THE DEVELOPMENT OF A NOVEL *IN VITRO* MODEL OF HUMAN LIVER FOR THE STUDY OF DISEASE PATHOGENESIS

Liqiong Chen, MSc

Thesis submitted to the University of Nottingham for the degree of Doctor of Philosophy

November 2009

Abstract

The development of systems for the long term *in vitro* culture of functional liver tissue is a major research goal. The central limitation of experimental systems to date has been the early de-differentiation of primary hepatocytes in cultures. Several factors including cell-cell interaction, cell-matrix interaction, soluble factors and 3D structures have been identified as the keys to overcome this limitation. The first aim of this project is to compare the established 3D model, co-culture of hepatocytes and hepatic stellate cells (HSCs) on $P_{DL}LA$ coated surfaces, to other best available systems using collagen and Matrigel. The hypothesis is that hepatocytes functionalities, established by cell-cell interaction, 3D structures and soluble factors, can be further enhanced by introduction of cell-matrix interaction.

In order to test the hypothesis, rat hepatocytes were cultured in five different systems, including monoculture of hepatocytes on collagen gel, in collagen-Matrigel sandwich, co-culture of hepatocytes and HSCs on collagen gel, in collagen-Matrigel sandwich and on $P_{DL}LA$ coated surface. Hepatocyte specific function assays, namely albumin secretion, urea secretion, testosterone metabolism by HPLC and CYP activities by LC-MS-MS, were used to analyze cell functionalities.

Homo-spheroids were only formed in monoculture on collagen gel, but hetero-spheroids were developed in all the co-culture systems. The results of function

assays showed hepatocytes in collagen-Matrigel sandwich configuration had the best secretion of albumin and urea and best CYP activities during the culture period. These data demonstrated the hypothesis that hepatocyte functions of the established model can be further improved by introduction of cell-matrix interaction.

In addition to establishment of rat hepatocyte culture systems, hetero-spheroids of primary human hepatocytes and primary human HSCs on $P_{DL}LA$ coated plates were developed successfully, due to the great improvements of isolation and culture of primary human HSCs. However, hepatocyte function assays have not been applied yet.

Hepatic cell lines have several advantages that are not applicable to primary cultured human hepatocytes, namely unlimited lifespan and stable phenotype. The immortalized Fa2N-4 cell lines have recently been assessed as replacements of primary human hepatocytes in CYP induction studies. The second aim of this study was to simultaneously characterize CYP1A2, CYP2C9, CYP3A4 and CYP2B6 induction in Fa2N-4 cells through assessment of mRNA, protein and activity endpoints for a range of prototypical compounds (previously assessed in human hepatocytes) with known positive and negative induction potential. LC-MS-MS and RT-PCR were used for assessment of activity and mRNA endpoints respectively. As a result, it is considered that Fa2N-4 cells offer a substitute for primary human hepatocytes for CYP1A2 and CYP3A4 induction but not for CYP2B6 due to lack of cytosolic CAR expression.

Acknowledgments

I would like to thank my supervisor, Brian Thomson, for his great supervision and support during the course of this PhD. I also thank my supervisor, Kevin Shakesheff, for his supervision and help with the tissue culture work. I express many thanks and gratitude to my industrial supervisor, Ken Grime, for assisting me with Fa2N-4 cells CYP induction work during my second year. Many thanks go to my internal examiner, Will Irving, and other members of the pharmacy school and molecular medical school that contributed to useful discussions about the project during meetings and seminars. I am also thankful to University of Nottingham and AstraZeneca for funding.

I thank all the members of the tissue engineering group from 2005 to 2008 for being a great team, especially Laura Dexter for great help in primary human hepatocytes isolation and culture, Amanj Saeed for assisting and providing with primary human stellate cells, Chafika Dehili for help in hepatocytes specific function assays (albumin and urea secretion) and Rob Thomas for guideness in HPLC technology. Many thanks go to all the technicians in the pharmacy school, particularly great help from Mrs Teresa Marshall. I also thank all the members of the DMPK from 2006 to 2007 in AstraZeneca, especially Jane Kenney for great guideness and help in Fa2N-4 cell line culture and CYP induction studies and James Bird for assisting in LC-MS-MS technology.

Finally, I would like to express my deepest gratitude and love to the most important people in my life: my parents Mr Minghao Chen and Mrs Xiuyun Xu, and my fiance Mr Ming Wu. I thank them for providing me with lots of support and encouragement that enabled me to finish my PhD. I dedicate this PhD to all of them.

Publications and Presentations

The following are attended meetings where some of the work reported in this thesis has been presented:

Poster presentation:

19th June 2006

The development of *in vitro* models of liver,

School of Molecular Medical Sciences presentation, University of Nottingham

2nd May 2007

The development of a novel *in vitro* model of human liver for the study of disease pathogenesis

School of Pharmacy presentation, University of Nottingham

School seminars:

04th April 2007

Assessment of CYP induction in Fa2N-4 cell line

DMPK, Charwood, Astrazeneca

28th April 2008

Co-culture of primary rat hepatocytes and stellate cells in 3D spheroids

School of Pharmacy presentation, University of Nottingham

2nd July 2008

The development of a novel *in vitro* model of human liver for the study of disease pathogenesis

School of Molecular Medical Sciences presentation, University of Nottingham,

Publications:

Kenny, J. R., Chen, L., McGinnity, D. F., Grime, K., Shakesheff, K. M., Thomson, B. and Riley, R. (2008). Efficient assessment of the utility of immortalized Fa2N-4 cells for cytochrome P450 (CYP) induction studies using multiplex quantitative reverse transcriptase-polymerase chain reaction (qRT-PCR) and substrate cassette methodologies. *Xenobiotica*, **38**, (12), 1500-1517.

Abbreviations

AFP	alpha-fetoprotein
AhR	Arylhydrocarbon receptor
AMBP-1	Adrenomedullin binding protein-1
ARNT	AhR nuclear translocator
BAL	Bio-artificial liver
BECs	Biliary epithelial cells
BLSS	Bio-artificial liver support system
BMCs	Bone marrow cells
BSA	Bovine serum albumin
° C	Degree Celsius
CAR	Constitutive androstane receptor
CK	cytokeratin
cm	centimetre
cm^2	centimetre square
CYP	Cytochrome P450
2D	Two-dimensional
3D	Three-dimensional
DBD	DNA binding domain
DMEM	Dulbecco's Modified Eagle Media
DMSO	Dimethyl sulphoxide
ECM	Extracellular matrix
EGF	Epidermal growth factor

EGTA	Ethylene glycol-bis (β-aminoethylether)-N, N, N', N'-tetraacetic acid
EHS	Engelbreth-Holm-Swarm
ELAD	Extracorporeal liver assist device
ERK	Extracellular-signal regulated kinase
EROD	7-Ethoxyresrufin-O-deethylase
ET-1	Endothelin-1
FACS	Fluorescence activated cell sorting
FAK	Focal adhesion kinase
FCS	Foetal calf serum
G	Gram
GST	Glutathione S-transferase
HGF	Hepatocyte growth factor
HGI	Hepatocyte growth inhibitor
HNF	Hepatic nuclear factor
H_2SO_4	Sulphuric acid
HSCs	Hepatic stellate cells
HemSCs	Hematopoietic stem cells
HS	Extracellular sulphate
IFN	Interferon
IGF	Insulin-like growth factor
IL	Interleukin
ILK	Intergrin-linked kinase
KCs	Kupffer cells
l	Litre

LBD	Ligand binding domain
LCT	Liver cell transplantation
LDL	Low density lipoproteins
LPS	Lipolysaccharides
LRP	Liver-regulating protein
MCP	Monocyte chemotactic protein
MELS	Modular extracorporeal liver support
mg	miligram
ml	mililitre
µCP	microcontact printing
µl	microlitre
µg	microgram
µmol	micromole
MARS	Molecular adsorbent recirculatiing system
MMP	Matrix metalloproteinase
mm	milimeter
mM	milimoles
nm	nanometer
NADPH	Nicotinamide adenine dinucleotide phosphate
NaCl	Sodium chloride
NPCs	Non-parenchymal cells
OLT	Orthotropic liver transplantation
PBS	Phosphate buffered Saline
PCs	Parenchymal cells

PDAC	Poly (diallyldimethylammonium chloride)
PDMS	Poly (dimethylsiloxane)
PEM	Polyelectrolyte multilayer
PGA	Polyglycolic acids
PGDF	Platelet-derived growth factor
PLGA	Polylactic-glycolic acid
$P_{DL}LA$	Poly (LD-lactic acid)
pmol	Picomole
PIPAAm	poly (N-isopropylacrylamide)
PXR	Pregnane X receptor
PVDF	Poly (vinylidene difluoride)
ROS	Reactive oxygen species
RER	Rough endoplasmic reticulum
rpm	Revolutions per minute
RPEn	Rat prostate endothelial cell line
RXR	Retinoid X receptor
SECS	Sinusoidal endothelial cells
SD	Standard deviation
SER	Smooth endoplasmic reticulum
SPS	Sulfonated polystryrene
ST	Sulfotransferase
TBS	Tris buffered saline
TMB	3, 3', 5, 5'-Tetramethylbenzidine
TNF	Tumour necrosis factor

TGF	Transforming growth factor
TIMP	Tissue inhibitor of metalloproteinase
TLR4	Toll-like receptor 4
UDPGT	Uridine diphosphate-glucuronosyltransferase
UNOS	United Network for Organ Sharing
VEGF	Vascular endothelial growth factor

Table of Contents

Table of Figures

Chapter One:

General Introduction

1 Introduction

1.1 The liver

1.1.1 Liver anatomy and microscopic structure

The liver is the largest gland of the body, weighing approximately 1200-1500 g and making up to one-fiftieth of the total adult body weight. It is situated in the upper right portion of the abdominal cavity. The organ enveloped in a thin capsule (Glisson's capsule), is divided by fissures into four lobes, namely the right (the largest lobe), left, quadrate and caudate lobes. (Sherlock and Dooley, 2005)

The entire liver consists of thousands of functional units, usually visualised as a six-side structure, known as the ‘classical lobule’. In addition, portal lobule and liver acini are two other common ways to consider parenchyma of liver structure, and simply use different aspects of liver vasculature to demarcate the functional unit. The structure of the classical lobule is shown in Figure 1.1. Each corner is made up of portal triads, which contain branches of the bile duct, the portal vein, and the hepatic artery. Along the central axis of each lobule runs the central vein, and cords radiate from the central vein towards the portal triad. These cords occupy the bulk of the lobule and are separated by sinusoids. (Rodés *et al*., 2007)

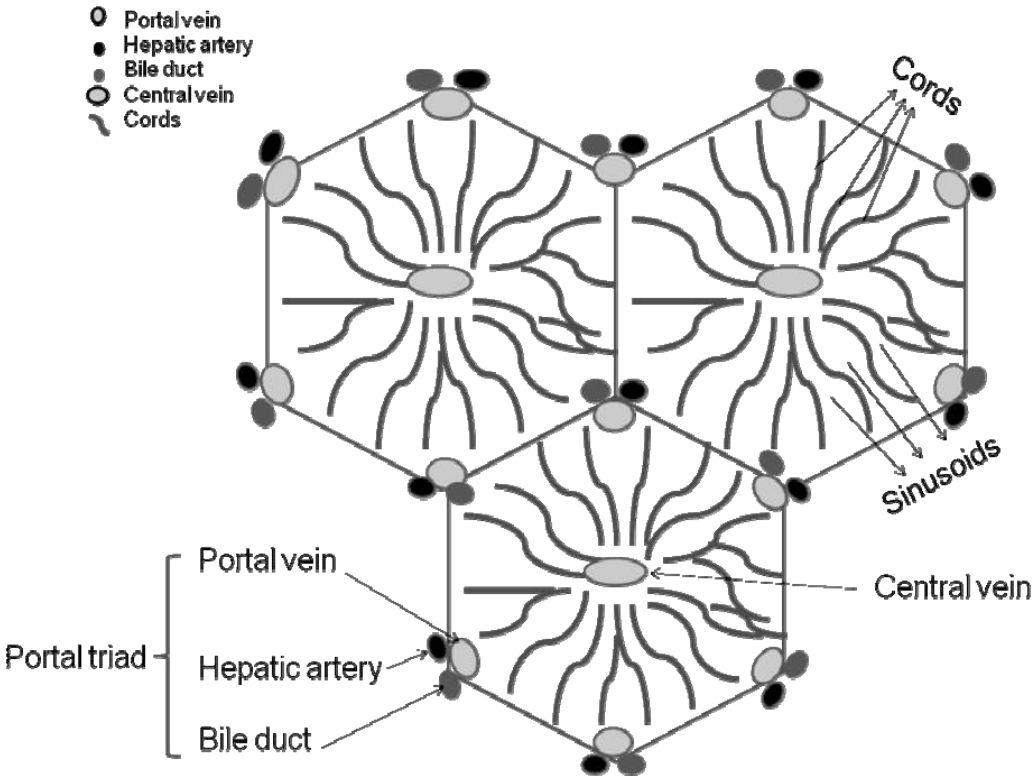

Figure 1.1: A schematic diagram of three classical liver lobules. Portal triad consists of bile duct, hepatic artery and portal vein. Central vein is located at the center of lobule and cords are separated by sinusoids.

A cord is composed of thousands of hepatocytes and each hepatocyte attaches to its neighbor. The tissue space between hepatocytes and sinusoidal endothelium is named the space of Disse and the sinusoids are vascular spaces lined by fenestrated endothelium. (Figure 1.2) The space of Disse contains a network of reticular fibers, for example collagen type III, which bring hepatocytes together. More importantly, since the endothelium has no underlying basement membrane, the blood plasma passages freely into the space of Disse. As, further, there is no epithelial basement membrane, the hepatocyte is the only epithelial cell in the body not separated from the vasculature by two continuous basement membranes. This facilitates rapid bidirectional macromolecular exchange between plasma and hepatocytes. (Sherlock and Dooley, 2005)

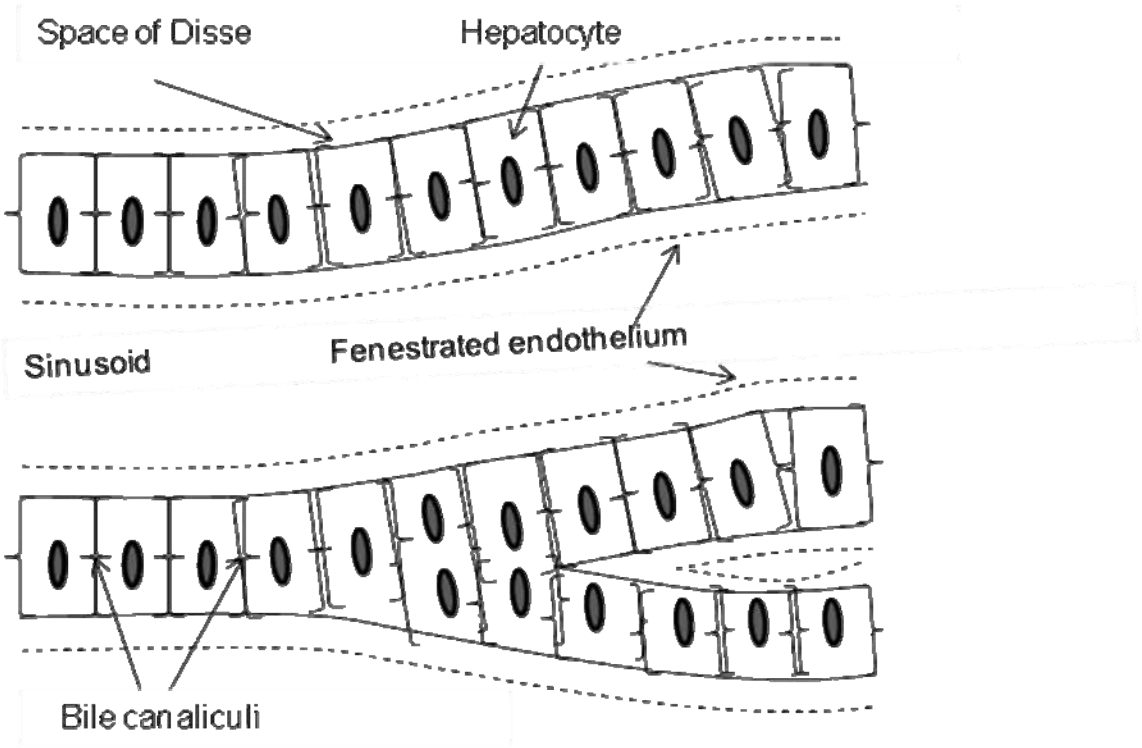

Figure 1.2: A schematic diagram of hepatic cords, sinusoid and fenestrated endothelium. Hepatocytes are arranged as cords and the apical surfaces of adjacent hepatocytes form bile canaliculi. Sinusoids are the space between fenestrated endothelium.

Unlike other organs, the liver is supplied with blood by two sources. One-third of the blood and 50% of the oxygen is delivered through the hepatic artery; the remaining two-thirds and 50% of the blood supply is provided by the hepatic portal vein. The latter source of the blood travels from the digestive tract where it collects the nutrients, which are delivered to liver for future storage. After the blood enters the liver by these two sources, it flows through the sinusoids and drains through three major hepatic veins into the vena cava (Rodés *et al*., 2007).

1.1.2 Cells of the liver

The predominant cell type, which performs the majority of liver functions, is the hepatocyte. These cells are present at a density of about 10^8 cells/g liver tissue in humans (Stacey *et al*., 2001). In addition to hepatocytes, at least 15 different cell types can be observed in the liver, including hepatic stellate cells (HSCs), Kupffer cells (KCs), sinusoidal endothelial cells (SECs), bile duct cells, liver-associated lymphocytes and nerve cells (Rodés *et al*., 2007). Of these, HSCs, KCs and SECs are the major non-parenchymal cell types and line the walls of the hepatic sinusoid (Rodés *et al*., 2007). The schematic in Figure 1.3 illustrates the position of these cells in relation to each other.

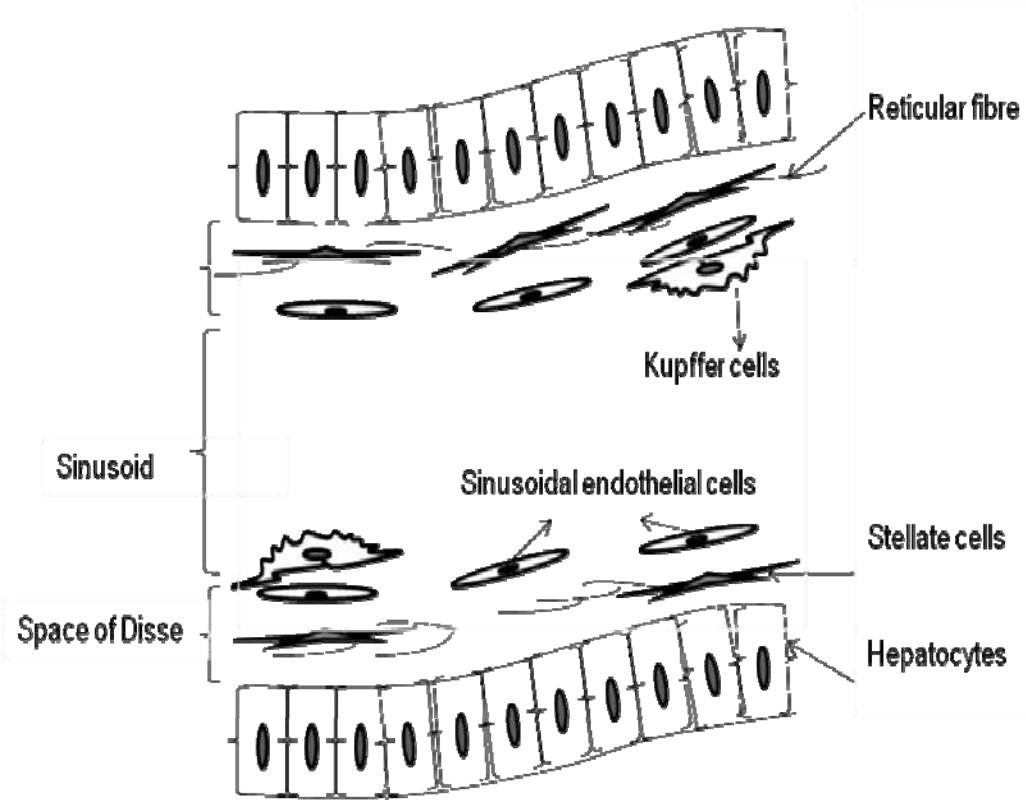

Figure 1.3: A schematic of the liver sinusoid and relation of parenchymal (hepatocytes) and non-parenchymal cell types (sinusoidal endothelial cells, Kupffer cells and hepatic stellate cells)

1.1.2.1 Hepatocytes

Highly differentiated hepatocytes make up approximately 80% by mass of the cell population of the liver (Rodés *et al*., 2007). The majority of hepatocytes possess single nuclei, although approximately 15% to 25% of the population is bi- or multi-nucleate. It has been reported that polyploidy affects the secretion of plasma protein and proliferation of hepatocytes (LeGuilly *et al*., 1973).

In vivo, human hepatocytes contain three membranes. They are highly polarized cells (Musat *et al*., 1993), which depend on the maintenance of two main membrane domains, namely apical (bile canalicular) and basal (sinusoidal) surfaces. The edges of the apical surface are attached by junctional complexes to those of adjacent hepatocytes, forming the bile canaliculi; the basal surfaces of the cells face the sinusoid and the space of Disse. (Figure 1.4) These two membranes show different hepatocellular functions (Dunn *et al*., 1989). Bile acids are excreted into the bile duct by traversing the bile canaliculi (apical surface), whereas proteins associated with the transport of metabolites are secreted into the circulation through the basal surface. (Figure 1.4)

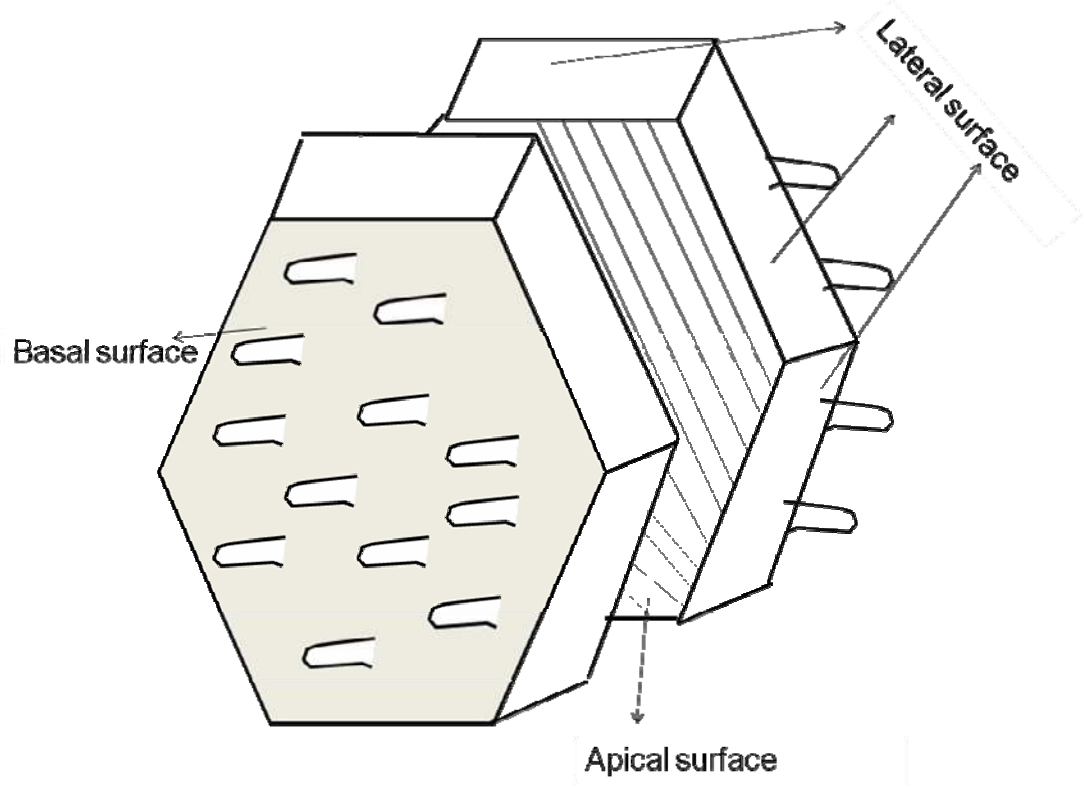

Figure 1.4: A schematic of three faces of a hepatocyte. Basal surface faces the sinusoid and space of Disse, apical surface faces bile canaliculous and lateral surface faces neighboring hepatocytes.

Hepatocytes are the “functional units’ of the liver. They perform many functions including uptake, transport, synthesis, biotransformation and degradation of proteins, lipids, hormones, xenobiotics, etc. They contain numerous mitochondria, where numbers of energy-providing processes take place, particularly oxidative phosphorylation. These mitochondria contain enzymes involved in citric acid cycle and β-oxidation of fatty acids. Ion balance and water metabolism are relevant to the mitochondria as well. In addition, hepatocytes have extensive endoplasmic reticulum, including both smooth (SER) and rough endoplasmic reticulum (RER). RER, where ribosomes are located, is responsible for synthesis of specific proteins, particularly albumin and Glucose-6-phosphatase. It may also participate in glycogenesis; SER, which contains microsomes, is the site of bilirubin conjugation and the detoxification of many drugs and other foreign compounds, particularly cytochrome P450-dependent monooxygenase system. Steroids are also synthesized on SER, including cholesterol and the primary bile acids. Moreover, peroxisomes, which are distributed near the SER and glycogen granules, have complex catabolic and biosynthetic roles. They contain the enzymes involved in the β-oxidation cycles, the glyoxalate cycle, ether lipid synthesis, and cholesterol and dolichol biosynthesis. Also, hepatocytes contain lysosomes, which have numerous hydrolytic enzymes and play a role in the degradation of extracellular and intracellular macromolecules. Furthermore, Golgi apparatus is found in hepatocyte cytoplasm, which is regarded as a 'packaging' site before excretion into the bile and is involved in the synthesis of glycoproteins. Finally, the cytoskeleton, consisting of microtubules, micro-

filaments and intermediate filaments, is fundamental for the stability and spatial organization of the hepatocyte. (Figure 1.5) (Sherlock and Dooley, 2005)

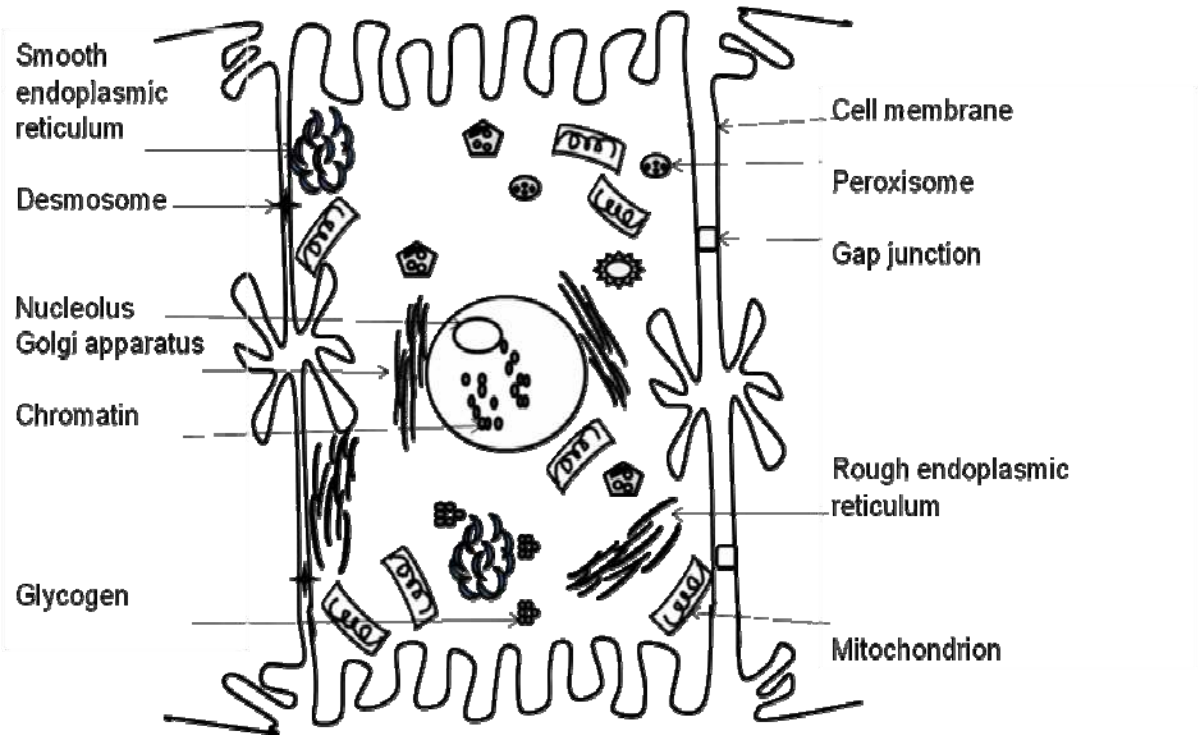

Figure 1.5: The organelles of the hepatocyte

1.1.2.2 Non-parenchymal cells

A functional and histological unit is formed by sinusoidal cells, including SECs, KCs and HSCs, in combination with the sinusoidal aspect of hepatocytes (Sherlock and Dooley, 2005). SECs line the sinusoids and KCs are associated with endothelium. HSCs lie in the space of Disse between the hepatocytes and endothelial cells. (Figure 1.3)

1.1.2.2.1 Endothelial cells

Endothelial cells form a continuous lining to the sinusoid. They differ from endothelial cells elsewhere as they do not possess a regular basal lamina but have numerous fenestrae. Fenestrae act as a biofilter between sinusoidal blood and the plasma within the space of Disse, and permit the exchange of macromolecules of different size with nearby hepatocytes. Particles > 0.2 μm do not pass, but smaller triglyceride-depleted, cholesterol-rich and retinol-rich residues can enter the space of Disse (Sherlock and Dooley, 2005). Therefore, the fenestrae might play a vital role in chylomicron and lipoprotein metabolism. Endothelial cells have a high capacity for receptor-mediated endocytosis and are active in clearing both macromolecules and small particles from the circulation (Sherlock and Dooley, 2005). In addition, they are known to secrete IL-1, IL-6, interferon and hepatocyte growth factor (HGF) and proteins that effect extracellular matrix (ECM) (Noji *et al*., 1998), together with a variety of mediators, such as tumour necrosis factor, prostaglandin E2, prostacyclin, and angiotensin-converting enzyme, which could regulate hepatocyte function (Hashimoto *et al*., 1992).

1.1.2.2.2 Kupffer cells

KCs, derived from circulating monocytes, are attached to the endothelial lining of the sinusoid. These highly mobile macrophages are responsible for removing old and damaged blood cells or cellular debris, also bacteria, viruses, parasites and tumour cells by several different mechanisms (Sherlock and Dooley, 2005).

KCs are activated by a number of agents, including endotoxin, sepsis, shock, interferon-γ, arachidonic acid and tumour necrosis factor (TNF). Interestingly, activated KCs can release an array of inflammatory mediators, growth factors, and reactive oxygen species, including cytokines, hydrogen peroxide, nitric oxide, TNF, interleukin (IL) 1, IL6, interferon-α and β, and transforming growth factor (TGF- β). (Sherlock and Dooley, 2005)

The role of KCs in liver biology has not been fully understood, but can be described into two categories: KCs as the primary target of toxic signals and KCs as a second target responsive to the toxic signals received by the hepatocytes. For the first category, these cells might be the primary site of an initially protective response that develops to cause damage with further stimulation (Ito *et al*., 2003). They could act as not only a protector (He *et al*., 2005; Kresse *et al*., 2005) but also as a mediator of damage (Prins *et al*., 2004). For the second category, the KCs play a more supportive role in the overall response to the toxicant. However, the detailed mechanism of KC-hepatocyte interaction is still uncertain.

1.1.2.2.3 Hepatic stellate cells

HSCs were firstly identified by Von Kupffer in 1876 as "*sternzellen*"; however, these cells were not identified as unique vitamin A-storing lipocytes with an important role in hepatic fibrosis until 1952 by Ito and Nemeto. In 1985, Friedman and colleagues found out that hepatic "lipocytes" were the main cells responsible for collagen production in rat. After that, with the development of techniques of isolation and culture of HSCs, research has established HSCs as key elements in liver fibrosis at many levels.

HSCs reside in the space of Disse, between endothelial cells of sinusoids and hepatocytes. They comprise approximately 1.4% of total liver volume and 15% of the total number of cells, respectively (Geerts, 2001; Friedman, 2004). They are present at a ratio of about 3.6 to 6 cells per 100 hepatocytes (Moreira, 2007). HSCs exhibit mainly two phenotypes. In quiescent state, HSCs are characterised by large perinuclear lipid droplets and long cytoplasmic processes with fine branching (Sato *et al*., 2003). They are essential in the regulation of retinoic acid homeostasis (Li and Friedman, 1999; Geerts, 2001). The storage of vitamin A is not homogeneous, and particular lobules and sub-lobules appear to be the major site of storage for retinoid (Ballardini *et al*., 1994). Also, they play a vital role in the maintenance of basement membrane matrix, mainly type IV, VI collagen and glycoproteins, essential for the maintenance of the normal hepatic perisinusoidal environment (Pinzani *et al*., 1992). In addition, quiescent HSCs are responsible for the regulation of hepatic blood flow (Tanikawa, 1995) and portal venous pressure (Rockey and Weisiger, 1996). Furthermore, quiescent HSCs express the hepatocyte mitogen,

hepatocyte growth factor, which may play a role in control of regeneration in the normal liver.

Besides the quiescent state, HSCs can undergo activation or transdifferentiation to a myofibroblast-like cell, which is regulated by paracrine and autocrine loops of growth factors in association with fibrosis in pathological conditions such as liver injury and cirrhosis (Friedman, 2000; Lieber, 2005). The activated HSCs are with several new phenotypic characteristics, including enhanced cell adhesion and migration, expression of α-SMA, increased proliferation, production of chemotactic substances capable of recruiting inflammatory cells, contractibility, loss of normal retinoid-storing capacity, increased rough endoplasmic reticulum, changes in cytockeletal organization and cellular morphology and acquisition of fibrogenic capacity. Conceptually, activation occurs in two phases, namely initiation and perpetuation (Friedman, 2000). Initiation refers to the early events which make cells responsive to a great number of proliferative and fibrogenic cytokines, including TGF-β (Gressner *et al*.,1993), TNF-α, matrix metalloproteinase (MMP)-9 (Winwood *et al*., 1995) and reactive oxygen species (ROS) (Nieto *et al*., 2002) from KCs; interferon (IFN)-γ and IL from lymphocytes (Wynn, 2004 and Sugimoto *et al*., 2005); Toll-like receptor 4 (TLR4) from both HSCs themselves and KCs. Also, initiation is associated with the events resulting from early changes in ECM caused by the transcriptional activation of many profibrogenic genes including α1 (I) collagen, TGF-β1, type I and II TGF-β (Li *et al*., 2008).

Perpetuation is the result of a continuously dynamic process of release of cytokines to the cells, which can be subdivided into at least seven distinct events occurring simultaneously. These events include proliferation, chemotaxis, contractility, fibrogenesis, release of cytokines, degradation of the liver's normal matrix and loss of vitamin A droplets. (Friedman, 2006)

The molecular mechanism of the above phenotypic responses of activated HSCs is related to a numerous number of cytokines and mediators. Platelet-derived growth factor (PGDF) is identified as the main mediator for proliferation (Borkham-Kamphorst, 2004) and endothelin-1 (ET-1) and other contraction-stimulating cytokines secreted by HSCs are the key contractile stimuli (Shi-Wen *et al*., 2004). A variety of mediators, however, have been demonstrated to promote HSCs fibrogenesis, for example, TGF-β is the most potent fibrogenic factor for HSCs (Olaso and Friedman, 1998) and leptin has been regarded as a profibrogenic hormone in the liver (Bethanis and Theocharis, 2006; Niu *et al*., 2007). In addition, HSCs express virtually all the key components required for matrix degradation, mainly matrix metalloproteinase (MMP)-2 and MMP-3. A rapid decrease of expressions of tissue inhibitor of metalloproteinase (TIMP)-1 and -2 is caused by increased activity of MMP-2 (Arthur, 2000). Moreover, several chemo-attractants, including PDGF, insulin-like growth factor (IGF)-1, ET and monocyte chemotactic protein (MCP)-1, have a role in HSCs chemotaxis.

1.1.3 Liver extracellular matrix

The liver ECM relates to the array of various macromolecules which consist of the scaffolding of the liver. In addition to a physical scaffold, it is a modulator of biologic processes including cell attachment, migration, differentiation, repair and development. In normal liver, apart from Glisson's capsule, ECM is restricted to portal triads, sinusoid walls and central veins. (Bedossa and Paradis, 2003)

Collagens, elastin, structural glycoprotein and proteoglycans are the four major components of ECM in normal liver. Of these, collagens are the most frequently found proteins and serve as scaffolding that supports the parenchyma and maintains hepatic integrity. Small bundles of type I and fibrillar collagen type III are confined to the space of Disse (Clement *et al*., 1985). However, type V collagen is more abundant near portal triads and central veins (Schuppan *et al*., 1986). Type IV collagen takes part in the formation of basement membrane of nerves, bile ducts, arterial and venous vessels (Martinez-Hernandez, 1984), together with laminin, entactin and perlecan. Glycoproteins, including fibronectin, laminin, tenascin and entactin, are major ECM constituents with a role in cell adhesion (Schuppan, 1990). They share epidermal growth factor-like domains, polymer-forming capacities and specific amino acid sequences interacting with cell receptor integrins (Ilynes, 1987; Alhelda and Buck, 1990). In addition to collagens and glycoproteins, proteoglycans including heparin, dermatan, chondroitin sulphate, perlecan, hyaluronic acid, biglycan and decorin (Gressner, 1983), are another key component in ECM. Proteoglycans are present in the intracellular space,

on the cell surface and in the extracellular space (Lozzo, 1985); however, their function is not clear as that of other ECM components.

1.2 Liver function and hepatic metabolism

The liver has the ability to perform a vast array of functions. These include:

- Metabolism - the regulated synthesis or degradation of a wide range of molecules. This includes the metabolism of carbohydrate, lipid, amino acid, nitrogen, vitamin, normal iron/copper and xenobiotics. It is also involved in mitochondria and energy formation, bile formation and secretion, ammonia and urea production, glutathione, haem biosynthesis and excretion of porphyrins.

- Synthetic function. Albumin and other carrier proteins are synthesized in the liver, which bind to other molecules. In addition, most of coagulation factors, anticoagulant proteins and components of the fibrinolytic systems required for haemostasis are synthesized by hepatic parenchymal cells. Extracellular matrix proteins, mainly collagen, are also produced in liver and play an important role in liver function in health and disease. (Rodés *et al*., 2007)

In terms of metabolic function of the liver, it can be summarized into several major categories, namely carbohydrate metabolism, fat metabolism and protein metabolism. Most of these compounds entering the body are lipophilic, which are not easily excreted. By transforming one substance to another water-soluble compound by increasing its polarity, the liver facilitates the excretion of toxins. Hepatocytes are the main cell type involved in the metabolism and the processes of it can be divided into two stages.

(i) Phase I reactions

Phase I reactions are sometimes called "functionalization reactions", since they often introduce new hydrophilic functional groups to compounds by oxidation, reduction or hydrolysis. These groups are then recognized as the attachment points for other molecules in the process of conjugation. (Rang *et al*., 2007) The enzymes involved in phase I reactions include oxygenases and oxidases, reductase, hydrolytic enzymes and enzymes that scavenge reduced oxygen. They are mostly located on endoplasmic reticulum (microsomes), cytosol, mitochondria and lysosomes. (Kwon, 2001)

Specifically, cytochrome P450 (CYP) monooxygenases are the major enzymes involved in the Phase I reactions. Their mechanism of action is rather complex, but the outcome of the reaction is relatively simple - that is formation of a hydroxyl group by the addition of an oxygen atom from molecular oxygen and formation of water by the other oxygen atom. (Rang *et al*., 2007) They are also regarded as the most important metabolizing enzymes for xenobiotics. More than 85% of the drugs in the market are metabolized by CYP enzymes. (Kwon, 2001)

(ii) Phase II reactions

Phase II reactions mostly refer to "conjugation reactions", which are binding of a substance (parent compound), or its metabolites from a phase I reaction, with endogenous molecules (conjugation), and making more water soluble derivatives that may be excreted in the urine or bile.

The types of phase II reactions include glucuronidation, sulfation, glutathione-conjugation, acetylation, methylation and conjugation with amino acids (e.g. glycine, taurine, glutamic acid). Most conjugation reactions are to replace a hydrogen atom present in a hydroxyl, amino or carboxyl group by conjugating agents. Among all of them, glucuronidation is the most common and quantitatively most important type of conjugation. (Figure 1.6) (Kwon, 2001)

The Phase II enzymes, located on endoplasmic reticulum (microsomes), cytosol, mitochondria and nucleus, include uridine diphosphate-glucuronosyltransferase (UDPGT), sulfotransferase (ST), N-acetyltransferase, glutathione S-transferase (GST), methyl transferase, and amino acid conjugating enzymes. Particularly, UDPGT is responsible for glucuronidation. (Kwon, 2001)

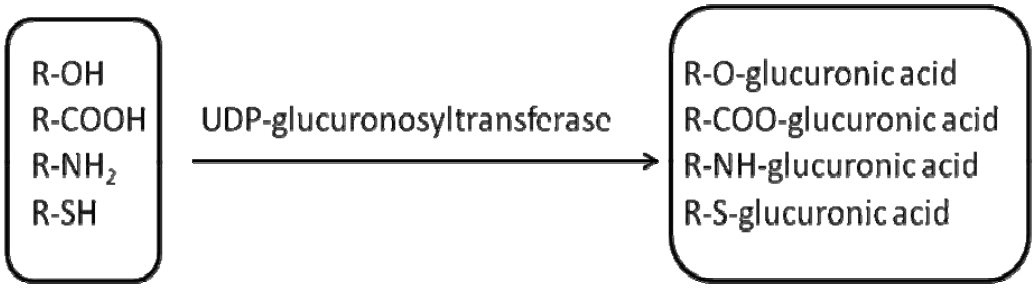

Figure 1.6: The glucuronide conjugation reactions by UDP-glucuronosyltransferase. A hydrogen atom present in a hydroxyl, amino or carboxyl group is replaced by glucuronic acid.

1.2.1 Cytochrome P450 enzymes

1.2.1.1 Cytochrome P450 enzyme system

The P450 system is made of three protein components set in the phospholipid environment of the endoplasmic reticulum. The first component is cytochrome P450, which is a three-dimensional structure arranged into a series of helices and folds and contains a ferroprotoporphyrin IX heme prosthetic group, and can directly contact substrates and molecular oxygen. Another component is NADPH-cytochrome P450 reductase, which transfers electrons from NADPH to the cytochrome P450-substrate complex. With the help of the other protein, cytochrome b_5, together with the cytochrome b_5 reductase, the second of the two electrons required for cytochrome P450 reactions is delivered to enhance the catalytic efficiency and proceed to the reduction step. (Figure 1.7) (Kwon, 2001)

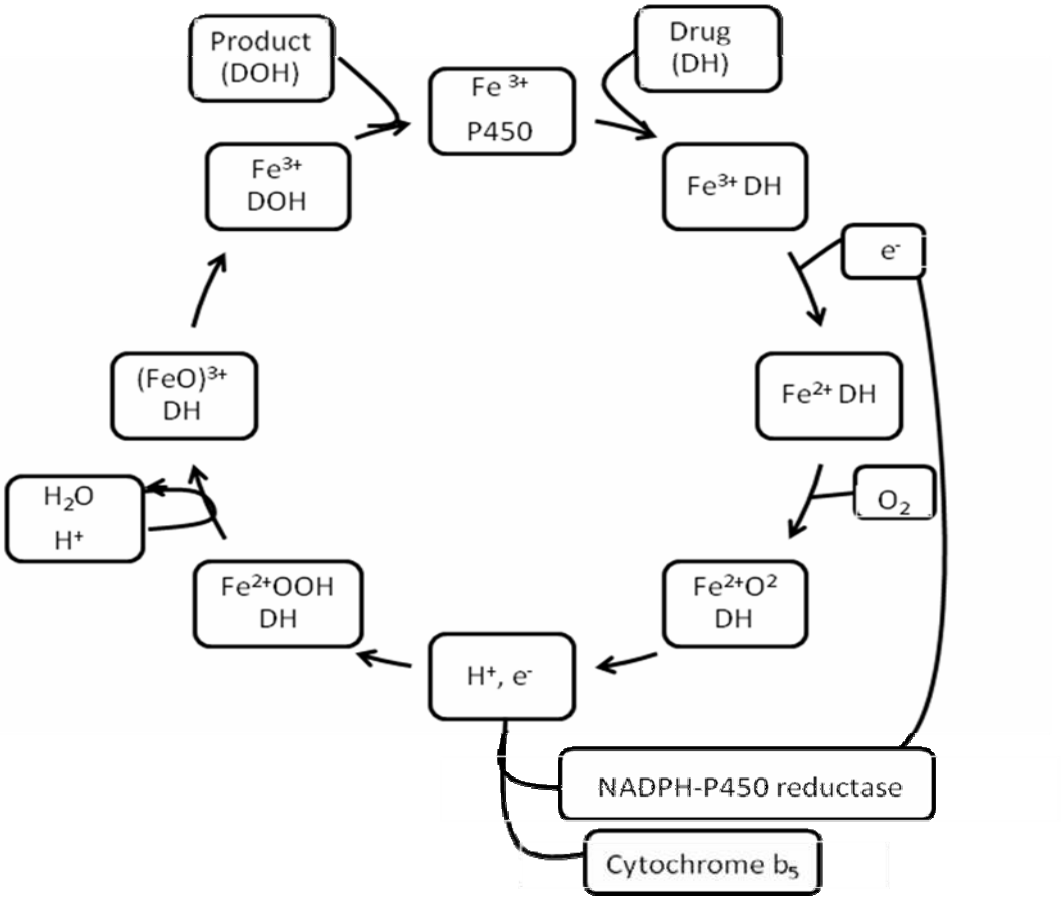

Figure 1.7: Schematic representation of catalytic cycle of cytochrome P450. P450 with Fe^{3+} combines with a molecule of drug (DH), reduces to Fe^{2+} DH after receiving an electron from NADPH-P450 reductase and then combines with O_2 to form $Fe^{2+}O_2$ DH. Fe^{2+}OOH DH is then formed after combing with a proton and a second electron from NADPH-P450 reductase/Cytochrome b_5. The addition of a second proton is to convert Fe^{2+}OOH DH to $(FeO)^{3+}$ and to yield water. DOH is finally liberated from the complex of oxidised drug and P450 enzyme is regenerated. (Rang *et al*., 2007)

1.2.1.2 Nomenclature

When the oxidised form of cytochrome P450 (Fe^{+3}) is reduced to the ferrous (Fe^{+2}) state, cytochrome P450 is able to bind ligands such as O_2 and CO. The name of cytochrome P450 is derived from the ability of the enzyme to bind with carbon monoxide in the reduced form and then form a complex with the maximal absorbance between 447 and 452 nm (an average of 450 nm). However, when the heme moiety of cytochrome is disrupted, cytochrome P450 is converted to a catalytically inactive form called cytochrome P420, which absorbs light maximally at 420 nm upon binding with carbon monoxide in the reduced form. (Kwon, 2001)

1.2.1.2.1 Cytochrome P450 isoforms

Classification of cytochrome P450 into gene families, subfamilies and isoforms does not depend on the catalytic activities or substrate specificity but on amino acid sequence homology. (Kwon, 2001)

(i) Gene families (e.g. CYP1, CYP2, CYP3, etc): The genes of the enzymes sharing less than 40% amino acid homology are regarded as different gene families.

(ii) Subfamilies (e.g. CYP2A, CYP2B, CYP2C, etc): The similarities of gene sequence of the enzyme between 40% and 55% are assigned to different subfamilies.

(iii) Isoforms (e.g. CYP2C8, CYP2C9, etc): P450 enzymes with more than 55% amino acid sequence identity are classified as members of the same subfamily.

Currently, there are possibly four P450 gene families involved in drug metabolism, namely CYP1, 2, 3 and 4 and the first three are the main P450 gene families in the human liver. (Kwon, 2001) Table 1.1 illustrates all the CYP gene families, subfamilies and isoforms in human liver. Of these, CYP3A4 and CYP2D6 are the main metabolical isoforms for drug metabolism and CYP2C9, 2C19, 1A2, and 2E1 are less commonly involved. (Figure 1.8)

Table 1.1: Human cytochrome P450 isoforms

Category	Cytochrome P450 isoforms			
Family	CYP1	CYP2	CYP3	CYP4
Subfamily	1A	2A,B,C,D,E	3A	4A
Isoforms	1A1,1A2	2A6	3A3,3A4,3A5,3A7	4A9,4A11
		2B6		
		2C8,2C9,2C10,2C18,2C19		
		2D6		
		2E1		

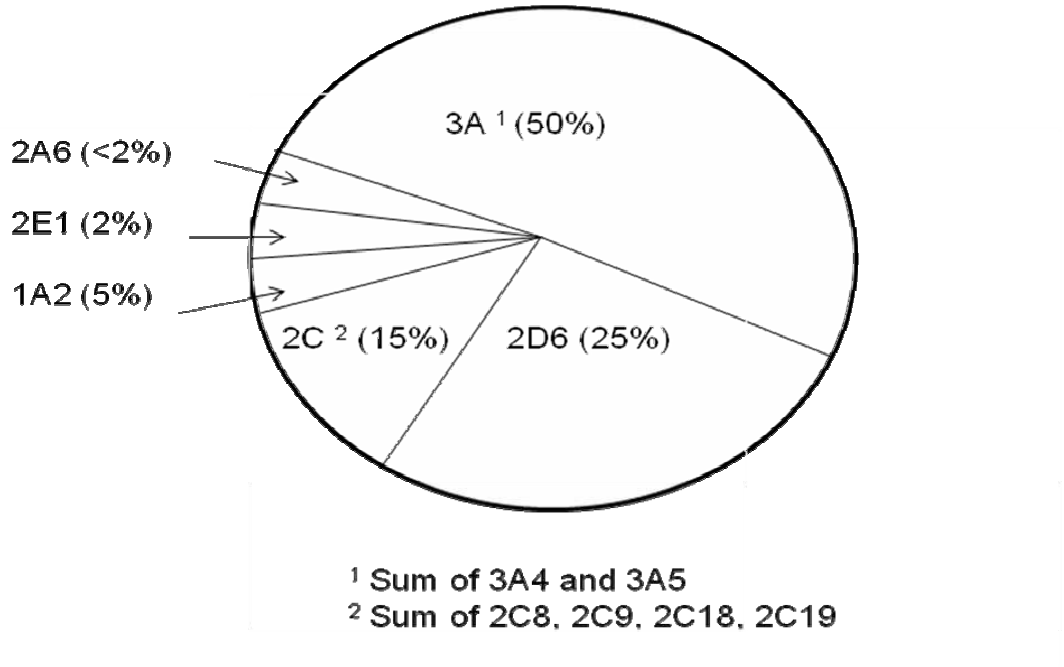

Figure 1.8: Percentage of individual P450 isoforms in the total P450 in human (Kwon, 2001).

1.2.1.3 Variability of cytochrome P450 in human liver

Human CYP enzymes, responsible for metabolism of xenobitics, are mainly localized in the membrane of endoplasmic reticulum (microsomes). However, during the last few decades, these microsomal CYPs have been reported to be present in other cellular organelles, such as at the extracellular face of plasma membrane (Loeper *et al*., 1990; 1993). CYP1A2. CYP3A4, CYP2C, CYP2D6 and CYP2E1 were recognized in the human hepatocyte plasma membrane by three autoantibodies in the immunofluorescence and immunoperoxidase studies (Loeper *et al*., 1993). It was also demonstrated that this particular content of CYPs in the plasma membrane was 9% of that in microsomes. Moreover, Golgi apparatus, lysosome and mitochondria (CYP3A1 and CYP3A2) are the localizations of rat and mouse CYPs (Ronis et al., 1991; Neve et al., 1996; 2001).

In addition to variability of localization, phenotypic and genotypic differences in the expression of CYPs in human liver have been investigated. CYP2C9, CYP2C19 and CYP2D6 are the major enzymes with polymorphisms in the human liver (Gómez-Lechón *et al*., 2007). In particular, CYP2D6, which is responsible for the metabolism of 25% of drugs in clinical practice, has a high number of allelic variants, some of them resulting in significant changes in enzyme functions (Gómez-Lechón *et al*., 2007). However, other CYP isoforms such as CYP3A4, CYP1A1 and CYP2E1 are relatively well conserved, with only a few variants causing the enzyme functions (Ingelman-Soudberg, 2005).

The hepatocyte is the major cell type expressing the majority of CYPs in human liver. However, other cells such as Kupffer cells, endothelial cells and hepatic stellate cells may contribute to the expression of CYPs to some extent. It has been reported that CYP2C11, CYP3A2 and CYP2D1 have been recognized in rat HSCs, at levels of 14-38% of those in rat hepatocytes (Yamada *et al*., 1997). Also, CYP2E1 in Kupffer cells have been involved in alcoholic liver disease (Adachi *et al*., 1995).

1.2.1.4 Cytochrome P450 in diseased human liver

Significant alternations in the hepatic expression of CYPs have been observed in the patient with liver diseases. For example, in the non-alcoholic fatty liver, the level of CYP1A2, CYP2D6 and CYP2E1 mRNAs were decreased in parallel with the disease progression, while CYP2A6, CYP2B6 and CYP2C9 mRNA expressions increased. At the protein level, CYP1A2, CYP2C19, CYP2D6, CYP2E1 and CYP3A4 expression tended to decrease with disease progression. (Fisher *et al*., 2009) Also, the level of both CYP1A2 mRNA and protein was reduced in the liver with hepatocellular and cholestatic types of cirrhosis, but the level of CYP3A4 mRNA and protein was only reduced in hepatocellular disease (George *et al*., 1995). Taking these observations together, the disease-specific CYP alternation is partly due to a pre-translational mechanism.

In addition, cigarette smoking and alcohol drinking have great effects on the expression of microsomal CYPs. Cigarette smoking is known to cause clinically significant induction of microsomal CYP1A2 with the indication of

the N-demethylation of caffeine to paraxanthine (Rasmussen *et al*., 2002). The expression of microsomal CYP2E1 is greatly induced by alcohol consumption with the increased activity of 6-hydroxylation of chlorzoxazone (Girre *et al*., 1994). However, other factors, either genetic or environmental, may contribute to the variations in CYP1A2 and CYP2E1 levels. For example, a strong correlation of CYP1A2 activity between identical twins was reported and certain drugs, vegetables and infectious diseases had effects on CYP1A2 expression (Vistisen *et al*., 1991; Rasmussen *et al*., 2002).

1.2.1.5 Cytochrome P450 inhibition and induction

The inhibition or induction of CYP enzymes is regarded as the most common mechanism for drug-drug interactions (Lin and Lu, 1998). CYP inhibition results from competition between two drugs which are metabolised by the same CYP. It may cause an unexpected increase in the plasma concentration of one or both drugs and also lead to a variety of minor or severe adverse effects. On the other hand, the induction arises from an elevation in the total amount of CYP which may lead to a marked decreased in plasma concentrations of a drug metabolised by the induced CYP. It can have significant consequences in the pharmacokinetics and toxicity of drugs. Therefore, it is necessary to understand the regulatory mechanisms of enzyme inhibition and induction to prevent potential harmful drug-drug interactions. (Hollenberg *et al*., 2002)

1.2.1.5.1 Cytochrome P450 inhibition

The CYP inhibitors can be divided into three categories depending on their different mechanisms. Reversible inhibitors are those that take part in the

catalytic cycle before the formation of the activated-oxygen intermediate, while either quasi-irreversible or irreversible inhibitors are those that interfere during or after the formation of the activated-oxygen intermediate. Generally, reversible inhibition is regarded as the most common cause of drug-drug interactions, which exhibits only dose-dependent inhibition of substrate metabolism. However, quasi-irreversible and irreversible inhibitions show both dose-dependent and time-dependent inhibition. (Hollenberg *et al*., 2002)

(i) Reversible inhibition

In the reversible inhibition of CYPs, the normal metabolic functions of the enzymes will continue after the removal of the inhibitors from the body. It can be further classified as competitive, noncompetitive and uncompetitive inhibition. In competitive inhibition, binding of the substrate to the active site of the enzyme is stopped due to the interaction between inhibitor and the enzyme (e.g. quinidine); in the noncompetitive inhibition, the inhibitor binds to the enzyme at a site rather than the active site, but enzyme-substrate-inhibitor complex is unable to function catalytically (e.g. ketoconazole); uncompetitive inhibition seldom happens in drug metabolism. In this case, the inhibitor binds to the enzyme-substrate complex rather than the enzyme, which leads to a non-productive formation. (Hollenberg *et al*., 2002)

(ii) Quasi-irreversible inhibition

In the quasi-irreversible inhibition, the inhibitors coordinate very tightly to the prosthetic heme in the CYP active site after the catalytic activation by the enzyme to transient intermediates. The interaction between the inhibitors and

CYP metabolic intermediates are so effective that it can covert the enzyme to a catalytically non-functional state. More importantly, the release of native catalytically active enzyme can be achieved only under special experimental conditions. Several different types of compounds are involved in this inhibition, including those containing a dioxymethylene function and nitrogen containing compounds like 1, 1-disubstituted hydrazines, acyl hydrazines, and a variety of alkylamines. (Hollenberg *et al*., 2002)

(iii) Irreversible inhibition

This final category of inhibitors is those compounds that bind irreversibly to the prosthetic heme, or the protein, or that their metabolites bind to the enzyme (e.g. gestodene). They can be referred to as "catalysis-dependent", "suicide" or "mechanism-based" inactivators. They are generally considered to be a relatively unusual occurrence with most enzymes. (Hollenberg *et al*., 2002)

1.2.1.5.2 Cytochrome P450 induction

Transcriptional gene activation, which is mediated by nuclear receptors, is the most common mechanism of CYP enzyme induction (Allen *et al*., 2001). Nuclear receptors, including arylhydrocarbon receptor (AhR), constitutive androstane receptor (CAR) and pregnane X receptor (PXR), serve as transcription factors in the whole process. In the absence of a ligand (drug), the nuclear receptor combines with co-repressor complexes, which gives a basal level of transcription. However, in the presence of a ligand (drug), the nuclear receptor binds to the ligand through the ligand binding domain (LBD), which leads to the release of co-repressor complexes and recruitment of co-activator

complexes. After the activated receptor binds to the dimerization partner, the chromatin of nuclear receptor is remodelled and then transcription is activated. The transcription of the respective CYP isoform is regulated through the DNA binding domain (DBD) of the nuclear receptor binding to the response element in the CYP gene promoters. Retinoid X receptor (RXR) is the partner for CAR and PXR and the AhR nuclear translocator (ARNT) is the one for AhR. (Wang and LeCluyse, 2003; Lemaire *et al*., 2004)

AhR and CAR are mainly located in the cytoplasm of hepatocytes. Once they are activated, they are transolcated to the nucleus; while PXR is predominantly located in the nucleus. Figure 1.9 shows an example of AhR/CAR-mediated mechanism of enzyme induction. However, it should be noted that not all the enzyme inductions are due to this direct ligand binding mechanism. Both AhR and CAR can be activated by ligand binding independent mechanism. (Backlund and Ingelman-Sundberg, 2005; Hu *et al*., 2007)

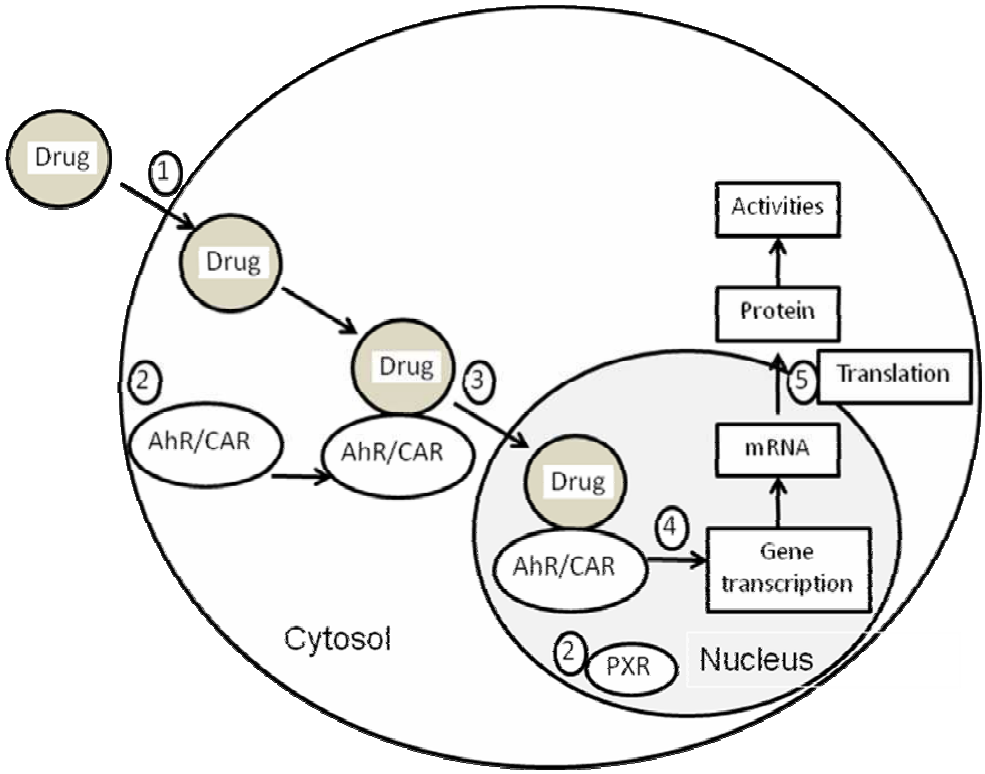

Figure 1.9: Overview of the receptor-mediated mechanism of enzyme induction. 1) The drug enters the cell. 2) AhR and CAR are located in cytoplasm, and PXR is mainly located in nucleus. This schematic diagram shows AhR/CAR-mediated pathways only; but PXR is activated in the same way in the nucleus. 3) AhR and CAR are translocated to nucleus after binding to the drug. 4) The activated receptor binds to the dimerization partner to activate the transcription. 5) mRNA is translocated to cytoplasm and translated into CYP and other proteins.

1.3 Engineering liver tissue

The 70% liver resection model was first described by Higgins and Anderson in 1931. The regenerative response of the liver is proportional to the loss of tissue mass for resections. The removal of up to 70% of the tissue mass can allow the remaining tissue to enlarge. However, a greater than 70% resection leads to a remarkable decline in the regenerative response (Nagasue *et al*., 1987). In liver tissue engineering, the aim is to exploit and expand this liver regenerative potential in order to grow liver tissue *in vitro*. There are various potential applications of engineered liver tissue, particularly in bio-artificial liver devices and *in vitro* toxicology models.

1.3.1 Bio-artificial liver device

Liver transplantation is the only recognized curative therapy available for end stage liver disease (Schiff and Schiff, 1993). However, due to donor shortages and substantial morbidity, it remains an unsatisfactory approach. According to the United Network for Organ Sharing (UNOS), only 5846 liver transplants were performed in 2004 against more than 17,000 patients on the national waiting list for liver transplantation in 2007 (Fiegel *et al*., 2008) The number of people on the liver transplant waiting list is increasing much faster than the number of transplants from deceased donors. Liver transplantation is also one of the most expensive surgical procedures available nowadays (Evans, 1993; Mendeloff *et al*., 2004). Consequently, work on engineering of liver tissue has attempted to develop extracorporeal liver support systems in order to either extend patient's period for bridge to liver transplantation or let the diseased liver regenerate itself.

Early research aimed to develop detoxification (artificial liver) devices, which are directed at removing toxins that cannot be removed by conventional dialysis. Biologic-DT (Aladag *et al*., 2004), molecular adsorbent recirculating system (MARS®) (Stange *et al*., 2002) and Prometheus (Kramer *et al*., 2003) have reached the clinical evaluation. However, even if the toxins are removed from blood stream for each of the systems, these systems are unsuccessful in maintaining the critical biochemical functions of liver.

Due to the shortages of effective detoxification devices, cell-based (bio-artificial liver, BAL) therapies and devices have been developed, aiming to combine the new techniques with previous methods to provide more support to the patients. The HepatAssist™ is the first generation of BAL, which is based on the use of hollow fibre cartridges (Demetriou *et al*., 2004). It has been followed by the extracorporeal liver assist device (ELAD®) (Millis *et al*., 2002), the modular extracorporeal liver support (MELS) (Mundt *et al*., 2002; Saucer *et al*., 2002) and the bio-artificial liver support system (BLSS) (Mazariegos *et al*., 2002). Two more recent developments, the radial flow bioreactor (Morsiani *et al*., 2002) and the Academic Medical Centre (AMC)-BAL (Van de Kerkhove *et al*., 2002) have reached clinical evaluation. Both of these two BALs directly perfuse the patient's plasma over and around cultured primary porcine hepatocytes. However, the impact of these BALs on patients' survival and clinically significant outcomes still remains unclear.

Cell transplantation is another cell-based therapy for liver disease. The method is to seed hepatocytes into the portal vein and then they are transported with

blood into liver sinusoids. Only a few studies have been reported because of the limited availability of human hepatocytes (Smets *et al*., 2008).

Researchers have turned to bioreactors for hepatic cell culture. The most successful devices incorporate features of the native liver structure. Early hepatocyte tissue culture has been mostly in monolayer, where hepatocytes rapidly lose their specific functions (Bissell *et al*., 1987). Culture of hepatocytes in a static manner is also very unlike the natural condition where the nutrients and waste metabolites are continuously supplied and removed. The bioreactor perfusion setting, which overcomes the shortages of early hepatocyte tissue culture system, is supported by adequate levels of oxygenation, nutrient gradients to a more *in vivo* like liver structure. 3D hepatocyte culture, which maintains extended liver specific functions in comparison to monolayer, has shown great potential for bio-artificial liver support (Ijima *et al*., 1998).

Appropriate cell sources for extracorporeal liver support remain as a controversial topic. The majority of bio-artificial liver support systems have used primary porcine hepatocytes, which show similar biochemical functions and activities to human hepatocytes. However, potential immunogenic response and unwanted transmission of pathogens have limited the use of these cells (Schrem *et al*., 2006). Due to limited human hepatocyte availability, cell lines including tumour-derived line and immortalized cell lines (Tsiaoussis *et al*., 2001) have been recommended as an alternative. However the cell lines have been demonstrated to express altered functions or reduced functions

compared to primary human hepatocytes. Therefore, stem cells may be the ideal cell source for cell-based therapies, since they have the potential to differentiate into mature cell types, benefiting to the damaged liver tissue (Odorico *et al*., 2001). The effects of growth factors, cytokines or mediators have been studied regarding to their roles on growth/differentiation of liver stem cell (Yoon *et al*., 1999). However, there are still many questions and challenges with regard to the use of stem cells in BAL.

1.3.2 *In vitro* toxicology model

In the drug development process, one of the major factors that delay the development is the potential for toxicity. The efficacy and safety of the compound in human have to be tested before clinical trials. Therefore, various *in vitro* toxicology models have been established to assess this factor, because traditional *in vivo* animal models are limited due to animal welfare/ethical concerns and inter-species differences between animal and human being.

Current engineered liver tissue models for use in toxicology studies are of three major types, namely, isolated perfused organ, liver slices and isolated hepatocyte model. The major advantages of isolated perfused organ are to maintain the 3D structure of organ with tight cell-cell interactions and the potential for bile collection and analysis (Hobbs *et al*., 1968a, 1968b). However, it is very complex to keep the function of organs within the physiological ranges and it is hard to achieve the integrity of the function over a prolonged period. In contrast to the complexity of isolated perfused organs, liver slices are relatively easy to prepare. This model retains tissue organization

and cell-cell and cell-matrix interactions and preserves the lobular structure of the liver as well (Hillesheim *et al*., 1995; Gandol *et al*., 1996); however, bile flow and portal flow cannot be analyzed. More importantly, poor diffusion of oxygen and nutrients cannot be fully solved. Although some of these problems have been improved due to the development of new slice model (Vickers, 1994), the short viability and the lack of bile collection are still unresolved.

The isolated hepatocyte model, however, is the most frequently used *in vitro* liver cell model (Acosta *et al*., 1985). Primary hepatocyte culture has been regarded as a golden standard in the study of drug metabolism and has been used to give predictive information on the pharmacokinetics of potential drug molecules (Butterworth *et al*., 1989; Guillouzo *et al*., 1993). Although the traditional monoculture rapidly loses the hepatocyte function, great progress has been made in terms of the methodology of liver cell cultures over the last few years. A variety of culture techniques for long-term *in vitro* culture have been established and evaluated. For example, poor preservation of native liver structure has been improved by introduction of three-dimensional spheroids formed by hepatocytes with non-parenchymal cells in specific basement membrane (Riccalton-Banks *et al*., 2003; Thomas *et al*., 2005, 2006); lack of exchange of oxygen and nutrients in static culture has been overcome by the novel bioreactor system (Morsiani *et al*., 2002; Van de Kerkhove *et al*., 2002). Therefore, well-differentiated hepatocytes in long-term culture would provide a major advantage in contrast to isolated perfused organ and liver slices for the metabolism and toxicology studies.

1.4 Approaches to engineering liver tissue

Although the liver has extraordinary regenerative capacity *in vivo*, creation of long-term viable and functional liver tissue *in vitro* has not been achieved yet. The central problem is the determination of the environmental signals necessary to maintain hepatocyte specific functions. In simple primary cultures, the characteristic morphology of hepatocytes changes within the first few days and hepatocyte-specific functions rapidly diminish after isolation (Bissell *et al*., 1987; Carr *et al*., 1986). Several approaches have been developed to recreate the microenvironment of hepatocytes, including soluble factors, cell-cell interaction and cell-matrix interaction. These are discussed below.

1.4.1 Medium supplementation and long-term hepatocyte culture

Many investigators have made significant advances toward the development of culture conditions which promote hepatocyte proliferation or preserve differentiated function of hepatocytes. Some of the most commonly used additives are described below.

(i) Growth factors and cytokines

Richman *et al.* first showed that epidermal growth factor (EGF) could induce DNA synthesis in primary hepatocytes in 1976. Interestingly, it is still the most commonly used polypeptide hormone for hepatocyte proliferation, since EGF can lead the hepatocytes to enter the cell cycle for two to three consecutive cycles, after DNA synthesis stops. TGF-α, which shares the same receptor as EGF, is also mitogenic for hepatocytes and may be a stronger mitogen than EGF (Brenner *et al*., 1989; Mead and Fausto, 1989). HGF, which is purified

from rat platelets, has the ability to promote hepatocyte proliferation as well. Together with EGF, they are two main growth factors widely used in hepatocyte medium. However, both of these mitogens are inhibited by TGF-β in hepatocyte culture (Carr *et al*., 1986). Other factors, such as soluble TGF-β, IL-1β, IL-6 (Nakamura *et al*., 1988) and hepatocytes growth inhibitor (HGI) (Huggett *et al*., 1987), are capable to inhibit EGF mitogenesis in the culture.

(ii) Nicotinamide

Nicotinamide can enhance the DNA repair synthesis of cultured hepatocytes caused by chemical carcinogens (Althaus *et al*., 1982) and stimulate proliferation of hepatocyes *in vitro* (Sato *et al*., 1999). Also, the presence of nicotinamide in cultured hepatocytes inhibits the loss of CYP activities (Paine *et al*., 1979) and mRNA expression of albumin (Inoue *et al*., 1989). The effects of nicotinamide on both proliferation and differentiation are probably due to the inhibitory effect on poly (ADP-ribose) polymerase activity, an enzyme which catalyses polymerization of the ADP-ribosyl moiety of NAD (Ueda and Hayaishi, 1985).

(iii) Amino acids

Amino acids mainly act as liver cell nutrients (Seglen and Solheim, 1978) and inhibitors of hepatic protein degradation (Schworer and Mortimore, 1979). Stimulation of protein synthesis by high concentration of amino acids could be further enhanced by the addition of insulin and glucocorticoid (Seglen *et al*., 1983). Also, amino acids could be considered as a growth trigger, since hepatic DNA synthesis is observed in the starved rat followed by an amino acid meal

(Bucher *et al*., 1978). In particular, proline is necessary to induce DNA synthesis of hepatocytes and 30μg/ml in the medium is enough for the induction of the maximum DNA synthesis of cultured hepatocytes (Nakamura *et al*., 1984; Houck and Michalopoulos, 1985). Other amino acids, such as arginine, also play a role in hepatocyte growth.

(iv) Insulin

In vivo, the liver receives a continuous supply of insulin from the islets of Langerhans, so it is not surprising to see insulin is crucial for hepatocyte attachment, survival, protein synthesis and many specific functions (lipid and carbohydrate metabolism) in *in vitro* cultures (Agius *et al*., 1990). In particular, the glycogen storage is directly affected by insulin depending on the glucose concentration (Agius and Peak, 1993).

(v) Dexamethasone

Dexamethasone is usually applied to enhance matrix gene transcription (fibronectin and collagen) (Jefferson *et al*., 1985), and to increase protein synthesis, including albumin. In addition, phenobarbital induced hepatocyte DNA synthesis is further enhanced by certain concentrations of dexamethasone. However, it inhibits hepatocyte spheroid formation (Abu-Absi *et al*., 2005) and suppresses CYP 1A2 induction at a concentration of 1 μM (Harada *et al*., 2003). Therefore, it may not be beneficial for long-term hepatocyte culture.

(vi) Trace metals

Trace metals are usually added into chemically defined medium for hepatocytes culture in a prolonged period, although no evidence has shown they could improve hepatocyte proliferation (Block *et al*., 1996; Cable and Isom, 1997). However, the presence of selenium in the hepatocye culture medium could maintain the synthesis of CYP induced by phenobarbital (Newman and Guzelian, 1982). In addition, copper, iron and zinc are all required in the hepatocyes long-term culture (Cable and Isom, 1997), since prolonged absence of these metals causes the activity of ribonucleotide reductase in leukaemic lymphocytes to be decreased (Oblender and Carpentieri, 1991a, 1991b).

(vii) Dimethyl sulphoxide (DMSO)

2% DMSO in the hepatocyte culture medium is considered as the most effective concentration in terms of cell morphology, proliferation and differentiation. Kojima *et al.* reported that typical cuboidal morphology, cell-cell adhesion structures, gap junctions and bile-canaliculus-like structure were observed in the presence of 2% DMSO in 1997. In addition, DNA synthesis of hepatocytes stopped after removal of DMSO from the medium (Cable and Isom, 1997), but the proliferation ability could be regained by the presence of DMSO and trace metals. Also, secretion of albumin and transferrin was recovered by adding 2% DMSO to the medium after hepatocyte proliferation *in vitro* (Mizuguchi *et al*., 1996).

1.4.2 Culture surface

The role of ECM in the control of development and differentiation of hepatocyte has been the subject of intense research for many years (Hay, 1981; Martin and Garbion, 1987). Numerous studies have demonstrated the importance of the extracellular matrix in the modulation of many aspects of cellular function including growth, adhesion, migration, differentiation and gene expression (Lee *et al*., 1993). The interactions between hepatocytes and ECM are complicated, which are involved in a variety of specific receptors. The significance of this relationship has been focused on by many researchers, who have attempted to restore the contact of hepatocytes with a range of culture surfaces to resemble the *in vivo* ECM.

1.4.2.1 ECM and liver derived surfaces

Several natural ECM proteins have been applied to liver tissue engineering, including type I collagen, type IV collagen, fibronectin and laminin, which are known to influence hepatocyte morphology and functions. In addition, liver derived biomatrix from rat, pig or human have been developed and compared with the natural ECM proteins in terms of hepatocyte morphology and function.

(i) Collagen, fibronectin and laminin

Collagen is the most abundant expressed protein in liver ECM and a variety of isoforms are distributed in different locations with distinct functions. Type I and type IV are the most common isoforms used as ECM in hepatocyte culture *in vitro*. Comparing to collagen, fibronectin and laminin contribute less to the

composition of liver ECM, but still are used widely as ECM for hepatocytes *in vitro*.

The morphology, proliferation, migration, growth and survival of hepatocytes are relatively diverse when cells are cultured on fibronectin, laminin or collagen coated surfaces. Hepatocytes cultured on these three ECM proteins show spread morphology and mostly maintain in a monolayer. However, if the amount of fibronectin, laminin or collagen is limited on coated dishes, the spherical morphology, which is more like *in vivo*, is exhibited (Mooney *et al*., 1992). Although the morphology of hepatocytes on these ECM proteins is quite similar, the responses to HGF are different. Cells are proved to undergo proliferation on the collagen type I and fibronectin coated surfaces by the stimulation of HGF, but no proliferation is shown from the cells on laminin (Schuppan *et al*., 1998). These different responses are dependent on the interaction between cells and ECMs, which is mainly mediated by integrin signalling, focal adhesion kinase (FAK) or extracellular-signal regulated kinase (ERK) (Giancotti and Ruoslahti, 1999; Hynes, 2002). In addition, the growth of stress fibres in hepatocytes cultured on these ECM proteins is dissimilar. The stress fibre is developed by hepatocytes on the collagen type I and fibronectin coated surfaces but not on the laminin coated surface (Kim *et al*., 2003; Hoshiba *et al*., 2006). Moreover, only laminin, particularly laminin-10/11, is demonstrated to enhance cell migration in hepatocyte culture *in vitro*. (Fujiwara *et al*., 2001; Gu *et al*., 2001) Furthermore, hepatocytes cultured on collagen type I are less protected from apoptosis than those cultured on

collagen type IV, fibronectin and laminin (Gomez-Lechon *et al*., 1995; Morita *et al*., 1995).

The CYP inductions on hepatocyte monolayers cultured on these ECM proteins are distinct to some extent. For example, CYP2B1/2B2 induction is poor in hepatocyte monolayers cultured on type I and IV collagen by phenobarbital. Also, the cells cultured on high concentration of laminin only display substantial induction (Caron, 1990; Brown *et al*., 1995), and the addition of soluble laminin to the media does not have any effects on the CYP induction by phenobarbital (Oda *et al*., 2008). On the contrary, cells cultured on low concentration of type I collagen and laminin exhibit greater CYP2B1/2B2, perhaps due to spherical morphology formation. (Oda *et al*., 2008)

(ii) Collagen sandwich & collagen-Matrigel sandwich

Hepatocytes cultured on substrata like collagen or fibronectin exhibit spreading morphology with nearly no polarized structure. Cells also show deteriorating differentiated function after a few days *in vitro*. However, this process can be modulated by overlay of another layer of collagen or Matrigel. Matrigel, extracted from Engelbreth-Holm-Swarm (EHS) mouse sarcomas, contains several ECM proteins, including 61% laminin, 30% collagen I, 7% entactin, as well as several growth factors (BD Matrigel). This double layer sandwich culture has been demonstrated to maintain hepatic polarity (Musat *et al*., 1993; LeCluyse *et al*., 1994) and long-term stable differentiated functions (Dunn *et al*., 1992; Berthiaume, *et al*., 1996). Therefore, it has been used for liver physiology studies (Liu *et al*., 1999; Turncliff *et al*., 2006), drug

metabolism/toxicity testing (Nussler *et al*., 2001; Kemp and Brouwer, 2004; Kemp *et al*., 2005) and hepatocyte-based bioreactors (LeCluyse *et al*., 1994; Allen *et al*., 2001).

Collagen sandwich configuration also has utility. Tuschl and Mueller reported that hepatocytes cultured in this sandwich culture with serum-free medium showed typically polygonal shaped cells with well-defined cell borders and plasma membrane over time. Also, the bile canaliculi-like network was relatively stable after 72 hours. More importantly, the CYP1A1 expression over time was much less reduced in the serum-free sandwich culture and the level of cellular stress was lower than the monolayer. (Tuschl and Mueller, 2006)

In addition to double layer of collagen culture, collagen-Matrigel sandwich has been used and applied widely to hepatocyte culture. Besides rat hepatocyte morphological and functional improvements in this culture configuration with low concentration of dexamethasone (Sidhu *et al*., 2004), the cultivation re-establishes and maintains CYP expression levels (Omiecinski *et al*., 1999) as well as enhances the gene induction response to phenobarbital (Sidhu *et al*., 2004). It has also been applied to human hepatocyte culture and demonstrated great achievements in cell morphology, exhibiting formation of cell-cell adhesion, bile canaliculi, microtubules and cytoskeletal elements (Hamilton *et al*., 2001; LeClyuse *et al*., 2001). The effect of Matrigel on CYP induction in human hepatocytes is less clear. LeCluyse *et al*. reported in 2000 that induction of CYP3A4 activity by rifampicin was not affected by overlay of Matrigel.

However, Gross-Steinmeyer *et al*. (2005) demonstrated that the same CYP was greatly induced by phenobarbital in the collagen-Matrigel sandwich. The disparity between the two groups could be explained by differences in media and the effects of different cell densities (Hamilton *et al*., 2001). The molecular mechanism of the maintained hepatocytes differentiation in the presence of Matrigel are most likely regulated by β-catenin (Monga *et al*., 2006) and /or integrin-linked kinase (ILK) (Gkretsi *et al*., 2007).

1.4.2.2 Non-ECM-derived surfaces

Synthetic ECMs, which mostly lead hepatocytes to a three-dimensional architecture, have been used widely in recent years due to their mechanical properties and processability (Gupta *et al*., 2002). Also, they replace several functions of natural ECM, for example, offering appropriate mechanical strength as well as providing the space to supply nutrients and oxygen (Putnam and Mooney, 1996). Two types of synthetic ECM are available, including synthetic polymer and natural polymer.

Biodegradable synthetic polymers, mostly including polyester and polycarbonate, have a long history of use as scaffolds in liver tissue engineering. The ability of changeable structure to meet mechanical properties requirements and the kinetics of biodegradation to suit various applications are the key advantages of these synthetic polymers. Polyglycolic acids (PGA) (Mooney *et al*., 1996; Lee *et al*., 2003), polylactic acid (PLA) (Riccalton-Banks *et al*., 2003; Thomas *et al*., 2005, 2006) and their copolymer (polylactic-glycolic acid, PLGA) (Hasirci *et al*., 2001; Li *et al*., 2006) have been applied *in*

vitro. Natural polymers including alginic acid (Yang *et al*., 2002), chitosan (Park *et al*., 2003), xyloglucan (XG) (Seo *et al*., 2004), silk sibroin (Gotoh *et al*., 2004) and gelatine (Hong *et al*., 2003) have also been used for liver tissue engineering.

In order to improve the cell attachment on poor adhesive polymer surfaces, a number of ECM-derived proteins or other bioactive components have been applied to coat polymers. The morphology and functions of hepatocytes are enhanced when cells are cultured on the polymer conjugated with ECMs. For example, Akon *et al*. (2005) reported that hepatocytes cultured on the membrane of polyvinyl alcohol (PVA) coated with ECM proteins showed higher albumin and urea secretion than cells on the membrane of polyvinyl alcohol-co-ethylamine (PVA-EA). Among all the ECMs, the viability of hepatocytes was higher on PVA coated with collagen than PVA coated with other ECM proteins, including laminin, fibronectin and vitronectin. (Akon *et al*., 2005) Also, hepatocytes cultured on gelatine with the presence of chondroitin sulphate and hyaluronic acid show higher viability and better functionalities comparing to those on gelatine scaffold without ECMs (Barbetta *et al*., 2008).

A few advantages of synthetic ECMs over conventional ECMs include no variation of ECM from batch to batch, no non-uniformity in the gel thickness and no transport barrier for nutrients or metabolite waste. Particularly, in the conventional sandwich culture system, the top ECM not only holds back transport of nutrients or waste but also sheds during culture. Some researchers

demonstrate that synthetic sandwich culture is better than conventional collagen sandwich culture. For example, hepatocytes in a sandwich between a porous Si3N4 membrane conjugated with galactose (top) and a polyethylene terephthalate (PET) film (bottom) show improved differentiated functions than those of cells in collagen sandwich (Zhang *et al*., 2008). Also, RGD-modified PET (top) / PET coated with galacose (bottom) synthetic sandwich show better cell-cell interaction and functions than conventional collagen sandwich (Du *et al*., 2008). Furthermore, hepatocytes forming spheroids in a three-dimensional PuraMatrix scaffold demonstrate higher CYPIA1 activity than cells in collagen sandwich throughout the culture period (Wang *et al*., 2008).

1.4.3 Co-cultures

1.4.3.1 Patterned co-culture

A limitation of random co-culture is the lack of controlling cell placement, cell-cell and cell-ECM interaction. Micropatterning technology has overcome this limitation, including photolithography (Ranucci *et al*., 2000), microfluidic channel (Ostuni *et al*., 2000), elastomeric membrane (Folch and Toner, 2000; Folch *et al*., 2000), microcontact printing (μCP) (Kumar and Whitesides, 1993; Xia and Whitesides, 1998) and layer-by-layer assembly technique (Decher, 1997). For example, a polyelectrolyte multilayer (PEM) template that is either resistant or adhesive to primary hepatocytes is prepared by coating poly (diallyldimethylammonium chloride) (PDAC) and sulfonated polystyrene (SPS) on the PEM surface. Hepatocyte co-cultured with NIH3T3 on this PDAC/SPS surface secretes higher albumin and urea than cells on the PEM surface alone. (Kidambi *et al*., 2007)

The success of this novel approach is dependent on the relative adhesiveness of two cell types to the substrates. The surfaces have been developed to switch from cell-repulsive to cell-adhesive by several mechanisms, including electroactive polymers (Jiang *et al*., 2003; Yeo *et al*., 2003), thermally responsive polymers (Yamato *et al*., 2002; Tsuda *et al*., 2005) and magnetic beads (Ito *et al*., 2004). However, these polymers or magnetic beads could be cytotoxic (Choksakulnimitr *et al*., 1995; Tiwari *et al*., 2003) and most of the patterned co-cultures are 2D, therefore, development of a biocompatible and 3D versatile micropatterning approach is of interest.

1.4.3.2 Co-culture with fibroblasts

Fibroblasts, derived from the mesenchyme, are involved in formation of the intercellular substance of the connective tissue and fibres and play an important role in the regeneration of the liver. Since human fibroblasts offer a better attachment and enhance cyclophosphamide metabolism for hepatocytes (Kligerman *et al.*, 1980), fibroblasts and their cell lines, such as NIH3T3, have been widely used for liver tissue engineering.

Although random 2D co-culture systems of these two cell types have been demonstrated to provide better hepatocyte functions comparing to hepatocyte culture alone (Washizu *et al*., 2001; Kang *et al*., 2004), 3D structure is required to rebuild the liver as it is *in vivo*. Novel techniques, such as 3D biodegradable scaffolds (Seo *et al*., 2006), 3D microencapsulation (Chia *et al*., 2005), and multilayer cell sheets technique (Ito *et al*., 2007) have been applied for co-culture of hepatocytes and 3T3. For example, magnetic forced based (MFB)

HepG2 monotypic cell sheet co-cultured with MFB NIH3T3 cell sheet and MFB HepG2 and NIH3T2 mixed cell double sheets are used to assess hepatocyte functions. The higher albumin in the mixed cell double sheets indicates more heterotypic cell contacts facilitate hepatocyte function. (Ito *et al*., 2007) Also, enhanced hepatocyte CYP activity is observed when cells are co-cultured with NIH3T3 in a 3D microcapsule formed with a hybrid matrix in the presence of soluble factor, TGF-β1 (Chia *et al*., 2005). In addition to the 3D environment, hepatocyte spheroids co-culture with NIH3T3 improves hepatocyte function by both homotypic and heterotypic cell-cell interaction (Lu *et al*., 2005; Fukuda *et al*., 2006). For example, albumin secretion and CYPIA1 enzyme activity are enhanced by spontaneous adhesion of NIH3T3 on the rat hepatocyte spheroids on the galactosylated poly (vinylidene difluoride) (PVDF) surface (Lu *et al*., 2005). In addition to NIH3T3, other fibroblasts, like 3T3-J2, have been shown to offer better hepatocyte functions (Cho *et al*., 2008).

1.4.3.3 Co-culture with sinusoidal endothelial cells

Compared with endothelial cells from many other tissues, liver SECs do not adapt well and are notoriously difficult to culture *in vitro*. Traditional culture methods could maintain the differentiation functions of SECs for only 48 hours. Although some improvements have been achieved to maintain the cells with media supplemented with tumour cell-conditioned media (Irving *et al*., 1984; Gatmaitan *et al*., 1996), phorbol ester (De Zanger *et al*., 1997), vascular endothelial growth factor (VEGF) (Yamane *et al*., 1994) or hepatocyte-conditioned media (Krause *et al*., 2000), SECs start to dedifferentiate after 5 or 6 days. Only recently, it has been reported that endothelial fenestrae could be

induced in M1-SEC cells or primary cultured SECs using anti-actin agents (Braet *et al*., 2007; Saito *et al*., 2007). More recently, co-culture of SECs with hepatocytes improves the survival and function of SECs for a longer period. For example, rat liver SECs co-cultured with hepatocytes in a 3D microreactor survive after 13 days with the indication of SECs specific marker SE-1 (Hwa *et al*., 2007). In addition, SECs co-cultured with hepatocytes on ECM substrates scaffold derived from liver maintain a near-normal fenestration as well as SECs differentiation (Sellaro *et al*., 2007).

Due to the extreme difficulty to culture *in vitro*, SECs have been hardly used for co-culture with hepatocytes for the purpose of enhancing hepatocyte functions. In the 1980s, random co-culture of rat hepatocytes with primary or cell line SECs was initially setup and demonstrated to maintain albumin secretion (Morin and Normand, 1986; Goulet *et al*., 1988). Since then, several culture techniques have been developed. For instance, biodegradable polymers have been applied to co-culture rat hepatocytes with SECs under flow conditions; however, there is no effect of SECs on survival rate and or hepatocyte function as compared to hepatocyte culture alone (Kaihara *et al*., 2000). Only recently, patterned co-culture has been applied to these two cell types because of the development of thermo-responsive culture dishes. Before this, no other parameters for patterned co-culture are suitable, since similar substrates are required for both hepatocytes and SECs. For example, poly (N-isopropylacrylamide) (PIPAAm) is utilized to achieve overlaying aortic endothelial cell sheets onto monolayer hepatocytes. Hepatocytes maintain the differentiated cell shape and express albumin for over 41 days of culture.

(Harimoto *et al*., 2002) In addition, rat hepatocytes and bovine endothelial cells are co-cultured on a dually patterned co-culture using the same polymer. Albumin secretion and ammonium metabolism are improved by the heterotypic cell-cell interaction. (Tsuda *et al*., 2006) The molecular mechanism underlying this co-culture is most likely regulated by the expression of α2-macroglobulin (Talamini *et al*., 1998) and gap junctional intercellular communication (Saito *et al*., 2007).

1.4.3.4 Co-culture with biliary epithelial cells

Biliary epithelial cells (BECs), which are involved both in the biliary ductular morphogenesis and in efficient regeneration of bile drainage system, has received less attention relative to hepatocytes. However, many studies have focussed on the relationship between BECs and hepatocytes. In 1980s, addition of BECs into hepatocyte cultures enhanced hepatocyte function by showing stable high level of albumin more than 2 months. Type III collagen secreted by BECs was regarded as the key to correlate with the long-term survival. (Clement *et al*., 1984) A few years later, liver-regulating protein (LRP) was found to be involved in maintenance of hepatocyte differentiation (Corlu *et al*., 1991) IL-6 was then showed to be secreted by BECs and had mitogenic and anti-apoptotic effects on hepatocytes. (Matsumoto *et al*., 1994; Sakamoto *et al*., 1999)

Since then, hepatocytes co-cultured with BECs have been demonstrated to maintain many differentiated liver functions and may provide a useful model for studying enzyme regulation. Hepatocyes are induced to undergo several

waves of division without loss of differentiation when cells co-culture with BECs in the presence of both TNF-α and HGF/EGF (Sérandour *et al*., 2005). In another study, albumin synthesis, urea production and CYP activities maintain over 3 three weeks when human hepatocytes are co-cultured with human BECs (Auth *et al*., 2005). In addition, the effects of phenobarbital and 3-methylcholanthrene on the expression of monooxygenase activities as well as mRNA levels in co-cultures of BECs and rat hepatocytes have been examined (Lerche *et al*., 1997). Direct and indirect effects of various hormones on glutathione S-transferases (GSTs), which play a role in the detoxification of xenobiotics or metabolites of xenobiotics by oxygenases, have been further investigated (Coecke *et al*., 2000).

1.4.3.5 Co-culture with Kupffer cells

In vivo, KCs have direct contact with hepatocytes through their cytoplasmic extension. Cellular communication between these two cell types is mainly considered to produce cytokines and excrete inflammatory mediators such as eicosanoids, nitric oxide, and reactive oxygen species (Decker, 1998). In particular, TNF-α, IL-1 and IL-6 have been regarded as early mediators for the hepatic inflammatory response. Biosynthesis of acute phase proteins and down regulation of xenobiotic metabolizing enzyme systems is mainly induced by these cytokines (Andus *et al*., 1988; Hartung *et al*., 1997). Hepatocyte structure is dramatically changed in co-culture with KCs and cortisol, low density lipoproteins (LDL) and lipolysaccharides (LPS). Ribosomes on the rough ER membrane, the volume of smooth ER and the number of lysosomes all increase due to KCs' derived pro-inflammatory cytokines (Panin *et al*., 2002). In

addition, KCs release pro-inflammatory cytokines such as IL-1, IL-6 and TNF-α, which are responsible for directly suppressing CYP3A activity (Abdel-Razzak *et al*., 1993; Muntane-Relat *et al*., 1995). For example, a 50-70% suppression of CYP3A activity dependent on the concentration of KCs was observed by Jeffrey *et al.* and KCs-mediated IL-2 is the key to alter CYP3A expression (Sunman *et al*., 2004). LPS-induced hepatic injury can be observed in the co-culture of hepatocytes and KCs with almost complete suppression of CYP3A activity by the extensive expression of TNF-α (Hoebe *et al*., 2001) mediated by reduction of AhR/Arnt (Wu *et al*., 2006). Therefore, the direct interaction between KCs and hepatocytes supports the extensive cytokines production but in turn suppresses hepatocyte function.

1.4.3.6 Co-culture with hepatic stellate cells

Due to the close interaction of HSCs with hepatocytes *in vivo*, HSCs are regarded as an ideal candidate for an *in vitro* co-culture component. They play a profound role in the pathogenesis of liver disease (Gressenger, 1998; Friedman, 2000) and, on a cellular level, are considered as the key in the development of liver fibrosis (Bedossa and Paradis, 2003). Many co-culture studies have been focused on the activation of HSCs (Nieto *et al*., 2001; Myung *et al*., 2006), deposition of ECM (Arthur, 2000; Bedossa and Paradis, 2003), or any other fibrogenesis related parameters (Nieto *et al*., 2002; Nieto and Cederbaum, 2003; Xu *et al*., 2005). For example, the activation of HSCs is regulated by activation of TGF-β through the induction of thrombospondin-1 by bile acids treatment in the co-culture of Huh-BAT and LX-2 cell lines (Myung *et al*., 2007). Also, an abundant extracellular matrix, including laminin,

fibronectin, and collagen proIII and IV is observed when hepatocytes are co-cultured with HSCs (Loreal *et al*., 1993). Moreover, MMP-13 mRNA is up-regulated and collagen type I is down-regulated when HSCs are co-cultured with hepatocytes (Schaefer *et al*., 2003).

In addition, HSCs contribute to both proliferation and differentiation of hepatocytes *in vitro*. Co-cultures with rat primary HSCs supports rat hepatocyte DNA synthesis by HSCs' derived factors, including HGF, extracellular sulphate (HS) and HS proteoglycan (Uyama *et al*., 2002). HSCs induce the expression of connexion 43, a gap junction protein, and lead to enhanced hepatocyte albumin mRNA expression (Rojkind *et al*., 1995). More importantly, 3D spheroids formed by co-culturing primary rat hepatocyes and HSCs on $P_{DL}LA$ coated surface, show enhanced albumin secretion and CYP activities (Riccalton-Banks *et al*., 2003; Thomas *et al*., 2005, 2006).

Besides primary HSCs, HSCs cell lines, such as spontaneous or genetically immortalized cell lines, have been applied to improve hepatocyte functions. For example, hepatocytes co-cultured on gene-transferring HSCs on CFSC/HGF feeder layers maintain higher viability, albumin and urea secretion than hepatocytes monoculture on collagen type I coated surface. c-Met, which is highly expressed in the co-culture system, is considered as the key to the enhanced function (Wang *et al*., 2005). Also, immortalized human hepatocytes NKNT-3 show increased CYP3A4 and CYP2C9 activity with increased urea synthesis co-cultured with TWNT-1 cell line, one of SSR#197-immortalized HSCs (Watanabe *et al*., 2003). However, not all the HSCs cell lines are

beneficial to hepatocyte function. For example, activated CFSC-2G HSCs cell line affects negatively the proliferation, functionality and ECM production of hepatocytes (Arnaud *et al*., 2003).

1.4.3.7 Co-culture with NPC fraction

A co-culture system involving only two cell types does not represent the complexity of cross regulation of all cell types *in vivo*. This is supported by successful co-culturing of hepatocytes and non-parenchymal cell (NPC) fraction *in vitro*. A special isolation method is used by Schmelzer *et al*. to get an approximately 20-30% NPCs fraction compared to only 1% NPCs from the conventional Percoll purification method. This co-culture in collagen sandwich shows the level of biotransformation of cyclosporine corresponding to the respective *in vivo* metabolism. (Schmelzer *et al*., 2006) Also, a method of co-culturing of rat hepatic parenchymal cells (PCs) and NPCs (stromal) in a 3D mesh has been developed (Naughton *et al.,* 1995). Fresh isolated PCs are cultured on pre-cultured stromal cells to show dioxin-inducible CYP activity for 56 days and albumin, fibrinogen, transferrin and fibronectin expression for 48 days. Ries *et al.* then demonstrate that HSCs and KCs are the prominent cell types of stromal cells after 8 days in a specific medium condition. Phosphoenolpyruvate carboxykinase activity and urea production are increased in this co-culture system for a long period. (Ries *et al*., 2000) The mechanism of the co-culture effect of stromal cells has been investigated by using a micromachined silicon substrate with moving parts. Cell direct contact for a limited time followed by soluble signal is required to maintain hepatocellular phenotype. (Hui and Bhatia, 2007)

1.4.4 Spheroids

Various types of 3D culture techniques in the liver tissue engineering have been developed including spheroid formation, biodegradable polymer scaffolds, sandwich culture configuration and microspheres (Brieva and Moghe, 2004). Among all of these methods, spheroids are the most commonly used method to form 3D cell constructs. The physiological state of hepatocytes is changed when they form spheroids, resulting in a series of changes in the morphology and function. In other words, hepatocytes in either homo-spheroids or hetero-spheroids display higher viability and exhibit higher level of liver-specific functions than monoculture of hepatocytes. This enhanced functionality of spheroids is probably due to the extensive cell-cell interaction as well as soluble factors in 3D structures. (Kim *et al*., 2001; Lu *et al*., 2003; Yin *et al*., 2003)

In particular, hetero-spheroids are of great interest due to the combination of the benefits of a 3D microenvironment and improved hetero-cell-cell interaction. Conventional preparation of spheroids requires a suitable culture substratum and a large surface area for initial attachment as well (Takezawa *et al*., 1992), which are the limitations for bio-artificial device development. However, suspension co-culture of self-organization hetero-spheroids has overcome these limits (Lee *et al*., 2004). For example, spheroids are formed by suspension co-culture of hepatocytes and rat prostate endothelial cell line (RPEn) in a spinner vessel and then sub-cultured in a Ca-alginate gel bead after 20 hours. Significantly higher albumin secretion and ammonia removal activities are observed in hetero-spheroids than those in homo-spheroids.

Similar to *in vivo* location of SECs and hepatocytes, RPEn cells are located on the surface of hetero-spheroids. (Lee *et al*., 2004) Also, hetero-spheroids developed by hepatocytes and whole NPCs fraction in the presence of Eudragit S100 on a untreated dish or spinner flask show higher albumin secretion, ammonia removal and CYP1A1 activity as well for over 4 weeks *in vitro*. NPCs are randomly distributed in the hetero-spheroids, either on the surface or inside the spheroids. (Yamada *et al*., 2001)

However, these above suspension hetero-spheroids do not favour the cell-ECM interaction. Lu *et al.* report a type of hetero-spheroids with not only higher degree of cell-cell interaction but also maintenance of cell-ECM interaction. Rat hepatocytes self-form into spheroids covered with NIH3T3 on the poly (vinylidene difluoride) (PVDF) surface. Albumin synthesis and CYPIA1 activity are maintained over 15 days and then decline afterwards due to detachment of spheroids because of over-confluence of NIH3T3. (Lu *et al*., 2005)

The size of the spheroids is critical due to the limited oxygen and nutrient supply in the centre of spheroids if they are bigger than 100 μm in diameter (Takabatake *et al*., 1991). Spheroids formed in the patterned co-culture could control the size, shape and space between them (Fukuda *et al*., 2006). For example, thousands of hetero-spheroids 100 μm in diameter are formed by bovine aortic endothelial cells and rat primary hepatocytes on micro-patterned surface with glass domains 100 μm in diameter and surrounded by 100 μm spacing of a-lactosyl-PEG/PLA. (Otsuka *et al*., 2004) In addition to patterned

co-culture, another novel method for rapid spheroid formation is reported by Okubo *et al*. They demonstrate mixed liver cells spheroids 60 μm in diameter could be developed using an isolation method without EGTA and calcium in 6 hours. The ultra-structure of these spheroids shows bile canaliculi, tight junctions and mitochondria, which is identical to *in vivo* liver tissue. (Okubo *et al*., 2002)

1.4.5 Bioreactor

Hepatocytes in conventional cultures do not operate under continuous perfusion conditions and, gradients and vectors for metabolite transfer are significantly altered, which is not corresponding to cells *in vivo*. However, the use of bioreactors for liver tissue engineering, which overcomes the limitations of conventional culture, has been considered as the most successful application to mimic liver *in vivo* situation.

Several critical engineering designs of bioreactor, including maximum of long-term hepatocyte specific functionality, ability of cell scale-up, minimum of preparation volume and elimination of transport limitations, should be considered. In terms of maintaining the long-term hepatocyte function, oxygen transport, which cannot be achieved well in the conventional culture, is one of the most vital parameters in the design of bioreactor due to high oxygen uptake of hepatocytes (Foy *et al*., 1994) and relative low efficiency of oxygen carrier (oxygen ECM). In addition to oxygen transport, shear stress induced by flow rate is another crucial factor to influence hepatocyte function (Kan *et al*, 2004),

since reduction of shear stress could allow higher medium flow rate in order to supply sufficient oxygen.

There are several different types of bioreactors, including hollow fibre bioreactors, monolayer bioreactors, perfused scaffolds and cell suspension. Hollow fibre technology can protect the cells from shear stress and provide a high number of cells in a small volume (Obermayer *et al*., 2001); monolayer bioreactor and perfused scaffold expose the cells under the medium flow induced shear stress, but 3D architecture, co-culture with NPCs or scale-up cell number could be easily achieved (Fiegel *et al*., 2006; Wen *et al*., 2008); suspension culture demonstrated poor cell viability but good transfer between plasma and hepatocytes (Doré and Legallais, 1999). In addition, radial flow bioreactor has recently been developed using stacked microfabricated grooved substrates instead of hollow fibre (Park *et al*., 2008). Co-culture of hepatocytes and 3T3-J2 is applied to the system and the albumin synthesis is about 250 $\mu g/10^6$ hepatocyes per day, which is higher than other bioreactors in development (De Bartolo *et al*., 2000). The success of this bioreactor is probably due to the reduction of shear stress by microgrooves to provide high medium flow with enough oxygen. The bioreactor is the basis for the extracorporeal liver assist device (ELAD) (Millis *et al*., 2002), HepatAssist (Stadlbauer and Jalan, 2007), modular extracorporeal liver support (MELS) (Sauer *et al*., 2003), Amsterdam Medical Centre (AMC)-BAL (Van de Kerkhove *et al*., 2002) and bio-artificial liver support system (BLSS) (Patzer *et al*., 2002).

1.4.6 Stem cells

Although liver cell transplantation (LCT) has emerged with some success to replace the gold standard treatment, orthotropic liver transplantation (OLT), for end-stage liver failure (Najimi and Sokal, 2005; Stephenne *et al*., 2006), it is still limited by the cell viability, tissue supply and engraftment techniques. The recent demonstration of stem cells' plasticity has led to the increasing interest in applying them in the tissue regenerative medicine (Verfaillie *et al.*, 2002). Some key theoretical advantages of stem cells include easy harvest, high level of proliferation, efficient *in vitro* transfection and potential autologous cell usage. However, many questions are still opened in this area and stem cell therapies need further development to become competitive. The morphology of stem cell-derived hepatocyte-like cell is rarely similar to that of the mature hepatocyte. Also, the functional characterization of stem cell-derived hepatocyte-like cells has not been standardized and normalized. More importantly, liver repopulation after stem cell transplantation *in vivo* remains limited. In this context, the development of several types of hepatic stem cells in liver tissue engineering is briefly described.

1.4.6.1 Fetal hepatic stem cells

The origin of the fetal hepatic stem cell has been a controversial topic. Hematopoietic cells were regarded as the major components in the fetal liver in early development (Lemmer *et al*., 1998; Zaret, 2000; Monga *et al*., 2001), but others suggest hepatic progenitor cells are an independent stem cell population (Nierhoff *et al*., 2005). In addition, the subject of markers is as controversial as the origin of the fetal hepatic stem cells. However, some potentially useful

markers have been identified in the fetal liver, including Thy-1 (Fiegel *et al*., 2003), CK18 (Fiegel *et al*., 2003) and c-kit (Fujio *et al*., 1994).

A few types of hepatic progenitors have been identified during fetal liver development. With the help of fluorescence activated cell sorting (FACS), liver hepatic progenitors are isolated, which display clonogenetic potential and have a bipotential differentiation to liver or biliary cells (Taniguchi, *et al*., 2000). Fetal liver epithelial cells are also identified (Sandhu *et al*., 2001). They are proved to have bipotential differentiation by forming both hepatocytes and cholangiocytes after transplanted into adult liver (Tateno *et al*., 1996).

1.4.6.2 Bone marrow derived stem cells

Petersen *et al.* first described that bone marrow cells transplanted into lethally irradiated mice could differentiate into liver stem cells or mature liver cells (hepatocytes) (Petersen *et al*., 1999). This observation has been confirmed in patients who receive a bone marrow transplantation or peripheral blood stem cell transplantation for haematological disorders (Korbling *et al*., 2002). Several *in vitro* data also demonstrate that certain types of bone marrow cells/stem cells could differentiate to hepatocytic cells in the presence of appropriate culture conditions (Fiegel *et al*., 2003; Kakinuma *et al*., 2003). Hematopoietic stem cells (HemSCs) were initially considered to be able to differentiate into hepatocytic cells when FACS-sorted mouse HemSCs showed liver-specific gene expression and function after transplantation into FAH-deficient mice (Lagasse *et al*., 2000). The potential differentiation ability of these HemSCs is further confirmed by the expression of albumin and CK genes

in cultured human CD34-positive HemSCs induced by HGF (Fiegel *et al*., 2003).

Besides HemSCs, the possibility of mesenchymal stem cells (MSCs) differentiated into hepatocytic cells is indicated by the fact that MSCs can express the liver specific marker, alpha-fetoprotein (AFP) and cytokeratin-18 (CK-18), produce albumin and urea as well as display CYP activity under certain conditions (Hong *et al*., 2005; Kang *et al*., 2005). Co-culture with other cell types has a strong influence on the induction of liver specific gene expression of MSCs. Adult rat liver cells used to co-culture with MSCs enhance the differential potential of MSCs (Lange *et al*., 2005). This co-culture influence is highlighted by the finding by Okumoto *et al.* that immune-selected bone marrow cells co-cultured with hepatocytes express HNF-1α and CK-8 in the presence of HGF and FBS (Okumoto *et al*., 2003). Fetal liver cells, however, cause a faster differentiation of MSCs in to hepatocytic cells compared to adult liver cells (Lange *et al*., 2006). Overall, MSCs have the characteristics to be highly proliferative *in vitro* and to display a large *in vitro* and *in vivo* differentiation potential.

1.4.6.3 Adult liver stem cells

Four main types of hepatic progenitors are described in this context, namely, oval cells, small hepatocytes, liver epithelial cells and mesenchymal-like cells. The activation of oval cells has been regarded as the most promising process to facilitate liver regeneration (Oh *et al*., 2002). Oval cells were observed by microscopy in experimental hepatic degeneration in 1961 (Grisham and

Hartroft, 1961) and they were small in size with a large nucleus-to cytoplasm ratio. In the rodents, they are believed to be potential liver progenitor cells and express immature markers (α-fetoprotein), mature hepatic markers (e.g. albumin) and biliary markers (e.g. cytokeratin-19) (Wang *et al*., 2003). The cells are responsible for liver regeneration after the treatment of 2-acetylaminofluorene (2-AFF) in the injury model (Alison *et al*., 1996). However, in the human, the concept of the bipotential oval cells is still controversial. OV-6-positive oval cells are analogous to those seen in rodent model and might be characterized as human liver progenitor, which could differentiate into OV-6-positive ductal cells or lobular hepatocytes in Heather's experiments (Crosby *et al*., 1998). In addition, the appearance of "ductular reactions", which is described as the proliferative response to several types of liver injury, has been considered as the most common evidence to support the existence of oval cells in human (Kiss *et al*., 2001).

1.5 Aims

The development of systems for the long term *in vitro* culture of functional liver tissue is a major research goal. The central limitation of experimental systems to date has been the early de-differentiation of primary hepatocytes in cultures. Rat primary hepatocytes and hepatic stellate cells have been isolated and co-cultured on Poly (*DL-lactic acid*) ($P_{DL}LA$) surface to form three-dimensional spheroids successfully (Riccalton-Banks *et al*., 2003; Thomas *et al*., 2005, 2006). It has been previously demonstrated that this co-culture model maintains tight cell-cell interaction and enhances long-term growth and hepatocyte specific functions. However, it is reported that not only cell-cell interaction but also cell-matrix interaction has great effects on hepatocyte morphology and functionality. Therefore, the aim of this project is to compare this model to other best available systems using collagen and/or Matrigel. It is hypothesised that this model can be further enhanced by the inclusion of extracellular matrix. We also wished to compare the function of the Fa2N-4 cell line to our primary cell models.

To test this hypothesis, the studies described in this thesis aim to:

- Apply and optimize common primary hepatocyte function assays
- Optimize cell density and culture conditions for co-culture of rat hepatocytes and hepatic stellate cells in collagen-Matrigel sandwich
- Compare the established 3D model to the co-culture of rat hepatocytes and hepatic stellate cells in collagen-Matrigel sandwich using albumin secretion, urea production and testosterone metabolism assays

- Use Mass spectrometry to confirm and extend our observations on CYP enzyme functions
- Establish the co-culture of human hepatocytes and hepatic stellate cells in 3D spheroids
- Compare CYP induction potential in the Fa2N-4 cell line via activity and mRNA endpoints for a range of prototypical compounds with known induction potential in primary human hepatocytes

Chapter Two:

Preliminary Study of Co-culture of Hepatocytes and Hepatic Stellate Cells (HSCs)

2.1 Introduction

2.1.1 Why use primary hepatocytes?

Primary cultured hepatocytes can be isolated from liver and maintained *in vitro* for a few days, where they retain their adult function and phenotype for a variable length of time. Primary cells have evident inherent advantages that make them the closest model to *in vivo* (Nagaki *et al*., 1995; Margarita *et al*., 2005). Good preservation of plasma membrane and active uptake/excretion mechanisms and metabolisms is similar to hepatocytes *in vivo* (Berthiaume *et al*., 1996; Jigorel *et al*., 2005). Also, maintenance of metabolism pathways (both phase I and phase II enzymes), physiological cofactor-enzyme levels and active gene expression remains well conserved for several days in culture (Gomez-lechon *et al*., 2003, 2004). Comparison of CYP expression in cultured hepatocytes with hepatic tissue demonstrates that the metabolic capabilities of primary cultured cells are comparable in important ways to those of intact liver (Martin-Aragon *et al*., 2001). However, common use of human hepatocytes is held back by the restricted access to human liver tissue and the limited proliferation abilities of the differentiated hepatocytes in *in vitro* culture. Therefore, other primary cells including rat, mouse, pig, as well as hepatic cell lines are used as alternative options in most laboratories.

2.1.2 The effects of seeding density on hepatocyte morphology and functionalities

Cell seeding is one of the key procedures in the construction of a long-term culture system that maintains several hepatic functionalities, and therefore a necessary component of a tissue-engineered bioartificial liver that can replace

liver functions in patients with severe liver insufficiency. Due to inability to proliferate under the usual culture conditions and rapid loss of cell viability after a few days *in vitro*, a variety of efficient culture techniques applied to achieve highly-maintained hepatic function by using proper seeding density is vital. Primary 3D culture of hepatocytes with non-parenchymal cells, which is considered as a highly stable long-term culture as well as a more physiologic environment, has to be achieved at the appropriate densities of both cell types. Rat hepatocytes (200,000 cells/cm^2) are co-cultured with NIH/3T3 mouse fibroblasts at the ratio of 1:1 to enhance hepatocyte functional maintenance (Lu *et al*., 2005), while in another research paper using the same two cell types, the densities are 1.1 $x10^5$ cells/cm^2 and 1.0 $x10^5$ cells/cm^2 respectively, but in a double-layer culture pattern (Nishikawa *et al*., 2008); When rat hepatocytes were co-cultured with primary rat HSCs at the ratio of 2:1 on a $P_{DL}LA$ coated 6-well plate, CYP450 functions were prolonged compared to monoculture (Riccalton-Banks *et al*., 2003; Thomas *et al*., 2005, 2006). Instead of primary HSCs, a HSC-T6 cell line co-cultured with rat hepatocytes on scaffolds in a perfusion bioreactor, at the same ratio as that of primary HSCs to hepatocytes, also achieved higher albumin, urea and CYP450 functions (Wen *et al*., 2008). These diverse systems illustrate the importance of using the right seeding density.

2.1.3 Assessments of hepatocyte function *in vitro*

2.1.3.1 7-ethoxyresorufin O-dealkylase (EROD) activity assay

The assay was adapted from an assay originally described by Burke and Mayer in 1974. It is mainly based on a CYP1A-catalysed O-dealkylation of 7-ethoxyresorufin (ER). The resorufin metabolite formed can be measured fluorometrically. The EROD assay is now a widely used indicator of hepatocyte functionality (Figure 2.1).

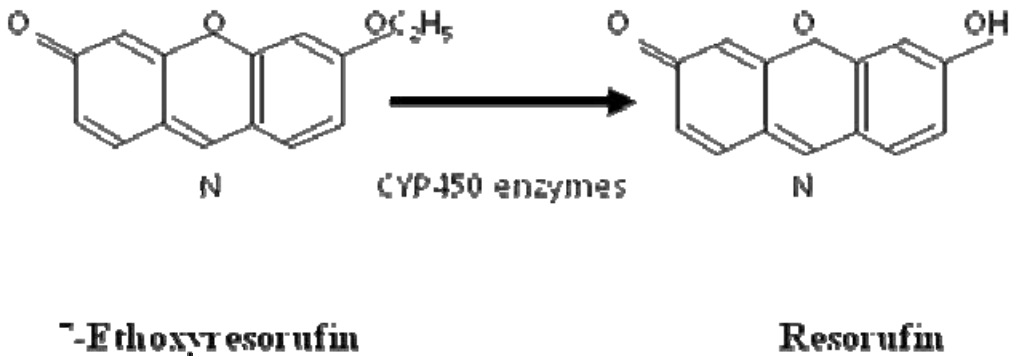

Figure 2.1: Chemical structure of the substrate 7-Ethoxyresorufin and the resulting fluorescent metabolite resorufin by CYP1A.

2.1.3.2 Testosterone metabolism assay

One of the major metabolic pathways in hepatocytes is cytochrome P450-dependent monooxygenase activity, which is assessed by testosterone metabolism (Donato *et al*., 1994; Thomas *et al*., 2005). The 6β-hydroxylation of testosterone is mainly catalysed by CYP3A1 and the oxidation of testosterone to 4-androstene-3, 17-dione is predominately mediated by CYP2B and CYP2C. High-performance liquid chromatography (HPLC) is applied to assess the CYP activities in this chapter. HPLC is a form of liquid chromatography to separate compounds which are dissolved in solution. Compounds are separated by injecting a plug of the sample mixture onto a column, which pass through it at different rates due to differences in their partitioning behaviour between the mobile liquid phase (solvent) and the stationary phase (column) (Figure 2.2).

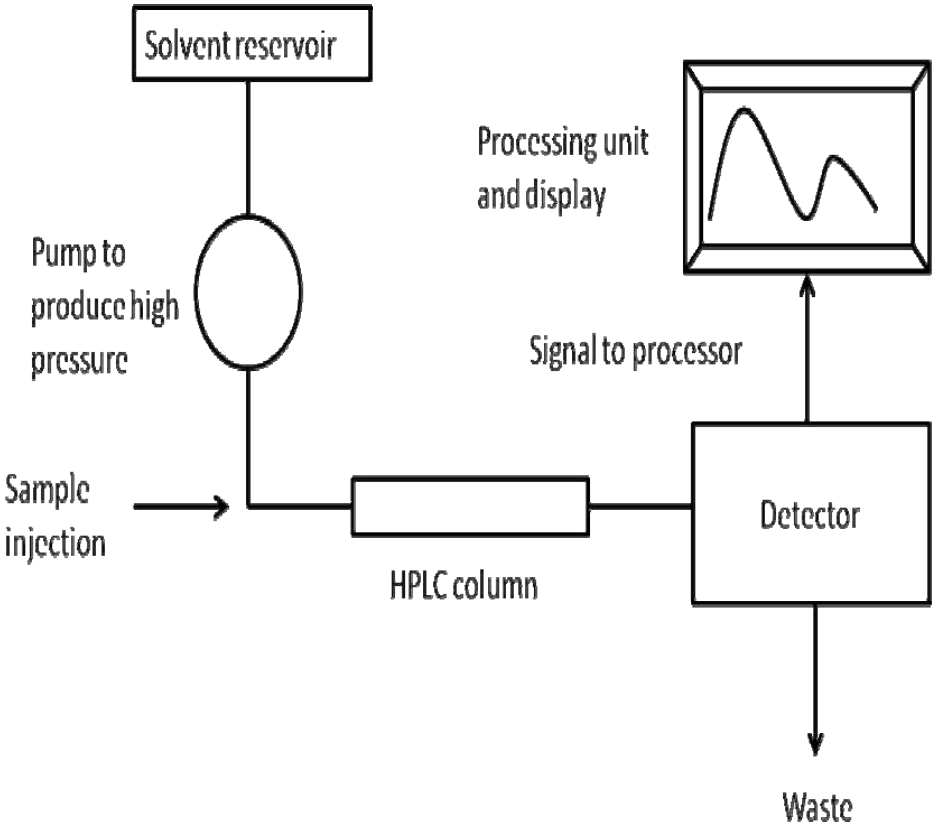

Figure 2.2: A flow scheme for HPLC. The pump provides a steady high pressure and can be programmed to vary the composition of the solvent. The liquid sample containing different material is injected and each material is separated through the different attraction between column and solvent. Each material travels in different retention time (the time taken for a particular compound to travel through the column to the detector) and each particular material can absorb UV light of specific wavelengths by the detector (UV absorption). Finally, the output is shown in the peak proportional to the amount of each material.

2.1.3.3 Albumin secretion assay

The amount of albumin was identified and measured by enzyme-linked immunosorbent assay (ELISA). Cell culture media, where albumin is secreted, are collected and transferred to a high protein-binding plate. An anti-rat albumin antibody conjugated with horseradish peroxidase (HPO) is then added to the plate. The HPO enzyme converts the o-phenylenediamine dihydrochloride (OPD) substrate to a detectable coloured product. The enzyme activity and albumin concentration can then be quantified by the colour change (Figure 2.3).

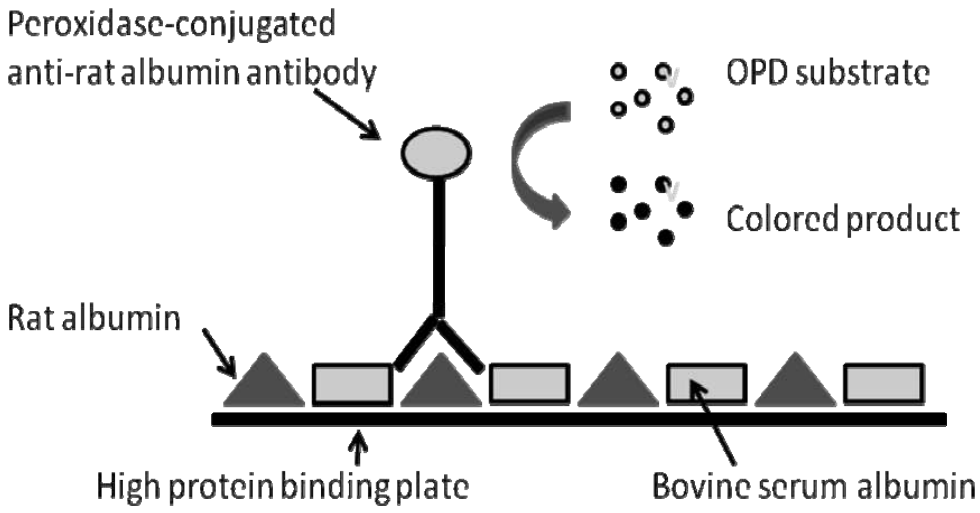

Figure 2.3: Schematic diagram of ELISA assay. An anti-rat albumin antibody conjugated with horseradish peroxidase (HPO) is bound to albumin from the medium in cell culture. The HPO enzyme converts the o-phenylenediamine dihydrochloride (OPD) substrate to a detectable coloured product.

2.1.3.4 Urea secretion

The QuantiChrom Urea assay kit (Centaur), which is an improved Jung's method (Jung *et al*., 1975), utilizes a chromogenic reagent that forms a coloured complex specifically with urea. The intensity of the colour, measured at 520 nm, is directly proportional to the urea concentration in the sample.

2.1.4 Aims

The preliminary studies described in this chapter were designed to confirm the method of isolation of primary rat hepatocytes and HSCs using a two-step collagenase perfusion method, followed by monoculture of hepatocytes and co-culture of hepatocytes with HSCs in different *in vitro* culture systems, especially in collagen- Matrigel sandwich configuration and on a $P_{DL}LA$ coated surface. Also, hepatic function assays including albumin secretion, urea secretion, EROD and testosterone metabolism applied to monoculture of hepatocytes were optimized. The chapter specifically aims to study:

- isolation of primary rat hepatocytes and HSCs;
- seeding density of hepatocytes in monoculture and co-culture; the ratio of hepatocytes and HSCs in co-culture;
- effects of Matrigel overlay on morphology of hepatocytes monoculture and co-culture; and
- effects of plate change on hepatic function assays: albumin secretion, urea secretion, EROD and testosterone metabolism.

2.2 Material and Methods

2.2.1 Animals

Male Wistar rats (Charles River, UK), weighing between 180-250 g were used. The animals were fed commercial food and tap water and were housed in small groups on soft wood bedding.

2.2.2 Chemicals

Bovine serum albumin (BSA), H_2SO_4, 2, 2, 2-trifluoroethanol (TFE), rat tail collagen type I and polyoxyethylene sorbitan monolaurate (Tween 20) were purchased from Sigma, UK. Crystals of polymer poly (DL-lactic acid) ($P_{DL}LA$) were from Alkermes Inc., USA. Matrigel was from BD Biosciences, UK. Methanol, ethanol and industrial methylated spirit (IMS) were from Fisher Chemicals, UK. Formal buffered saline (10% v/v) and Cryo-M-bed embedding compound were purchased from Bright, Huntington, UK. Rat Albumin ELISA Quantification Kit was from Bethyl Laboratories Inc., UK. QuantiChrom Urea Assay Kit was purchased from Gentaur, Belgium.

2.2.3 Plasticware

12-well tissue culture treated dishes and tissue culture flasks (75 cm^2) were bought from Nunclon, Denmark. 12-well collagen type I coated dishes were bought from BD Biosciences, UK. Costar 96-well flat bottom, non-treated, polystyrene assay plates and enzyme immunoassay high binding plates were purchased from Corning, USA.

(i) P_{DL}LA coating of culture plates

P_{DL}LA (Polyscience Inc) was dissolved in 2,2,2-Trifluoroethanol at a concentration of 1.5 mg/ml. 500 µl of P_{DL}LA solution was added to each 962 mm^2 nunclon dish. The dishes were placed in an oven at 70ºC for approximately 40 minutes to evaporate the solvent and then exposed under a sterilising UV lamp for 30 minutes before being stored at -20ºC.

2.2.4 Primary rat hepatocyte isolation

The hepatocyte isolation was based on the two-step collagenase perfusion method described by Seglen in 1976 using the apparatus shown in Figure 2.4A and 2.4B. A Millipore peristaltic pump was set at a flow rate at 20 ml/minute and the water bath was maintained at 40˚C during the perfusion so that the perfusion buffer temperature was approximately 37˚C when it reached the tissue. Hepatocytes were isolated from male Wistar rats (Section 2.2.1). After the rat was killed by cervical dislocation, the right and middle liver lobes were carefully removed and placed on the perfusion platform. The liver lobes were cannulated with a 1.5-inch, 21 gauge winged needle infusion set (Venisystem, UK) through a vein of an exposed cut surface on top of the Buchner funnel. In order to flush out the blood and to destroy cell-cell interaction, the lobes were perfused with chelating buffer (Appendix 1.5) for 10 minutes followed by a 20 minute perfusion with collagenase perfusate buffer (Appendix 1.6) to break down cell-extracellular matrix interaction. The lobes were then removed carefully and placed in a pertri dish containing hepatocyte complete medium (Appendix 1.8.1). The cells were released from the extracellular matrix of the tissue by breaking the capsule and agitating the tissue with sterile scissors and

forceps (Figure 2.4C). The tissue suspension was filtered through 64 μm sterile cotton gauze placed over a funnel into two 50 ml falcon tubes. The filtrate was centrifuged at 50 ×g for 5 minutes. The resulting pellets were resuspended in 10 ml hepatocyte complete medium diluted with the same amount of 90% percoll solution (Appendix 1.7) and centrifuged at 50 ×g for a further 5 minutes. All the viable hepatocytes were eventually harvested in the pellets. The supernatants from both spins were poured off and kept for the use of isolation of hepatic stellate cells.

The viable hepatocytes were resuspended in appropriate amount of hepatocyte complete medium and the viability of the cells was assessed using Trypan Blue exclusion. 100 μl of cell suspension and an identical amount of Trypan Blue solution were gently mixed together. The solution was placed on a 0.0025 mm^2 haemacytometer (Sigma, UK) covered with a slide. Under the examination of light microscope, the number of cells taking up the blue dye were counted and regarded as non-viable cells. The proportion of viable cells was calculated as a percentage of the total number of cells. A viability of at least 85% (viable cells/total cells) was considered necessary for experimental work.

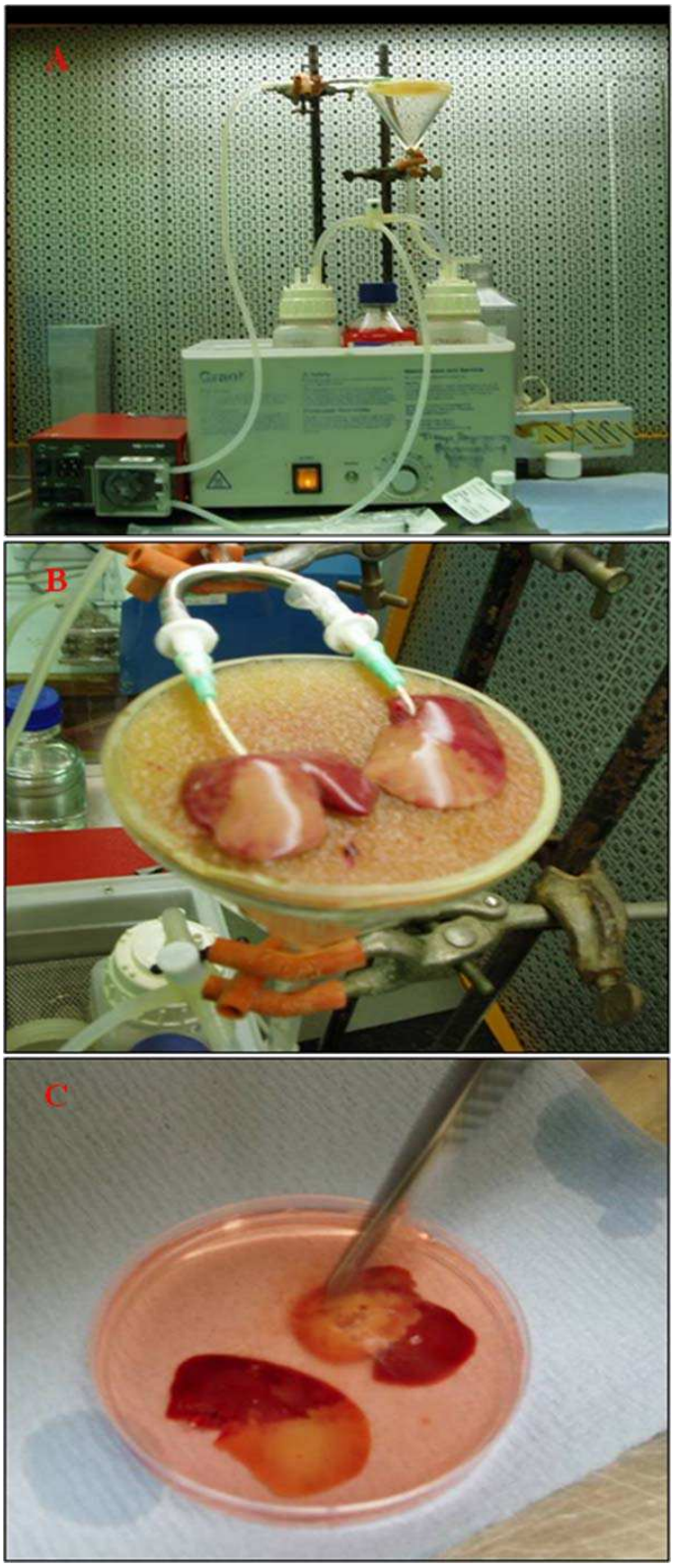

Figure 2.4: The setup for rat hepatocyte isolation (A); perfusion of the liver lobes with a 1.5-inch, 21 gauge winged needle infusion set (B); release of hepatocytes from tissue by mincing with forceps (C).

2.2.5 Primary rat hepatic stellate cell isolation

The supernatants from primary hepatocyte isolation were centrifuged at 50 × g for 5 minutes. The resulting pellets were discarded, and the preceding two steps repeated so as to get rid of the hepatocytes remaining in the supernatants. After that, the supernatant from the second spin was centrifuged at 250 × g for 10 minutes and the pellets, containing HSCs, were collected and re-suspended in the proper amount of HSCs medium (Appendix 1.8.3).

2.2.6 Culture conditions

Cell culture was carried out using aseptic techniques in a class II biosafety cabinet for primary rat hepatocytes and HSCs (Envair, UK). All cell cultures were maintained at 37˚C in a humidified atmosphere with 5% CO_2 / 95% O_2 in air.

(i) Cell culture: overlay with extracellular matrix - Matrigel

The stock Matrigel was thawed out slowly and fully by placing in slushy ice for 2 to 3 hours. The Matrigel was then diluted in ice-cold hepatocyte incomplete medium (Appendix 1.8.2) to give a final concentration at 0.25 mg/ml using an ice-cold pipette. The medium was removed from 12 well plates after the cells initial attachment, 2 hours for rat hepatocytes and 4 hours for human cells respectively. 1 ml of Matrigel-containing medium was added to each well using ice-cold pipette and the cells were returned to the incubator immediately. The cells were undisturbed until 24 hours. After this time, the Matrigel-free medium was replaced for subsequent experiments and treatments.

2.2.7 Functional analysis

2.2.7.1 Cytochrome P-450 enzyme activity assays

(i) 7-ethoxyresorufin O-dealkylase (EROD) activity assay

The mediums were aspirated and the cells were washed with PBS buffer before the assay was started. The required amount of Krebs buffer (Appendix 2.1.1) was created to wash the cells, which contained 10 μM dicoumarol (Appendix 2.1.3) and 5 μM substrate 7-ethoxyresorufin (Appendix 2.1.2), and the cells were incubated for 30 minutes at 37˚C, 5% CO_2 in air. No cells controls with Krebs buffer containing 10 μM dicoumarol and 5 μM substrate 7-ethoxyresorufin permitted assessment of cell independent substrate breakdown to resorufin. No substrate controls with Krebs buffer containing 10 μM dicoumarol only provided non-resorufin fluorescence. After incubation, 200 μl of the buffer was removed from each well and transferred to another 96-well plate in triplicate containing 40 μl of 1600 units/ml β-glucuronidase (Appendix 2.1.5) in 0.1 M sodium acetate buffer (Appendix 2.1.4). After that, the cells were washed with sterile PBS buffer, resuspended in fresh medium and then returned to the incubator at 37˚C, 5% CO_2 in air. The 96-well plates containing buffer with β-glucuronidase were incubated at 37˚C for a minimum of 2 hours before the reaction was terminated by adding 50 μl of 0.1 M sodium hydroxide to each well. Finally, fluorescence of samples was measured by using either a Hitachi F-4500 fluorescence spectrophotometer or a Bio-Tek FL600 plate reader at 530 nm excitation and 590 nm emission. The fluorescence readings from no cell controls were subtracted from the sample readings. A standard curve of resorufin (0-100 pmol/ml) was prepared in Krebs buffer (Appendix 2.1.6).

(ii) Testosterone metabolism assay

Analysis of testosterone metabolism by HPLC has been established by the Tissue Engineering Group, School of Pharmacy, University of Nottingham. Rat hepatocyte cultures were incubated at 37˚C for 1 hour with 1.5 ml EBSS, supplemented with 1 mM Ca^{2+} and 1 mM Mg^{2+}, containing 100 µM testosterone. The supernatant was centrifuged at 250 ×g for 5 minutes to remove cell debris and then analyzed using a Beckman high-performance liquid chromatography (HP 1090) fitted with a Zorbax 300 SB-C18 4.6 mm x 15 cm column at 50˚C. Mobile phase A (Appendix 2.3.1) and mobile phase B (Appendix 2.3.2) started at 15% B / 85% A and reached to 50% B / 50% A gradually over 10 minutes at a consistent speed of 1 ml/min. Sample injection volume was 40 µl and UV absorbance was detected at 245 nm with an integral diode array detector. The activities of CYP3A and CYP2B/2C were measured by the amount of 6β-hydroxytestosterone and 4-androstene-3, 17-dione metabolised by CYP3A and CYP2B/2C, respectively. The standard of 6β-hydroxytestosterone and 4-androstene-3, 17-dione were run intermittently as controls.

2.2.7.2 Urea secretion assay

At each day points the medium was removed from the wells and centrifuged at 13000 rpm for 5 minutes by using a MSE Microcentaur centrifuge. The supernatant was kept in 1.5 ml eppendorf tube and stored at -20˚C until needed. 5 µl of each sample was incubated with 100 µl reagent A mixed with the same volume of reagent B in a 96-well plate for 10 minutes at room temperature and read at 492 nm in a plate reader (Bio-Tek FL600).

2.2.7.3 Albumin secretion assay

The capture anti-rat albumin antibody (1 mg/ml) was diluted with coating buffer (Appendix 2.2.1) to the concentration of 10 µg/ml and 100 µl aliquots were added to each well of a 96-well high affinity binding plate. The plate was then incubated for 60 minutes at room temperature or kept at 4˚C overnight. After incubation, the captured antibody from each well was aspirated. The plates were then washed by wash solution (Appendix 2.2.2) three times followed by the addition of 200 µl of blocking solution (Appendix 2.2.3) to each well. The plate was then incubated for another 30 minutes at room temperature. After aspirating the block solution, the plate was washed three times as before. 100 µl of each sample, together with standards with appropriate dilutions (Appendix 2.2.6) by sample/conjugate diluents (Appendix 2.2.4), were transferred to each well and incubated for 60 minutes at room temperature. After that, the standards and samples were removed and washed as in the previous steps for five times. 100 µl of HRP conjugated antibody (1 mg/ml) (Appendix 2.2.7), diluted to the concentration of 25 ng/ml, was added to each well and covered with foil and incubated for 60 minutes at room temperature. After the incubation, the HRP conjugated antibody from each well was aspirated and the plates were then washed as in the previous steps for five times. Finally, 100 µl of TMB was added to each well and the reaction was terminated by adding 100 µl of 2 M H_2SO_4 (Appendix 2.2.5) after 10 minutes (with foil present at all times). The samples were read at 450 nm in the plate reader.

2.2.8 DNA content analysis HOECHST 33285

Cells were freeze-dried and stored at -70˚C until needed. Cells were washed with PBS buffer before 500 µl of papain solution (Appendix 2.4.7) was added to each well and incubated at 37˚C for 1 hour to lyse the cells. After that, 500 µl of working solution (Appendix 2.4.3) was added and mixed well with papain solution. 100 µl mixed solution was then transferred to a fresh 96-well plate. Finally, the cells were read at excitation 360 nm and emission 460 nm on a plate reader.

2.2.9 Rat hepatic stellate cells stain

2.2.9.1 Lipid staining

10% formalin solution (approximately 4% formaldehyde) was used to fix the HSCs for 5 minutes and then sterile distilled water was used to wash the cells. The cells were incubated with oil red O staining solution (Appendix 2.5.2) for 10 to 15 minutes at room temperature and then washed with sterile distilled water before examination by light microscopy. Lipid droplets were visible as pink/red vesicles. Other techniques, such as immunocytochemistry for desmin and glial fibrillary acidic protein (GFAP), will also be used in future within the Tissue Engineering Group, School of Pharmacy, University of Nottingham.

2.2.10 Experimental design and data analysis

In order to optimize the hepatocyte specific function assays, including albumin secretion, urea secretion, EROD and testosterone metabolism, and to assess whether hepatocyte functions are effected by the repeated assays, hepatocyte monolayers were cultured on collagen type I coated 12-well plates at the

density of 500, 000 per well. The medium was changed every 24 hours and replaced by fresh medium. Hepatocyte functions were assessed on seven day points, namely day 1, 3, 5, 7, 9, 11, 14 and 21. The assays were applied to the same plate on seven day points (one plate), to seven different plates on each day point (daily plate), or to four different plates on every two day points (every two day plate). Each hepatocyte function assay was carried out three times in duplicate on 12 well plates. Duplicates were averaged to create independent data points for statistical analysis. Data was analysed using one way ANOVA for differences in three different ways of applying hepatocyte function assays. Post tests with Tukeys error control were conducted to identify these differences. All data analysis was done in Excel and Prism. Graphs show mean values ± the standard error of the mean.

Testosterone metabolism CYP activities are expressed as percentage of initial activity, not per mg protein, while both albumin and urea secretion assays were normalized to mg/ml/24 hours on 12 well plates by the assumption that the number of hepatocytes on monoculture was 500,000 through the whole culture period.

2.3 Results

2.3.1 Morphology

The first objective of the study was to determine the optimum seeding density for hepatocytes in monoculture and to then assess the impact of Matrigel overlay on hepatocyte morphology in monocultures and co-cultures. All the following experiments have been repeated at least three times.

2.3.1.1 Rat hepatocyte seeding density on 12 well collagen type I coated plates

Rat hepatocytes were obtained as described previously (Section 2.2.4) and were plated onto 12 well collagen type I coated plates at a density of 500,000 to 700,000 cells per well in the complete medium for two hours initial attachment. The floating cells were then removed and the remaining cells were washed and cultured in the incomplete medium. Figure 2.5 shows the morphology of hepatocytes in different densities on 12 well collagen type I coated plates by light microscope.

An assessment of the ratio of well coverage to the numbers of floating cells (Figure 2.5) indicated that high seeding densities led to excess cell death. Cultures at seeding densities of 500,000 and 550,000 appeared healthier and these cultures were examined after 48 and 72 hours (Figure 2.6). The hepatocytes cultured at both these densities showed more than 80% confluence after 48 hours, however, less viable cells were observed when the hepatocytes were cultured at the density of 550,000 after 72 hours. Therefore, rat hepatocytes cultured at 500,000 per well would be used in the future study.

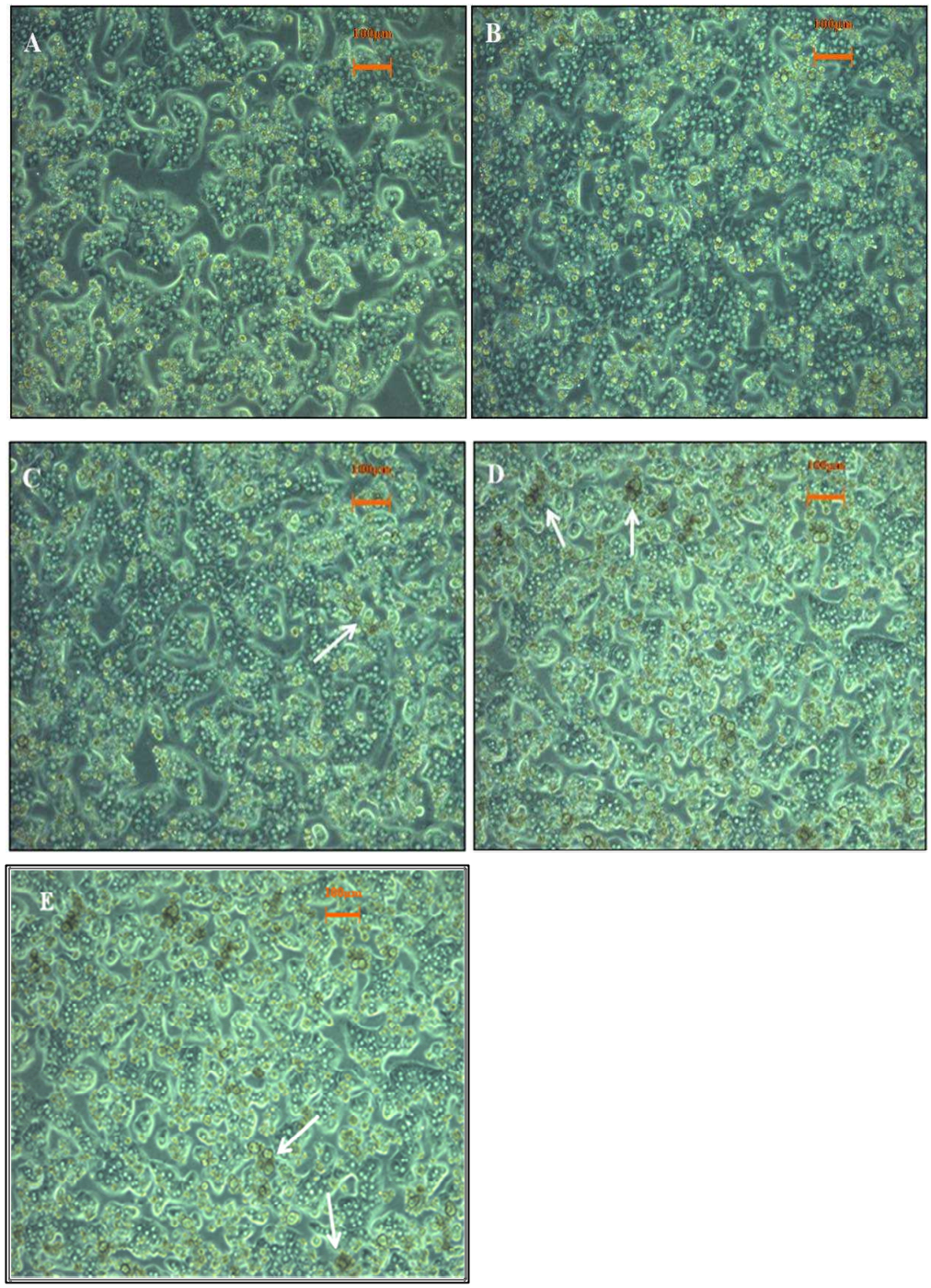

Figure 2.5: Phase contrast microscope images of rat hepatocyte cultures on 12-well collagen type I coated plates after 24 hours. Images A to E show rat hepatocytes at the density of 500,000, 550,000, 600,000, 650,000 and 700,000 cells per well respectively. Floating (dead) cells are shown by white arrows. There are less of these in Image A and B.

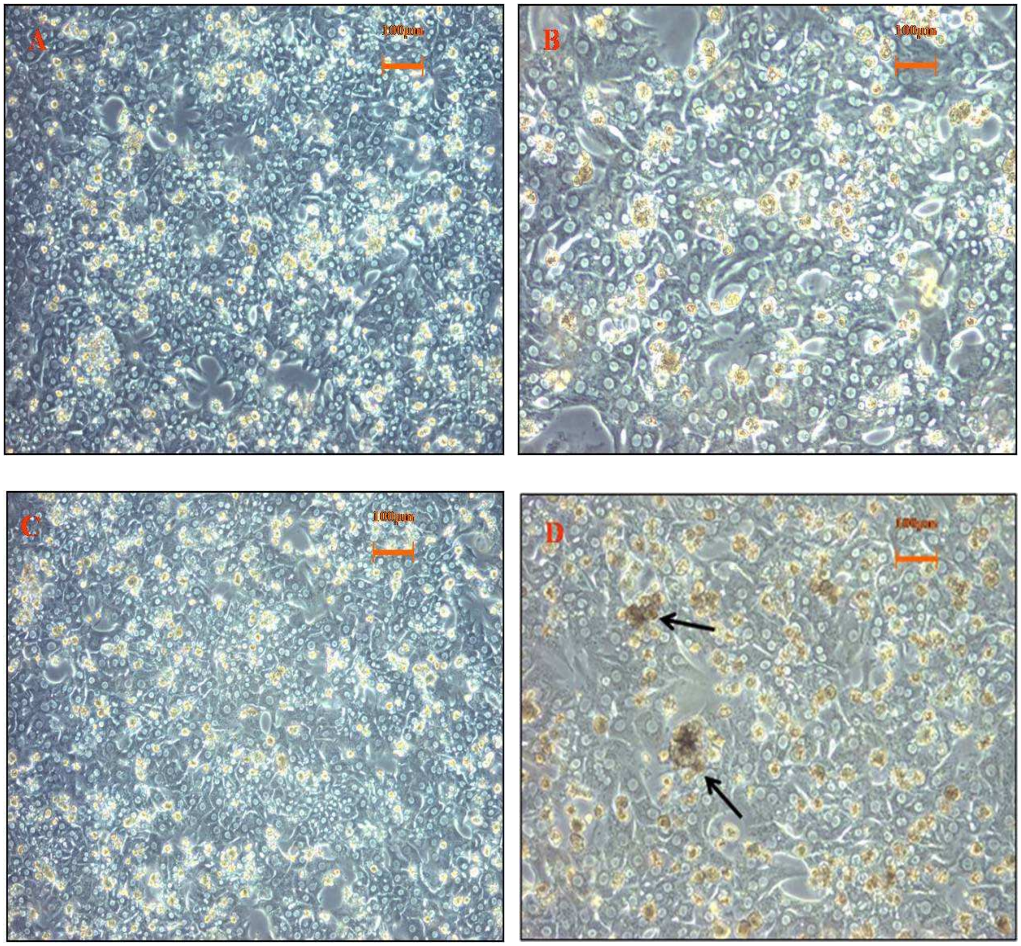

Figure 2.6: Phase contrast microscope images of rat hepatocyte cultures on 12-well collagen type I coated plates after 48 and 72 hours, respectively. Images A and B are hepatocytes at a density of 500,000 cells per well after 48 and 72 hours, respectively. Images C and D are hepatocytes at the density of 550,000 cells per well after 48 and 72 hours, respectively. Floating (dead) cells are shown by black arrows. There are more of these in Image D than Image B.

2.3.1.2 Impact of Matrigel overlay

Rat hepatocytes were cultured on a 12 well collagen type I coated plate at the density of 500,000 per well. After 2 hours initial attachment, Matrigel was overlaid on the top of the cells described previously (Section 2.2.6). The cells without overlaying Matrigel were used as controls. Figure 2.7 shows morphology of hepatocytes in the collagen-Matrigel sandwich configuration.

After 24 hours of isolation, rat hepatocytes in the collagen-Matrigel sandwich configuration reached approximately 90% confluence and cells retained hepatocyte characteristic morphology (well-defined cell borders, distinct nuclei and bile canaliculi-like structure) after 48 hours, while the cells without Matrigel overlay showed less confluence after 24 hours and started to spread and lose cuboidal shape after 48 hours. Therefore, Matrigel overlay had great effects on the confluence and morphology of rat hepatocytes.

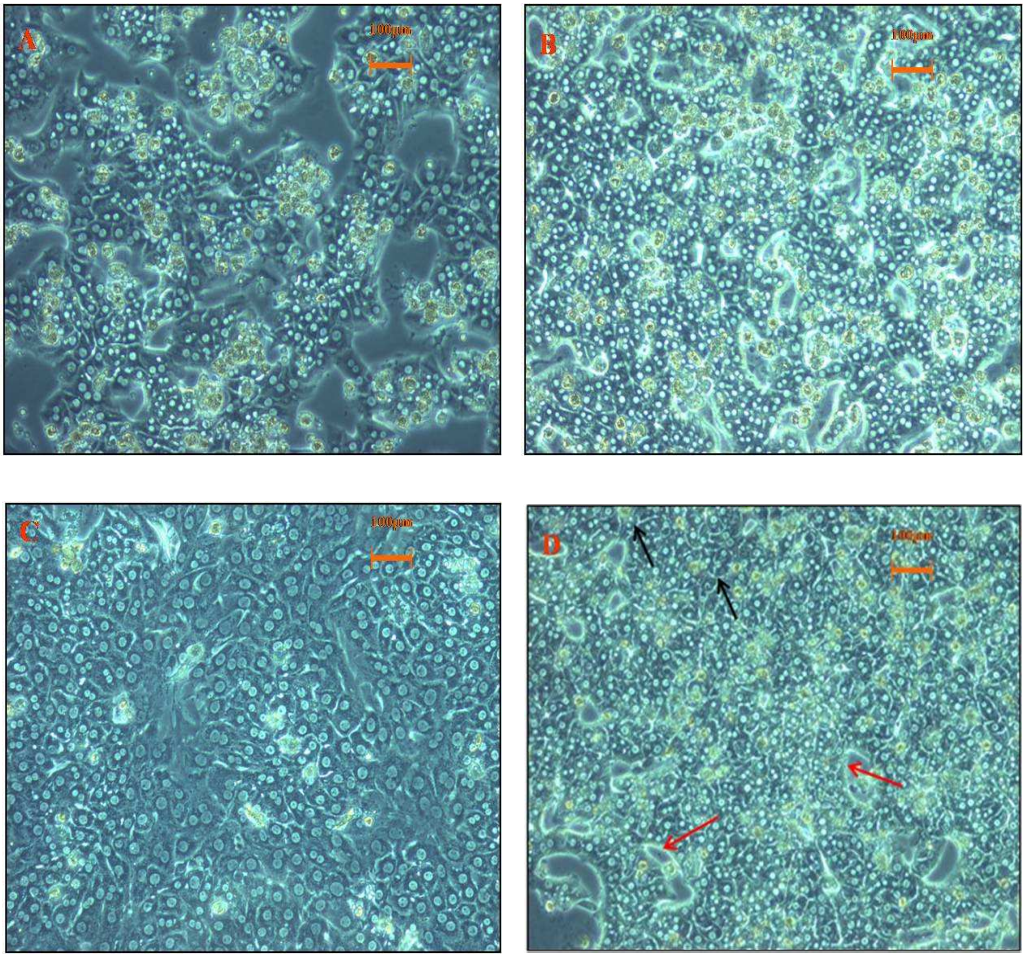

Figure 2.7: The morphology of hepatocytes after 24 and 48 hours of isolation. Images A and C are hepatocytes cultured on the collagen type I coated plates after 24 and 48 hours, respectively. Cells are spread out and lose the cuboidal shape in Image C. Images B and D are hepatocytes cultured in the collagen-Matrigel sandwich configuration after 24 and 48 hours respectively. Distinct cell borders (black arrows) and bile-canaliculi-like structures (red arrows) are shown in Image D.

2.3.1.3 Co-culture of hepatocytes with HSCs in the collagen-Matrigel sandwich configuration and P_{DL}LA coated surface

Rat hepatocytes and HSCs were isolated as described previously (Section 2.2.4 and 2.2.5). Co-culture of hepatocytes and HSCs at the ratio of 2:1 in total number of 500,000 was cultured in collagen-Matrigel sandwich and P_{DL}LA coated surface. The medium for the cells in sandwich configuration were used as described previously (Section 2.3.1.1).

For the cells on P_{DL}LA surface, incomplete medium was used all the time and the medium was not changed until the formation of 3D spheroids. The morphology of co-culture of hepatocytes and HSCs in collagen-Matrigel sandwich was showed in Figure 2.8A and 2.8B. Three-dimensional self-organizing spheroids were formed on the P_{DL}LA surface plates (Figure 2.8D).

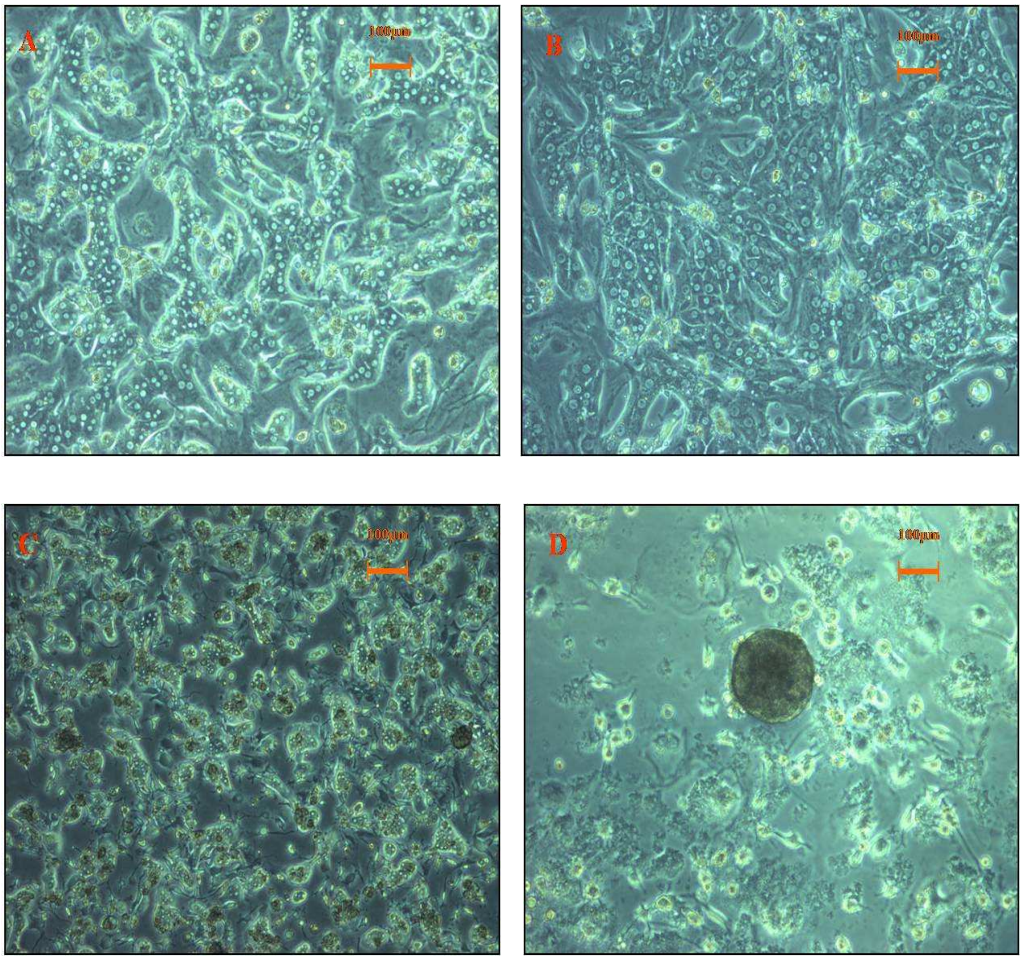

Figure 2.8: Co-culture of hepatocytes and HSCs in collagen-Matrigel sandwich after 24 and 48 hours, respectively (Image A and B), on PLA surface after 24 hour and 72 hours, respectively (Image C and D). A spheroid is shown in Image D.

2.3.2 Function analysis

The experiments presented in Section 2.3.1 provide a basis for comparing the function of hepatocytes maintained as either monocultures or co-cultures in collagen/Matrigel overlays and as 3D co-cultures within spheroids. In order to ensure that functional assays were working consistently and in optimal conditions, the effects of repeated assays on hepatocyte functions were first examined.

Rat hepatocytes were consistently isolated at >85% viability and cultured on collagen I coating plate. The effects of different protocols for assay application were examined in terms of albumin secretion assay, urea secretion assay, EROD assay and testosterone metabolism. Data from all four assays are shown in Figures 2.9, 2.10, 2.11 and in Table 2.1. The medium from all plates was changed every day at the similar time point. Old medium was used for albumin and urea secretion assays, and then it was replaced by the fresh medium. Three different ways of assay application were used to assess the effects of repeated assay application on hepatocyte function. Assays were only applied on one plate during the whole period of experiment, or assays were applied on different plate for every single day point, or assays were applied on the same plate only for two day points.

2.3.2.1 Albumin secretion

Albumin levels in the medium were measured by sandwich ELISA. Cultures were assayed 24 hours (day 1) after cell seeding and then on days 2, 3, 4, 5, 7, 9, 11, 14 and 21 days of culture. The method for this procedure was described in Section 2.2.7.3

The amount of albumin secreted was calculated from the standard curve of known rat albumin concentrations by Prism software (Figure 2.9A). The amount of albumin reached the peak on day 1 and afterwards, the amount decreased dramatically. No albumin could be detected after day 7. Also, no obvious difference of amount of albumin could be assessed from three different methods of changing plates (Figure 2.9B).

A)

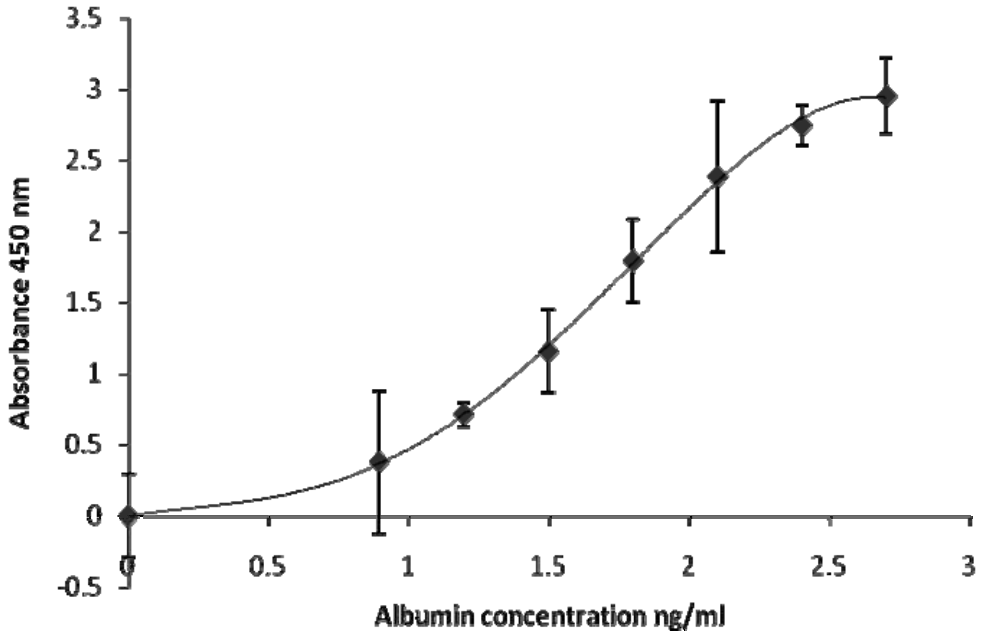

B)

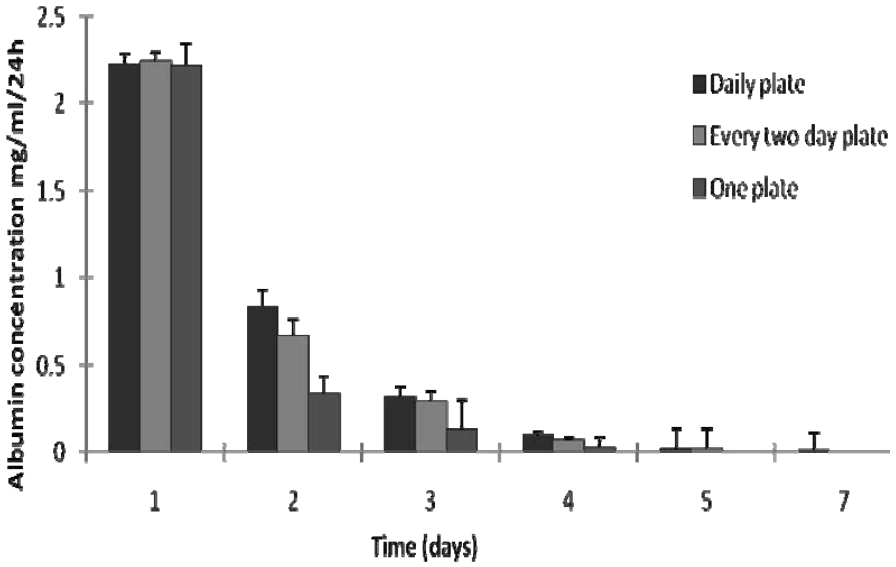

Figure 2.9: A representative albumin standard curve (A), albumin secretion per ml of medium of hepatocyte cultures over 7 days in a 24-hour period (B). Medium were changed every 24 hours. The assays were applied to the same plate on six day points (one plate), to six different plates on each day point (daily plate), or to three different plates on every two day points (every two day plate) (n=3, error bars indicate ±SD)

2.3.2.2 Urea secretion

Urea levels in the medium after 24 hours of cultures were measured by quantitative colorimetric determination at 520 nm. Cultures were assayed the same way as described in Section 2.3.2.1. The method was introduced in Section 2.2.7.2.

The amount of secreted urea was calculated from the standard curve of known urea concentration by Microsoft Excel (Figure 2.10A). The amount of urea kept at a similar level from day 1 to day 9, although the peak was on day 1, indicating that the ability of primary cells to secrete urea may require less hepatocyte specific differentiation than the secretion of albumin (Figure 2.10B).

No urea was detected on day 7 and 9 from the plates that were changed every two-day points and no amount was detected on day 9 from the plates that were not changed at all. The possible reason to explain this phenomenon might be the internal error of plating rat hepatocytes on different wells. Except day 7 and 9, there was no major difference in the amount of secreted urea between different plates.

A)

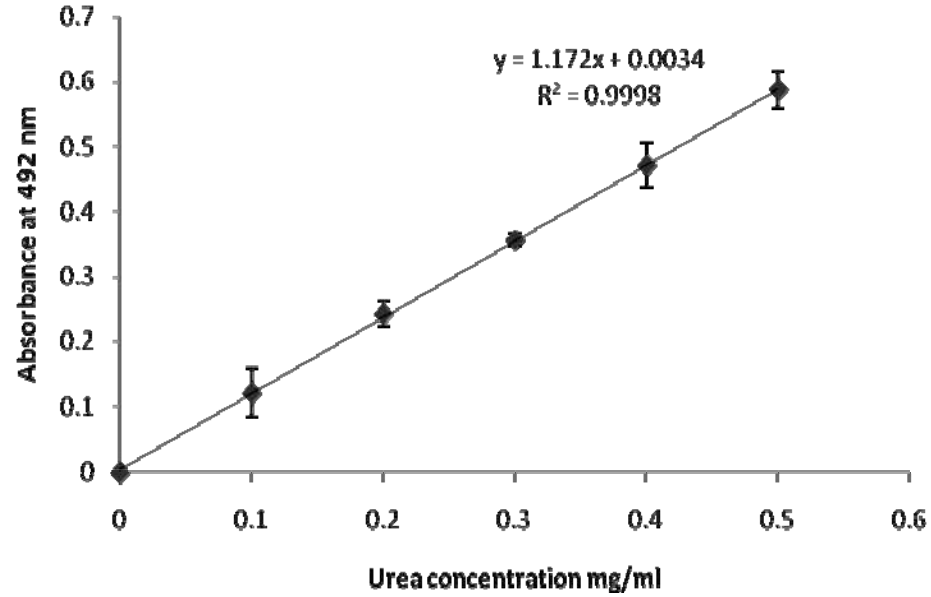

B)

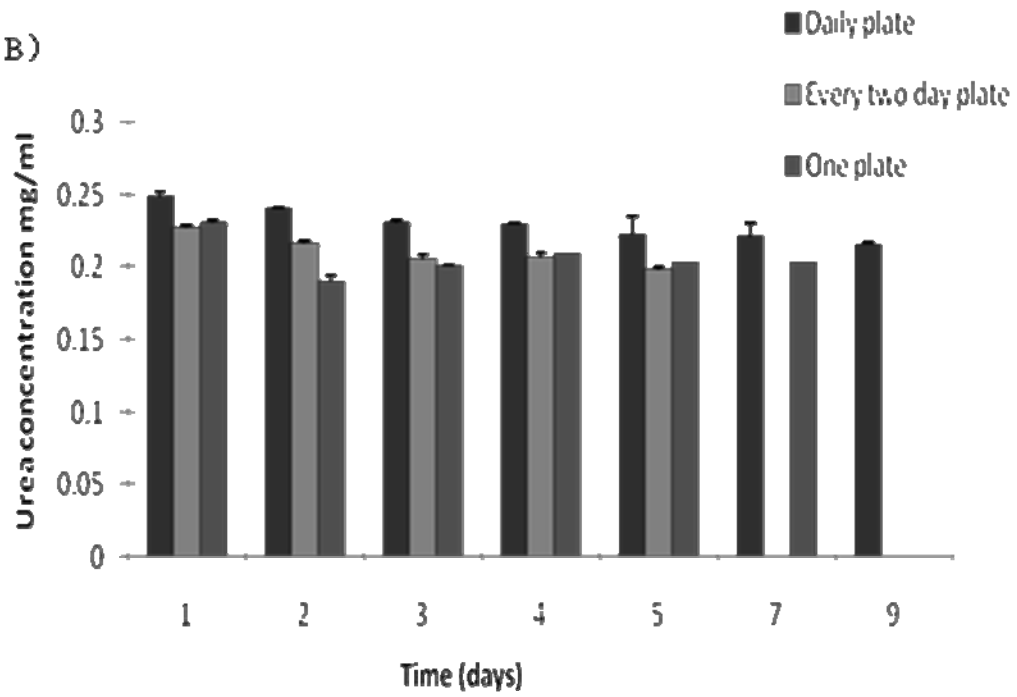

Figure 2.10: A representative urea standard curve (A), urea secretion per ml of medium of hepatocyte cultures over 9 days in a 24-hour period (B). Medium were changed every 24 hours. The assays were applied to the same plate on seven day points (one plate), to seven different plates on each day point (daily plate), or to four different plates on every two day points (every two day plate) (n=3, error bars indicate ±SD)

2.3.2.3 EROD assay

CYP-450 mono-oxygenase activity was assessed *via* an EROD assay (Section 2.2.7.1 (i)). Cultures were assessed 2 hours after cell seeding and then after 1, 2, 3, 4, 5, 7, 9, 11, 14 and 21 days of culture. The amount of ethoxyresorufin (ER) converted by the hepatocytes was calculated from a standard curve, measuring the fluorescence of various concentrations of resorufin in solution (Figure 2.11A).

The CYP-450 mono-oxygenase activity of rat hepatocytes in monoculture reached its highest value at day 2 and decreased sharply on day 3. After that, the activity remained relatively constant at between 4 and 7 pmol resorufin/ml until 7 days after seeding. No apparent difference of amount of resorufin was detected from different plates (Figure 2.11B).

A)

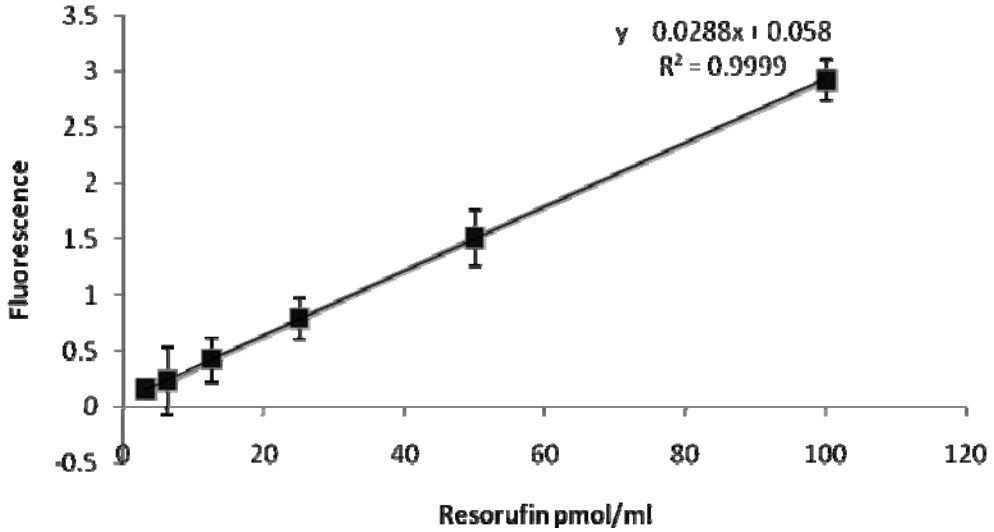

B)

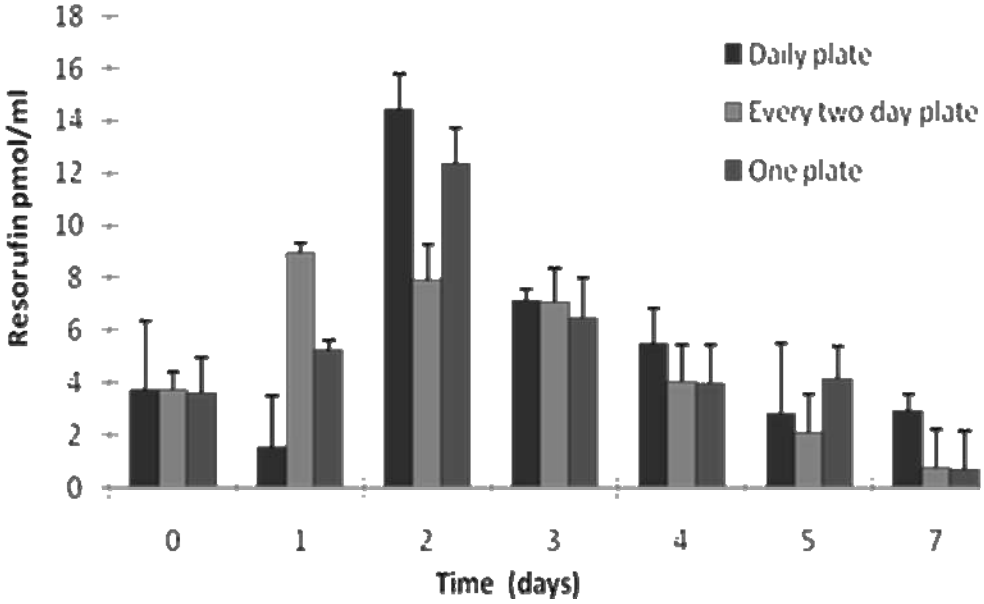

Figure 2.11: A representative resorufin standard curve (A), the CYP-450 monooxygenase activity of rat hepatocytes (B). Medium were changed every 24 hours. The assays were applied to the same plate on seven day points (one plate), to seven different plates on each day point (daily plate), or to four different plates on every two day points (every two day plate) (n=3, error bars indicate ±SD)

2.3.2.4 Testosterone metabolism

Function of CYP-450 enzymes in the culture system was further assessed by hydroxylation of testosterone. The method, which was run by HPLC, was shown in Section 2.2.7.1 (ii). Both 6β-hydroxylation of testosterone and the oxidation of testosterone to 6β-hydroxytestosterone and 4-androstene-3, 17-dione respectively was assessed at 1, 2, 3, 4, 5, 7, 9, 11, 14 and 21 days of culture. In rats, 6β-hydroxylation of testosterone was mediated by CYP3A1 and oxidation of testosterone was mediated mainly by CYP2B1 with minor contribution by 2C11and 2B2.

No 6β-hydroxylation of testosterone was detected during the whole experiment, while the oxidation of testosterone to 4-androstene-3, 17-dione only remained on day 1 (Figure 2.12).

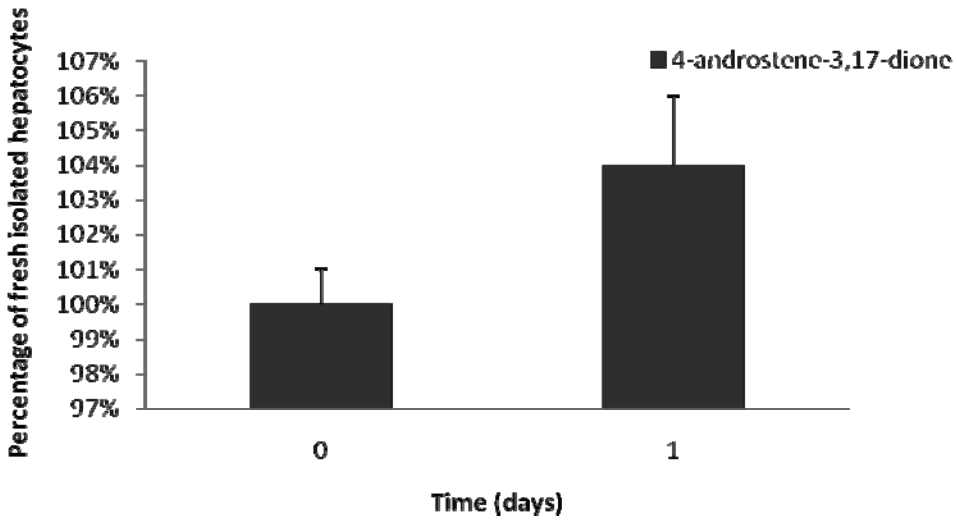

Figure 2.12: The oxidation of testosterone to 4-androstene-3, 17-dione of rat primary hepatocytes by CYP2B on day 0 (straight after isolation) and day 1. Medium is changed every 24 hours. (n=3, error bars indicate ±SD)

2.3.3 DNA content analysis Hoechst 33258

A cell number standard curve was prepared by a series of number of cells, namely 0.125, 0.25, 0.5, 1, 2, 4, and 8 million cells. Each of them was incubated in 2 ml papain solution (Appendix 2.4.7) at 60˚C overnight. After cells were washed with PBS buffer, the same amount of HOECHST 33285 working solution (Appendix 2.4.3) was added in each solution. 100 µl mixed solution was then transferred to a fresh 96-well plate. Finally, the cells were read at excitation 360 nm and emission 460 nm on a plate reader.

A DNA standard curve was prepared by stock DNA (sodium salt from salmon testes, Sigma, UK) at the concentration of 0, 0.5, 1, 1.5, 2, 3, 4, 5, 10, 15 and 20 µg/ml in papin buffer (Appendix 2.4.6). The same amount of HOECHST 33285 working solution was mixed with each DNA solution before read on the plate reader in the above condition.

A)

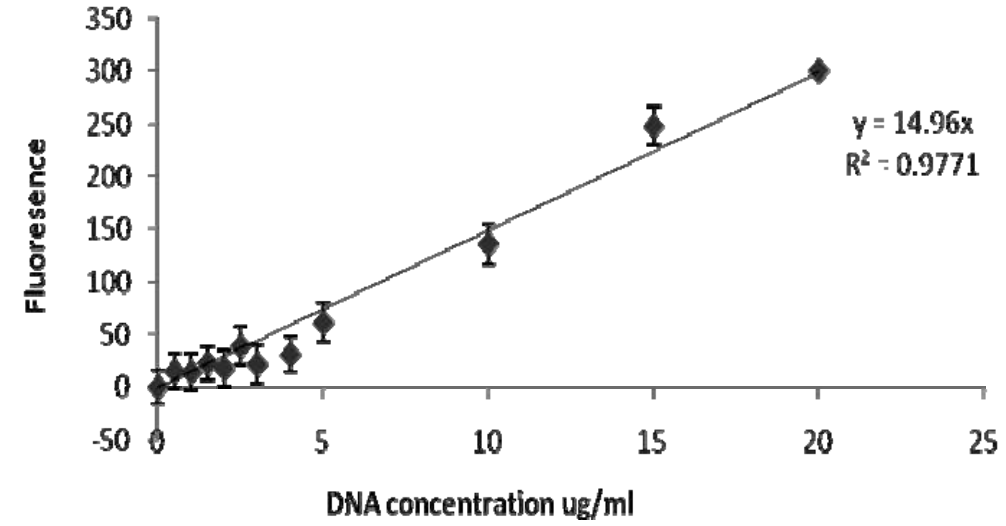

B)

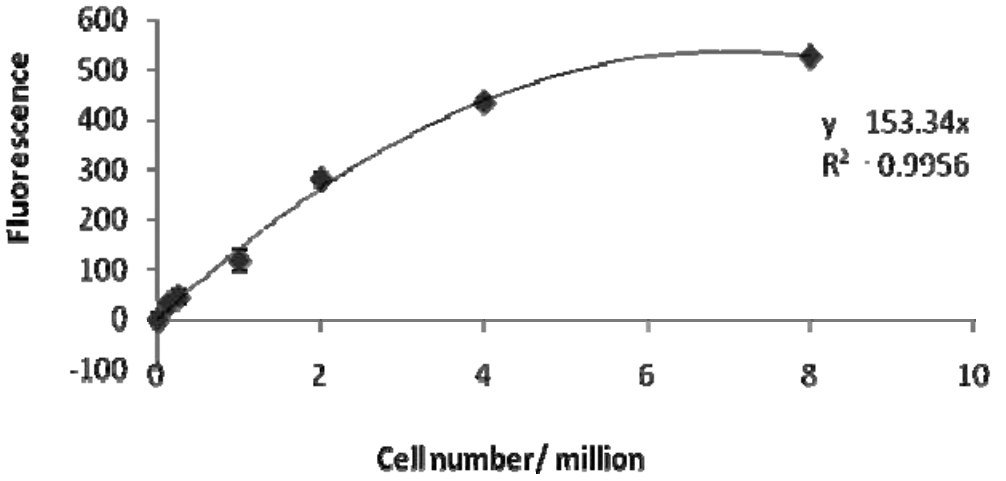

Figure 2.13: DNA standard curve for DNA content analysis Hoechst 33285 (A), cell number standard curve for DNA content analysis Hoechst 33285 (B). (n=3, error bars indicate ±SD)

2.3.4 Hepatic stellate cells

2.3.4.1 Morphology

HSCs were isolated by the method mentioned in Section 2.2.5. The cells were cultured in the HSCs medium after isolation. The characteristic morphology of active HSCs examined by phase contrast light microscope was shown in the Figure 2.14.

Phase contrast microscope revealed that within 48 hours of seeding, HSCs had adhered and had begun to project fine processes on the tissue culture plastic surface (Figure 2.14A). After approximately 7 days in the culture, the HSCs became confluent and showed longer, thicker processes, which had increased in number (Figure 2.14B).

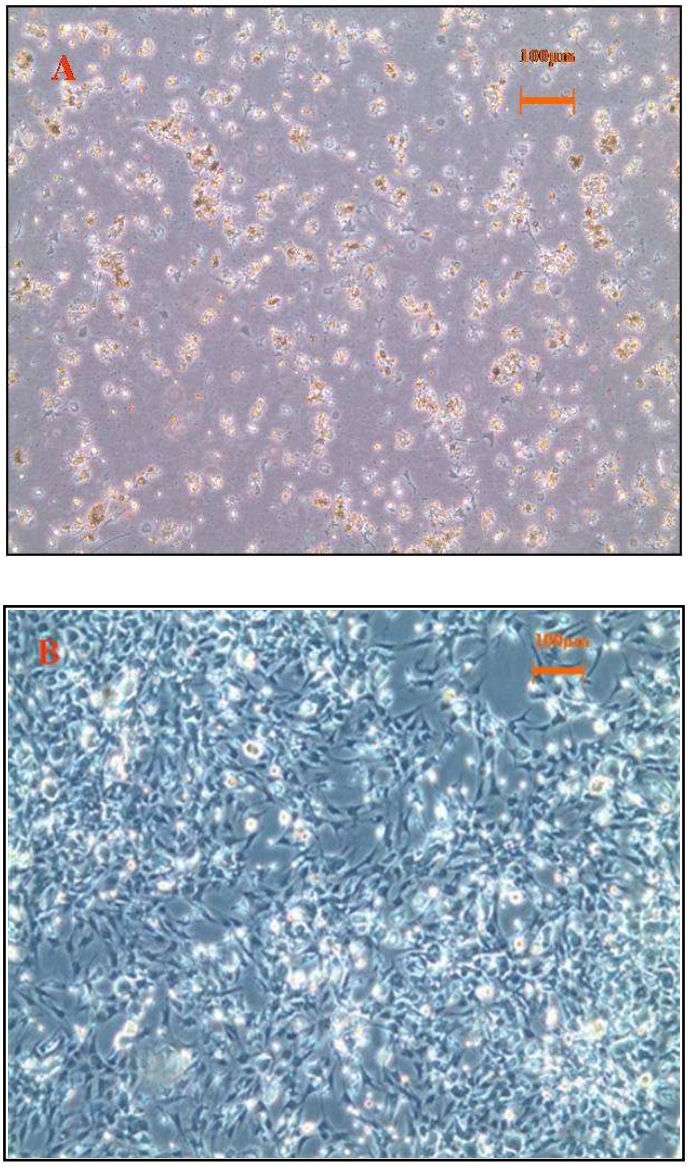

Figure 2.14: Phase contrast light microscope images of primary rat HSCs in culture. (A) Cells show quiescent state after 48 hours in culture, (B) cells are activated and confluent after 7 days in culture.

2.3.4.2 Lipid staining

The method was described in Section 2.2.9. The visible lipid droplets could be seen in Figure 2.15.

Figure 2.15: Visualization of lipid droplets within the HSCs (10 days in culture). HSCs incubated with Oil Red O to stain lipid vesicles pink/red. Arrow indicates lipid vesicle.

2.4 Discussions

2.4.1 The effects of seeding density on morphology of hepatocyte monoculture

The key variables controlling differentiated functions of hepatocytes are believed to be cell-cell and cell-ECM interactions. The role of homotypic cell-cell interactions is typically studied by varying cell seeding density. It has been reported that the cell density of 500,000 to 700,000 is recommended for 12-well plates (LeCluyse *et al*., 2005). In this study, the lowest density was demonstrated to be the most suitable density in terms of morphology. Considering both good coverage and apoptosis, cells at a seeding density of 500,000 had more than 90% confluence, with the least non-viable cells after 48 hours post-isolation. The observation suggests that the disadvantages of the limitation of nutrients, oxygen supply and the removal of waste products at high seeding density may outweigh the advantages of the increase in cell-cell contacts which accompany higher densities.

2.4.2 The effects of ECM on morphology of hepatocyte monoculture as well as co-cultures

The role of cell-ECM interaction on hepatocyte morphology was studied by the method of Matrigel overlay. The cells with Matrigel overlay reached above 90% confluence more quickly and retained round shape with well-defined cell borders, distinct nuclei and bile canaliculi-like structure longer when compared with the cells with no overlay of Matrigel. Matrigel is well known to contain a mixture of ECM including type IV collagen (Rojkind and Ponce-Noyola, 1982), type I collagen, heparan sulfate proteoglycan (Stow *et al*., 1985), fibronectin

(Oh *et al*., 1981) and laminin and it provides the cells with a more *in vivo*-like microenvironment, which might have great effect on hepatocyte specific functions.

It has been demonstrated in this study that 3D self-organizing spheroids formed on $P_{DL}LA$ surface but not in the collagen-Matrigel sandwich configuration on 12 well plates. It is believed that the formation of spheroids on static cultures of hepatocytes is a result of poor cell attachment and repulsion of the cells from the culture surface (Tzanakakis *et al*., 2001). The $P_{DL}LA$ surface is more hydrophobic than collagen surface and consequently, cell to surface interactions are not as strong as on $P_{DL}LA$, which results in poor adherence of the cells to the surface. In addition, TGF-β has previously been shown to play a role in the detachment of cardiac cells from the endothelium (Brown *et al*., 1985) and is known to be secreted by HSCs (Pinzani *et al*., 1995). Therefore, a non-adhesive surface as well as HSCs contributes to form spheroids.

However, in addition to hydrophobicity of $P_{DL}LA$ surface and HSCs, other factors, such as surface area, HSCs status and NPCs (e.g. Kupffer cells and endothelial cells), might contribute to spheroid formation to some extent, which have not been considered in this study. For the self-assembled spheroids, which depend on the culture substratum, a large surface area is required for initial cell attachment (Kamihira *et al*., 1997), therefore, 6 well plates with bigger attachment area might be applied in future work. In addition, HSCs used in this study are not completely pure isolation by the two-step collagenase perfusion method and they are contaminated with different portion of other

NPCs from isolation to isolation. It has been reported that rat prostate endothelial cell line is used to co-culture with hepatocytes to form hetero-spheroids in a spinner vessel in approximately 20 hours (Lee *et al*., 2004) and spheroids are formed by co-culture of hepatocytes and NIH3T3 on the poly (vinylidene difluoride) (PVDF) surface as well (Lu *et al*., 2005). Therefore, the contribution of spheroid formation from these NPCs cannot be excluded completely. Also, the ratio of quiescent and activated status of HSCs and repeated trypsinisation of HSCs may play a role in the spheroid formation. A certain range of passage number of HSCs used for spheroid formation need to be considered. Taken these observations together, the reproducibility of spheroid formation on $P_{DL}LA$ coated plate or non-spheroid formation in collagen-Matrigel sandwich need further experiments.

2.4.3 The effects of repeated assay application on hepatocyte functionality

Four common hepatocyte function assays have been applied successfully and optimized in this study. The initial question addressed was the pragmatic issue of the effects of repeated assay applications on hepatocyte functions. There are no apparent effects on the ability of hepatocytes in monoculture to secrete albumin, urea and the activity of CYP1A-catalysed O-dealkylation of 7-ethoxyresorufin. The effects of repeated assay applications on the metabolisation of testosterone cannot be assessed due to lack of data shown after day 1. The hepatocytes lost their CYP mono-oxygenase activity rapidly after short period *in vitro*. This could be explained by a rapid down-regulation of degradation pathways relative to enzyme expression and the initial rise is

part of the de-differentiation process as opposed to a general recovery of cell function (Robert *et al*., 2005).

It is notable that, while the secretion of urea was well preserved, the secretion of albumin was rapidly lost in monoculture, which shows similar trend compared to other data of albumin and urea secretion (Bissell *et al*., 1987; Sivaraman *et al*., 2005)

In terms of CYP enzyme activity tested by EROD assay, diminished activity on day 0 and day 1 after hepatocyte isolation was confirmed on three time occasions. The reason for this initial reduction in the activity of hepatocytes has yet to be elucidated, but may be a result of some environmental factors causing the down regulation of genes transcribing for CYP-450 enzymes immediately following cell isolation. After the peak on day 2, the activity decreased markedly on day 3. It has been suggested that declining levels of CYP may be a result of decreased synthesis or increased degradation (Paine *et al*., 1980).

The accuracy and specificity of the EROD and testosterone metabolism assays has been considered. Although hepatocyte is not the only cell type contributing to the expression of CYPs, CYP1A by EROD and CYP2B by testosterone metabolism are unique to hepatocytes. HSCs play a role mainly in the expression of CYP2C11, CYP3A2 and CYP2D1 (Yamada *et al*., 1997) and Kupffer cells are basically involved in CYP2E1 expression (Adachi *et al*., 1995).

2.4.4 Conclusions and future work

The development of systems for the long term *in vitro* culture of functional liver tissue is a major research goal. The central limitation of experimental systems to date has been the early de-differentiation of primary hepatocytes in cultures. Rat primary hepatocytes and hepatic stellate cells have been isolated and co-cultured on $P_{DL}LA$ surface to form 3D spheroids successfully. It has been previously demonstrated that this co-culture model enhances long-term growth and maintenance of hepatocyte specific functions. However, it is important to compare this model to the best available other systems and to assess whether the model can be further enhanced by the inclusion of extracellular matrix proteins. Therefore, the effect of Matrigel, which contains key ECM components, and collagen, will be assessed on the morphology and functions of hepatocyte. The successful completion of these experiments will identify an effective model for the preservation of rat hepatocyte functions.

This chapter specifically has achieved confirmation of:

- the method of isolation of primary rat hepatocytes and HSCs previously established by Tissue Engineering Group;
- successful spheroids formation by co-culture of rat hepatocytes and HSCs on $P_{DL}LA$ coated surface;
- the specific hepatocyte functions assays including albumin secretion, urea secretion, EROD and testosterone metabolism;

and demonstration of:

- seeding density of hepatocytes in monoculture and co-culture (500,000 cells per well on 12-well plate); the ratio of hepatocytes and HSCs in co-culture (2:1);
- great effects of Matrigel overlay on confluence and morphology of hepatocyte monoculture and co-culture with HSCs; and
- no specific effects of plate change on albumin secretion, urea secretion, EROD except testosterone metabolism.

The next stage of the project will compare rat hepatocyte functions in the following culture systems, including monoculturing hepatocytes on collagen gel and in collagen-Matrigel sandwich, as well as co-culturing hepatocytes with HSCs on collagen gel, in collagen-Matrigel sandwich and on $P_{DL}LA$ coated surface. Mass spectrometry for the simultaneous measurement of multiple CYP functions (DMPK, Charwood, AstraZeneca) will be used to facilitate future work on both rat and human cells.

Chapter Three:

Co-culture of Primary Rat Hepatocytes and Hepatic Stellate Cells (HSCs)

3.1 Introduction

3.1.1 The advantages of 3D cell culture

There have been long-recognized difficulties in maintaining the survival and differentiated function of hepatocytes in *in vitro* cultures. 3D spheroids have been proposed as an important system for the preservation of hepatocyte morphology and liver specific functions. Ultrastructural characteristics of liver tissue, such as indistinguishable cell-cell boundaries, abundant cytoplasmic organelles, bile canaliculus-like structures, and space of Disse-like architecture are observed at the surface of, or within, spheroids (Abu-Absi *et al*., 2002; Lee *et al*., 2004; Fukuda *et al*., 2006). Spheroids exhibit higher levels of homologous and cell-cell interactions than hepatocyte monocultures and permit heterologous interactions in spheroids containing more than one cell type. This increased intercellular contact is a potentially important mechanism for regulating cell communication and reconstructing cellular polarity. In addition, accumulation and deposition of specific ECM generated by co-culture of hepatocytes and non-parenchymal cells can be found at the surface of hetero-spheroids, but cannot be observed in homo-spheroids (Lee *et al*., 2004) or hepatocyte monoculture (Landry *et al*., 1985). Moreover, higher levels of liver specific functions have been maintained for extended period in spheroids in comparison to 2D monocultures (Fukuda *et al*., 2003; Tamura *et al*., 2008). Overall, 3D spheroids provide an environment in which some of the complexity of the spatial organisation found *in vivo* can be reproduced and there is evidence that this is reflected in improved function.

3.1.2 Methods of formation of 3D spheroid

Since hepatocyte spheroids are considered to maintain hepatocyte functions for a longer period than hepatocyte monolayer culture, various cultivation methods and techniques for hepatocyte spheroid formation have been investigated. These methods can be generally separated into two groups. The first group is dependent on the surface property of the culture substratum. The spheroids using this method are usually formed in a stationary environment. The culture substrata include extracellular matrix or synthetic components, such as proteoglycan (Koide *et al*., 1990), positively charged culture dishes (Hasebe *et al*., 2003), porous polyurethane foam (Ijima *et al*., 1998; Fukuda *et al*., 2003), poly-*N*-isopropyl acrylamide (Takezawa *et al*., 1992), and titanium dioxide gel surface (Nakazawa *et al*., 2006). 48 to 96 hours is required for production of hepatocyte spheroid using these methods. The second group depends on a non-stationary dynamic culture system, such as rotation culture with shaking (Surapaneni *et al*., 1997) or spinning culture, using a spinner vessel (Lee *et al*., 2004) or spinner flask (Yang *et al*., 2000; Okubo *et al*., 2002). Hepatocyte spheroids are formed in 24 to 48 hours in dynamic cultures. The speed of spheroid formation is not only critical for establishing cell-cell contact but also necessary for the maintenance of liver-specific function (Glicklis *et al*., 2000). Other methods for the production of spheroids include both growth factor supplementation and extracellular matrix (Semler *et al*., 2001), 3D scaffold (Wang *et al*., 2008), application of microfabrication and microcontact printing (Fukuda *et al.,* 2006; Nakazawa *et al*., 2006).

3.1.3 Mechanisms of formation of 3D aggregates

One of the key mechanisms of spheroid formation in a stationary environment is the attachment substratum. Most attachment substrata require non-adhesive surfaces, which cause poor cell attachment and repulsion of the cell from the culture surfaces. In the situation using scaffold as a substratum, in addition to its chemical composition, its physical property, and especially the pore size and the pliability, profoundly influences cell organization (Semler and Moghe, 2001; Haouzi *et al*., 2005). Cell-cell interaction is critical for spheroid formation, since it is believed that the intercellular forces (e.g. F-actin and connexin-32) in hepatocyte spheroids modulate the works of adhesion and cohesion (Liu *et al*., 2007). Although some soluble factors (e.g. MMPs), generated by cell-cell interaction play a role in cell-ECM interaction (Sato *et al*., 2003), spheroid formation always occurs when cell-cell interaction is greater than cell-ECM interaction (Powers *et al*., 1997). In other words, reduction of cell-ECM interaction can promote spheroid formation, which is probably modulated by fibrinolytic factors and filamentous actin network (Tzanakakis *et al*., 2001; Hasebe *et al*., 2003). Two fibrinolytic factors, namely tissue-type plasminogen activator (tPA) and urokinase-type plasminogen activator (uPA) are expressed in the hepatocytes (Hasebe *et al*., 2003). Plasmin generated by plasminogen *via* these two activators is involved in the regulation of ECM remodelling. This process has a great effect on the initial adhesion of hepatocytes to culture dishes and then migration and detachment of hepatocytes from culture dishes in the formation of hepatocyte spheroids. Besides fibrinolytic factors, an intact filamentous actin (F-actin) network is required for the reorganization of cytoskeleton in self-assembly spheroids

(Tzanakakis *et al*., 2001). Consequently, attachment substratum, cell-cell interaction and cell-ECM interaction are the keys for spheroid formation in a stationary environment.

However, the mechanism of spheroid formation in a non-stationary culture system has not been completely understood. It is believed that cell density, collision frequency, oxygen supply, and cell-cell interaction play significant roles in spheroid production. (Wu *et al*., 1995)

3.1.4 The effects of HSCs and Matrigel on 3D structures

The contribution of HSCs to the formation of 3D structures is likely to vary in different stages of the whole process. HSCs form tight adhesion to hepatocytes, which results in a well-defined hepatic ultrastructure, and this cell-cell interaction triggers HSCs activation during early liver regeneration in the rat (Mabuchi *et al*., 2004). Then, the expression of actin filaments and microtubules of activated HSCs helps to change the shape of rat hepatocyte and rearrange the cytoskeletal structure of the hepatocytes into self-assemble three-dimensional spheroids (Tzanakakis *et al*., 2001). Next, intercellular communication between activated HSCs *via* gap junction, mainly regulated by connexin-43, may enhance the coordination of HSC contraction *in vitro*, which plays a role in assembling hepatocyte monolayer to groups of aggregates (Fischer *et al*., 2005). Endothelin (ET)-1 and other contraction stimulating cytokines secreted by activated HSCs are highly responsible for the contractility as well, since ET-1 has been reported to promote the ability of contraction in normal dermal fibroblasts (Appleton *et al*., 1992) and lung

fibroblasts (Shi-Wen *et al*., 2004). After that, the expression of various MMPs of activated HSCs is required for matrix degradation, particularly MMP-2 and MMP-3 (Li *et al*., 2008). Together with the expression and activity of different forms of activator protein (AP)-1, a fine balance between the activity of AP-1 proteins and their target genes (MMP and TIMP) promotes the activated HSCs to remodel the hepatic ECM in cultured HSCs (Smart *et al*., 2001). This step of remodelling ECM is necessary for spheroid formation, since spheroid formation always occurs when cell-cell interaction is greater than cell-ECM interaction (Powers *et al*., 1997). Taking these observations together, HSCs are likely to play a key role in the formation and maintenance of spheroids. HSCs provide a series of cell signals for the regulation of formation of hepatocyte 3D structure (Sato *et al*., 2003).

The specific factors in Matrigel leading to spheroid formation are not known, although Matrigel, which contains various growth factors and ECM components produced by sarcoma cells, is considered the most effective substratum for hepatocyte differentiation (Bissell *et al*., 1987; Takashi *et al*., 2007). In 1993, Mackay *et al*. hypothesized that inactive proteases derived from Matrigel, but not from hepatocytes, contribute to spheroid formation. In particularly, epimorphin found in Matrigel (Hirai *et al*., 1993) induced MMP9, MMP3 and urokinase type plasminogen activator (uPA) in hepatocytes (Segawa *et al*., 2005). These epimorphin regulated proteases were required to induce hepatocyte aggregation to spheroids (Miura *et al*., 2007), as evidenced by the fact that an epimorphin-neutralizing antibody blocked the development of the cystic ductal structures of hepatocytes cultured on Matrigel (Tulachan *et*

al., 2006). Consequently, the proteases of Matrigel contribute to spheroid formation at least to some extent.

Self-forming 3D spheroids by co-culture of hepatocytes and HSCs on $P_{DL}LA$ coated surface has been previously established by the Tissue Engineering Group, School of Pharmacy in the University of Nottingham (Riccalton-Banks *et al*., 2003; Thomas *et al*., 2005, 2006). This 3D model shows better hepatocyte functions than monoculture on tissue culture plastic. In this chapter, we test the hypothesis that the inclusion of extracellular matrix in the form of Matrigel can further enhance the capacity of our established 3D model to maintain hepatocyte specific functions in culture.

3.1.5 Methods of measuring cytochrome P450 enzyme activity

A variety of methods could be used to analyse CYP activities. Generally speaking, the amount of one metabolite of the related substrate, which is metabolized by the specific enzymes, is measured either by a plate reader (i.e. metabolism of ethoxyresorufin to resorufin by CYP1A1 activity) or by a more accurate analytical method like HPLC (i.e. 6β- hydroxylation of testosterone and oxidation of testosterone mainly mediated by CYP3A and CYP 2B1). However these methods measure the activity of metabolic pathways, rather than the activity of individual enzymes, and it is difficult to reach conclusions about specific CYP activity. For this reason, a more accurate and specific method, high performance liquid chromatography - tandem mass spectrometry (LC-MS/MS), was selected and is introduced in this chapter. Both methods are used to detect the quantity of respective metabolites in the incubation media. A

new cassette of CYP substrates for several specific CYP measurements was used in LC- MS/MS (Kenny *et al*., 2009). CYP1A2, CYP3A1 and CYP2B6 enzyme activities are measured by their capacity to metabolise specific probes, namely: phenacetin deethylation (CYP1A2) (paracetamol); bupropion hydroxylation (CYP2B6) (1'-hydroxybuproprion); midazolam 1'-hydroxylation (CYP3A1) (1'-hydroxymidazolam). This technique therefore provides detailed information, not only about the major enzyme CYP3A1, but also other enzymes CYP1A2 and CYP2B6 activities.

3.1.6 High performance liquid chromatography - tandem mass spectrometry (LC-MS/MS)

LC-MS/MS is potentially the most useful technique for the characterization of drug metabolites, and combines a high resolution chromatography step with a further analysis giving both molecular weight and structure information on trace components. The remarkable advantage of LC-MS/MS is the capacity to simultaneously analyze a much wider range of compounds, including those which are thermally labile, of high polarities or of high molecular mass.

The sample solution is injected onto an HPLC column that consists of a narrow stainless steel tube filled with fine, chemically modified silica particles. Compounds are separated on the basis of their relative attraction (stationary phase) either between polar silica and non-polar solution (normal phase HPLC), or between non-polar silica and polar solution (reverse phase HPLC), which is the most commonly used form of HPLC; non-polar and polar compounds in solution travel through the column more quickly (mobile phase). Components

eluting from the chromatographic column are then introduced to the mass spectrometer *via* a specialized interface. The two most common interfaces used for HPLC/MS are the electrospray ionization (ESI) and the atmospheric pressure chemical ionization (APCI) interfaces.

In electrospray ionization, the compound is introduced to the source at typical flow rates of 1µl min^{-1} and the compound solution passes through an electrospray needle, the end of which is maintained at a high negative or positive potential at the range from 2.5V to 4V. This creates a strong electric field to produce a fine spray of tiny droplets and then to charge the droplets with the same polarity as on the needle. The droplets are forced towards the source sampling cone on the counter electrode and solvent evaporation occurs. The droplets then start to evaporate and shrink until the densities of electrical charge on the surfaces increase and reach the point that the surface tension can no longer sustain the charge (the Rayleigh limit). Then the droplets come apart. This produces smaller droplets that can repeat the process as well as naked charged compound molecules. Eventually, the ions are sorted in the mass analyzer according to their mass to charge (m/z) ratios and collected by a detector. An electrical signal is then generated proportional to the number of ions from the detector. It is the measurement of mass to charge ratio rather than mass per se that allows high molecular weight components such as proteins to be analyzed. Therefore, CYP metabolites are analyzed using this interface in this chapter.

APCI is an equivalent ionization method to ESI. The major difference is the process of ionization. In ESI, the ionization is created by the potential difference between the spray needle and cone; while in APCI, the compound solution is introduced into a pneumatic nebulizer and evaporated in a heated quartz tube before interacting with cone to create ions. Low mass compounds are primary applications of APCI.

3.1.7 Aims

The principal aims of the work presented in this chapter are:

- to test whether our established model of spheroid co-cultures on $P_{DL}LA$ coated plates could be further enhanced by supplementation with ECM proteins, including collagen and Matrigel, and
- to assess whether HSCs, ECM or both were the cause of any observed effect by measuring hepatocyte functions using albumin secretion, urea secretion, testosterone metabolism by HPLC and LC-MS/MS.

3.2 Material and Methods

3.2.1Chemicals

Midazolam was purchased from Sequoia Research Products Ltd. (Oxford, UK). Paracetamol, diclofenac and buproprion were purchased from Sigma-Aldrich (Gillingham, UK) and were of the highest grade available. 1 x DPBS was bought from Introvigen, UK. QIAamp® DNA Mini Kit was purchased from QIAGEN, UK. Other chemicals were listed in Chapter 2 (Section 2.2.2).

3.2.2 Plasticware

$P_{DL}LA$ coated 12 or 6 well plates were prepared as described in Chapter 2 (Section 2.2.3). 12 well and 6 well collagen type I coated dishes were bought from BD Biosciences, UK. Other plasticware were shown in Chapter 2 (Section 2.2.3).

3.2.3 Cell isolation and culture conditions

Primary rat hepatocytes and HSCs were isolated as described in Chapter 2 (Section 2.2.4) and they were co-cultured on either 12 or 6 well plates. Rat hepatocytes were seeded in five different culture systems, including hepatocyte monocultures on collagen gel and in collagen-Matrigel sandwiches, as well as hepatocytes co-cultured with HSCs on collagen gel, in collagen-Matrigel sandwiches and on $P_{DL}LA$ coated surface. The method for Matrigel overlay was described in Chapter 2 (Section 2.2.6). The seeding density of hepatocyte monocultures on 12 and 6 well plates was 500,000 cells per well and 900,000 cells per well respectively; co-culture of hepatocytes and HSCs at the ratio of 2:1 in total number of 500,000 cells per well and 900,000 cells per well was

cultured on 12 and 6 well plates, respectively. Cells on 12 and 6 well plates were maintained in 1 ml and 2 ml culture medium, respectively.

3.2.4 Passage of HSCs

HSCs were isolated as described previously. After the HSCs reached 80% confluence on a normal T75 flask, they were passaged using a trypsin/ EDTA method. Before the cells were trypsinized by 3 ml trypsin/EDTA, warm PBS buffer was used to wash the cells. After 5 minutes incubation, 5ml of HSCs medium was added to stop the trypsin/EDTA reaction and the cells were scraped from the flask using a cell scraper. The cell suspension was centrifuged at 250 g for 5 minutes and the pellets were re-suspended in fresh HSCs medium. Finally, the cells were placed on a new flask with fresh medium and then were passaged again when they were confluent. Different passage numbers of HSCs were used to test the effects on spheroids formation on 6 well $P_{DL}LA$ coated plates. Passage number 0, 3, 4, 6, 7, 14, 17 and 30 of HSCs were created by the above method.

3.2.5 Disaggregation of spheroids

The medium and spheroids from each well were aspirated and centrifuged at 50 g for 5 minutes. Each pellet was then re-suspended in 2 ml pre-warmed PBS and added back to matching wells briefly to wash. PBS and loose spheroids from each well were aspirated and centrifuged again at 50 g for 5 minutes. After that, each aliquot was re-suspended in 2 ml pre-warmed accutase, added back to matching well and incubated at 37ºC for 10 minutes. After retrieval from the incubator, the cells were scraped in order to detach residual cells or

adherent spheroids and then returned to incubator for a further 30 minutes. Finally, each cell suspension was aspirated, centrifuged at 350 g for 5 minutes and re-suspended in PBS.

3.2.6 DNA quantification

QIAamp® DNA Mini Kit was used to isolate the total DNA from cell cultures. The cell suspension from each well of 6 well plates was obtained either by a cell scraper or disaggregation of spheroids as described in Section 3.2.5. After the cell suspension was centrifuged at 50 g for 5 minutes, the cell pellets were re-suspended in 200 µl PBS. DNA was then isolated according to manufacturer's instructions (QIAamp®) and the amount of DNA obtained from each well was measured by NanoDrop® ND1000 UV-Vis Spectrophotometer to give a final concentration in ng/µl.

3.2.7 Function analysis

Testosterone metabolism, albumin secretion assay, and urea secretion assay have been previously described. For this section, EROD assay for CYP activity was supplemented by the more sensitive and reproducible LC-MS/MS.

(i) CYP activity measurements by LC-MS/MS

The medium from each well was aspirated and the cells washed with PBS buffer prior to assay. CYP1A2, CYP3A1 and CYP2B6 enzyme activities were measured by their capacity to metabolise specific probes, namely phenacetin deethylation, midazolam 1'-hydroxylation and bupropion hydroxylation. Probe stocks were prepared in methanol at the concentrations of 0.6, 0.2 and 1 mg/ml,

respectively. Three probe mixed solutions was mixed, evaporated to dryness under nitrogen gas, and reconstituted in PBS to give final incubation concentrations of 4.48, 9.06 and 23.7 μg/ml respectively. 2 ml of the diluted mixed substrate cassette was added to each well of cultured rat hepatocyte monocultures and co-cultures after day 1, 3, 5, 7, 9, 11, 14 and 21. Cells were then incubated on an orbital shaker for gentle agitation (~ 30 rpm; 37°C). Aliquots (100 μl) were removed at 20 minutes and 60 minutes after adding the probe substrates and the samples were quenched in ice-cold methanol (100 μl). The samples were then stored at -30°C until analysis by LC-MS-MS as described below. A 4 CYP metabolite standard curve was prepared from 1, 2, 5, 10, 20, 50, 100, and 200 to 500 ng/ml, which was used to quantify the amount of metabolite produced by samples at each point of time. Following the completion of the activity assay, cells were lysed in RLT buffer (600 μl; Qiagen, West Sussex, UK) containing β-mercaptoethanol (10 μl/ml) and stored at -80˚C until required for mRNA analysis.

The samples stored at -30°C were thawed and then centrifuged at 2000 *g* for 15 minutes at 4˚C and the supernatant (10 μl) was injected from a 96-well plate onto a Symmetry C18 (3.5 μm) column (2.1×100 mm, Waters, Hertfordshire, UK) maintained at 40°C. HPLC separation was performed using Jasco PU-2085 plus semi-micro pumps coupled to Jasco DG-2080-54 degasser, MX-2080-32 dynamic mixer and a CO-2067 plus column oven (Jasco, Essex, UK). The mobile phase consisted of solvent A (0.1% formic acid in acetonitrile) and solvent B (0.1% formic acid in water), using a linear gradient of 10% A (0-0.1

min), 54% A (0.1-3.0 min), 100% A (3.0-3.5 min), 10% A (3.51 min) with a run time of 5.5 minutes and flow rate 0.5 ml/min. This procedure allowed chromatographic separation of all probe substrates and their respective metabolites. This was coupled to a triple quadruple Platinum Ultima (Waters, Hertfordshire, UK) operating in ESI+ mode, with Masslynx v.4.1 running in MRM mode monitoring for paracetamol (transition 152.27 > 110.24, cone voltage 59 V, collision energy 17 eV), hydroxybupropion (256.32 > 139.26, 24 V, 31 eV), 4'-hydroxydiclofenac (312.26 > 231.22, 52 V, 17 eV) and 1'-hydroxymidazolam (342.35 > 203.23, 31 V, 24 eV). These metabolites were subsequently quantified by the standards prepared as above. Results were calculated as pmoles of metabolite formed per million cells per minute of incubation. Representative control wells were trypsinsed and counted to ensure cell number was accurate.

3.2.8 Experimental design and data analysis

In order to test the hypothesis that our previous co-culture model could be further enhanced by addition of ECM components, and to assess whether NPCs, ECM or both were the cause of any effect, we established five distinct cultures including: hepatocyte monoculture on collagen gel; hepatocyte monoculture in a collagen-Matrigel sandwich; co-culture of hepatocytes with HSCs on collagen gel; co-culture of hepatocytes and HSCs in collagen-Matrigel sandwiches; co-culture of hepatocytes and HSC on $P_{DL}LA$ coated plates (Chapter 2, Section 2.3.1.3). Cells were firstly cultured on 12 well plates and the morphology and function were assessed. However, expected spheroids did not form on $P_{DL}LA$ coated plates after 72 hours. The influence of passage

number of HSCs on spheroid formation and morphology was then interrogated. 6 well plates were then applied for cell cultures with greater initial attachment area and correct range of passage numbers of HSCs were also used on 6 well plates. The morphology and hepatocyte functions were assessed as well. Each culture system was carried out three times in duplicate on 12 well plates but only once in duplicate on 6 well plates due to the development of difficulties in isolating viable primary rat hepatocytes as described in the Appendix 3. Duplicates were averaged to create independent data points for statistical analysis. Data was analysed using one way ANOVA for differences in metabolite production between the various culture conditions. Post tests with Tukeys error control were conducted to identify these differences. All data analysis was done in Excel and Prism. Graphs show mean values ± the standard error of the mean.

Testosterone metabolism CYP activities are expressed as percentage of initial activity, not per mg protein, while CYP activities analyzed by LC-MS/MS are expressed as pmol/min/μg DNA. For testosterone metabolism, the value for initial function used to calculate the percentage function is an average value from all experiments. Albumin and urea secretion assays were normalized to ng/ml/cell on 12 well plates by the assumption that the number of hepatocytes on monoculture and co-culture was 500,000 and 333,333 respectively through the whole culture period. However, DNA content analysis was subsequently applied to normalize these two assays on 6 well plates to mg/ml/μg DNA and ng/ml/μg DNA respectively.

3.3 Results

3.3.1 Morphology of rat hepatocytes on 12 well plates

Rat hepatocytes and HSCs were isolated as described previously (Chapter 2, Section 2.2.4 and 2.2.5). Hepatocytes were plated onto 12 well plates at a density of 500,000 cells per well for monoculture on collagen gel and in collagen-Matrigel sandwich, since this density has previously been demonstrated to be optimal (Chapter 2, Section 2.2.6). Co-culture of hepatocytes with HSCs was seeded at the density of 333,333 and 166,667 cells per well of 12 well plates for each of: collagen gel; collagen-Matrigel sandwich; $P_{DL}LA$ coated plates.

The morphology of both monocultures was similar to that observed in previous experiments (Chapter 2, Section 2.3.1.1). However, spheroids were not observed in co-cultures on $P_{DL}LA$ coated plates. Most of the cells on $P_{DL}LA$ coated plates maintained a monolayer (Figure 3.1A), except for a few small aggregates after 72 hours (Figure 3.1B). These small aggregates did not go on to become the multicellular islands which are the precursors of freely floating spheroids. No spheroids formed in the co-cultures on collagen gel and in collagen-Matrigel sandwich.

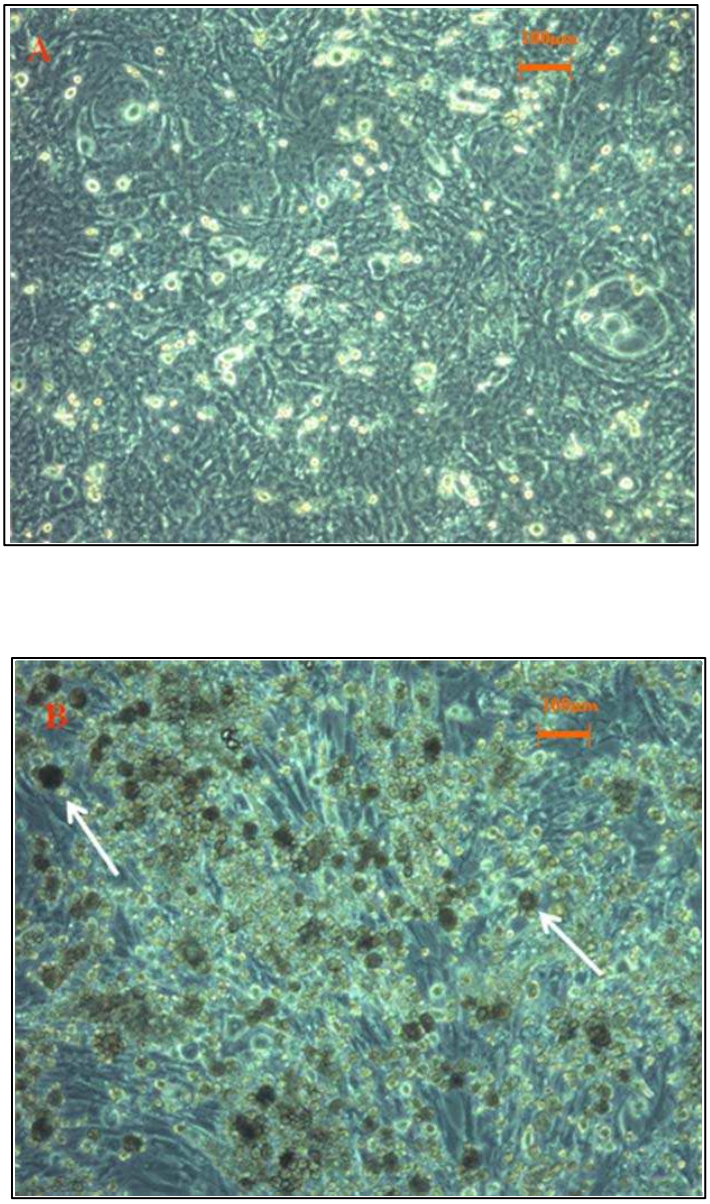

Figure 3.1: Rat hepatocytes co-cultured with rat HSCs (passage number 2) on 12 well $P_{DL}LA$ coated plates. Medium was not changed until 72 hours. Most of the cells maintained in a monolayer after 72 hours (A), but a few small aggregates (white arrows) were observed in some wells after 72 hours (B).

3.3.2 Functional analysis of cultures on 12 well plates

Functional analysis of albumin secretion, urea secretion and testosterone metabolism was carried out 24 hours after cell seeding (day 1) and then on day 3, 5 and 7 of cultures using the methods described previously.

3.3.2.1 Albumin secretion and urea secretion

Overall, the amount of albumin in each of the five different culture systems showed a similar pattern of reaching a peak on day 3 and decreasing on day 5 without further falls on day 7 (Figure 3.2A). In terms of hepatocyte monocultures, cells cultured in collagen-Matrigel sandwich showed higher albumin activity than cells cultured on collagen gel from day 3 to day 7; while among three hepatocyte co-cultures, cells cultured on $P_{DL}LA$ coated plates demonstrated the highest activity through the whole culture period. Particularly, the amount of albumin secreted by hepatocytes co-cultured on $P_{DL}LA$ coated plates was similar to that of albumin produced by cells mono-cultured in collagen-Matrigel sandwich on day 7, although cells of the monoculture revealed higher albumin amount than those co-cultured on $P_{DL}LA$ coated plates on day 5. (Figure 3.2A)

Comparing to albumin secretion data, the amount of urea showed much less variation in the different culture systems from day 1 to day 7, although cells of the co-cultures showed higher urea production than those of the monocultures (Figure 3.2B).

A)

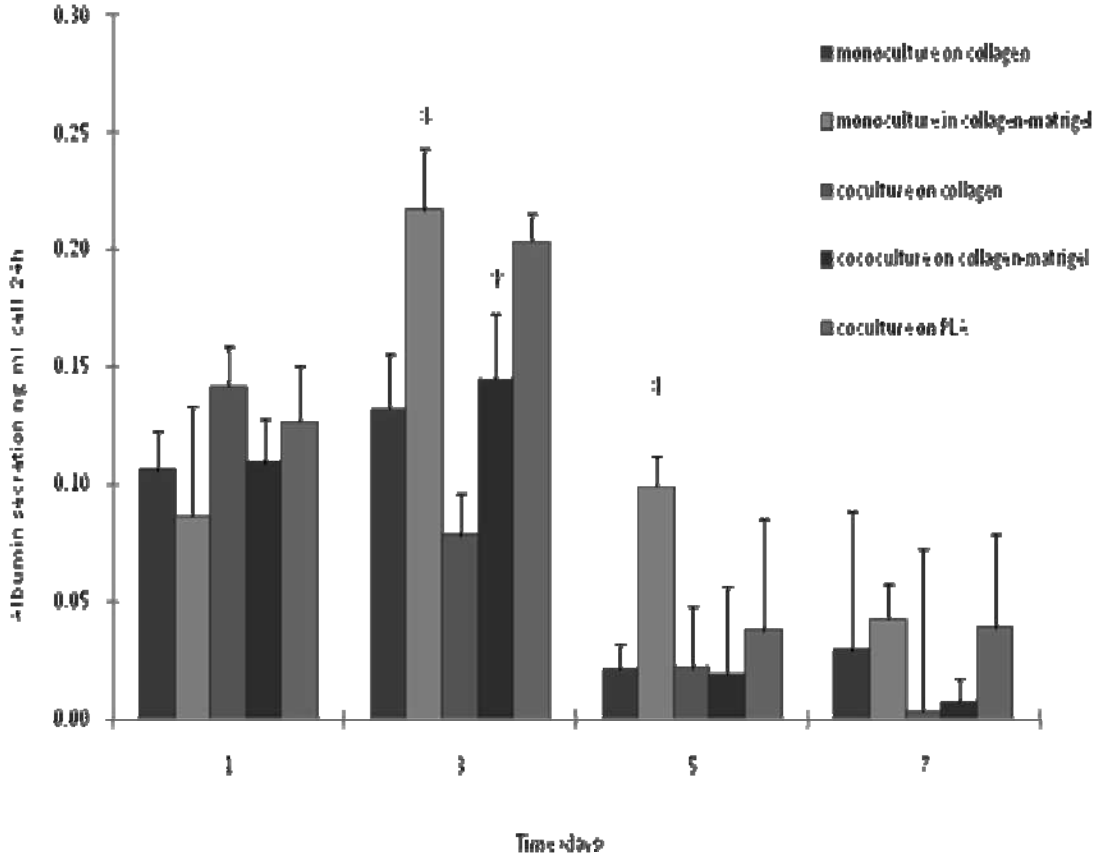

Figure 3.2A: The amount of albumin (ng/ml/cell/24h) secreted by rat hepatocytes on 12 well plates after 24 hours. Passage number 2 HSCs was used for the co-cultures and medium was changed every 24 hours. The error bars marked * on day 3 where data of cells of monoculture on collagen and co-culture in collagen-Matrigel sandwich are statistically significant than that of cells of co-culture on collagen ($P < 0.05$, 95% confidence). The error bars marked * on day 5 where data of cells of monoculture in collagen-Matrigel are statistically significant than that of cells of monoculture on collagen, co-culture on collagen and in collagen-Matrigel ($P < 0.05$, 95% confidence).

B)

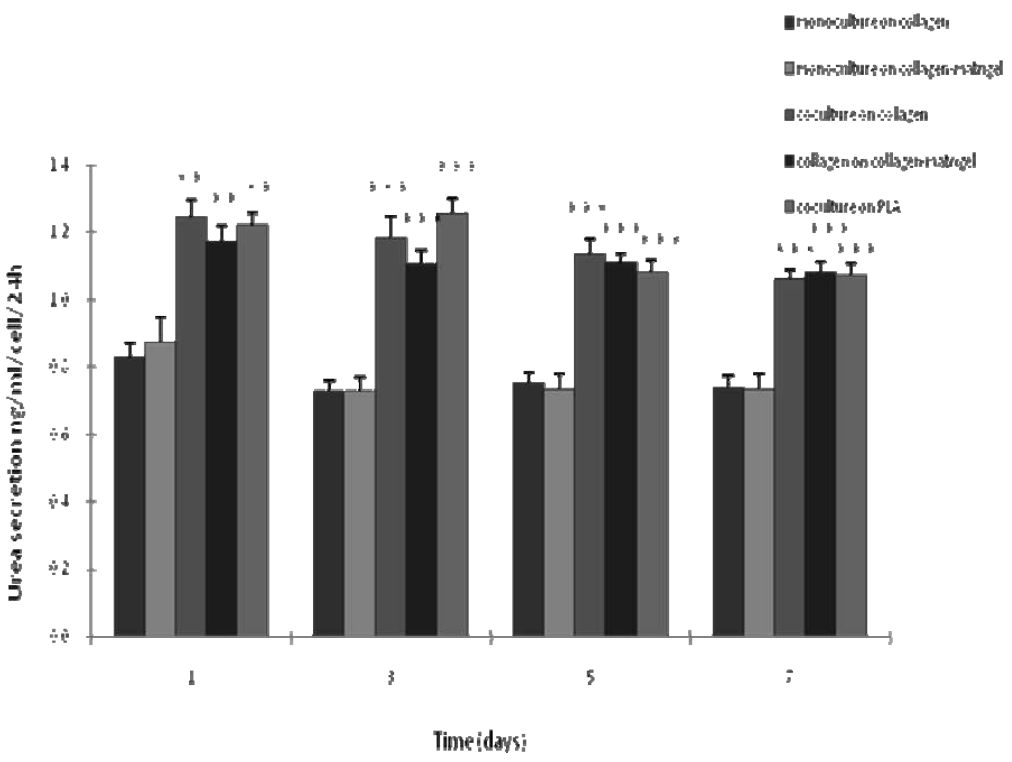

Figure 3.2B: The amount of urea (ng/ml/cell/24h) secreted by rat hepatocytes on 12 well plates after 24 hours. Passage number 2 HSCs were used and medium was changed every 24 hours. The error bars marked ** on day 1 where data of cells in the co-cultures are statistically significant than that of cells in monocultures at $P < 0.01$ (99% confidence) and the error bars marked *** on day 3, 5 and 7 where data of cells in the co-cultures are statistically significant than that of cells in monocultures at $P < 0.001$ (99.9% confidence).

3.3.2.2 Testosterone metabolism

Two testosterone metabolites, 6β-hydroxytestosterone and 4-androstene-3, 17-dione were measured by incubation of testosterone in the culture medium for 1 hour. The data have been normalized to percentage activity of freshly isolation cells (day 0).

6β-hydroxytestosterone production by CYP3A1 on day 1 only showed about 50% of day 0 activity in all five culture systems but subsequently increased to 100% ~ 300% activity of day 0 activity on day 3 and then decreased on day 5. The production of 6β-hydroxytestosterone could only be detected in three culture systems on day 5, namely monoculture in collagen-Matrigel sandwich, co-culture in collagen-Matrigel sandwich and co-culture on $P_{DL}LA$ coated plates. Among these three cultures, co-culture on $P_{DL}LA$ coated plates showed the highest CYP3A1 activity. (Figure 3.3A)

CYP2B1 activity, as assessed by 4-androstene-3, 17-dione production, was similar in all culture systems from day 1 (about 100% activity of day 0 cells) to day 3 (approximately 150% activity of day 0 cells) (Figure 3.3B). However, on day 5 cells co-cultured on $P_{DL}LA$ coated plates showed the highest activity, although the activity is not statistically significant compared to that of cells mono-cultured in collagen-Matrigel sandwich.

A)

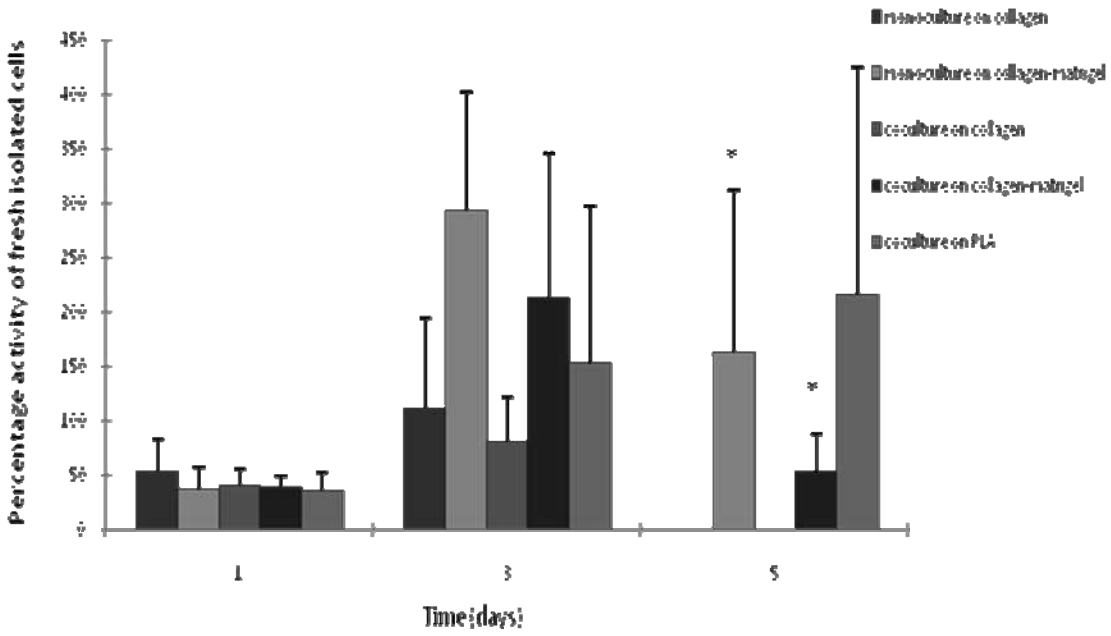

Figure 3.3A: 6β-hydroxytestosterone (CYP3A activity) production by rat hepatocytes on 12 well plates after 24 hours. Passage numnber 2 HSCs were used in the co-cultures and medium was changed every 24 hours. The error bars marked * on day 5 where data of cells of monoculture and co-culture in collagen-Matrigel are statistically significant than that of cells of co-culture on collagen ($P < 0.05$, 95% confidence).

B)

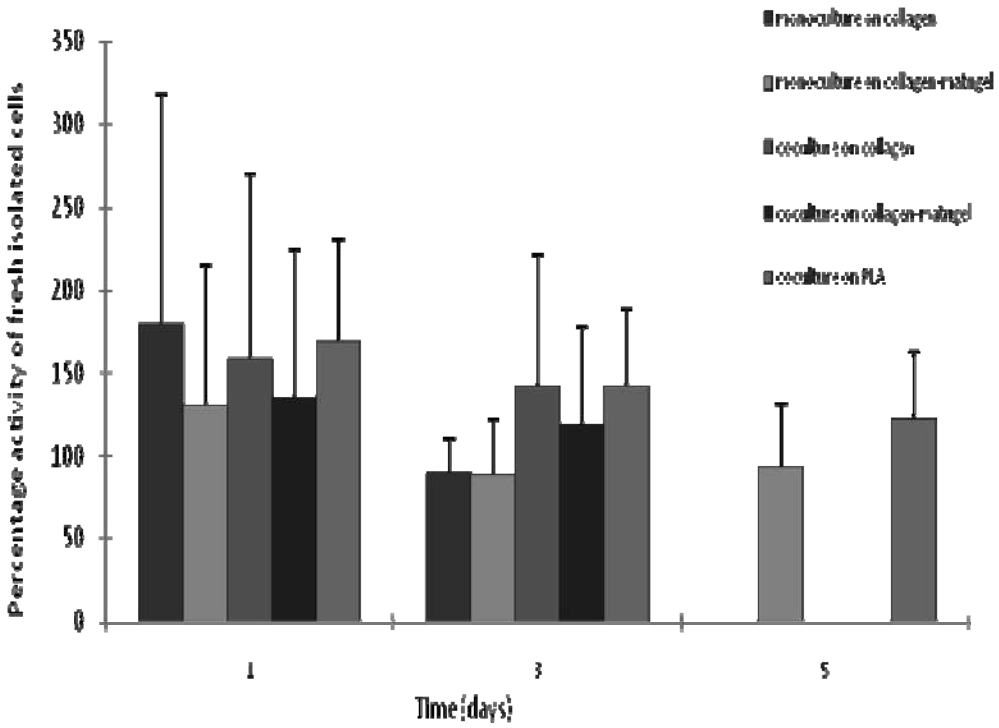

Figure 3.3B: 4-androstene-3, 17-dion (CYP2B activity) production by rat hepatocytes on 12 well plates after 24 hours. Passage number 2 HSCs were used in the co-cultures and medium was changed every 24 hours. The error bars indicating the differences between cells monocultured in collagen-Matrigel sandwich and those co-cultured on $P_{DL}LA$ coated surface are not statistically significant on day 5 ($P > 0.05$, 95 % confidence).

3.3.3 The effects of different passage numbers of HSCs on spheroids formation on 6 well $P_{DL}LA$ coated plates

Passage number 0, 3, 4, 6, 7, 14, 17 and 30 HSCs were used to co-culture with rat hepatocytes on $P_{DL}LA$ coated 6 well plates instead of 12 well plates. Spheroid formation was observed in the co-cultures using passage number 0, 3, 4, 6 and 7, but hepatocytes co-cultured with passage number 14 (Figure 3.4F), 17 (Figure 3.4G) and 30 (Figure 3.4H) HSCs mainly maintained in a 2D monolayer.

The size and number of spheroids formed by various passage number HSCs were dissimilar. In terms of the size of spheroids, those formed by passage number 0 (Figure 3.4A) and 3 (Figure 3.4B) HSCs (>200 μm) were bigger than others formed by passage number 4 (Figure 3.4C), 6 (Figure 3.4D) and 7 (Figure 3.4E) HSCs (<100 μm). However, the number of spheroids was *vice versa*. It was roughly less than 10 spheroids formed by passage number 0 and 3 HSCs and approximately 30 spheroids at maximum developed by passage number 4, 6 and 7 HSCs. Also, the morphology of spheroids was variable between those developed by passage number 0, 3 and 4, 6, 7. Better defined cell borders and tighter cell conjunctions were observed in the spheroids co-cultured by passage number 0 and 3 HSCs. In addition to the morphology, the time for spheroids formation was different. Spheroids formed by passage number 0 and 3 HSCs were observed within 48 hours, spheroids structured by passage number 4 and 6 HSCs were formed within 72~96 hours, and 144 hours (6 days) was necessary for spheroid formation using passage number 7 HSCs.

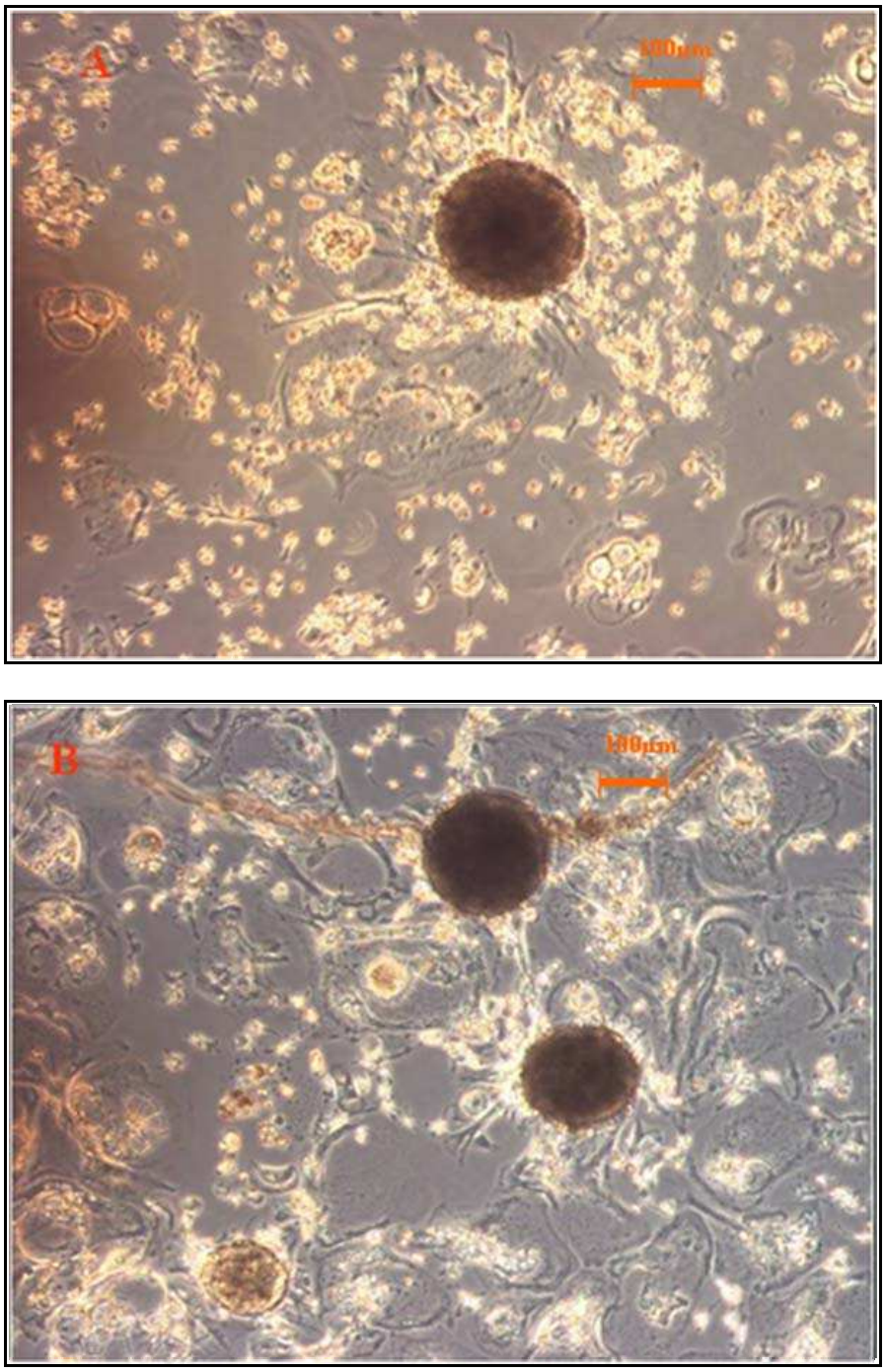

Figure 3.4: Formation of spheroids on 6 well $P_{DL}LA$ coated plates after 48 hours in co-cultures of rat hepatocytes with rat HSC passage number 0 (A) and 3 (B).

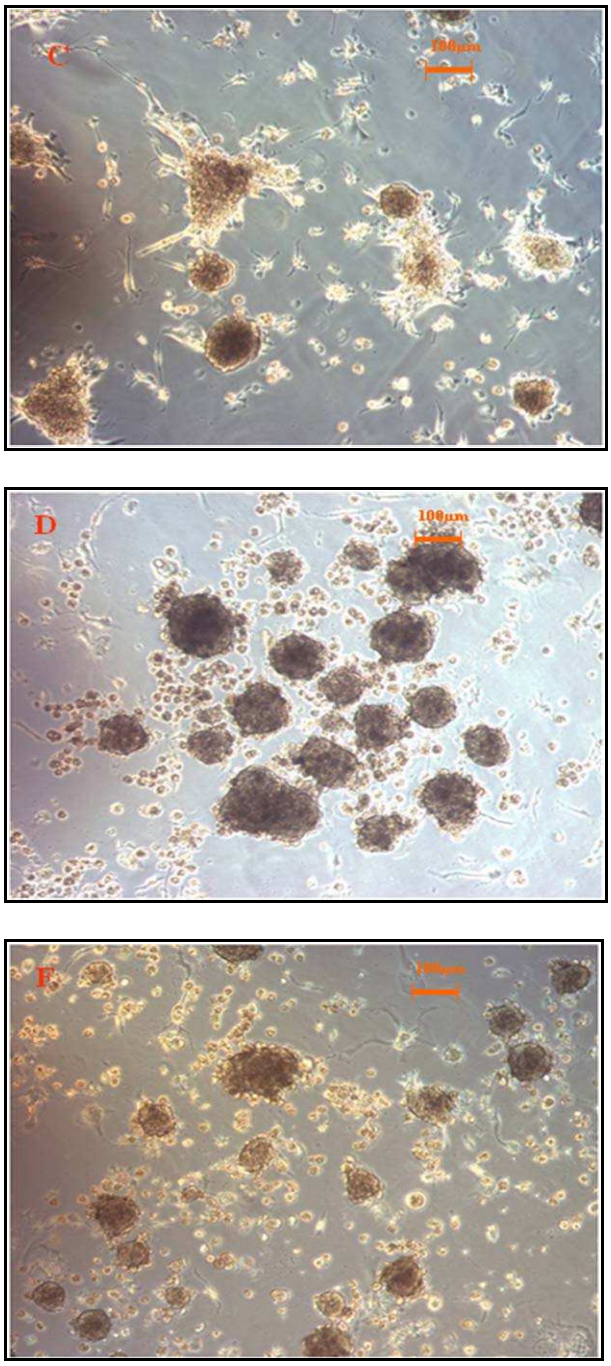

Figure 3.4: Formation of spheroids on 6 well $P_{DL}LA$ coated plates after 72~96 hours in co-cultures of rat hepatocytes with rat HSC passage number 4 (C), and 6 (D). Formation of spheroids on 6 well $P_{DL}LA$ coated plates after 6 days using rat HSC passage number 7 (E).

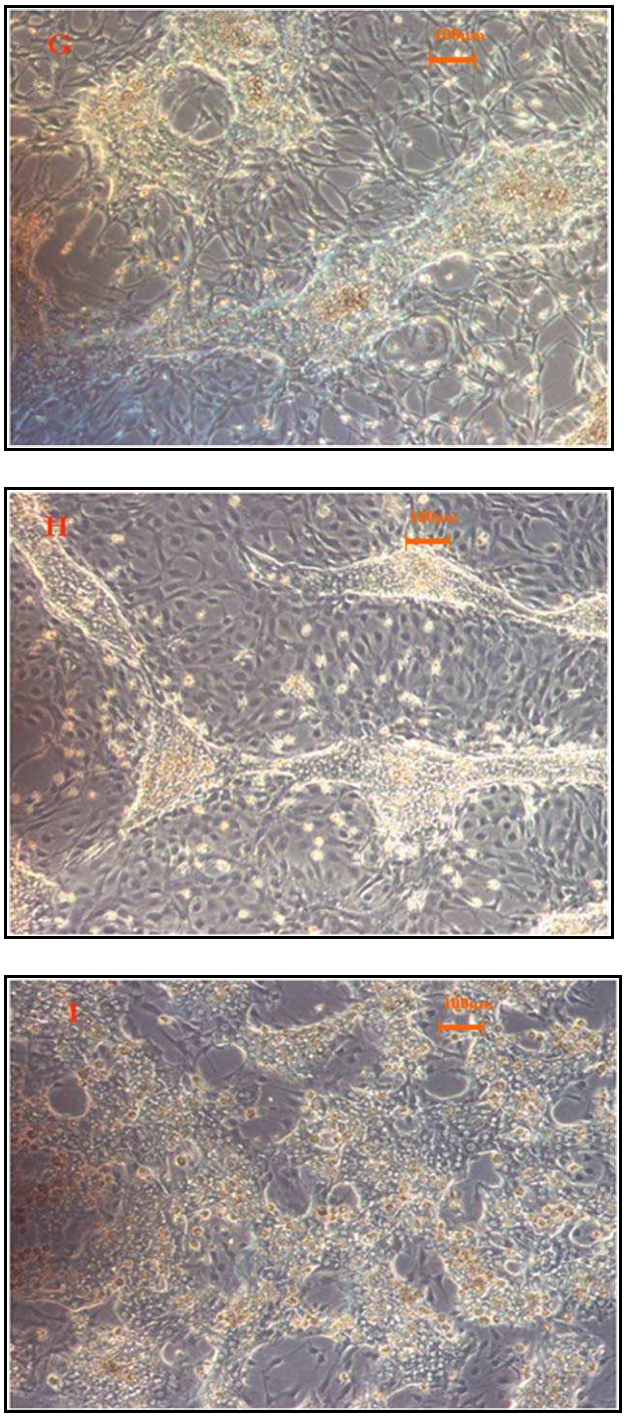

Figure 3.4: Rat hepatocytes co-cultured with rat passage number 14 HSCs (G) and 17 HSCs (H) and 30 HSCs (I) mainly maintain a monolayer on 6 well $P_{DL}LA$ coated plates after 6 days.

3.3.4 Morphology of rat hepatocyte on 6 well plates

Rat hepatocytes were plated onto 6 well plates at a density of 900,000 cells per well for monoculture on collagen gel and in collagen-Matrigel sandwich; co-culture of hepatocytes with passage number 4 HSCs were seeded at the density of 600,000 and 300,000 cells per well of 6 well plates on collagen gel, in collagen-Matrigel sandwich and on $P_{DL}LA$ coated plates.

The morphology of hepatocytes monocultured on collagen gel on 6 well plates showed exactly like that of cells cultured on 12 well plates. However, spheroids were surprisingly displayed in the monoculture of collagen-Matrigel sandwich and all three co-culture systems. Spheroids on $P_{DL}LA$ coated plates were formed in 72 hours (day 3), while spheroids on other culture systems were showed on day 6. Spheroids formed on $P_{DL}LA$ coated plates were smaller, denser and more numerous that those formed in other systems.

3.3.5 Functional analysis on 6 well plates

Functional analysis of albumin secretion, urea secretion and CYP activity by LC-MS/MS were measured after 24 hours (day 1) cells seeding and then on day 3, 7, 9, 11, 14 and 21 of cultures. The methods for these procedures were described previously. All the data in this section were normalized to DNA level.

3.3.5.1 DNA content analysis

The amount of DNA for each well for each day point was averaged by two experiments. The results were showed in Table 3.1.

Table 3.1: The amount of DNA (μg) for each well from day 1 to day 21 measured by Nanodrop (n=2)

Time/DNA (μg)	C/H	C/H/M	C/H&S	C/H&S/M	P/H&S
Day 1	12.90	21.82	17.96	21.83	16.32
Day 3	6.98	13.26	10.76	15.42	10.46
Day 7	8.58	11.74	7.05	6.28	6.20
Day 9	4.21	5.17	3.37	3.40	3.41
Day 11	3.21	4.16	3.12	3.22	3.33
Day 14	3.21	2.17	2.37	2.40	2.41
Day 21	1.22	2.11	1.37	1.40	1.41

C/H = Hepatocytes monoculture on collagen gel

C/H/M = Hepatocytes monoculture in collagen-Matrigel sandwich

C/H&S = Hepatocytes co-cultured with HSCs on collagen gel

C/H&S/M= Hepatocytes co-cultured with HSCs in collagen-Matrigel sandwich

P/H&S = Hepatocytes co-cultured with HSCs on $P_{DL}LA$

3.3.5.2 Albumin secretion and urea secretion

On the whole, cells in all five culture systems exhibited comparable albumin on day 1, increasing albumin on day 3 and gradually decreasing albumin from day 7 to day 21. All the co-culture systems showed higher albumin amount than both monoculture systems all the times except on day 1. Cells co-cultured in collagen-Matrigel sandwich and $P_{DL}LA$ coated plates demonstrated to maintain high albumin through the whole culture period. (Figure 3.5A)

The amount of urea in all culture systems was similar from day 1 to day 7. After day 7, cells of co-culture systems secreted more urea than those of the monocultures until day 21. In addition, higher urea secretion was displayed from day 7 to day 21 comparing to the amount from day 1 to day 7. However, there were no differences among three co-culture systems reached significance (Figure 3.5B).

A)

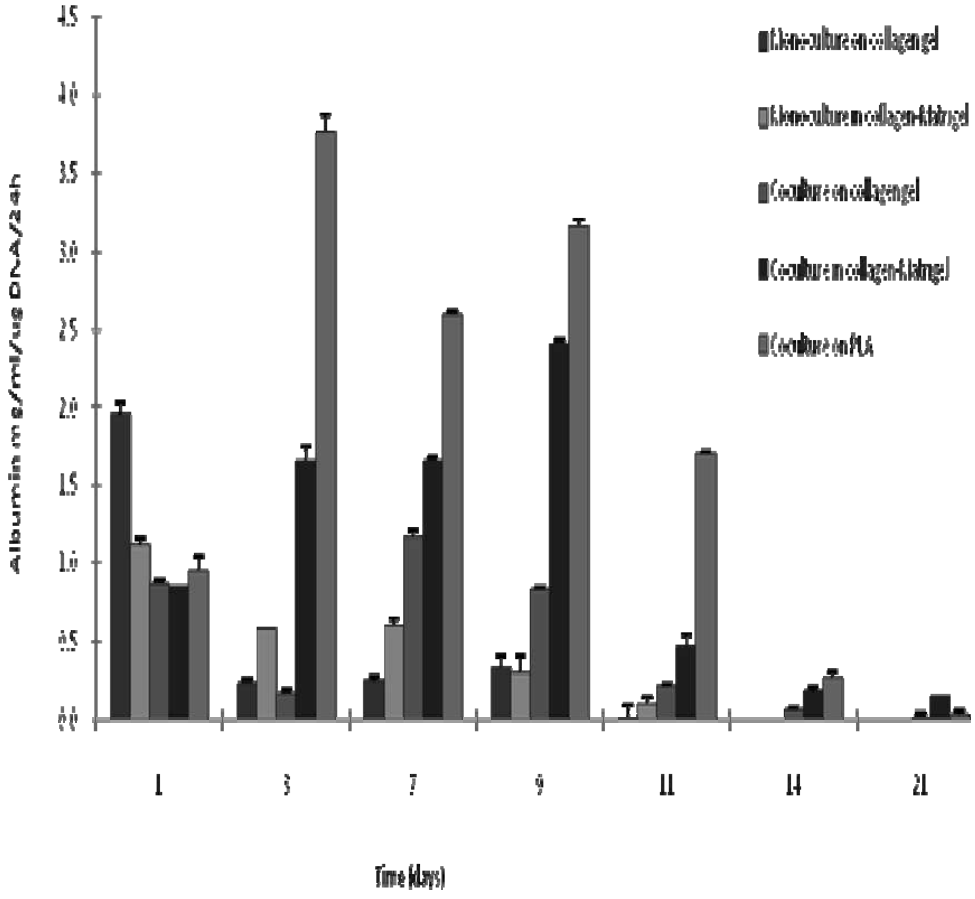

Figure 3.5A: The amount of albumin (mg/ml/µg DNA/24h) secreted by rat hepatocytes on 6 well plates after 24 hours. Passage number 4 HSCs were used in the co-cultures and medium was changed every 24 hours.

Table 3.2: Tukey's multiple comparison test for the amount of albumin secreted by rat hepatocytes on 6 well plates after 24 hours.

Tukey's Multiple Comparison Test	P value on day 1	P value on day 3	P value on day 7	P value on day 9	P value on day 11	P value on day 14	P value on day 21
A Vs B	P < 0.001	P < 0.001	P < 0.001	P > 0.05	P > 0.05	NA	NA
A Vs C	P < 0.001	P > 0.05	P < 0.001	P < 0.001	P < 0.01	NA	NA
A Vs D	P < 0.001	P < 0.001	P < 0.001	P < 0.001	P < 0.001	NA	NA
A Vs E	P < 0.001	P < 0.001	P < 0.001	P < 0.001	P < 0.001	NA	NA
B Vs C	P < 0.01	P < 0.001	P < 0.001	P < 0.001	P > 0.05	NA	NA
B Vs D	P < 0.01	P < 0.001	P < 0.001	P < 0.001	P < 0.001	NA	NA
B Vs E	P < 0.05	P < 0.001	P < 0.001	P < 0.001	P < 0.001	NA	NA
C Vs D	P > 0.05	P < 0.001	P < 0.001	P < 0.001	P < 0.001	P < 0.001	P < 0.001
C Vs E	P > 0.05	P < 0.001	P < 0.001	P < 0.001	P < 0.001	P < 0.001	P > 0.05
D Vs E	P > 0.05	P < 0.001	P < 0.001	P < 0.001	P < 0.001	P < 0.001	P < 0.001

A = mono-culture on collagen gel

B = mono-culture in collagen-Matrigel sandwich

C = co-culture on collagen gel

D = co-culture in collagen- Matrigel sandwich

E = co-culture on $P_{DL}LA$ coated surface

P > 0.05, not statistically significant

P < 0.05, significant

P < 0.01, very significant

P < 0.001, highly significant

NA = not available

B)

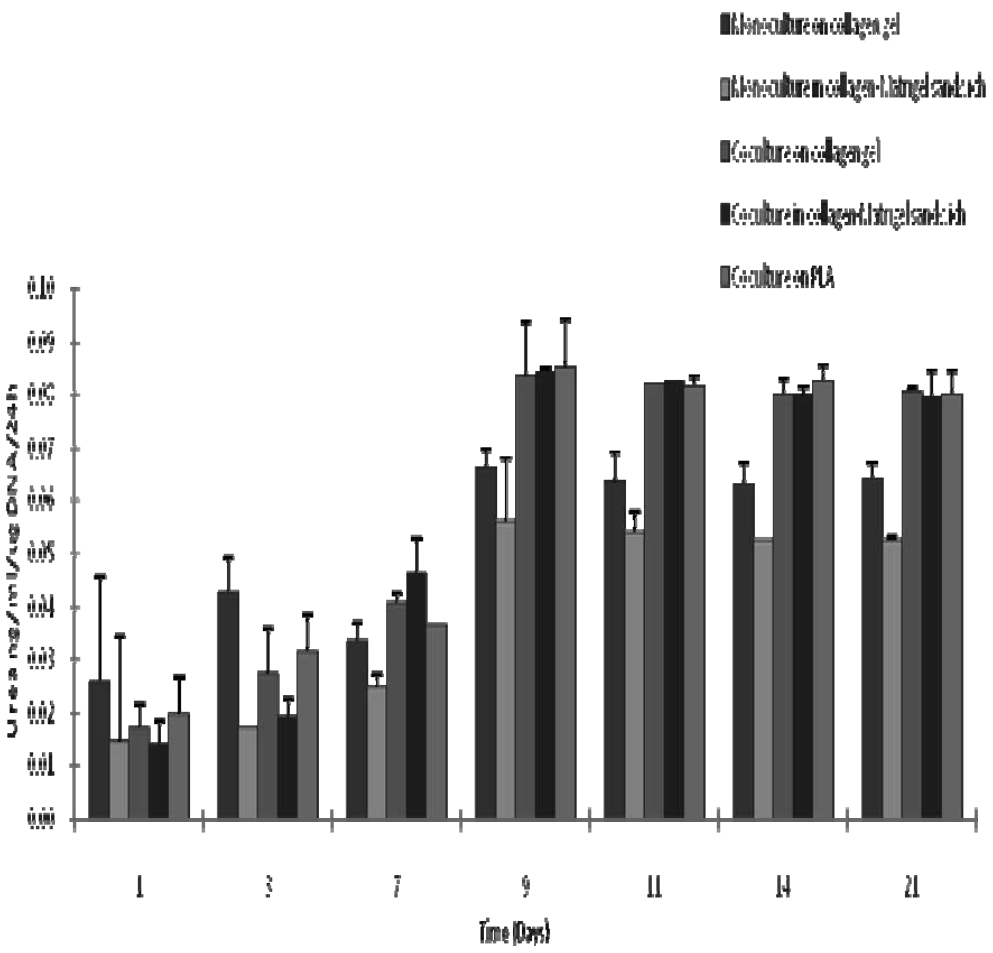

Figure 3.5B: The amount of urea (ng/ml/µg DNA/24h) secreted by rat hepatocytes on 6 well plates after 24 hours. Passage number 4 HSCs were used in the co-cultures and medium was changed every 24 hours.

Table 3.3: Tukey's multiple comparison test for the amount of urea secreted by rat hepatocytes on 6 well plates after 24 hours

Tukey's Multiple Comparison Test	P value on day 1	P value on day 3	P value on day 7	P value on day 9	P value on day 11	P value on day 14	P value on day 21
A Vs B	P > 0.05	P < 0.001	P < 0.05	P > 0.05	P < 0.05	P < 0.001	P < 0.001
A Vs C	P > 0.05	P < 0.01	P > 0.05	P > 0.05	P < 0.001	P < 0.001	P < 0.001
A Vs D	P > 0.05	P < 0.001	P < 0.01	P > 0.05	P < 0.001	P < 0.001	P < 0.001
A Vs E	P > 0.05	P > 0.05	P > 0.05	P > 0.05	P < 0.001	P < 0.001	P < 0.001
B Vs C	P > 0.05	P > 0.05	P < 0.001	P < 0.01	P < 0.001	P < 0.001	P < 0.001
B Vs D	P > 0.05	P > 0.05	P < 0.001	P < 0.01	P < 0.001	P < 0.001	P < 0.001
B Vs E	P > 0.05	P < 0.05	P < 0.01	P < 0.01	P < 0.001	P < 0.001	P < 0.001
C Vs D	P > 0.05	P > 0.05	P > 0.05	P > 0.05	P > 0.05	P > 0.05	P < 0.05
C Vs E	P > 0.05	P > 0.05	P > 0.05	P > 0.05	P > 0.05	P > 0.05	P > 0.05
D Vs E	P > 0.05	P < 0.05	P < 0.05	P > 0.05	P > 0.05	P > 0.05	P > 0.05

A = mono-culture on collagen gel

B = mono-culture in collagen-Matrigel sandwich

C = co-culture on collagen gel

D = co-culture in collagen- Matrigel sandwich

E = co-culture on $P_{DL}LA$ coated surface

P > 0.05, not statistically significant

P < 0.05, significant

P < 0.01, very significant

P < 0.001, highly significant

3.3.5.3 CYP activity measurements by LC-MS/MS

CYP1A2, 2B6 and 3A1activities were measured by metabolism of phenacetin deethylation, bupropion hydroxylation and midazolam 1'-hydroxylation of respective metabolites paracetamol, 1'-hydroxybuproprion and 1'-hydroxymidazolam. All the data were normalized to pmol/min/µg DNA.

Paracetamol production by CYP1A2 was maintained for 7 days. The activities of cells of monocultures were only detectable on day 1. Cells co-cultured in collagen- Matrigel sandwich illustrated gradually increased activity from day 1 (0.08 pmol/min/µg DNA) to day 7 (0.15 pmol/min/µg DNA); while cells co-cultured on P_{DL}LA coated plates showed decreased activity from day 1 (0.1 pmol/min/µg DNA) to day 3 (0.07 pmol/min/µg DNA) and no activity was shown on day 7. (Figure 3.6A)

1'-hydroxymidazolam production by CYP3A1 was maintained in monoculture for a longer period to day 3. However, the co-culture of collagen-Matrigel sandwich was the only culture system revealing the activity on day 7. Cells of other co-culture systems had no CYP3A1 activity after day 3. (Figure 3.6B)

1'-hydroxybuproprion production by CYP2B6, all five culture systems exhibited the CYP2B6 activity until day 7 and the activities of cells cultured on collagen-Matrigel sandwich and P_{DL}LA coated plates were extended until day 9. Although cells co-cultured on collagen-Matrigel sandwich demonstrated much higher CYP2B6 activity than those co-cultured on P_{DL}LA coated plates on day 7, they were similar on day 9. The reason why cells cultured on

collagen-Matrigel sandwich had much higher activity than cells cultured on other culture systems on day 7 was probably due to the big number and size of spheroids on that particular dish. (Figure 3.6C)

A)

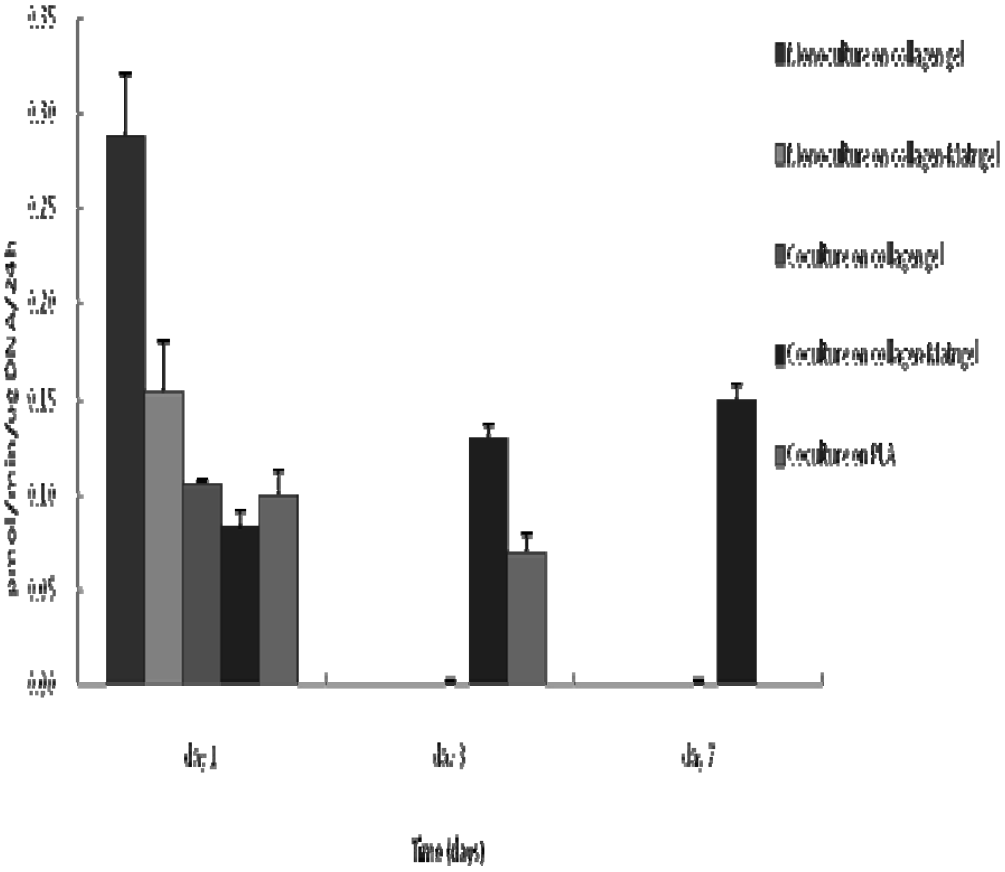

Figure 3.6A: Paracetamol production (CYP1A2 activity) by rat hepatocytes on 6 well plates after 24 hours. Passage number 4 HSCs were used in the co-cultures and medium was changed every 24 hours.

Table 3.4: Tukey's multiple comparison test for paracetamol production (CYP1A2 activity) production by rat hepatocytes on 6 well plates after 24 hours

Tukey's Multiple Comparison Test	P value on day 1	P value on day 3	P value on day 7
A Vs B	P < 0.001	NA	NA
A Vs C	P < 0.001	NA	NA
A Vs D	P < 0.001	NA	NA
A Vs E	P < 0.001	NA	NA
B Vs C	P > 0.05	NA	NA
B Vs D	P < 0.01	NA	NA
B Vs E	P < 0.05	NA	NA
C Vs D	P > 0.05	P < 0.001	NA
C Vs E	P > 0.05	P < 0.001	NA
D Vs E	P > 0.05	P < 0.01	P < 0.001

A = mono-culture on collagen gel

B = mono-culture in collagen-Matrigel sandwich

C = co-culture on collagen gel

D = co-culture in collagen- Matrigel sandwich

E = co-culture on $P_{DL}LA$ coated surface

P > 0.05, not statistically significant

P < 0.05, significant

P < 0.01, very significant

P < 0.001, highly significant

NA = not available

B)

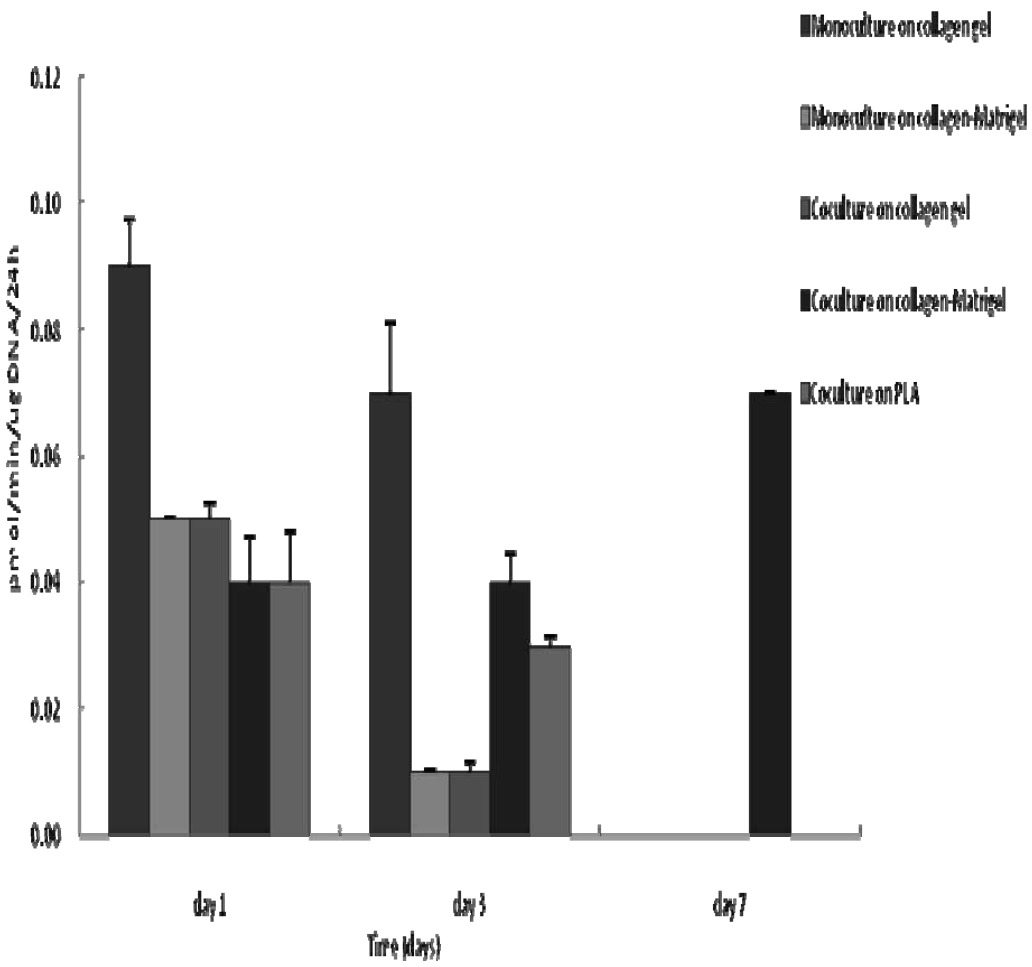

Figure 3.6B: 1'-hydroxymidazolam production (CYP3A1 activity) by rat hepatocytes on 6 well plates after 24 hours. Passage number 4 HSCs were used in the co-cultures and medium was changed every 24 hours.

Table 3.5: Tukey's multiple comparison test for 1'-hydroxymidazolam production (CYP3A1 activity) by rat hepatocytes on 6 well plates after 24 hours

Tukey's Multiple Comparison Test	P value on day 1	P value on day 3	P value on day 7
A Vs B	P < 0.001	P < 0.001	NA
A Vs C	P < 0.001	P < 0.001	NA
A Vs D	P < 0.001	P < 0.001	NA
A Vs E	P < 0.001	P < 0.001	NA
B Vs C	P > 0.05	P > 0.05	NA
B Vs D	P > 0.05	P < 0.001	NA
B Vs E	P > 0.05	P < 0.01	NA
C Vs D	P > 0.05	P < 0.001	NA
C Vs E	P > 0.05	P < 0.01	NA
D Vs E	P > 0.05	P > 0.05	NA

A = mono-culture on collagen gel

B = mono-culture in collagen-Matrigel sandwich

C = co-culture on collagen gel

D = co-culture in collagen- Matrigel sandwich

E = co-culture on $P_{DL}LA$ coated surface

P > 0.05, not statistically significant

P < 0.05, significant

P < 0.01, very significant

P < 0.001, highly significant

NA = not available

C)

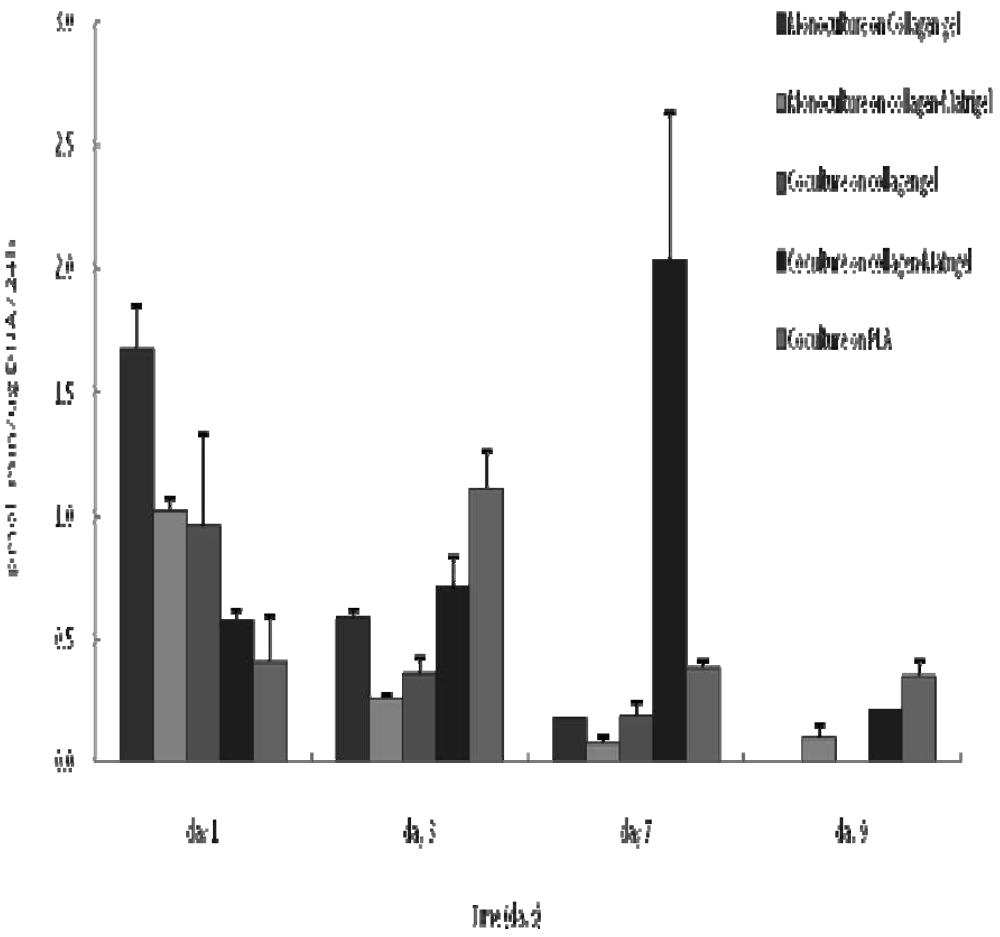

Figure 3.6C: 1'-hydroxybuproprion (CYP2B6 activity) production by rat hepatocytes on 6 well plates after 24 hours. Passage number 4 HSCs were used in the co-cultures and medium was changed every 24 hours.

Table 3.6: Tukey's multiple comparison test for 1'-hydroxybuproprion (CYP2B6 activity) production by rat hepatocytes on 6 well plates after 24 hours

Tukey's Multiple Comparison Test	P value on day 1	P value on day 3	P value on day 7	P value on day 9
A Vs B	P < 0.05	P < 0.01	P > 0.05	NA
A Vs C	P < 0.01	P > 0.05	P > 0.05	NA
A Vs D	P < 0.001	P > 0.05	P < 0.001	NA
A Vs E	P < 0.001	P < 0.001	P > 0.05	NA
B Vs C	P > 0.05	P > 0.05	P > 0.05	NA
B Vs D	P > 0.05	P < 0.001	P < 0.001	P < 0.05
B Vs E	P < 0.05	P < 0.001	P > 0.05	P < 0.01
C Vs D	P > 0.05	P < 0.01	P < 0.001	NA
C Vs E	P < 0.05	P < 0.001	P > 0.05	NA
D Vs E	P > 0.05	P < 0.01	P < 0.001	P < 0.05

A = mono-culture on collagen gel

B = mono-culture in collagen-Matrigel sandwich

C = co-culture on collagen gel

D = co-culture in collagen- Matrigel sandwich

E = co-culture on $P_{DL}LA$ coated surface

P > 0.05, not statistically significant

P < 0.05, significant

P < 0.01, very significant

P < 0.001, highly significant

NA = not available

3.4 Discussion

3.4.1 The morphology of rat hepatocytes on 12 well plates

The spheroids on 12 well $P_{DL}LA$ coated plates did not form as expected. There are two potential reasons to explain this phenomenon in this study. Firstly, surface area and seeding density could play an important role in self-forming spheroids. For the self-assembled spheroids, which depend on the culture substratum, a large surface area is required for initial cell attachment (Kamihira *et al*., 1997). In other words, a minimum cell number is necessary for the initiation of spheroids formation. The cell number of hepatocytes on a 12 well plate is approximately 333,000 in comparison to 500,000 in a 6 well plate. Secondly, different passage numbers of HSCs were used in this chapter. Passage number 1 and 2 of HSCs were co-cultured with hepatocytes to form spheroids successfully in previous studies, but passage number 4 and 5 were applied to the co-culture this time. The cytokine expression and responsiveness and the ability of remodelling ECM of activated HSCs from different passage numbers were possibly changed by the effects of several rounds of trypsinization *in vitro*. Therefore, the effects of different passage numbers of HSCs and the effects of seeding density were further studied for spheroid formation in the following section.

3.4.2 Functional analysis of rat hepatocytes on 12 well plates

The data of rat hepatocyte functions on 12-well plates are summarized in Table 3.7. It is demonstrated that the secretion of albumin exhibited an initial loss on day 1, reached the peak on day 3, and decreased dramatically after that. The initial loss of albumin secretion is probably a consequence of the recovery

process of cells after isolation. However, the amount of urea was maintained at a constant level from day 1 to day 7.

From the urea data, it is noticeable that all three co-cultures revealed higher secretion than the two monocultures during the whole culture period, but this urea assay is not sensitive enough to demonstrate which co-culture system is the best; while from the albumin data, among five culture systems, cells monocultured on collagen-Matrigel sandwich and co-cultured on $P_{DL}LA$ surface displayed similar activities during the whole time. The statistical analysis found no significant differences between them.

In terms of testosterone metabolism, CYP3A1, which is the most abundantly expressed CYP enzyme protein in the rat, was measured by the production of 6β-hydroxytestosterone. A reduced CYP3A1 activity after hepatocyte isolation was shown on day 1, most likely to represent, as with albumin, down regulation of CYP gene transcription immediately after cell recovery. After the peak on day 3, the activity of cells co-cultured on $P_{DL}LA$ surface was slightly higher than that of cells mono-cultured in collagen-Matrigel sandwich. In addition, the metabolism of testosterone to 4-Androstene-3, 17-dione was mainly metabolized by CYP2B1 with minor contributions by CYP2C11 and CYP2B2 (Sonderfan *et al*., 1989). The activities of all five culture systems were well preserved from day 1 to days 3, but the activity could only be observed in two culture systems on day 5, namely, monoculture in collagen-Matrigel sandwich and co-culture on $P_{DL}LA$. The cells cultured on $P_{DL}LA$ displayed higher activity.

It is not easy to compare culture systems between different research groups because of a large number of variables such as isolation methods, medium supplements and different endpoints. For co-culture of hepatocytes and HSCs on $P_{DL}LA$ coated surface, the percentage activity of CYP3A1 and CYP2B1 of fresh isolated cells on day 5 is around 200% and 130% respectively in this study, which is higher than only approximately 15% and 55% respectively from Thomas *et al*. 2005. For albumin and urea secretion, hepatocytes patterned co-cultured with NIH 3T3 on the polyelectrolyte multilayer template showed approximately 0.065 ng/cell/day and 0.07 ng/cell/day on day 5 respectively (Kidambi *et al*., 2007), which is similar to our albumin data and a slightly lower to our urea data from hepatocytes co-cultured with HSCs. In addition, our co-culture on $P_{DL}LA$ plates showed almost 1000 times and 100 times higher amount of albumin and urea secretion than the co-culture of hepatocytes and endothelial cells on P(IPAAm-BMA) patterned surface on day 3 (Tsuda *et al*., 2006), and co-culture of hepatocytes and Kupffer cells on PDMS micropatterned surface on day 5 (Yekaterina *et al*., 2005) respectively.

Table 3.7: a summary of data of hepatocyte function assays on 12-well plates

Summary of data on 12-well plates	**Albumin secretion (ng/ml/cell/24h)**	**Urea secretion (ng/ml/cell/24h)**	**CYP3A activity (% of fresh isolated cells)**	**CYP2B/2C activity (% of fresh isolated cells)**
A= Monoculture on collagen gel	Shown on day 7 at about 0.034	Maintained at around 0.8 from day 1 to day 7	not shown on day 5	not shown on day 5
B= Monoculture in collagen-Matrigel sandwich	Shown on day 7 at about 0.042		Shown on day 5 at about 160%	Shown on day 5 at about 90%
C= Co-culture on collagen gel	Shown on day 7 at about 0.004	Maintained at around 1.2 from day 1 to day 7	Not shown on day 5	not shown on day 5
D= Co-culture in collagen-Matrigel sandwich	Shown on day 7 at about 0.008		Shown on day 5 at about 60%	not shown on day 5
E= Co-culture on $P_{DL}LA$	Shown on day 7 at about 0.038		Shown on day 5 at about 210%	Shown on day 5 at about 125%
Conclusions	B/E higher than the others ($P>0.05$)	C/D/E higher than A/B ($P<0.01$)	E higher than the others ($P<0.05$)	E higher than the others ($P>0.05$)

3.4.3 Potential mechanisms of maintenance cultured rat hepatocytes on 12 well plates

Cell-cell interaction, cell-ECM interaction, soluble factors and 3D spheroids are the main potential mechanisms to explain maintenance of cultured hepatocytes function *in vitro*. It has been reported that hepatocytes mono-cultured in collagen-Matrigel sandwich maintained the differentiated functions through 2D homotypic cell-cell interaction and 3D cell-ECM interaction. Collagen is a major ECM component and is widely used as a substratum for hepatocyte in *in vitro* culture. Matrigel, however, contains not only collagen IV but also other ECM proteins including laminin and entactin. Besides ECM proteins, Matrigel also contains several growth factors, namely β-FGF, EGF, IGF-α, NGF, TGF-β etc. It is likely that these factors all contribute to the capacity of Matrigel to maintain hepatocyte function in monoculture, and underpin its utility for studies of drug metabolism and enzyme induction (Hewitt *et al*., 2007).

The molecular mechanisms of maintenance of liver specific functions of hepatocytes co-cultured with HSCs on 12 well $P_{DL}LA$ coated plates were not studied in this chapter. However, since *in vivo* hepatocytes make contact, not only with other neighbour hepatocytes, but also with non-parenchymal cells, the co-culture of hepatocytes and HSCs *in vitro*, which are two major cell type in the liver, provides a closer approximation to the *in vivo* environment. Further, soluble factors, including cytokines and MMPs, and ECM components secreted from HSCs could contribute to ECM remodelling and 3D structure formation (Section 3.1.4). More importantly, ECM remodelling might be a prerequisite

for hepatocyte proliferation after isolation (Galli *et al*., 2000). Other soluble factors including EGF, TGFα and HGF secreted from HSCs also promote hepatocyte proliferation (Martinez-Hernandez and Amenta, 1995). Therefore, HSC participation may promote the formation of small aggregates, although not big spheroids, on a non-adhesive surface, $P_{DL}LA$, which mimics the hepatic intercellular environment.

The finding on 12-well plates that cells co-cultured on $P_{DL}LA$ coated plates showed better hepatocyte specific functions than those mono-cultured in collagen-Matrigel sandwich suggests that combination of 3D aggregates formed by hetero-cell-cell interaction and soluble factors from NPCs might play a more important role in maintenance of hepatocyte function than cell-ECM interaction.

3.4.4 The effects of different passage number HSCs on spheroids formation on 6 well $P_{DL}LA$ coated plates

In order to test what is the appropriate range of passage number of HSCs for spheroids formation, different passage numbers of HSCs were used in the co-cultures on $P_{DL}LA$ surface. This variable was shown to have great effects on the size, number, morphology and generation time of spheroids on 6 well $P_{DL}LA$ coated plates (Figure 3.4).

100 μm to 200 μm in diameter is considered to be the ideal spheroid mean size. In spheroids of more than 200 μm in diameter, hepatocytes in the central section become necrotic (Takabatake *et al*., 1991). This is likely to be due to

hypoxia as oxygen is thought to directly permeate only up to 100 μm depth in the liver tissue (Smith *et al*., 1986; Lipinski, 1989). The sizes of spheroids formed by passage number 4, 6 and 7 HSCs were smaller than 100 μm in diameter, and would therefore maintain oxygenation throughout the spheroid. Also, the number of spheroids in each well of 6 well plates has not been calculated precisely in this study. However, about 30 spheroids at maximum formed by passage number 3, 4 and 7 was observed under the microscope, which shows a good agreement with the method using 20-30 spheroids per well of 6 well plate to prevent merge of adjacent two cell colonies (Lee *et al*., 2004). Efficiency of spheroid formation calculated by the number of cells that form into spheroids divided by the total number of cells can be used in future work (Wu *et al*., 1995). In addition, it has been reported that fast aggregation could be important in preventing early cell death and increasing the cell viability (Okubo *et al*., 2002). The spheroids formed by passage number 4 and 6 HSCs took less time than those generated by passage number 7 HSCs. Therefore, the combination of ideal size and rapid formation suggests that passage number 4 to 6 HSCs may best support viable and functional tissue aggregates.

Table 3.8: a summary of spheroid formations by different passage numbers of HSCs on $P_{DL}LA$ coated plates

	Spheroid formation	**Spheroid size**	**Time for spheroid formation**	**Spheroid morphology**
Passage 0 HSCs	Yes	>200 μm	48 hours	Better defined cell borders and tighter cell conjunctions
Passage 3 HSCs	Yes	>200 μm	48 hours	
Passage 4 HSCs	Yes	<100 μm	72-96 hours	Less defined cell borders and less cell conjunctions
Passage 6 HSCs	Yes	<100 μm	72-96 hours	
Passage 7 HSCs	Yes	<100 μm	114 hours	
Passage 14 HSCs	No	Not Available		
Passage 17 HSCs	No			
Passage 30 HSCs	No			
Conclusions	Best spheroids formed by passage 4/6			

3.4.5 The morphology and functional analysis of rat hepatocytes on 6 well plates

Although a few small aggregates formed on $P_{DL}LA$ coated 12 well plates, spheroids appeared in all culture systems on 6 well plates except on monoculture of collagen-Matrigel sandwich. Apart from spheroids on $P_{DL}LA$ coated plates established in 72 hours, all other spheroids were developed in 6 days.

The secretion of both albumin and urea was exhibited through the whole culture period of 21 days. All three co-cultures showed higher activities than two monocultures during the whole time. For the urea data, it is not sensitive enough to analyze the differences in three co-cultures like previous data; while for the albumin data, cells co-cultured in collagen-Matrigel sandwich and on $P_{DL}LA$ coated plate revealed higher activity all the times. Cells on both these co-cultures showed almost 1,000 times higher amount of albumin but approximately 100 times lower amount of urea than those in a 3D microarray perfusion bioreactor (Powers *et al*., 2002). The reason why the urea secretion is much lower in our model is most likely because of the great ability of waste and toxin removal in the bioreactor.

Due to less sensitivity, less accuracy and less specificity of testosterone metabolism by HPLC, LC-MS/MS was applied to measure 3CYP activities at the same time. CYP3A1 activity showed in all five culture systems on day 1 and day 3. However, it could be only observed from cells co-cultured in collagen-Matrigel sandwich on day 7. CYP1A2 activities were not detectable

in cells of both monocultures and the co-culture on collagen gel on day 3 and only cells co-cultured in collagen-Matrigel sandwich maintained it on day 7. CYP2B6 activities were maintained in cells of all culture systems until day 7, but cells mono-cultured on collagen gel and the co-cultured on collagen gel lost the activities on day 9. Cells co-cultured on $P_{DL}LA$ surface and collagen-Matrigel sandwich showed similar activities on day 9.

The observation that hepatocytes co-cultured with HSCs in collagen-Matrigel sandwich and on $P_{DL}LA$ coated plates exhibited better CYP functions than cells mono-cultured in collagen-Matrigel sandwich on 6 well plates is most likely to be attributable to the formation of the 3D spheroids in these two co-cultures. This further supports the notion that 3D spheroids produced by the combination of hetero-cell-cell interaction and soluble factors from NPCs have greater effects on hepatocyte function than cell-ECM interactions. However, while spheroids formed in both co-culture systems, hepatocytes co-cultured with HSCs in collagen-Matrigel sandwich showed slightly higher functions. This suggests that hepatocyte functions can be further enhanced by cell-ECM interaction within 3D spheroids and this suggestion will be interrogated in further experiments.

The spheroids formed by co-culture of hepatocytes and HSCs in collagen-Matrigel sandwich in this study are hetero-spheroids, which are closer to *in vivo* environment than other homo-spheroids formed by hepatocytes only (Fukuda *et al*., 2003; Nakazawa *et al*.,2006). These spheroids also maintain both high degrees of cell-cell interaction and cell-ECM interaction, while other

spheroids do not favour the cell-ECM interaction (Yamada *et al*., 2001; Lee *et al*., 2004). LC-MS/MS, an advanced method of measuring CYP450 enzyme activity, is applied to assess specific CYP activities including CYP1A2, CYP2B6 and CYP3A1, which shows more accurate data in mass to charge (m/z) ratios than HPLC technology (Thomas *et al*., 2005). Taken together these observations, this spheroid system developed by co-culture of hepatocytes and HSCs in collagen-Matrigel sandwich is a potential candidate for *in vitro* liver development.

Table 3.9: a summary of data of hepatocyte function assays on 6-well plates

	Albumin secretion (mg/ml/µg DNA/24h)	**Urea secretion (ng/ml/ µg DNA/24h)**	**CYP1A2 activity (pmol/min/ µg DNA/24h)**	**CYP3A1 activity (pmol/min/ µg DNA/24h)**	**CYP2B6 activity (pmol/min/µg DNA/24h)**
A	Shown maximum on day 1, decreased to about 0.5 on day 3 and maintained at about 0.5 till day 11	Increased from about 0.01 to 0.04 from day 1 to day 7 and maintained at about 0.06 till day 21	Not shown on day 3/7	Not shown on day 7	Not shown on day 9
B			Not Shown on day 3/7	Not shown on day 7	Shown on day 9 at about 0.13
C	Shown maximum on day 3 and decreased gradually from day 7 to day 21	Increased from about 0.01 to 0.04 from day 1 to day 7 and maintained at about 0.08 till day 21	Not shown on day 3/7	Not shown on day 7	Not shown on day 9
D			Shown on day 7 at about 0.15	Shown on day 7 at about 0.07	Shown on day 9 at about 0.25
E			Shown on day 3 at about 0.13	Not shown on day 7	Shown on day 9 at about 0.35
F	C/D/E higher than A/B (P<0.01), E higher than C/D (P<0.01)	C/D/E higher than A/B from day 9 to day 21 (P<0.01)	D higher than the others (P<0.01)	D higher than the others (P<0.01)	E higher than D (P>0.05), E higher than B (P<0.01)

A= Monoculture on collagen gel

B= Monoculture in collagen-Matrigel sandwich

C= Co-culture on collagen gel

D= Co-culture in collagen-Matrigel sandwich

E= Co-culture on $P_{DL}LA$

F= Conclusions

3.4.6 Conclusion

The key question in this chapter is to answer whether the model of spheroids formed from co-culture of hepatocytes with HSCs on $P_{DL}LA$ coated plates could be further improved by the addition of ECM components, collagen and Matrigel. Hepatocytes co-cultured with HSCs on $P_{DL}LA$ surface showed the best functions on 12 well plates, which is consistent with the formation of 3D aggregates formed by hetero-cell-cell interaction and soluble factors from HSCs. However, on 6 well plates, hepatocytes co-cultured with HSCs in collagen-Matrigel sandwich showed better function than cells co-cultured with HSCs on $P_{DL}LA$, although spheroids formation existed in both co-cultures. This suggests that the addition of ECM (collagen-Matrigel sandwich) can further enhance hepatocyte functions. The experiment on 6 well plates was, however, completed only once and has not been repeated successfully due to difficulties of isolation of primary rat hepatocytes, although a great deal of work has been put to solve the problem (Appendix 3). However, it is reasonable to expect this co-culture system is better than the previous co-culture on $P_{DL}LA$ surface. It combines the benefits of monotypic and heterotypic cell-cell interactions, soluble factors from non-parenchymal cells, 3D spheroids structure, and cell-ECM interaction, which is precise enough to mimic the environment of liver *in vivo*.

Chapter Four:

Cytochrome P450 Induction Studies in Immortalised Human Cell Line: Fa2N-4

4.1 Introduction

4.1.1 CYP induction and inhibition

The modification of the cytochrome P450 (CYP) enzyme activities by inhibition, induction, or activation is of great interest to drug discovery and development scientists, since these modifications represent common causes of drug interactions. CYP inhibition can result from competition between two drugs which are metabolised by the same CYP. It may cause an unexpected increase in the plasma concentration of one or both drugs and also lead to a variety of minor or severe adverse effects. On the other hand, the induction arises from an elevation in the total amount of CYP which may lead to a marked decrease in plasma concentrations of a drug metabolised by the induced CYP. Common tools for the *in vitro* study of drug metabolism and disposition include liver slices, primary hepatocytes and hepatic cell lines. (Hollenberg *et al*., 2002)

4.1.2 Why use hepatic cell lines for CYP induction study?

One of the main obstacles using primary hepatocytes *in vitro* has been the lack of prolonged maintenance of liver specific function. A variety of cell culture methods have been developed to preserve drug-metabolising functions of liver under *in vitro* conditions. These include culturing hepatocytes on or in different basement membranes, co-culturing with other liver-derived or non-liver cell types and culturing in media containing growth factors and cytokines (Riccalton-Banks *et al.*, 2003; Tuschl and Mueller, 2006). However, the goal of creating enduring tissue that fully retains its liver-specific function has yet to be achieved.

Dramatic changes in CYP gene expression are observed during the early culture of human hepatocytes possibly because of a perturbation in the levels of transcription factors (Gomez-lechon *et al.,* 2004). Additionally, large inter-individual variability in CYP expression occurs in human beings due to genotypic and phenotypic variability (Ingelman-sundberg, 2004). These, coupled with limited accessibility, mean that cultured primary human hepatocytes might not be the best model of long-term liver cell culture in terms of liver specific functions.

In contrast to primary hepatocyes, hepatic cell lines have a few advantages, namely, almost unlimited lifespan, stable phenotype, good availability and simple culture conditions. Several hepatic cell lines have been developed and used in liver tissue engineering, including cell lines isolated from human hepatomas, immortalized hepatocytes, cell lines isolated from transgenic animals expressing viral transforming genes, oncogenes or growth factors, hepatocye/hepatoma hybrid cells and 'humanised' metabolically competent hepatocytes. Several hepatic cell lines including HepG2, BC2 and HepaRG (Vermeir *et al.,* 2005; Castell *et al*., 2006; Kanebratt and Andersson, 2008) and the immortalized Fa2N-4 cell line (Mills *et al*., 2004; Ripp *et al*., 2006; Youdim *et al*., 2007; Hariparsad *et al*., 2008) have recently been assessed as replacements of primary human hepatocytes in CYP induction studies.

4.1.3 A novel immortalized human cell line: FA2N-4

Fa2N-4 cells are non-tumorigenic and derived from primary human hepatocytes immortalized by transfection with the SV40 large T-antigen (Steen,

2004; Vermeir *et al*., 2005). Other hepatic human cell lines produced by transfection of hepatocytes with oncogenes (Ha-rasEJ, met, c-Ha-ras, telomerase) lack the complex spectrum of liver specific gene expression of hepatic cells *in vivo* (Hohne *et al*., 1993; Sirica, 1997; Wege *et al*., 2003). However, the Fa2N-4 cell line maintains morphological characteristics of primary human hepatocytes as well as stable expression and inducibility of various drug-metabolising enzymes (Mills *et al*., 2004). More recently, this Fa2N-4 model system has been used to predict the *in vivo* induction response (potency (EC_{50}) and magnitude of effect (E_{max})) of CYP3A4 inducers (Ripp *et al*., 2006). Furthermore, a higher throughput cocktail assay for assessment of CYP1A2, 2C9, 2C19, 2D6 and 3A4 levels in Fa2N-4 cells has been published (Youdim *et al*., 2007; Kenny *et al*., 2008).

4.1.4 Mechanisms of expression and transcription of CYP genes

CYP enzymes are major players in the phase I oxidative metabolism of a wide range of xenobiotics and endobiotics (steroids, fatty acids) (Guengerich, 1993). Only a few CYP genes, out of total 57 in the human genome, are responsible for xenobiotic metabolism. In the human liver a limited number of CYPs, namely CYP1A2, 2B6, 2C8, 2C9, 2C19, 2D6 and 3A4 are responsible for drug biotransformation (Gonzalez *et al*., 1990). Among them, CYP3A4 is the most abundantly expressed, comprising approximately 30 - 40% of the total CYP in human adult liver (Guengerich *et al*., 1999). CYP1A2, 2B6, 2C9 and 3A4, the major inducible CYPs, are selected for this study.

Transcription of CYP genes is regulated by several key liver enriched transcription factors (LETFs) including CCAAT/enhancer binding protein (C/EBP) (Rodriguez-antona, *et al*., 2003) and hepatocyte nuclear factor (HNF) 1, 3 and 4 (Schrem *et al*., 2002, 2004). Control is exercised by repressors including the small heterodimeric partner (SHP) (Lee *et al*., 2000) and the chicken ovalbumin upstream promoter transcription factors (COUP - TFs) (Tsai *et al*., 1997) as well as two main co-repressors, silencing mediator of retinoid and thyroid receptor (SMAT) and nuclear receptor co-repressor (NCoR) (Burke *et al*., 2000). In addition, the transcriptional activation of CYP genes is regulated by nuclear receptor-dependent mechanisms: the arylhydrocarbon receptor (AhR), constitutive androstane receptor (CAR) and pregnane X receptor (PXR), which regulate genes CYP1A2, CYP2B6 and CYP3A4, respectively (Tirona and Kim, 2004). Recently, the expression of PXR and AhR has been showed to be similar between Fa2N-4 cells and human hepatocytes; however both CAR and several hepatic uptake transporters including the OATPs are significantly lower in the cell line compared to primary hepatocytes (Hariparsad *et al*., 2008).

4.1.5 CYP induction in Fa2N-4 at mRNA expression levels

Analysis of mRNA levels is considered the most sensitive method of determining liver specific function in hepatocytes *in vitro*. The transcription and translation of mRNA for a single CYP enzyme is a complex process mediated by cross-regulated components and it is therefore essential to understand the patterns of gene transcription underlying function and ultimately to control them in order to achieve prolonged hepatocyte function *in*

vitro. In this chapter, assessments of both CYP activity and mRNA level are made.

4.1.6 Reverse transcription polymerase chain reaction (RT - PCR)

Four methods are in common use for the analysis of gene transcription: northern blotting, *in situ* hybridization, RNAse protection assays (RPAs) and reverse transcription polymerase chain reaction (RT-PCR). Northern blotting and RPAs are gold standards but they require more RNA than is sometimes available, whereas *in situ* hybridization is qualitative rather than quantitative. RT-PCR is particularly valuable when amounts of RNA are low, since an amplification step is involved. It is an *in vitro* method for enzymatically amplifying defined sequences of RNA and permits the analysis of different samples from as little as one cell in the same experiment. It is the most sensitive and the most flexible of the quantification methods and it can discriminate closely related mRNA.

Currently four different methods, TaqMan® (Applied Biosystems, Foster City, CA, USA), Molecular Beacons, Scorpions® and SYBR® Green (Molecular Probes), are available for real-time PCR. In this chapter the use of TaqMan® is described. TaqMan probes are sequence-specific oligonucleotides with a fluorophore and a quencher. The fluorophore is at the 5' end of the probe and the quencher is usually located at the 3' end or internally. During the PCR extension step, the probe is cleaved by the 5'-3' exonuclease activity of Taq DNA polymerase, separating the fluorophore and quencher. This results in

detectable fluorescence that is proportional to the amount of accumulated PCR product (Figure 4.1).

In this chapter, experiments are described that use QuantiTect® Multiplex RT-PCR Kit (QIAGEN) for the RT-PCR technique. This allows one-step quantitative RT-PCR (qRT-PCR), which permits both reverse transcription and PCR to take place in a single tube, so there is no need to open the tube once the reverse transcription reaction has been started and the contamination of other non-related RNA is greatly reduced. Also, it contains omniscript and sensiscript reverse transcriptases, which are designed for reverse transcription of RNA amounts greater than 50 ng and smaller than 50 ng respectively. This combination provides highly efficient and sensitive reverse transcription over a wide of range of RNA template amounts. In addition, a modified form of Taq DNA polymerase (HotStar Taq DNA polymerase) is provided, which is in an inactive state and has no enzymatic activity at room temperature but is activated by a 15 minutes 95ºC incubation step. This prevents the formation of mis-primed products and primer-dimers during reaction setup and first denaturation step. Most importantly, the QuantiProbes (Figure 4.2) are sequence-specific dual labeled probes. Besides a fluorophore at the 3' end and a quencher at the 5'end, there is a minor groove binder at the 5' end. The minor groove binder prevents hydrolysis of the QuantiProbe by the 5'-3' exonuclease activity of Taq DNA polymerase and the QuantiProbe is simply replaced by the template using Superbases technology during the PCR extension step. This increases the annealing efficiency and enables successful detection of difficult templates. Together with QuantiTect Multiplex RT-PCR buffer, use of uracil-

N-glucosylase (UNG) and ROX passive reference dye, QuantiTect®Multiplex RT-PCR Kit is an ideal tool for RT-PCR technology.

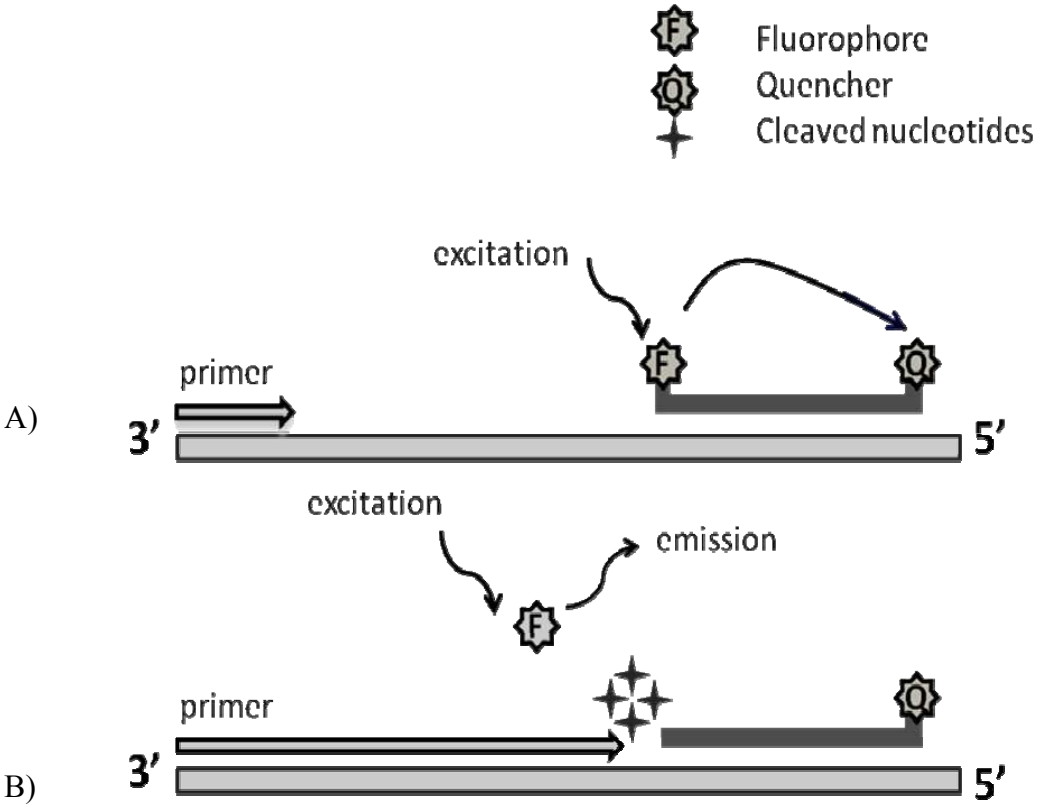

Figure 4.1: principle of Taqman probes in quantitative real-time PCR. A) Both the Taqman probe and the PCR primers anneal to the target sequence during the PCR annealing step. The proximity of the fluorophore with the quencher results in efficient quenching of fluorescence from the fluorophore. B) Taq DNA polymerase extends the primer. 5'-3' exonuclease activity of the enzyme degrades the probe, resulting in physical separation of the fluorophore from the quencher. Increased fluorescence from the released fluorophore is proportional to the amount of accumulated PCR product.

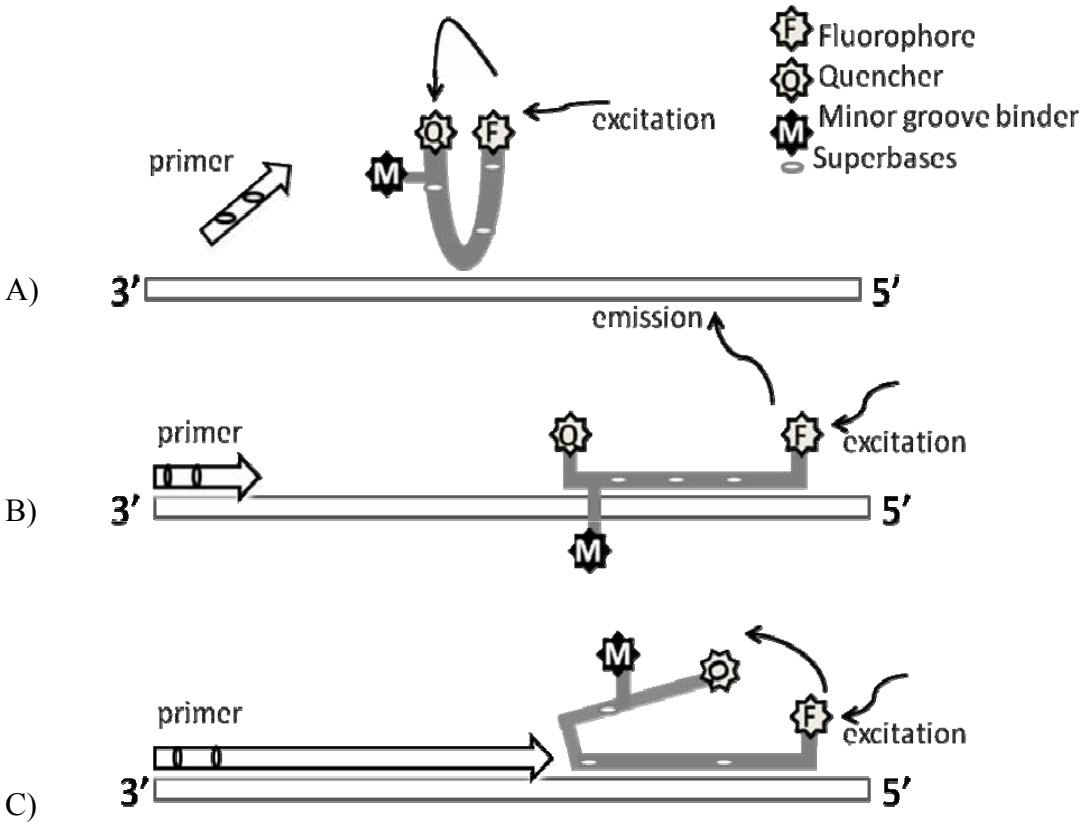

Figure 4.2: principle of QuantiProbes in quantitative real-time PCR. A) The QuantiProbe forms a random structure in solution when it is not bound to its target sequence. The proximity of the fluorophore with the quencher prevents the fluorophore from fluorescing. B) During the PCR annealing step, the QuantiProbe hybridizes to its target sequence, which separates the fluorophore and quencher, resulting in a fluorescent signal. The amount of signal is directly proportional to the amount of target sequence and it is measured in a real time to allow quantification of the amount of target sequence. C) During the PCR extension step, the QuantiProbe is displaced from the target sequence, bring the fluorophore and quencher into closer proximity, resulting in quenching of fluorescence.

4.1.7 Aims

The purpose of this study was to simultaneously characterize CYP1A2, CYP2C9, CYP3A4 and CYP2B6 induction in Fa2N-4 cells through assessment of mRNA, protein and activity endpoints for a range of prototypical compounds (previously assessed in human hepatocytes) with known positive and negative induction potential.

The induction assessment of both mRNA and activity is favorable and the series of experiments performed were:

- Time course of mRNA and activity CYP induction in Fa2N-4 cells
- Assessment of CYP1A2, CYP2C9, CYP2B6 and CYP3A4 induction in Fa2N-4 cells at the level of activity using 22 prototypical compounds by LC-MS/MS
- Assessment of CYP1A2, CYP2B6 and CYP3A4 induction in Fa2N-4 cells at the level of mRNA using 22 prototypical compounds by RT-PCR

The methodologies represented here have assisted a thorough evaluation of Fa2N-4 cells as a potential tool for CYP induction screening, using both activity and mRNA endpoints for the major inducible CYP isoforms.

4.2 Material and Methods

4.2.1 Chemicals and Reagents.

Bupropion, carbamazepine, 6-(4-chlorophenyl) imidazo[2,1-b][1,3]thiazole-5-carbaldehydeO-(3,4-dichlorobenzyl)oxime (CITCO), clotrimazole, dexamethasone, diclofenac, 4′-hydroxydiclofenac, mifepristone, β-naphthoflavone, nifedipine, omeprazole, paracetamol, phenacetin, phenobarbital, phenytoin, rifampicin, rifapentine, reserpine, troglitazone verapamil, and β-nicotinamide adenine dinucleotide phosphate, reduced form (NADPH), were purchased from Sigma-Aldrich (Gillingham, UK) and were of the highest grade available. Bufuralol, efavirenz, hydroxybupropion, hyperforin, S-mephenytoin, midazolam, 1′-hydroxymidazolam, paclitaxel, pioglitazone, rifabutin, ritonavir and sulfinpyrazone were purchased from Sequoia Research Products Ltd. (Oxford, UK). Acetonitrile, dimethyl sulfoxide (DMSO), ethanol and formic acid were purchased from Fisher Scientific (Loughborough, UK) and were of the highest grade available. Collagen type I coated 24-well plates, tissue-cultured treated flasks and trypsin-ethylene diamine tetracetic acid (EDTA) were purchased from BD Biosciences (Oxford, UK). Cryopreserved Fa2N-4 cells, Multi-Function Enhancing (MFE) plating media and MFE support media with supplement A were obtained from Xenotech Ltd (Lenexa, KA, USA). DNase I RNase free kit and RNase free water were from Invitrogen (Paisley, UK).

4.2.2 Cell Culture

Fa2N-4 cells were seeded on tissue culture treated T75 flask, maintained in MFE support media with supplement A (1 µl/ml) and incubated at 37˚C, 5%

carbon dioxide and 95% relative humidity. MFE support media was changed every two days and the cells were passaged until they were approximately 80% confluent. For passaging, the cells were trypsinized for 15 minutes, harvested in MFE plating medium, centrifuged at 120g for 5 minutes and resuspended in fresh MFE plating medium. Cells were then diluted to 0.2 x 10^6 cells/ml and either re-seeded in tissue culture treated flasks (~2 x 10^6 cells/flask) or seeded on type I collagen coated 24-well plates (0.1 x 10^6 cells/well; 0.5 ml/well). After 24 hours, MFE plating medium was replaced with MFE support medium containing supplement A. All Fa2N-4 cells used in the following experiments were between passages 2 and 8.

4.2.3 Enzyme induction experiment

Fa2N4 cells were supplemented with MFE support medium for a few days on type I collagen 24-well plates. Stock solutions (× 1000) of all test compounds at all concentrations were prepared in DMSO and diluted 1000-fold in MFE support medium containing supplement A to give a final DMSO content of 0.1% v:v. With the exception of phenobarbital (0.01-2 μM) prepared in MFE support medium to ensure solubility and hyperforin (0.01-2 μM) prepared in methanol, each inducer was prepared to a serial of six concentrations in DMSO to allow full induction dose response curves to be generated for each compound. According to the respective E_{max} concentrations from literature data for Fa2N-4 cells and human hepatocytes (LeCluyse *et al.*, 2000; Maden *et al.,* 2003; Faucette *et al.,* 2004, 2007; Ripp *et al.,* 2006), compounds and concentration ranges were as follows: Rifampicin 0.1 - 20 μM, Carbamazepine 3.13 - 250 μM, Clotrimazole 0.13 - 10 μM, Dexamethasone 3.13 - 250 μM,

Nifedipine 0.5 - 100 μM, Paclitaxol (Taxol) 0.38 - 30 μM, Phenytoin 3.13 - 250 μM, Pioglitazone 0.5 - 100 μM, Rifapentine 0.25 - 20 μM, Reserpine 0.63 - 50 μM, Rifabutin 0.1 - 20 μM, Ritonavir 0.06 - 5 μM, Troglitazone 0.1 - 20 μM, Sulfinpyrazone 3.13 - 250 μM, Mifepristone 0.13 - 10 μM, β-napthoflavone 0.63 - 50 μM, 50 μM Omeprazole, CITCO 0.13 - 10 μM, Verapamil 0.5 - 100 μM and Efavirenz 0.13 - 10 μM. Any higher concentration of each compound results in cell toxicity or drug insolubility. All aliquots were subsequently diluted in MFE support medium at the concentration of 1μl/ml and the solutions (0.5 ml) were added to appropriate wells of each 24-well plate. Some wells were supplemented with DMSO diluted in MFE support medium (1μl/ml) as controls. The MFE support medium with the inducers were changed every 24 hours for the next three days.

4.2.4 Isolation and quantification of mRNA

Total RNA was extracted from the cells in RLT buffer using RNeasy 96 kit (Qiagen, West Sussex, UK). The method 'isolation of RNA from animal cells by the vacuum protocol' was applied according to instructions supplied by QIAGEN. Quant-iT^{TM} RiboGreen RNA reagent and assay kit (Invitrogen, Paisley, UK) were used to quantify total RNA with a fluorescence microplate reader at 485 nm emission and 530 nm excitation wavelengths according to the manufacturer's instructions. The data from Ribogreen were used to normalize the CYP1A2, 2B6 and 3A4 mRNA results from qRT-PCR.

The standard curve of qRT-PCR was prepared from human hepatocyte mRNA pooled from cells that were induced separately with rifampicin, phenobarbital

and omeprazole. A no-reverse transcriptase control (No RT) and a no template control (NTC) should always be included to provide confidence that gene amplification is specific and that there has been no contamination of reagents.

The PCR primers and Taqman probes for CYP1A2, CYP2B6, and CYP3A4 were selected for their high specificity to the human CYP isoforms, afforded by their exon–exon spanning domains. Appropriate primers and probes were selected using primer express 2.0 software (Applied Biosystems, Foster City, CA, USA) and oligo mapping. A BLAST database search (http://www.ncbi.nlm.nih.gov/BLAST) was carried out to ensure selectivity. Primers and probes were synthesized by Eurogentec (Basel, Switzerland).

Duplex assay was used for CYP1A2 and CYP3A4, and single plex assay was used for CYP2B6 only. Both assays have been previously established and optimised in DMPK, Astrazeneca, Charnwood. The PCR reaction mixture containing the 2 primer-probe pairs/ 1 primer-probe pairs and complete mastermix was prepared using the two tables (Table 4.1 and 4.2) below for duplex and single plex assays respectively.

Table 4.1: the duplex reaction mixture for CYP1A2 and 3A4

	Volume (µl) per reaction	Volume (µl) for 105 reaction
CYP3A4 Forward primer (10 µM)	0.125	13.125
CYP3A4 Reverse primer (10 µM)	0.75	78.75
CYP3A4 Probe (5 µM)	2.5	262.5
CYP1A2 Forward primer (10 µM)	0.125	13.125
CYP1A2 Reverse primer (10 µM)	0.75	78.75
CYP1A2 probe (5 µM)	0.25	26.25
2 x NoRox Master mix	25	2625
Multiplex RT Mix	0.5	52.5
dH2O	15	1575
Total volume	45	4725

Table 4.2: the single reaction mixture for CYP2B6

	Volume (µl) per reaction	Volume (µl) for 105 reaction
Forward primer (10 µM)	0.125	13.1
Reverse primer (10 µM)	0.75	78.75
probe (5 µM)	0.25	26.25
2 x NoRox Master mix	12.5	1312.5
Multiplex RT Mix	0.25	26.25
dH2O	6.125	643.1
Total volume	20	2100

The mRNA samples, 2× Master mix, primer-probe sets (Table 4.3), QuantiTect Multiplex RT-PCR No ROX Master Mix Kit (Qiagen, West Sussex, UK) were thawed, kept on ice during the whole experiment period and returned to -20°C immediately after use. The Mx3005P real-time cycler with MxPro software (Stratagene, Amsterdam, Netherlands) was setup according to Table 4.4.

Table 4.3: primers and probes for CYP1A2, 2B6 and 3A4

Gene	**CYP1A2**
Forward Primer: (5′ → 3′)	CTCCTCCTTCTTGCCCTTCA
Reverse Primer: (5′ → 3′)	GGTTTACGAAGACACAGCATTTCTT
Probe: (5′ → 3′)	AGCACAACAAGGGACACAACGCTGAAT
Gene	**CYP2B6**
Forward Primer: (5′ → 3′)	CAAGAGTTCCTGAAGATGCTGAAC
Reverse Primer: (5′ → 3′)	AGGAAAGTATTTCAAGAAGCCAGAGA
Probe: (5′ → 3′)	TGTTCTACCAGACTTTTTCACTCATCAGCTCTGTATTC
Gene	**CYP3A4**
Forward Primer: (5′ → 3′)	GCAGGAGGAAATTGATGCAGTT
Reverse Primer: (5′ → 3′)	GTCAAGATACTCCATCTGTAGCACAGT
Probe: (5′ → 3′)	TACCCAATAAGGCACCACCCACCTATGA

Table 4.4: Mx3005P cycle times for one-step qRT-PCR

Step	Time	Temperature (º C)
RT	20 minutes	50
PCR initial activation	15 minutes	95
	2-step Cycling (40 –50 cycles)	
Denaturation	45 seconds	94
Annealing/extension	75 seconds	60

Each mRNA sample (5 µl) was added to a 96-well PCR plate and followed by a 45 µl or 20 µl of each PCR reaction mixture. After that, an optically clear plate lid was carefully taken and placed over a prepared PCR plate on the plate sealer bed. The plate sealer was then pushed down and held for 10 seconds. Finally, the plate was briefly centrifuged to remove air any bubbles before the qRT-PCR started.

4.2.5 Statistical analysis

All the results are expressed as mean and standard deviation of triplicate determinations in different cell passages unless otherwise specified.

The parameters E_{max} and EC_{50} were determined from dose–response data, where E_{max} is the maximum observed induction at an optimum concentration; and EC_{50} is the effective concentration that supports half-maximal induction. To estimate EC_{50} values, dose-response data were fitted to a simple E_{max} model with a Hill function according to the following equation:

$$Y= (E_{max} \cdot X^y)/(EC_{50}^y + X^y)$$

using Origin 6.0 (MicroCal, Northampton, MA, USA). Similar to the approach taken by Ripp *et al*. (2006), data points from wells with some evident toxicity, based on visual inspection of cell morphology, were excluded from the fits and the E_{max} was set at the observed E_{max} to prevent extrapolation of the curve fit beyond measured data.

4.3 Results

4.3.1Time course of mRNA and activity CYP induction in Fa2N-4 cells

The Fa2N-4 cells were treated with rifampicin and β-naphthoflavone for 24, 48 or 72 hours. The CYP3A4 enzyme activity and mRNA levels were measured at these three time points. For CYP3A4 activity (after rifampicin treatment), the fold increased gradually from 24 hours to 72 hours and reached maximal fold at 72 hours (Figure 4.3A). For the rifampicin mRNA data, the fold-induction at 48 hours was much higher than at 24 hours, but the fold-induction at 72 hours was similar with that at 48 hours (Figure 4.3B). For the β-naphthoflavone mRNA data, maximal CYP1A2 induction occurred at 24 hours and was maintained up to 72 hours (Figure 4.4B), whilst β-naphthoflavone induced CYP1A2 activity increased to 72 hours at the top two concentrations (6 and 25 μM) (Figure 4.4A). Therefore, 72 hours was chosen as the optimal incubation time for measuring mRNA as well as activity of CYP1A2 and CYP3A4.

A)

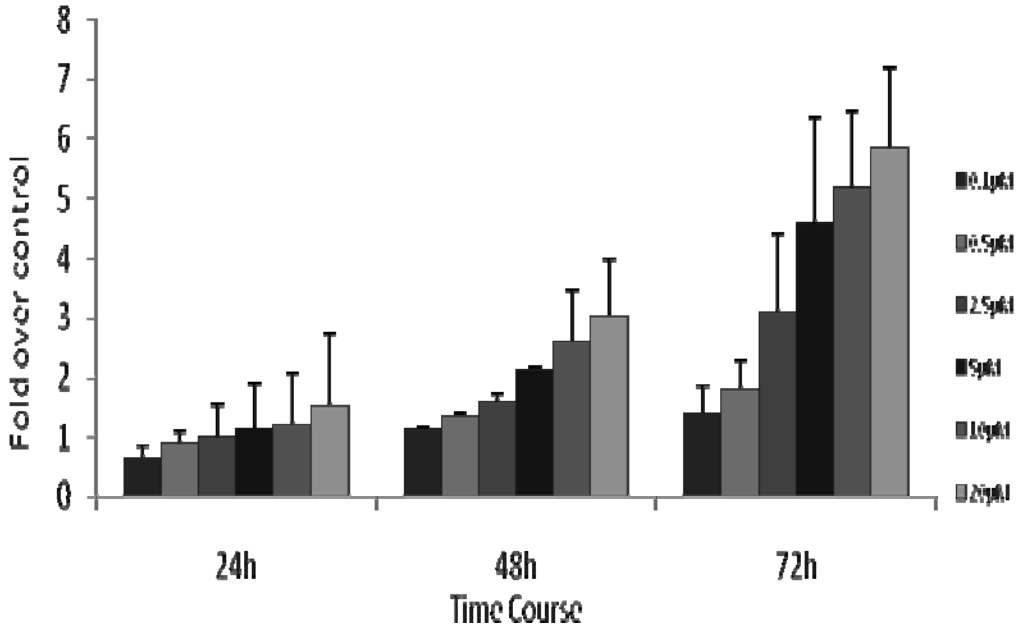

B)

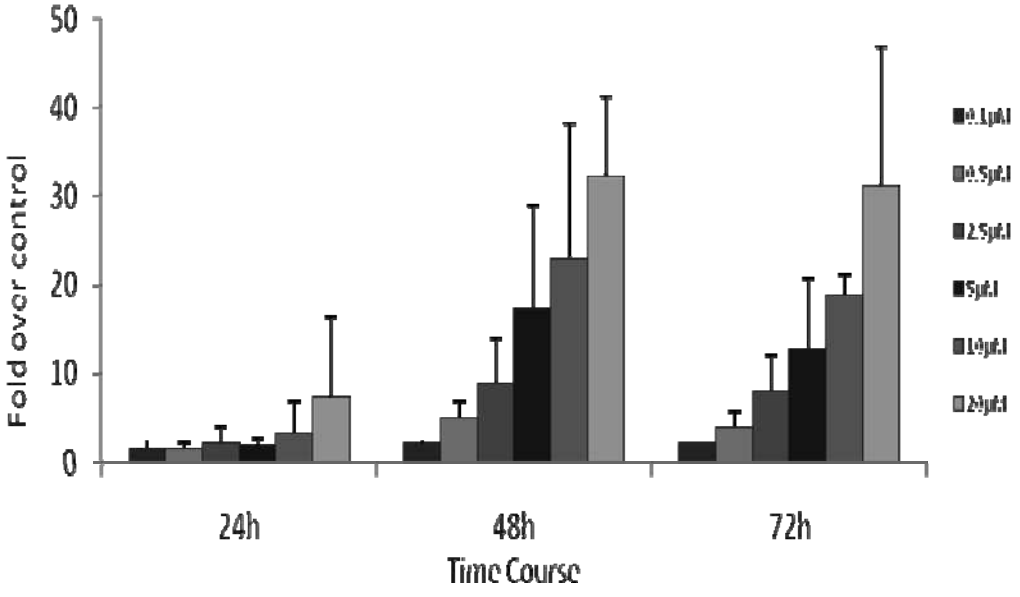

Figure 4.3: rifampicin CYP3A4 activity (A) and mRNA (B) at 24, 48 and 72 hours. Data are mean n=2 experiments ± S.D.

A)

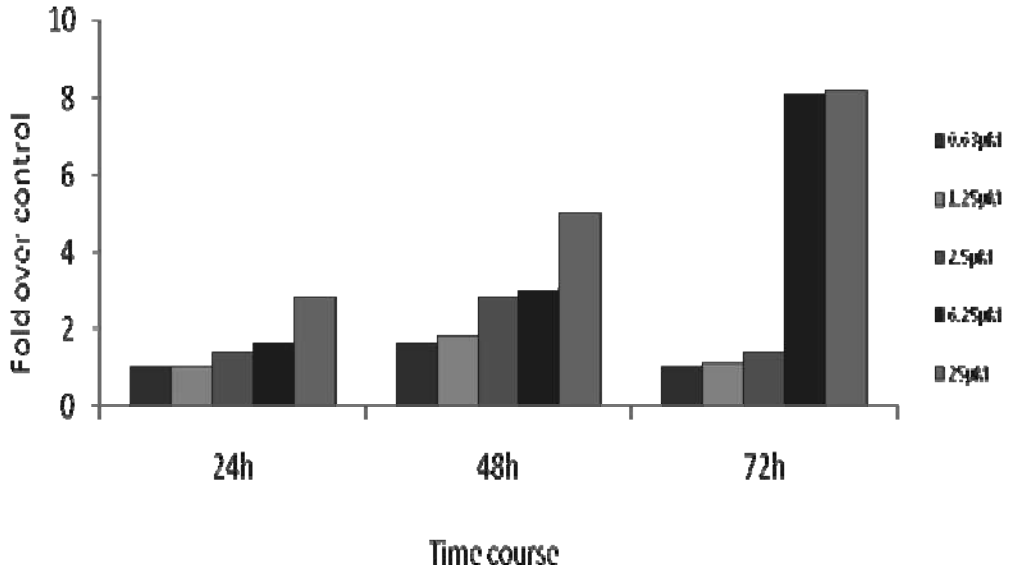

B)

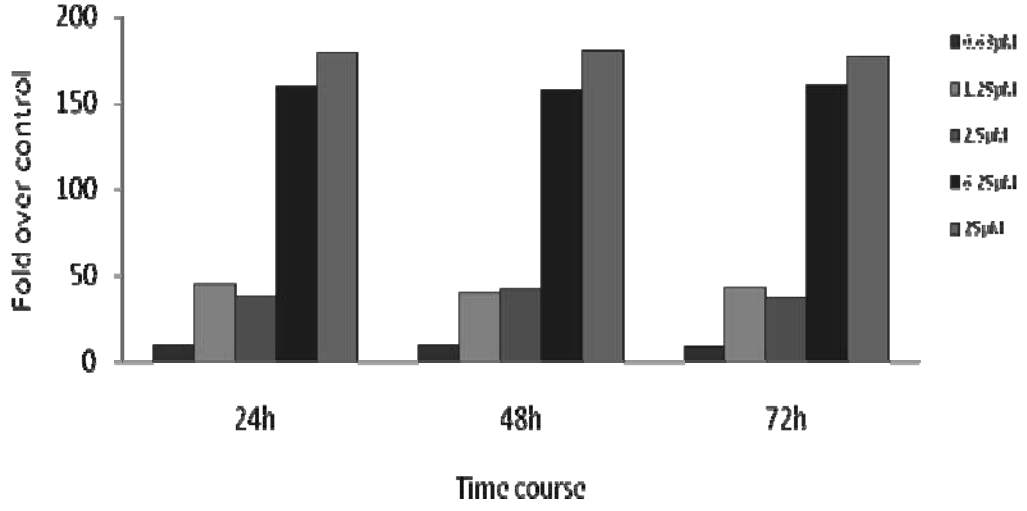

Figure 4.4: β-naphthoflavone CYP1A2 activity (A) and mRNA (B) at 24, 48 and 72 hours. Data are n=1 experiment

4.3.2 Induction profiles of prototypical CYP1A2, CYP2C9, CYP2B6 and CYP3A4 inducers in Fa2N-4 cells

The impact of 22 prototypical compounds on CYP1A2, CYP2C9, CYP3A4 and CYP2B6 activity and mRNA levels has been investigated using the Fa2N-4 cell line. Compounds were selected to represent a range of positive and negative inducers of CYP3A4 (Ripp *et al*., 2006), CYP1A2 and CYP2B6 through activation of pregnane X receptor (PXR), Aryl hydrocarbon receptor (AhR) and constitutive androstene receptor (CAR) respectively.

Fa2N-4 cells were treated for three days with varying concentrations of test compounds. Both CYP activities and mRNA levels were normalised to the vehicle control, and expressed as fold induction. Treatment with rifampicin resulted in an E_{max} of 6-fold and 3.5–fold induction of CYP3A4 and CYP2C9 activity respectively, whilst an E_{max} of 36-fold induction of CYP3A4 at the mRNA level was observed (Figure 4.5). Both CYP3A4 activity and mRNA were increased in a dose-dependent manner. Also, CYP2B6 was induced at the level of mRNA and activity by rifampicin (E_{max} 4-fold and 3-fold respectively). The E_{max} values for induction of CYP3A4 and CYP2C9 activity following for treatment with phenobabital were 4.5-fold and 3-fold respectively. (Figure 4.6A) The E_{max} value of CYP3A4 mRNA induction was 12-fold (Figure 4.6B). The effects of ß-napthoflavone on CYP1A2 activity and mRNA showed an E_{max} of 11-fold and 217-fold to the vehicle controls respectively (Figure 4.7). No induction of other isoforms mRNA and activity was noted.

A)

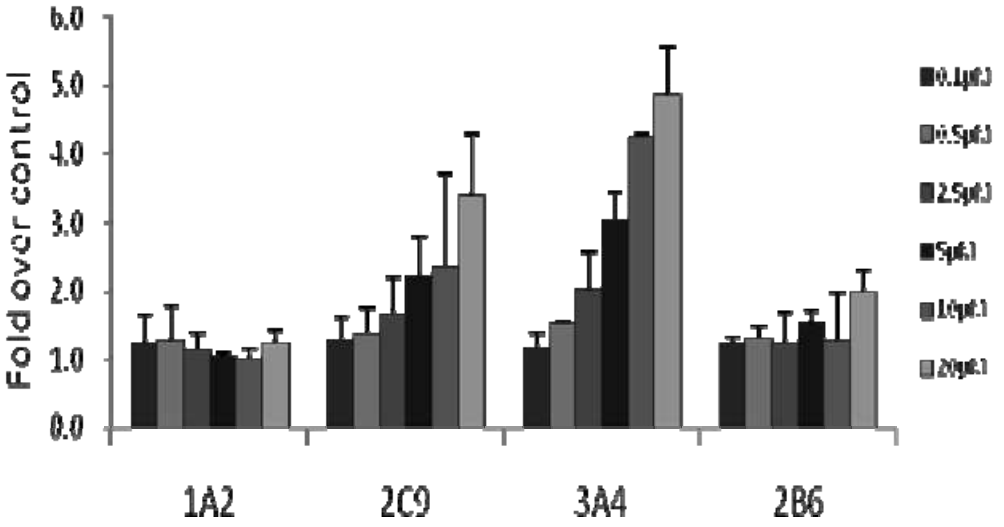

B)

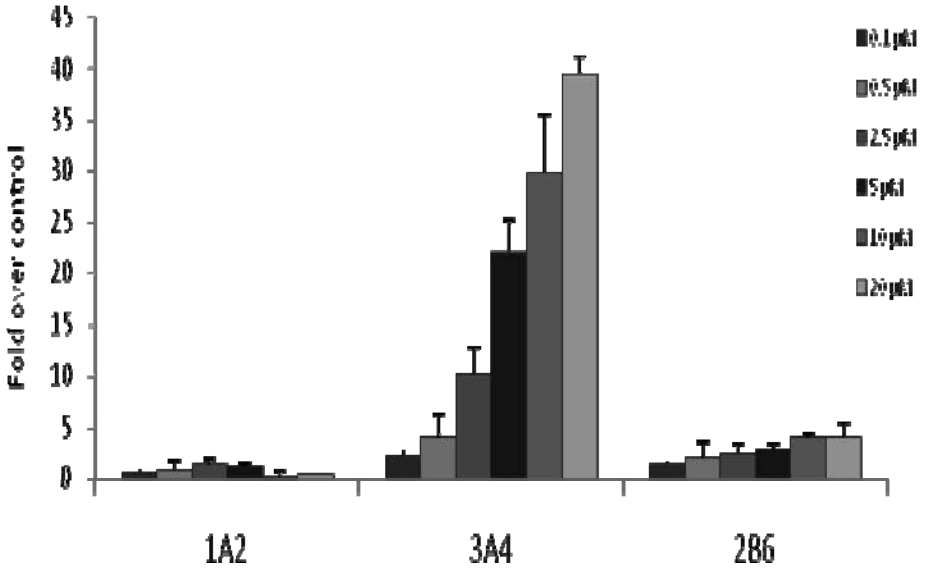

Figure 4.5: effects of rifampicin on CYP1A2, 2C9, 3A4 and 2B6 activity levels (A) as well as on CYP1A2, 3A4 and 2B6 mRNA levels (B). A serial of six concentrations of rifampicin was added to Fa2N-4 cells in the MFE support medium for continuous 72 hours. Medium containing the rifampicin was changed every 24 hours. CYP activities and CYP mRNA levels were measured by LC/MS-MS and qRT-PCR, respectively. Data are mean n=2 experiments ± S.D.

A)

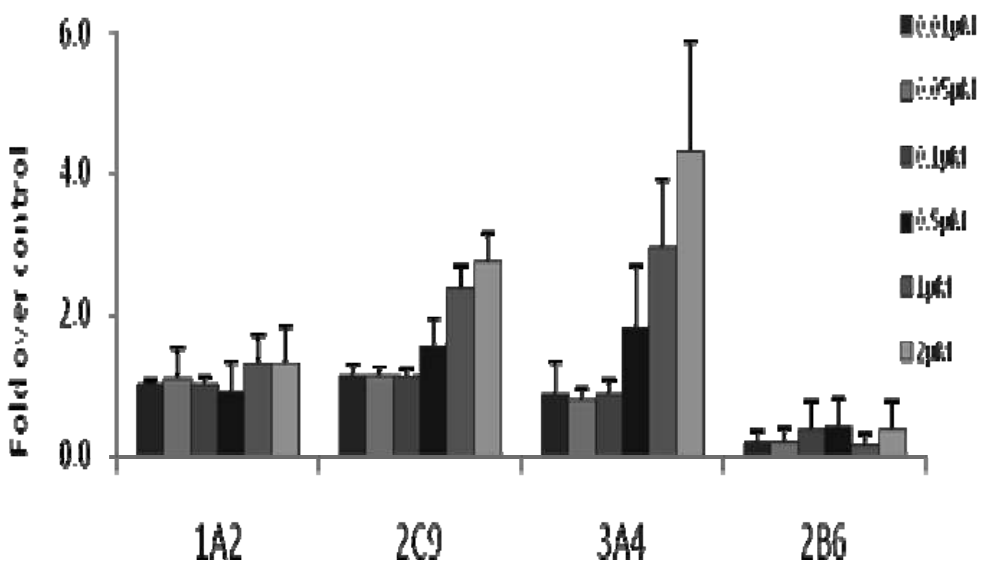

B)

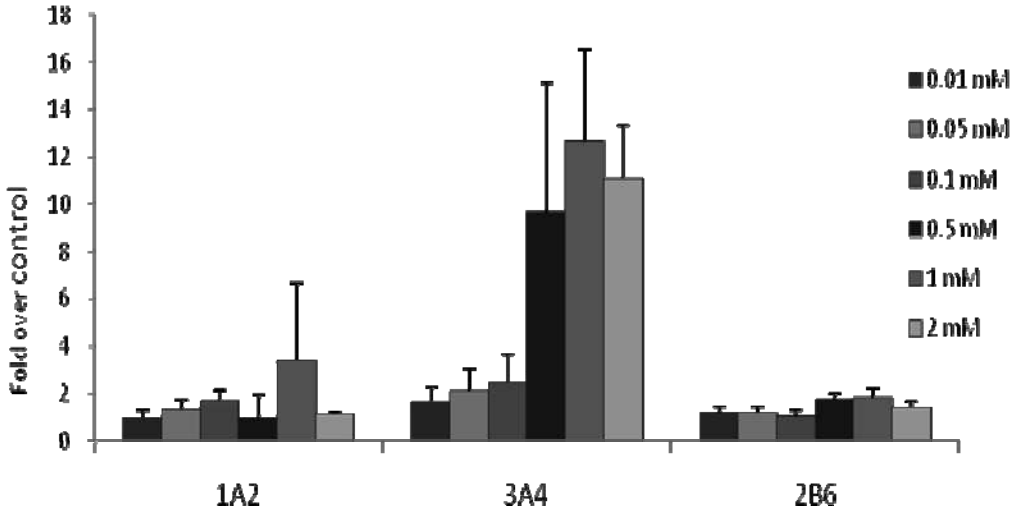

Figure 4.6: effects of phenobarbital on CYP1A2, 2C9, 3A4 and 2B6 activity levels (A) as well as on CYP1A2, 3A4 and 2B6 mRNA levels (B). A serial of six concentrations of phenobarbital was added to Fa2N-4 cells in the MFE support medium for continuous 72 hours. Medium containing the phenobarbital was changed every 24 hours. CYP activities and CYP mRNA levels were measured by LC/MS-MS and qRT-PCR, respectively. Data are mean n=2 experiments ± S.D.

A)

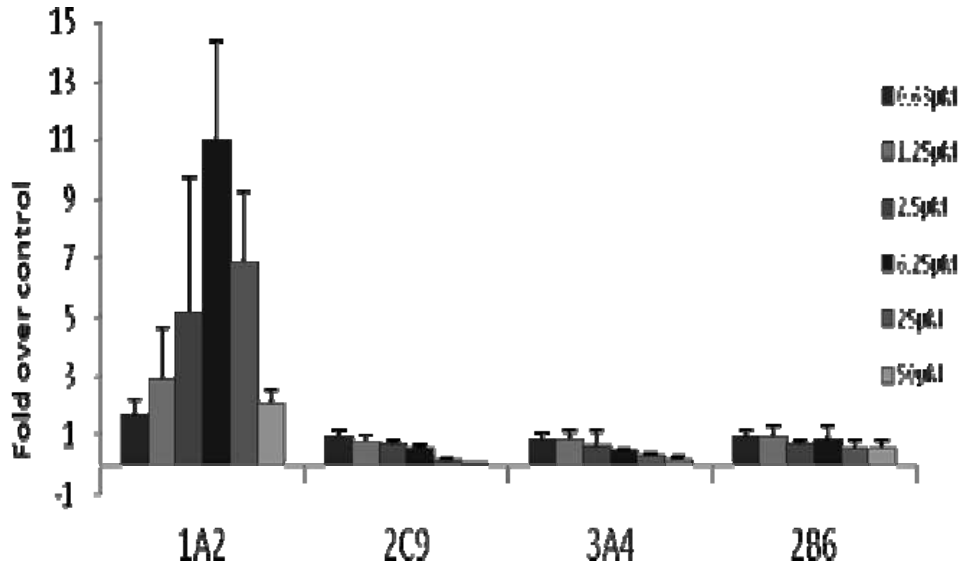

B)

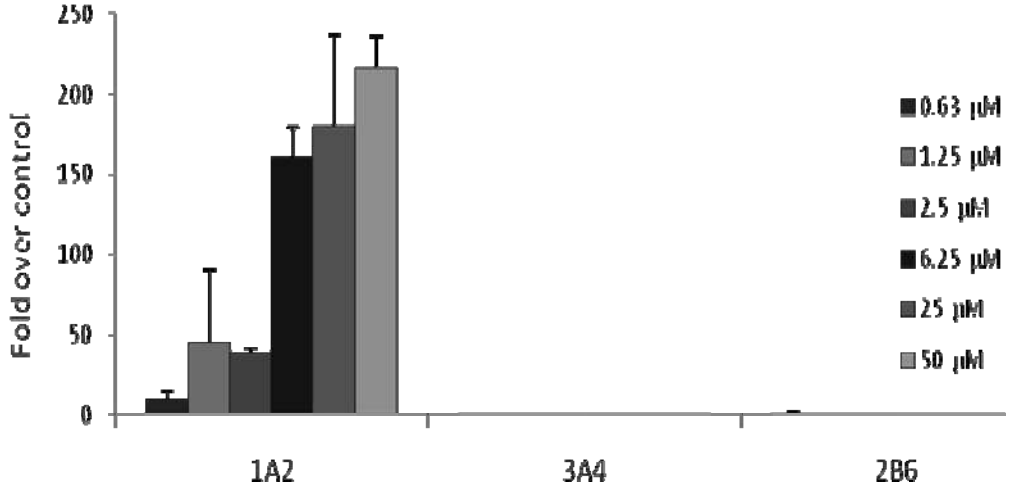

Figure 4.7: effects of β-naphthoflavone on CYP1A2, 2C9, 3A4 and 2B6 activity levels (A) as well as on CYP1A2, 3A4 and 2B6 mRNA levels (B). A serial of six concentrations of β-naphthoflavone was added to Fa2N-4 cells in the MFE support medium for continuous 72 hours. Medium containing the β-naphthoflavone was changed every 24 hours. CYP activities and CYP mRNA levels were measured by LC/MS-MS and qRT-PCR, respectively. Data are mean n=2 experiments ± S.D.

4.3.3 E_{max} and EC_{50} parameters for CYP1A2 and CYP3A4 inducers in Fa2N-4 cells

The E_{max} and EC_{50} values for CYP1A2 mRNA induction by all test compounds were estimated and are listed in Table 4.5. More than 2-fold induction of CYP1A2 mRNA was observed in a total of 6 compounds. β-naphthoflavone demonstrated both CYP1A2 mRNA and activity induction with an E_{max} of 217-fold and 11-fold observed, respectively. The EC_{50} for β-naphthoflavone CYP1A2 mRNA was 8 μM. CYP1A2 mRNA and activity induced by omeprazole gave E_{max} values of 425-fold and 16-fold respectively. CYP1A2 mRNA and activity showed does-dependent induction with E_{max} value of 35-fold and 3-fold respectively. No CYP1A2 induction was observed following treatment of Fa2N-4 cells with carbamazepine, clotrimazole, dexamethasone, efavirenz, paclitaxel, phenobarbital, phenytoin, rifabutin, rifampicin, rifapentine, ritonavir, pioglitazone, sulfinpyrazone, mifepristone, troglitazone, hyperforin or verapamil.

Table 4.5: E_{max} and EC_{50} values of CYP1A2 mRNA induction

	EC_{50} (μM)	E_{max} (fold induction)	CYP1A2 induction in human hepatocytes
Omeprazole	ND	425*	√
β-Naphthoflavone	8	217	√
CITCO	2	35	×
Clotrimazole	1	16	×
Nifedipine	2	16	×
Reserpine	NA	3	×

NA= not appropriate to define EC50 from data fit; ND = not determined;

*incubated at 50 μM only

√ (×) = CYP1A2 induction in human hepatocytes (not) shown in the literature

The E_{max} and EC_{50} parameters of CYP3A4 mRNA induction by all test compounds were calculated and are listed in Table 4.6. Mostly compounds (17 of the 22) exhibited greater than 2-fold induction of CYP3A4 mRNA, which were characterized to 6% of rifampicin E_{max}. Among these compounds, phenytoin, nifedipine, rifapentine, phenobarbital, rifabutin, and ritonavir induced CYP3A4 mRNA more than 20% of rifampicin mRNA E_{max}. Other compounds including phenytoin, dexamethasone, pioglitazone, phenobarbital and rifapentine achieved CYP3A4 activity greater than 2-fold, which was relvant to more than 40% of rifampicin CYP3A4 activity E_{max}. However, mifepristone, β-naphthoflavone, troglitazone and omeprazole demonstrated no CYP3A4 induction following exposure to Fa2N-4 cells.

Table 4.6: E_{max} and EC_{50} values of CYP3A4 mRNA induction

	EC_{50} (μM)	E_{max} (fold induction)	E_{max} (% maximal rifampicin induction)	CYP3A4 induction in human hepatocytes
Rifampicin	4	36	100	√
Rifapentine	3	27	75	√
Nifedipine	8	13	36	√
Phenobarbital	205	12	33	√
Phenytoin	74	10	28	√
Rifabutin	0.3	8	22	√
Ritonavir	0.2	8	22	√
Reserpine	3	7	19	√
Sulfinpyrazone	8	7	19	√
Paclitaxel	2	6	17	√
Efavirenz	0.7	5	14	√
Verapamil	1.3	5	14	√
Carbamazepine	11	4	11	√
Clotrimazole	0.4	4	11	√
CITCO	0.1	3	8	√
Dexamethasone	5	3	8	√
Hyperforin	0.1	3	8	√
Pioglitazone	1.2	2	6	√
β-Naphthoflavone	NA	1	3	×

NA= not appropriate to define EC50 from data fit

√ (×) = CYP3A4 induction in human hepatocytes (not) shown in the literature

Atypical or bell-shaped dose response curves for CYP3A4 mRNA were observed for rifampicin, rifapentine clotrimazole, paclitaxel, pioglitazone, reserpine and ritonavir. Among these compounds, rifampicin and rifapentine are two clearly CYP 3A4 inducers in Fa2N- 4 cells with E_{max} of 36 fold and 27 fold as well as EC_{50} of 4.2 μM and 3 μM respectively (Figure 4.8 and 4.9). The E_{max} of rifapentine is corresponded to 75 % of rifampicin maximal induction. However, in order to fit the dose response curve the final data point was omitted as induction decreased as concentration increased (Figure 4.10 and 4.11). In terms of clotrimazole, paclitaxel and pioglitazone, they were cytotoxic at their top concentrations tested under microscope through their morphology, but no other quantitative assessment of cytotoxicicty was carried out.

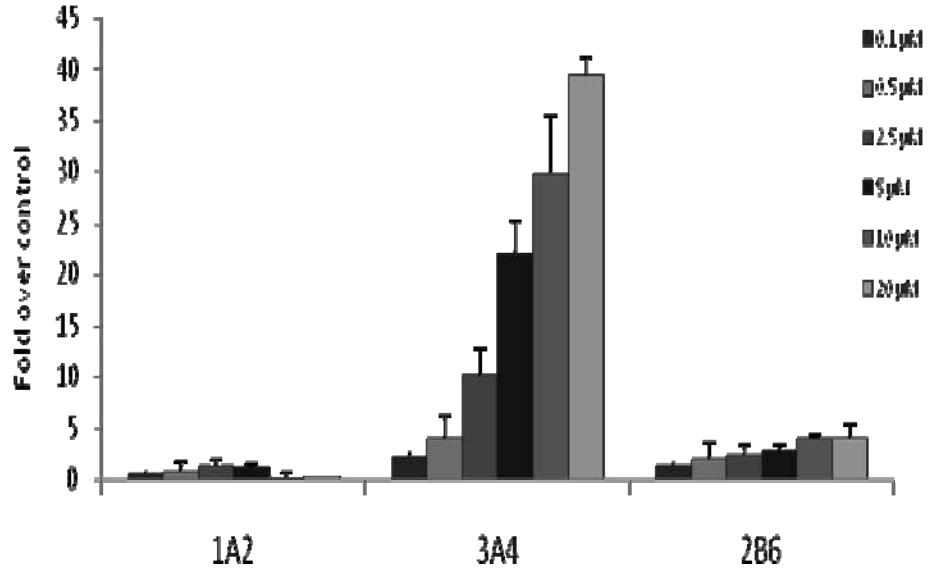

Figure 4.8: the effect of rifapentine on CYP3A4 mRNA level. Data are mean n=2 experiments ± S.D.

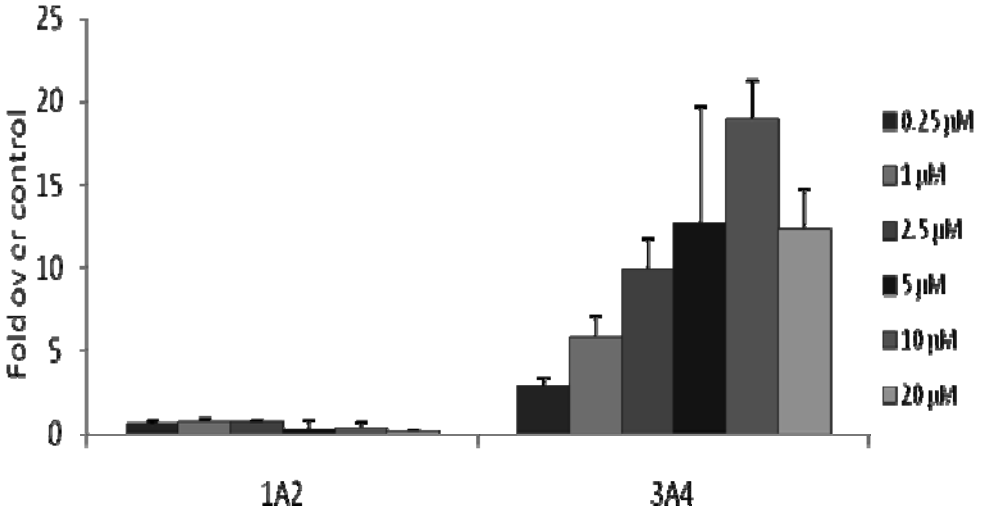

Figure 4.9: the effect of rifampicin on CYP3A4 mRNA level. Data are mean n=2 experiments ± S.D.

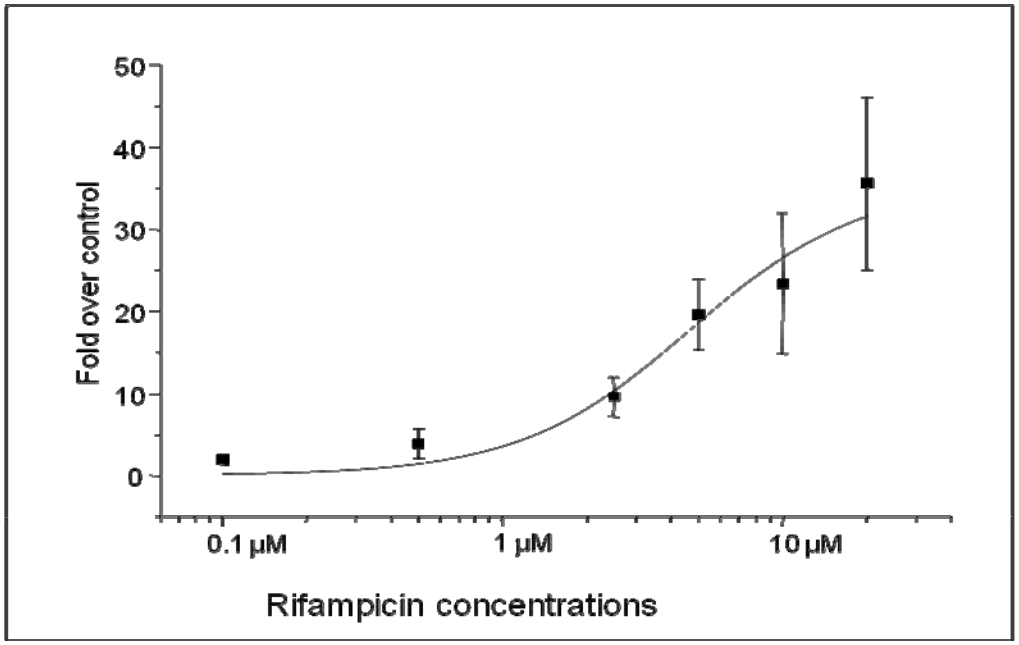

Figure 4.10: the does repose curve of rifampicin on CYP3A4 mRNA level

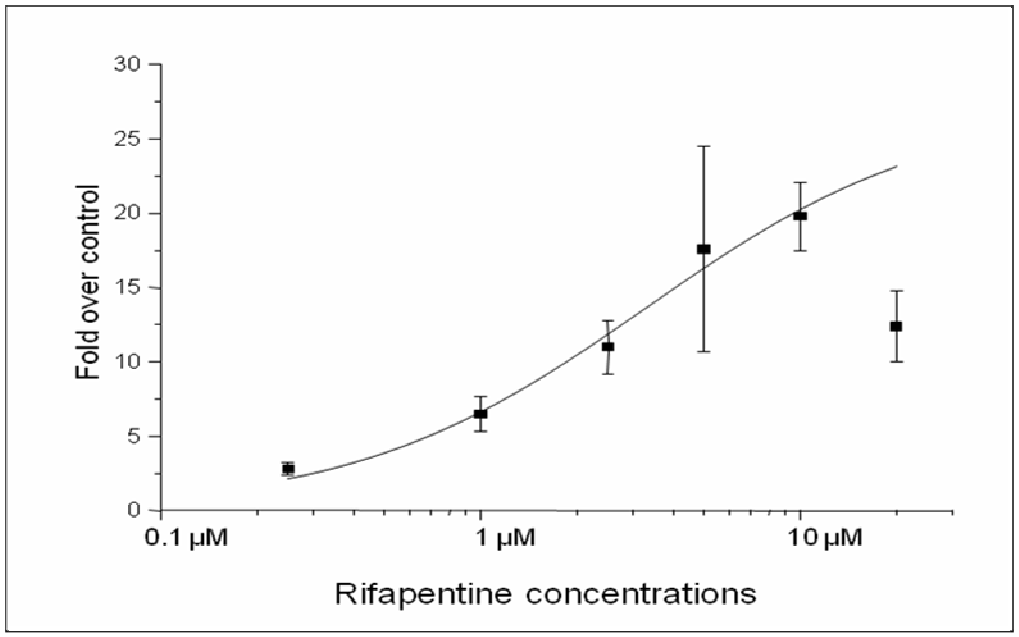

Figure 4.11: the does repose curve of rifapentine on CYP3A4 mRNA level

4.3.4 CYP2B6 Response in Fa2N-4 cells

Rifampicin is the only compound among all those tested compounds that showed a marked effect on CYP2B6 mRNA and activity. (Figure 4.5) No other tested compound demonstrated greater than 2-fold in CYP2B6 induction either at the mRNA or activity level. All CAR ligands like CITCO (Figure 4.12), phenobarbital (Figure 4.6) and β-naphthoflavone (Figure 4.7) did not induce a CYP2B6 response in Fa2N-4 cells.

A)

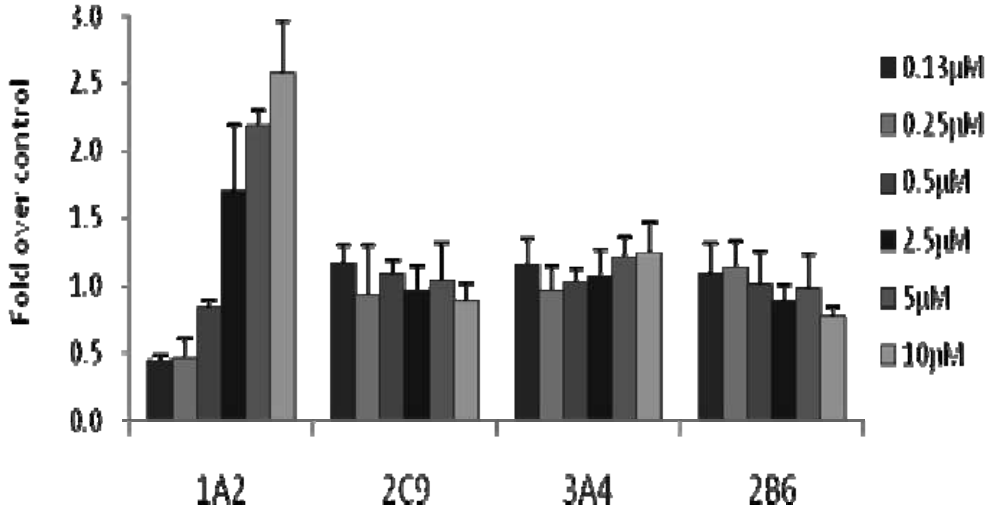

B)

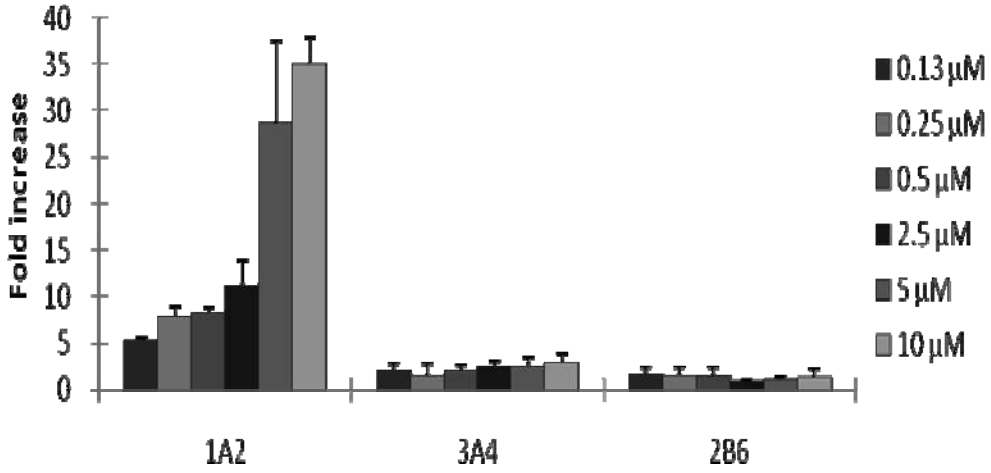

Figure 4.12: the effects of CITCO on CYP1A2, 2C9, 3A4 and 2B6 activity levels (A) as well as on CYP1A2, 3A4 and 2B6 mRNA levels (B). Data are mean n=2 experiments ± S.D.

4.4 Discussion

Evaluating CYP induction is an ultimate functional assessment for prolonged hepatocyte culture system as well as being a routine in the pharmaceutical industry. Due to phenotypic instability, genotypic variability and limited accessibility to primary human hepatocytes, a novel immortalised hepatic cell line has been developed and an evaluation is described in the chapter. In order to facilitate the evaluation of Fa2N-4 cells for CYP induction screening, qRT-PCR and cassetted CYP probe substrate methodologies, which have been previously established in DMPK, Astrazeneca, Charnwood, were used in the study.

4.4.1 Time course of mRNA and activity CYP induction in Fa2N-4 cells

Assessment of CYP induction in primary human hepatocytes on average takes 48 – 96 hours incubation with a test inducer (LeCluyse, 2001; Hewitt *et al.,* 2007b), whilst using mRNA as an endpoint may require a shorter induction period (Drocourt *et al.,* 2001; Meneses-Lorente *et al.,* 2007). A time course study with Fa2N-4 cells showed that the cells were similar to primary human hepatocytes in terms of the period of incubation time required for maximal induction. CYP3A4 mRNA and activity were induced by rifampicin reaching maximal induction at 72 hours. CYP1A2 activity, induced by β-naphthoflavone, showed a similar time course of induction, whilst CYP1A2 mRNA reached maximal induction by 24 hours and was maintained until 72 hours. Consequently, 72 hours was established as the optimal incubation time mRNA and activity end-points for CYP1A2 and CYP3A4.

4.4.2 CYP1A2 and 3A4 induction in Fa2N- 4 cells

Induction of CYP3A4 and CYP2C9 has been previously demonstrated in Fa2N-4 cells in response to rifampicin, phenobarbital and dexamethasone (Mills *et al*., 2004). Recently a larger set of inducers was investigated at mRNA levels using these immortalized hepatocytes (Ripp *et al*., 2006). The current work indicates Fa2N-4 cells can appropriately identify CYP1A2, 3A4 and 2B6 inducers at the enzyme activity or mRNA level. Generally, it is considered that a compound is a CYP inducer if it produces a maximal fold-induction of greater than or equal to 2. Omeprazole (E_{max} of 425) and β-naphthoflavone (E_{max} of 217) were recognized as prototypical CYP1A2 inducers *in vitro*, while other inducers include CITCO (mRNA E_{max} of 35), clotrimazole (mRNA E_{max} of 16), nifedipine (mRNA E_{max} of 16) and reserpine (mRNA E_{max} of 3). No other published literature shows the data of CYP1A2 induction in Fa2N-4 cells.

The prototypical *in vitro* inducers of CYP3A4 including carbamazepine, clotrimazole, dexamethasone, efavirenz, hyperforin, nifedipine, paclitaxel phenobarbital, phenytoin, pioglitazone, reserpine, rifabutin, rifapentine, rifampicin, ritonavir, sulfinpyrazone, verapamil were also correctly identified using Fa2N-4 cells (Figure 4.14). Although mifepristone, omeprazole and troglitazone have been previously identified as CYP3A4 inducers in primary human hepatocytes, no CYP3A4 induction was observed in Fa2N-4 cells (Ramachandran *et al.,* 1999; Raucy, 2003; Nishimura *et al.,* 2007). The absence of CYP3A4 induction with these compounds was possibly as a result

of cytotoxicity, previously reported for Fa2N-4 cells (Ripp *et al.,* 2006) and for troglitazone with primary human hepatocytes (Masubuchi, 2006).

Taken as a whole, the CYP1A2 and CYP3A4 induction data described in this study with Fa2N- 4 cells matches well to that previously demonstrated with human hepatocytes (LeCluyse *et al*., 2000; Meunier *et al*., 2000; Roymans *et al*., 2004). In particular the E_{max} values for CYP1A2 mRNA and activity induced by β-naphthoflavone were 217 and 11- fold in Fa2N-4 cells respectively, similar to that in human hepatocytes (Royman *et al*., 2004; Meneses-Lorente *et al*., 2007). Also, the E_{max} values for CYP3A4 mRNA and activity induction by rifampicin of 36 and 6-fold respectively corresponded well to those previously reported using human hepatocytes (Hariparsad *et al*., 2004; Roymans *et al*., 2004). Also, the maximum fold induction of CYP3A4 mRNA from Ripp *et al*. (2006) and in this study is listed in Figure 4.13. Both data show similar trend and are in a good agreement overall, but CYP3A4 mRNA maximum induction of certain compounds is higher in this study. For example, both phenobarbital and rifampicin mRNA maximum inductions in this study show twice fold to those from Ripp *et al*. (2006). The differences between two groups are probably due to the application of different concentration of the compound and induction time.

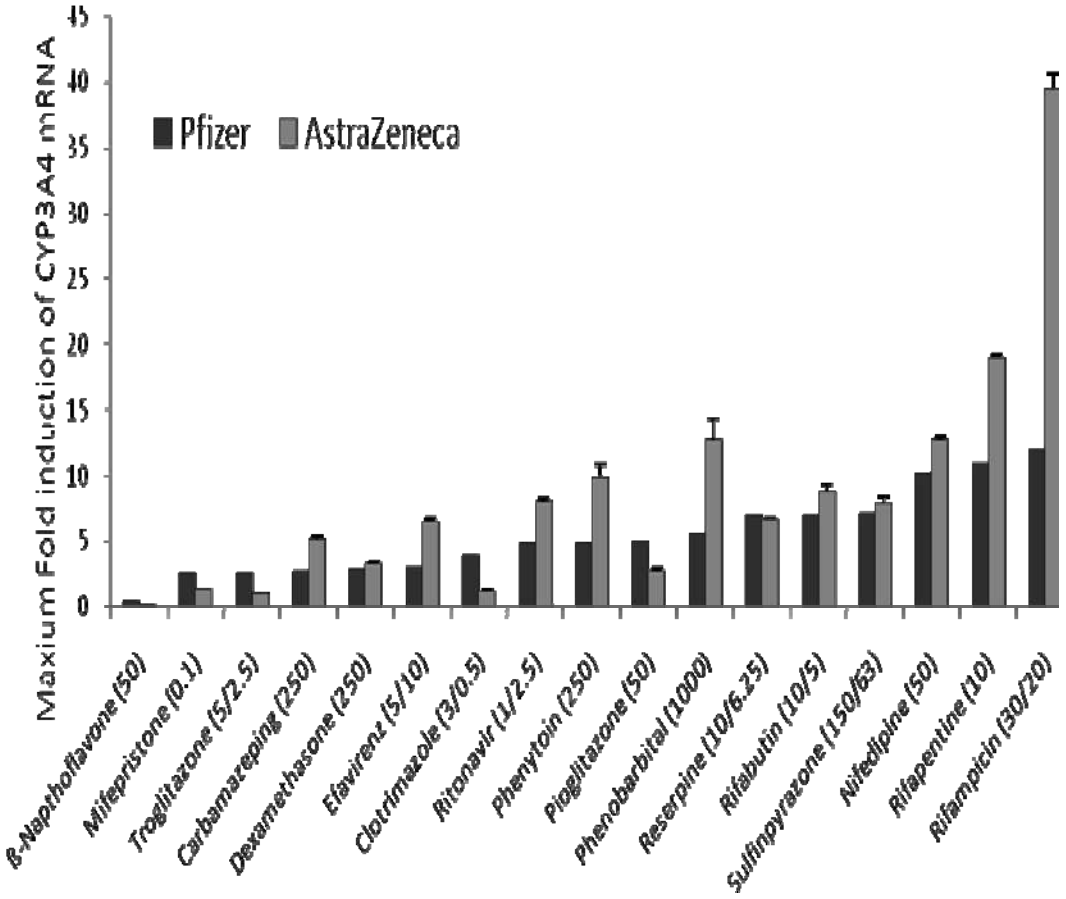

Figure 4.13: maximum fold induction of CYP3A4 mRNA comparison between AstraZeneca (this study) and Pfizer (Ripp *et al*., 2006). X axis shows that 17 compounds were used in different maximum concentration in two studies. 72 hours and 96 hours were applied for maximum CYP mRNA induction in this study and Pfizer's, respectively.

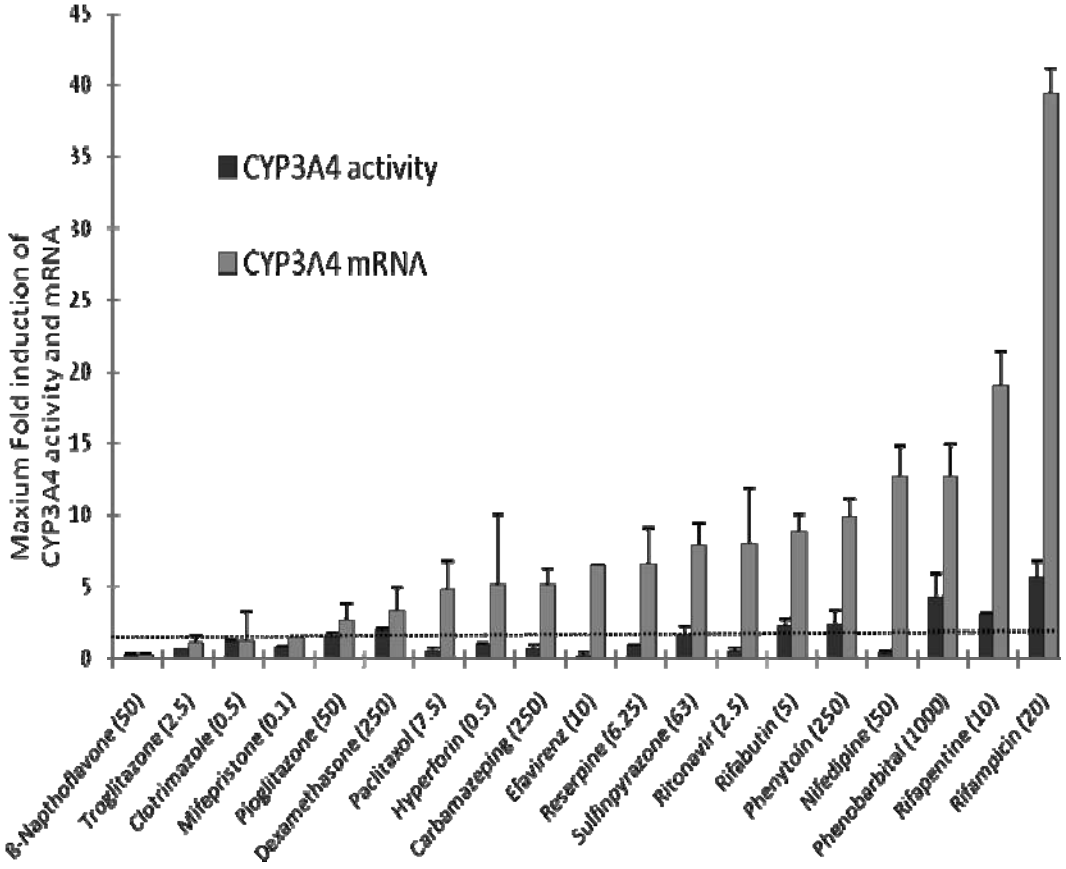

Figure 4.14: a summary of maximum fold induction of CYP3A4 activity and mRNA in Fa2N-4 cells at 72 hours induction time. 19 compounds at their maximum concentrations are shown in X axis. Majority of the compounds at mRNA level show greater than 2 fold (dash line).

4.4.3 CYP2B6 induction in Fa2N-4 cells

Nuclear hormone receptors play an important role in the regulation of transcriptional activation of CYP genes. Aryl hydrocarbon receptor (AhR) is capable of binding to the response elements in the promoter regions of the CYP1A2 gene. Constitutive androstene receptor (CAR) and pregnane X receptor (PXR) are regulators of CYP3A4 and CYP2B6 expression (Tirona and Kim, 2004) with PXR predominately relating to CYP3A4 and CAR predominately relating to CYP2B6 (Facuette *et al*., 2007). In Fa2N-4 immortalized cells, CAR exhibits high constitutive activity and spontaneous nuclear localization in contrast to its predominant cytosolic localization in primary hepatocytes (Faucette *et al*., 2007) therefore the expression level of CAR is considerably lower than in human hepatocytes (Hariparsad *et al*., 2008). Since CITCO, phenytoin and carbamazepine are selective activators of CAR (Faucette *et al*., 2006), phenobarbital activates both CAR and PXR and rifampicin activates CYP2B6 *via* PXR predominantly over CAR, there was no CYP2B6 induction by CITCO (Figure 4.12), weak induction by phenobarbital (Figure 4.6) but clear induction by rifampicin (Figure 4.5). Consequently, Fa2N-4 cell line may be used as a potential mechanistic tool for investigating CYP3A4 and CYP2B6 inducers *via* CAR/PXR.

4.4.4 Conclusion and future work

In conclusion, qRT-pCR and CYP1A2, CYP2C9, CYP2B6 and CYP3A4 substrate cassette methods described here have offered capacity to competently evaluate CYP induction in Fa2N-4 cells. It is considered that Fa2N-4 cells

offer a substitute for primary human hepatocytes for CYP1A2 and CYP3A4 induction but not for CYP2B6 due to lack of cytosolic CAR expression.

The next stage of this project will be to apply these CYP induction protocols to primary human hepatocyte culture models (e.g. co-culture of hepatocytes and hepatic stellate cells). Any reasons for differences in CYP3A4 expression and inducibility will be investigated at a molecular level, including liver-specific transcription factors (TFs), nuclear hormone receptors (NRs), binding of TFs and NRs to the regulatory element and promoter region of the CYP3A4 gene and the nature of chromatin in the region of CYP3A4, PXR regulatory and promoter region.

Chapter Five:

Co-culture of Primary Human Hepatocytes and Hepatic Stellate Cells (HSCs)

5.1 Introduction

5.1.1 Isolation of primary human hepatocytes

5.1.1.1 Sources of human liver tissues

The major sources of human liver tissues include whole organs from multiorgan donors (MODs) discarded for transplantation, tissue from split-liver transplantation, liver specimens obtained during partial therapeutic hepatectomy or small size surgical biopsies.

Donor livers and tissue from reduced-sized donor livers provide lower cell yield and viability than other sources. Also, the metabolic competence of cells shows a 30-35% reduction compared to other liver sources. (Serralta *et al*., 2003) The reasons why liver from organ donors are less competent are probably due to the use of a cold preservation solution to prevent warm ischemia and several hours of transportation under this condition before hepatocye isolation. Cold ischemia is not the only risk factor for the efficiency of isolation and the metabolic competence of cultured cells. The quality of University of Wisconsin (UW) solution, the most commonly used solution to preserve the livers (Quintana *et al*., 2003), is also a key factor (Spinelli *et al*., 2002). A new solution, Celsior, could be an effective alternative to UW preservation solution for donor liver samples (Straatsburg *et al*., 2002; Cavallari *et al*., 2003). Further, both the viability and the percentage of successful culture are higher for cells obtained from livers perfused with Celsior solution than with UW solution. However, no difference is observed in CYP activities in hepatocytes cultured in each preservation solution. These above results indicate that livers perfused and stored in Celsior solution offer

higher viability and better adaption to culture, but with similar metabolic activity.

In contrast to donor liver samples, liver specimens obtained from hepatectomy represent the most reliable source of healthy liver tissue, due to easier accessibility, more frequent availability and higher quality of isolated hepatocyes. (Brandenburg *et al*., 2005; Li, 2007) Although the surgery requires hepatic pedicle clamping (Pringle manoeuvre), which results in warm ischemia of the hepatic tissue, hepatocyte yield, viability and metabolic function are not greatly affected if the period of warm ischemia is no longer than 30 minutes (Lloyd *et al*., 2004; Richert *et al*., 2004). Reoxygenation after a hypoxic period, not the duration of the ischemia, seems to be the key to preventing decrease of hepatocye functionality (Alexandre *et al*., 2002).

5.1.1.2 Influence of donor characteristics on outcome of human hepatocyte functions

In order to maximize the availability of high quality hepatocytes from surgical specimens, donor factors with the potential to affect yield, viability and function of isolated hepatocytes need to be considered. The following parameters have been evaluated: age and gender; patients' health; steatosis and cholestasis.

For age of donor, no significant differences are observed in the viability and survival of cultured cells, but a significant reduction in cell yield is observed for donor aged >50 (Vondran *et al*., 2008). The total CYP-dependent oxidative

capability of hepatocytes is not greatly affected by the age. However, for certain specific CYP activity, such as CYP3A4, cultured hepatocytes from the older than 50 show lower activity than those under 50. This result is in good agreement with the observation that CYP variation exists in the adult and sometimes it can be greater than 50 fold for a particular CYP (Rodriguez-Antona *et al*., 2003), which is probably due to genetic predisposition and the individual induction status. No significant correlation between viability and survival of cultured cells and donor gender has been found (Serralta *et al*., 2003; Vondran *et al*., 2008). However, the total CYP-dependent oxidative capability of hepatocytes is lower, and the CYP3A4 activity higher, in female donors (Gómez-Lechón *et al*., 2004).

The state of the patients' liver also affects the yield, viability and functionality of hepatocytes (Chapman *et al*., 1993). Specimens with benign diseases (e.g. haemangioma) show the highest cell yield and viability, those with secondary tumours (e.g. chronic inflammation or cirrhosis) are lower in the cell yield and viability, but the lowest results are from those with primary tumours (Vondran *et al*., 2008). For the functionality of hepatocytes, the majority of CYP expressions are down-regulated and their related biotransformation pathways are changed during inflammation or infection (Gant *et al*., 2003). In particular, some CYPs are more susceptible by cirrhosis, including CYP1A, CYP2C and CYP3A (Bastien *et al*., 2000).

In addition, steatosis and cholestasis need to be considered. Both severe steatosis and cholestasis lead to a significant reduction in cell yield and

viability (Alexandre *et al*., 2002; Konera and Dikdan, 2002). In these studies steatosis appeared to have a particularly important effect on the total CYP-dependent oxidative capability of hepatocytes and CYP3A4 activity was lower in the livers with steatosis than normal tissue, which is in good agreement with previous studies (Weltman *et al*., 1998). However, the results from other published data are conflicting, showing either no influence of histopathological alteration (Richert *et al*., 2004) or even an increase in cell viability from tissue with steatosis (Lloyd *et al*., 2004).

Other factors, including previous chemotherapy, alcohol or tobacco consumption have not been shown to affect the yield, viability, attachment rate and function of isolated hepatocytes (Alexander *et al*., 2002).

5.1.1.3 Influence of isolation procedures and operative parameters on outcome of human hepatocytes

Several factors in the isolation procedures and operative parameters have been identified to affect the outcome of human hepatocytes. Warm ischaemic time longer than 30 minutes reduces the percentage of digested liver and cell yield (Alexander *et al*., 2002), while cold ischaemic time less than 5 hours does not affect the cell yield and viability (Richert *et al*., 2004). Also, an initial high-pressure washout is recommended to improve the efficiency, to shorten the warm ischaemic time and to reduce ischemia reperfusion-related injury (Hart *et al*., 2004). A liver biopsy weight of over 150 g affects the percentage of digested liver and a size of between 50 and 100 g is optimal for cell yield (Alexander *et al*., 2002; Richert *et al*., 2004). Reformation of Glisons' capsule

with glue or suture greatly enhances the cell yield and viability (Richert *et al*., 2004; Lloyd *et al*., 2004).

5.1.1.4 Isolation of primary human hepatic stellate cells

One of the most common methods of isolation of primary human HSCs is mince/enzymatic digestion. Briefly, finely minced liver tissue is digested with a combination of collagenase and pronase and then HSCs are separated from other NPCs by centrifugation over a gradient of Stractan (Bataller *et al*., 1998), Nycodenz (Siegmund *et al*., 2006), Larex (Muhanna *et al*., 2008) or Larcoll (Boers *et al*., 2006). The purity of HSCs in these isolates is usually more than 90% assessed by autofluorescence (Holt *et al*., 2009), transmission microscopy (Marra *et al*., 1993) or immunofluorescence (Boers *et al*., 2006). Cells reach 80% of confluence in approximately 15 days and generally exhibit typical myofibroblast-like phenotype after two serial passages. Overall, this is an effective, sensitive and reproducible method for isolation of HSCs. Another method is explant outgrowths (Levy *et al*., 2000). In brief, liver fragments in the size of approximately 1 cm^3 are plated on collagen coated flask and left to dry for 30 minutes to assist adherence. A confluence monolayer is usually achieved in 21 days, but it always represents a heterogeneous mixture of HSCs with other hepatic cell types and has limited number of passages (Schnabl *et al*., 2002).

A simple method using normally discarded washings of a two-step collagenase perfusion for isolation of primary human HSCs has been established in Tissue Engineering group, School of Pharmacy, University of Nottingham. It

outweighs other methods because this technique allows simultaneous isolation of HSCs and hepatocytes with less contamination of other NPCs. Also, comparing to mince/enzymatic digestion and explant outgrowths, it does not require matrix coated flask or density gradient centrifugation. Human HSCs by this method have been identified by positive staining of monoclonal anti alpha smooth muscle actin, anti glial fibrillary acidic protein and anti vimentin and negative staining of Kupffer cells and endothelial cells markers, namely monoclonal anti human CD68 and endothelial cell antibody (PAL-E). Overall, it is a rapid, effective and reliable method of isolation of human HSCs

5.1.2 Aims

The principal aims of the work presented in this chapter are:

- to study seeding density of human hepatocytes in monoculture on 12-well and 6-well collagen type I coated plates
- to test the effects of medium supplements on morphology of human hepatocytes on 6-well collagen type I coated plates
- to test the effects of Matrigel overlay on morphology of hepatocytes monoculture
- to establish 3D spheroids by co-culturing human hepatocytes and human hepatic stellate cells on $P_{DL}LA$ coated surface

5.2 Material and methods

5.2.1 Chemicals

Soltran kidney perfusion was purchased from Baxter Healthcare Ltd, UK. Gibco^{TM} Liver Perfusion Solution and Gibco^{TM} Liver Digest Media were bought from Invitrogen, UK. Penicillin/ streptomycin solution and dexamethasone were purchased from Sigma, UK. Human serum was bought from PAA Ltd., UK.

5.2.2 Human liver samples

Human liver tissues were obtained from therapeutic hepatectomy in Queen's Medical Centre, University Hospital in Nottingham. Patient consent and local Ethics Committee approval had been given to use the segments not required for transplantation (those remaining after cut-down) for research purposes. Patients with chronically deranged liver function or cirrhosis were excluded from the study.

5.2.3 Primary human hepatocytes isolation

Primary human hepatocytes were isolated by a method established by the Tissue Engineering group, School of Pharmacy, University of Nottingham and then improved by Astrazeneca, Sheffield. Segments (25-150 g), distal to the site of tumour or other pathology necessitating liver resection, cut from intact liver was immediately perfused with ice-cold Soltran kidney perfusion solution and immersed in ice-cold Soltran in order to reduce cellular deterioration during transportation to the laboratory, which was usually less than 30 minutes. On arrival at the laboratory the liver was transferred to the perfusion apparatus

and the cannulae connected to the perfusion lines within a Class II biosafety cabinet. Veins for cannulation were chosen to give maximum perfusion efficiency as tested by flushing with Soltran. The number of plastic cannulae used depended on the size of the segment and the distribution of veins, but was up to 4 in maximum. Once the perfusion system was connected to the liver tissue through cannulae, pre-warmed (37˚C) 1L Gibco^{TM} Liver Perfusion Solution was circulated through the system at a rate of 17-20 ml/min for 30 minutes. On completion, the initial perfusion medium was discarded and 1 L Gibco^{TM} Liver Digest Media was re-circulated at a rate of 17-20 ml/min for 40-60 minutes. After the digestion step, the liver tissue was disrupted gently with scissors and the resulting cells were re-suspended in pre-cooled (4˚C) human hepatocyte isolation medium (Appendix 1.8.6). The tissue suspension was then filtered through 100 μm sterile cotton gauze placed over a funnel into a cylinder. The filtrate was centrifuged at 50 g for 3 minutes in the pre-cooled (4˚C) centrifuge. The cell pellet was washed twice (50 g, 5 minutes) and finally re-suspended in pre-cooled human hepatocyte isolation medium with 90% Percoll in the 25% ($^{v}/_{v}$) gradient and centrifuged at 100 g for 10 minutes. The cell pellet was re-suspended in pre-cooled human hepatocyte plating medium (Appendix 1.8.4) and the supernatant was kept for hepatic stellate cell isolation. Cell yield and viability were estimated by Trypan Blue and 0.0025 mm^2 haemacytometer as described in Chapter 2, Section 2.2.4. A viability of at least 80% was considered necessary for experimental work.

Collaboration with FRAME Alternative Laboratory from School of Biomedical Science, University of Nottingham in September 2007, led to further

modification of the method of isolation of primary human hepatocytes. First perfusion of 1L Gibco^{TM} Liver Perfusion Solution for 30 minutes was replaced by 1 L perfusion buffer with EGTA for 15-20 minutes and the second perfusion of 1 L Gibco^{TM} Liver Digest Media was substituted with 1L perfusion buffer with collagenase for 20-30 minutes. Also, the centrifuge speed for filtrate and cell pellet at 527 rpm (50 g) for 5 minutes was changed to at 1000 rpm for 2 minutes. In addition, 90% Percoll in the 25% ($^{v}/_{v}$) gradient centrifuged at 745 rpm (100 g) was set with 90% Percoll in the 50% ($^{v}/_{v}$) gradient at 600 rpm. The remaining procedures were unchanged.

5.2.4 Primary human stellate cells isolation

The method of isolaton of primary human stellate cells was established and modified by the Tissue Engineering group, School of Pharmacy, University of Nottingham. All the supernatants from primary hepatocyte isolation were centrifuged at 50 g for 5 minutes at room temperature. The resulting pellets were discarded and then the supernatants were spinned twice at 50 g for 5 minutes to remove any contaminated hepatocytes. After that, the supernatant from the final spin was centrifuged at 4024 g (5000 rpm) for 20 minutes and the pellets, containing hepatic stellate cells, were collected and re-suspended in the proper amount of stellate cell medium containing 15% human serum (Appendix 1.8.7).

5.2.5 Cell culture

Primary human hepatocytes were seeded at the density of 0.1429 and 0.1875 million/m^2 and a total of 0.5 and 1.6875 million/well were cultured on 12-well

and 6-well collagen type I coated plate respectively. Two different sets of human plating media and human culture media were used. The first one included human plating medium (DMEM containing 4500 mg/L L-glucose and 25 mM HEPES, supplemented with 2 mM L-glutamine, 0.2 U/ml penicillin, 0.2 μg/ml streptomycin, 0.5 ng/ml amphotericin B and 10% fetal calf serum) and human culture medium (DMEM containing 4500 mg/L L-glucose and 25 mM HEPES, supplemented with 2 mM L-glutamine, 0.2 U/ml penicillin, 0.2 μg/ml streptomycin, 0.5 ng/ml amphotericin B, 10 μg/ml bovine pancreas insulin and 1 μM dexamethasone). The second set included human plating medium (DMEM containing 4500 mg/L L-glucose and 25 mM HEPES, supplemented with 100 U/ml penicillin, 100 μg/ml streptomycin, 0.1μM insulin from bovine pancreas, 1 μM dexamethasone and 5% FCS) and human culture medium (William's Medium E supplemented with 2mM L-glutamine, 100 U/ml penicillin, 100 μg/ml streptomycin, 0.1 μM dexamethasone and 0.1 μM (5.73 μg/ml) insulin from bovine pancreas).

5.2.6 Experimental design

The effect of seeding density on morphology of primary human hepatocytes was investigated. The effect of Matrigel overlay on morphology of primary human hepatocytes was also considered. Co-culture of primary human hepatocytes and human HSCs was then applied on $P_{DL}LA$ coated plates. All the cell cultures have been carried out three times except co-culture on $P_{DL}LA$ coated plate for twice.

5.3 Results

5.3.1 The effects of seeding density on morphology of human hepatocytes on 12-well and 6-well collagen type I coated plates

The primary human hepatocytes (viability above 80%) were cultured on 12-well and 6-well collagen type I coated plates at a density of 0.5 million cells/well (0.1429 million/m^2) and 1.6875 million/well (0.1875 million/m^2) respectively. The first human plating medium was used for the initial four hours for cell attachment and then the first human culture medium was used to wash off cell debris and replaced for further culture. For cells cultured on 12-well collagen type I coated plates, attachment to the collagen gel began after 4 hours with some cell debris and clumping. After 24 hours, cells exhibited uniform typical hepatocyte morphology with well-defined polyhedral shape and cell membrane, nuclei and a finely granular cytoplasm (Figure 5.1A). In 48 hours, hepatocyte monolayer became more than 80% confluent but with more cell debris and clumping (Figure 5.1B) and the monolayer deteriorated gradually within 72 hours (Figure 5.1C). Cells cultured on 6-well collagen type I coated plates showed better-defined cell shape and membrane, clearer nuclei and finer granular cytoplasm than those cultured on 12-well plates after 24 hours (Figure 5.2A). After 48 hours, they maintained most of these phenotypic characteristics (Figure 5.2B), but deterioration at 72 hours still occurred (Figure 5.2C).

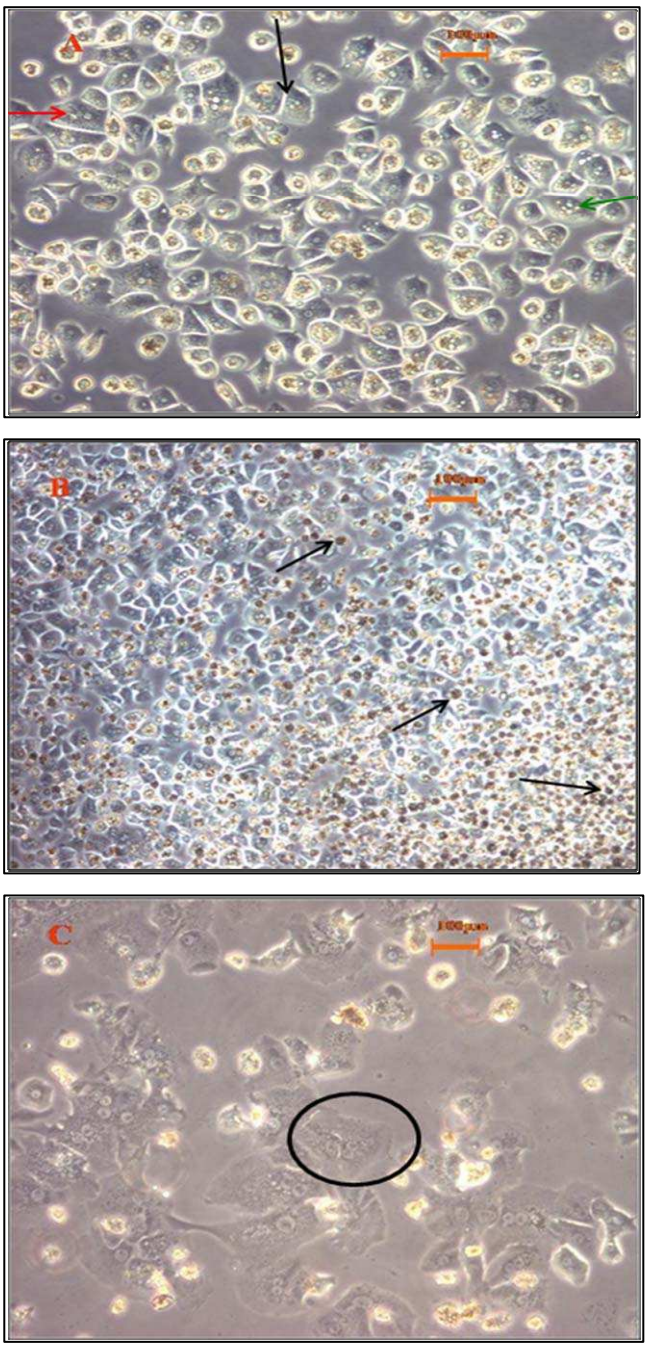

Figure 5.1: Primary human hepatocytes (0.5 million/well) cultured on 12-well collagen type I coated plates in first set media after 24 hours, showing cell border (black arrow), nuclei (red arrow) and granular cytoplasm (green arrow) (A), 48 hours, showing big amount of cell debris and floating cells (black arrows) (B) and 72 hours, showing cell deterioration without typical cuboidal shape (black circle) (C).

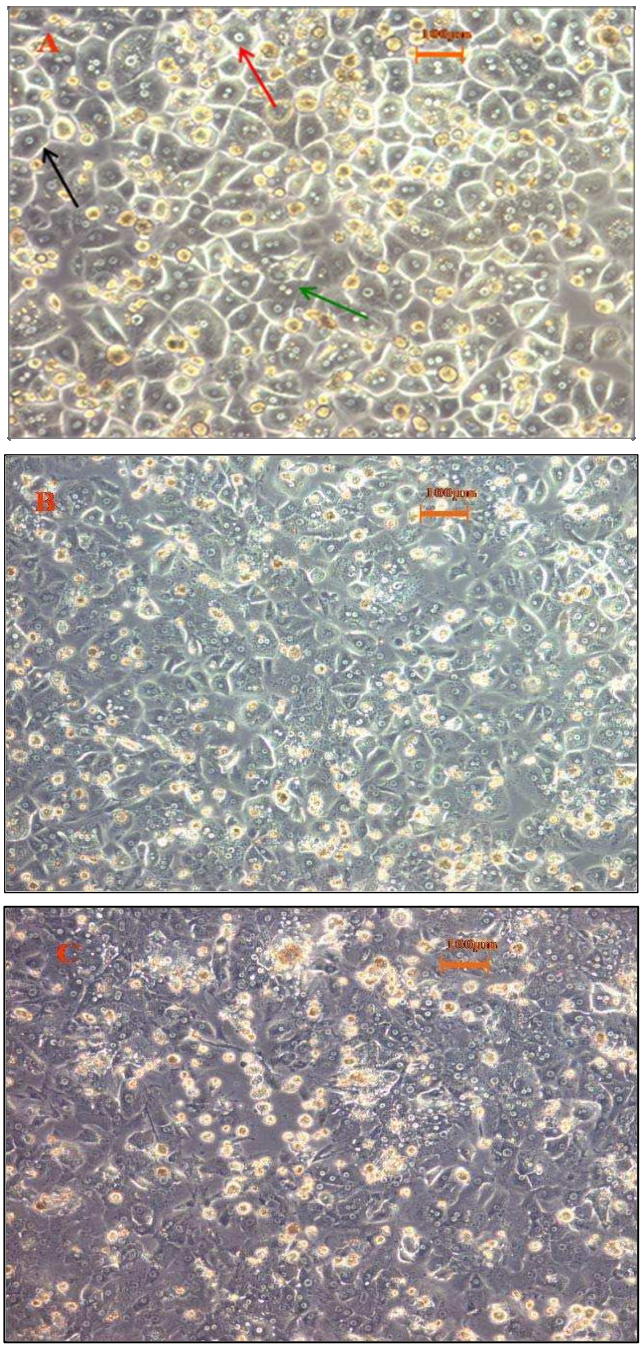

Figure 5.2: Primary human hepatocytes (1.68 million/well) cultured on 6-well collagen type I coated plates in first set media after 24 hours, showing clear cell border (black arrow), distinct nuclei (red arrow), and fine granular cytoplasm (green arrow) (A), 48 hours, showing small amount of cell debris and floating cells (B) and 72 hours, showing cell deterioration without typical cuboidal shape (C).

5.3.2 The effects of medium supplements on morphology of human hepatocytes on 6-well collagen type I coated plates

Different human plating media and culture media were used to demonstrate the effects of supplements on morphology of primary human hepatocytes. For the second human plating medium, the addition of 0.1 μM insulin from bovine pancreas and 1 μM dexamethasone was included and the amount of fetal calf serum was decreased to 5% rather than 10%. For the second human culture medium, the concentration of bovine pancreas insulin was decreased from 10 μg/ml to 5.73 μg/ml and that of dexamethasone was down to 0.1 μM instead of 1μM. For both second media, the combination of 100 U/ml penicillin and 100 μg/ml streptomycin were used as antibiotics with no addition of amphotericin B.

Human hepatocytes were seeded on 6-well collagen type I coated plates as previously described in Section 5.2.5. Cells cultured with second set media showed better attachment and higher survival percentage after 24 hours than those cultured with first set media (Figure 5.3A and B). They were more confluent and maintained better cell-cell interactions after 48 hours. Clearer nuclei and cell membranes were also observed. (Figure 5.4A and B) After 72 hours, cells cultured with first set media started to spread out and form fibroblast-like protrusions. The nuclear volume increased and the cytoplasm appeared granulated. (Figure 5.5A), which was a good agreement with previous result in Section 5.3.1. However, cells cultured with second set media maintained the typical hepatocyte shape and cell membranes and nuclei until day 5 (Figure 5.5B and Figure 5.6B).

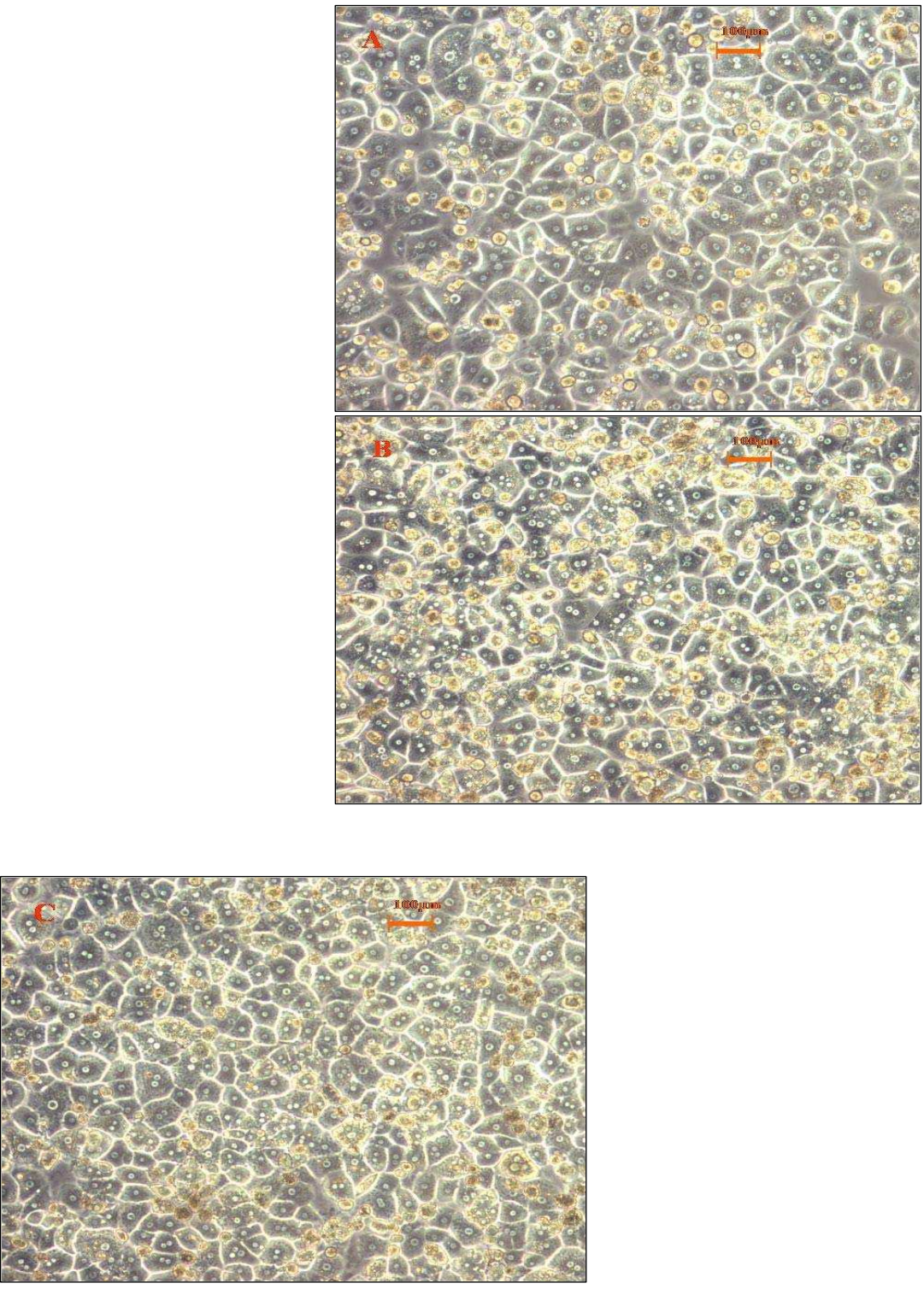

Figure 5.3: Primary human hepatocytes (1.68 million/well) cultured with first set media, showing about 90% confluence (A), second set media, showing about 95% confluence (B) and second set media with Matrigel overlay, showing about 100% confluence, best cell borders and the most distinct nuclei (C) on 6-well collagen type I coated plates after 24 hours

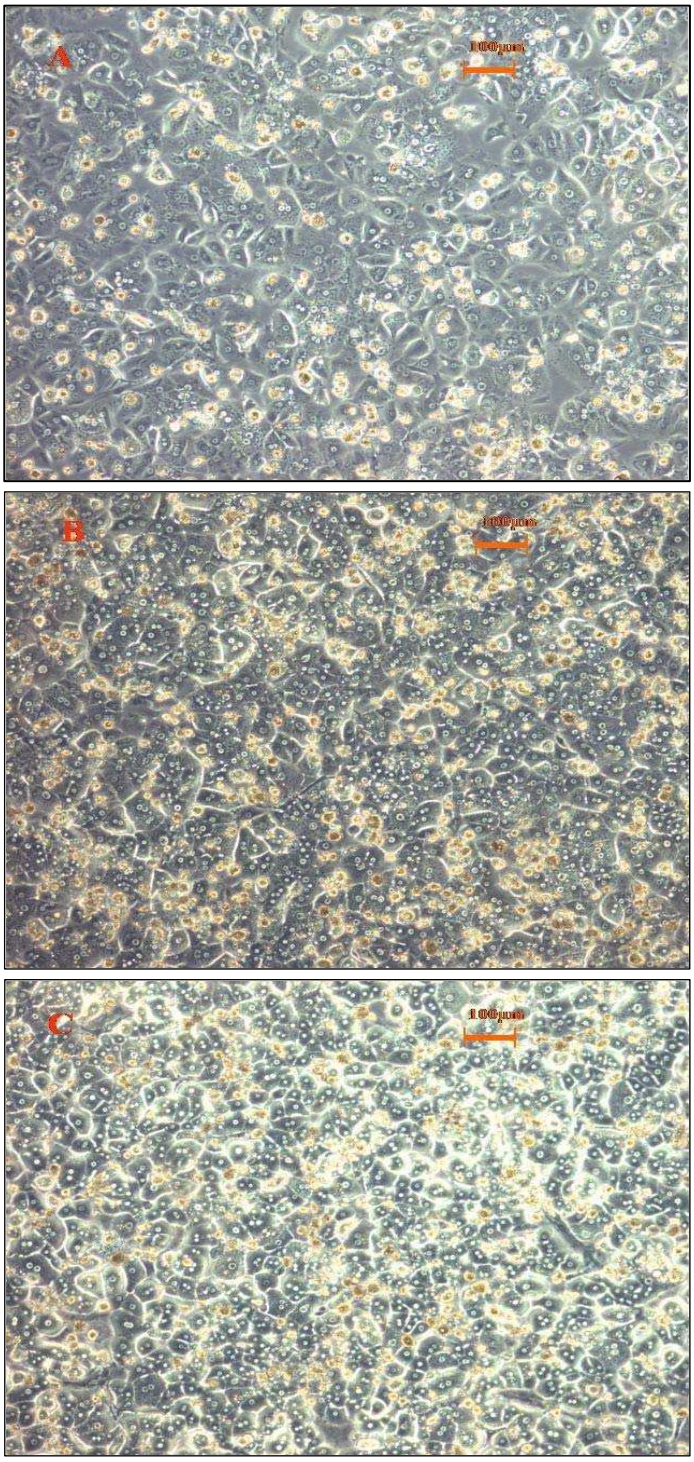

Figure 5.4: Primary human hepatocytes (1.68 million/well) cultured with first set media, losing almost all cell borders (A), second set media, losing about half cell borders (B) and second set media with Matrigel overlay, maintaining most of cell borders (C) on 6-well collagen type I coated plates after 48 hours

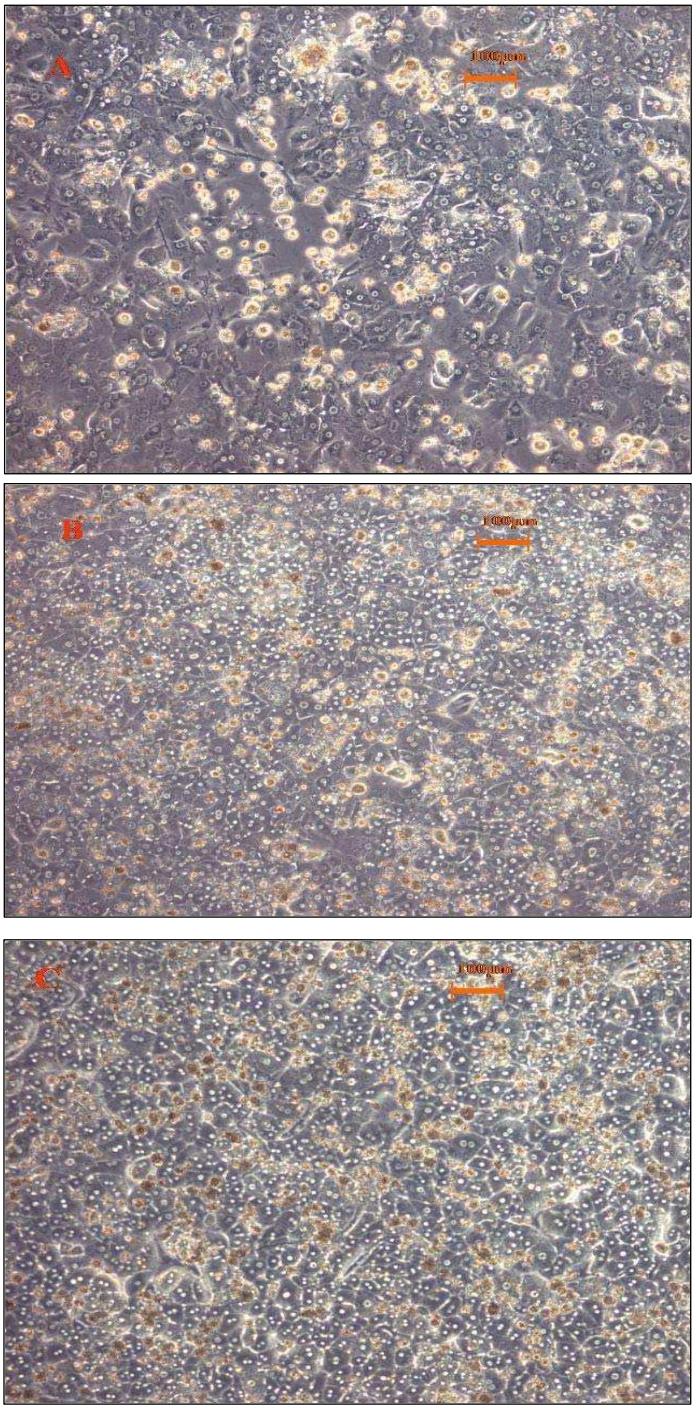

Figure 5.5: Primary human hepatocytes (1.68 million/well) cultured with first set media, showing cell deterioration and losing cuboidal shape (A), second set media, losing almost all the cell borders, but still maintaining the cuboidal shape (B) and second set media with Matrigel overlay, maintaining half of the cell borders and cuboidal shape (C) on 6-well collagen type I coated plates after 72 hours

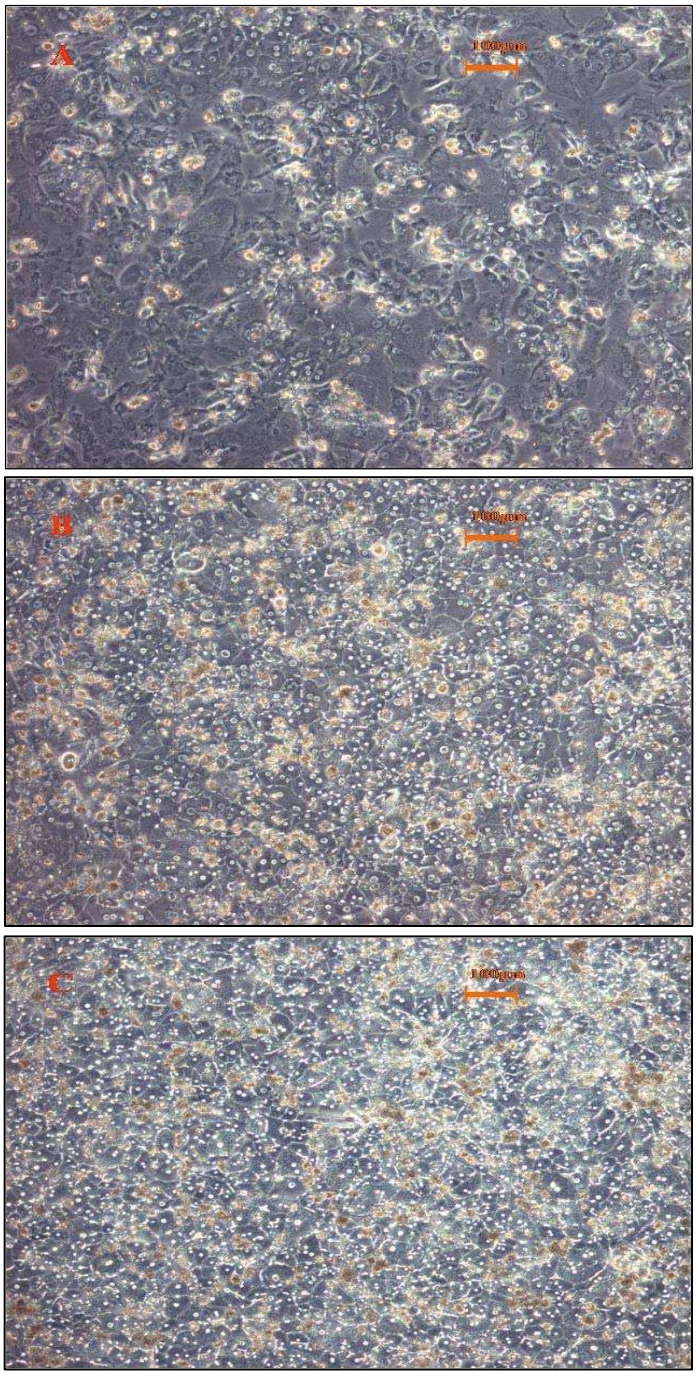

Figure 5.6: Primary human hepatocytes (1.68 million/well) cultured with first set media, showing cell deterioration and losing cuboidal shape (A), second set media, losing almost all the cell borders, but still maintaining the cuboidal shape (B) and second set media with Matrigel overlay, maintaining half of the cell borders and cuboidal shape (C) on 6-well collagen type I coated plates after 5 days

5.3.3 The effects of Matrigel overlay on morphology of primary human hepatocytes

The method of Matrigel overlay on human hepatocyte after 4 hours initial attachment was as described in Chapter 2 Section 2.2.6. Due to better maintenance shown by cells cultured with second set media, Matrigel overlay was only applied to those cells to investigate any further improvements on hepatocyte morphology. Compared to cells cultured with second set media but without Matrigel, cells cultured in collagen-Matrigel sandwich showed almost 100% confluence after 24 hours (Figure 5.3C). They demonstrated tighter cell-cell interactions, clearer nuclei, bile-canaliculi-like structures, better-delineated plasma membrane borders after 48 hours (Figure 5.4C) and maintained the better morphology until day 5 (Figure 5.5C and Figure 5.6C).

5.3.4 Co-culture of human hepatocytes with human hepatic stellate cells

The isolation of primary human hepatocytes and human HSCs were described previously in Section 5.2.3 and 5.2.4 respectively. The isolated human HSCs were not activated and ready to use until they were cultured in primary human stellate cell medium in T75 flask for approximately two weeks. The freshly isolated primary human hepatocytes (viability above 80%) and activated human HSCs (passage number 3) were co-cultured on 12-well $P_{DL}LA$ coated plates with second human culture medium at the density of 125,000 and 62,500 per well respectively. The ratio of these two cell types was 2:1, which was the same as co-culture of rat hepatocytes and rat HSCs in Chapter 2. Small aggregates were formed in 72 hours after isolation (Figure 5.7A) and then big

spheroids with better-defined cell borders were developed on day 5 (Figure 5.7B).

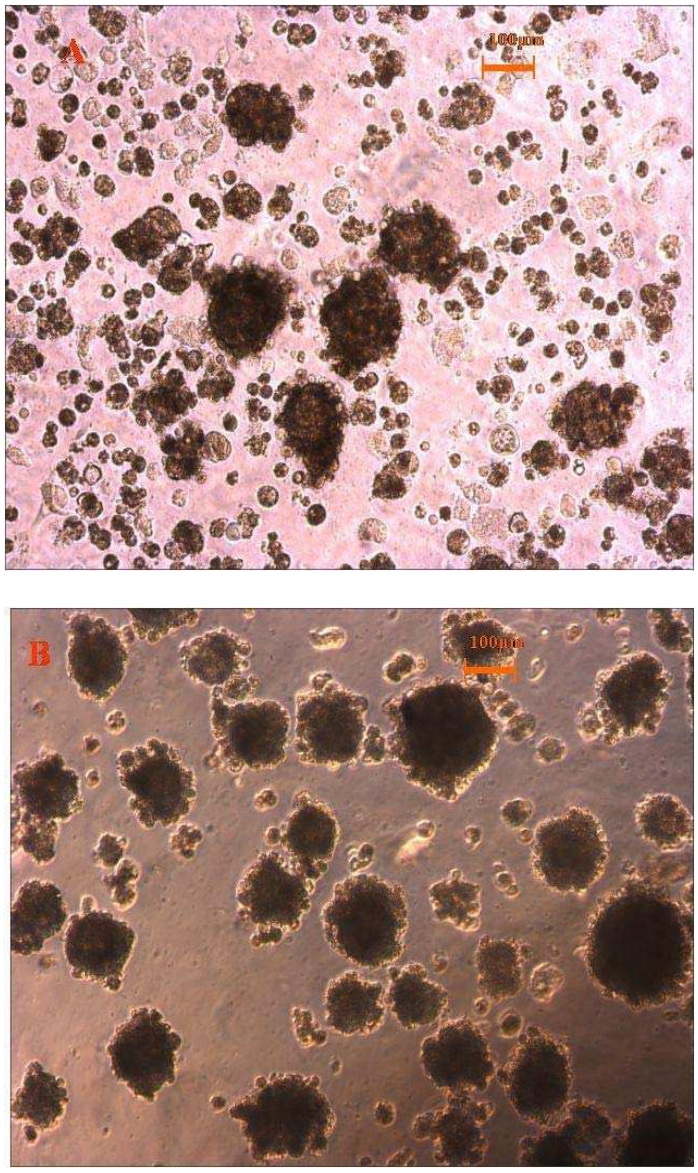

Figure 5.7: Co-culture of primary human hepatocytes (0.44 million/well) and human passage number 3 HSCs (0.22 million/well) on 12-well $P_{DL}LA$ coated plates after day 3, forming spheroids (A) and day 5, maintaining the spheroids (B). Second set media were used and the medium was not changed until 72 hours.

5.4 Discussion

5.4.1 The effects of cell density, media formulation and ECM application on morphology of human hepatocytes

The density of 0.1875 million/m^2 for primary human hepatocytes proved to maintain better cell morphology in the first 48 hours compared to the density of 0.1429 million/m^2. However, there was a strong perturbation of cell morphology after 72 hours even at a higher seeding density. This agreed with other reports in the conventional cultures (Hamilton *et al*., 2001). If cells were seeded at a very high density (almost 100% confluence), cells maintained hepatocyte-like morphology for only 1-2 days and then started to detach from the surface. Interestingly, the same high density did not result in the same confluence of cells in a three-dimensional ECM environment. Therefore, human hepatocytes in collagen-Matrigel sandwich with higher density showed better hepatocyte morphology in a longer period in this study.

In addition, media formulation had some influence on the morphology of hepatocytes in culture. For fetal calf serum, it can enhance the surface attachment ability of hepatocytes (William *et al*., 1977), but it may inhibit the re-establishment of bile canaliculi in hepatocytes culture (Terry and Gallin, 1994) and does not make a positive contribution to maintain cell differentiated phenotypes. Therefore, serum-containing medium was only applied to hepatocytes culture for the first 4 hours and serum-free medium was used for 3D spheroids formation over the whole culture period in this study. For dexamethasone, it is valuable for long-term preservation of hepatocyte-specific functions and polygonal hepatocyte morphology at the concentration of 1μM

(Yamada *et al*., 1980). However, the addition of dexamethasone at concentrations from 50 nM to 10 μM altered spheroid formation in a concentration-dependent fashion (Abu-Absi *et al*, 2005). Further, the supplement of 10 μM dexamethasone to the medium greatly enhanced LDH release and reduced the amount of urea secretion (Dong *et al*., 2008). Therefore, a low concentration of dexamethasone (0.1 μM) was applied to the medium in this study. For insulin, its administration to an endotoxemic rodent model decreased pro-inflammatory and increased anti-inflammatory mediators with enhanced hepatic functions and structure (Jeschke *et al*., 2005, 2007). Also, the addition of insulin at a dose of 10 IU/ml (approximately 10 μg/ml) to primary human hepatocytes cultures reduced the expression of pro-inflammatory cytokine proteins, including IL-6, TNF and IL-1β, IL-10 and IFN-α. Therefore, the supplement of insulin in the medium might help hepatocytes recover from the stress in the process of isolation.

Consequently, the combination of proper seeding density, media formulation and Matrigel overlay, which not only provides a 3D ECM environment but also offers a number of soluble factors, contributes to the maintenance of hepatocyte morphology over a long period.

However, the limitation of this section is lack of hepatocyte ultrastructure data to further confirm the formation and maintenance of hepatocyte architecture. Transmission electron microscopy (TEM) should be applied to show bile canaliculi, tight junctions, desmosomes, and fat and glycogen storage. Myosin

fibre-containing HSC and multiple junctions with the adjacent hepatocyte can be identified in a spheroid as well by TEM. (Thomas *et al*., 2005)

5.4.2 Co-culture of primary human primary hepatocyte and human HSCs

Spheroids formation of primary human hepatocytes and rat HSCs on 12-well $P_{DL}LA$ coated plates has been previously achieved by Tissue Engineering group, School of Pharmacy, University of Nottingham. However, due to the difficulties of isolation and culture of primary human HSCs, spheroid formation from co-culture of human hepatocytes and human HSCs was not demonstrated. Recently, because of great improvements made on perfusion method of isolation HSCs and maintenance of human HSCs *in vitro* within the group, the co-culture of human hepatocytes and human HSCs was finally established successfully in this study.

As was described in Chapter 1, hepatocyte homo-spheroids and hetero-spheroids showed higher viability and higher level of liver-specific functions than hepatocyte monolayer. In particular, hetero-spheroids were of great interest due to the combination of the benefits of a 3D microenvironment and improved hetero-cell-cell interaction. However, in the literature, most of the hetero-spheroids were formed by co-culture of rat hepatocytes (Lee *et al*., 2004; Otsuka *et al*., 2004) or human hepatic cell lines (Fukuda *et al*. 2006), which could not represent the hepatocyte environment *in vivo*. Therefore, spheroids formed by primary human hepatocytes and human HSCs in this study could provide a highly stable long-term hepatocyte culture and offer the capacity to mimic a more physiologic environment. It will be extremely interesting to

interrogate the maintenance of hepatocyte specific functions under these culture conditions.

Chapter Six:

General Conclusions

6.1 Project overview

In vitro long-term culture of hepatocytes that exhibit high levels of metabolic functions is essential to the success of liver tissue engineering, drug metabolism studies, disease modelling and many other applications. In this thesis, we have demonstrated that the function of hepatocytes in 3D spheroids, formed by co-culture of rat hepatocytes and hepatic stellate cells (HSCs) on $P_{DL}LA$ surfaces, is enhanced by the addition of extracellular matrix, including collagen and Matrigel. The functional capacity of this 3D spheroid model in collagen-Matrigel sandwich, as assessed by albumin secretion, urea secretion and a number of important CYP activities, is superior to spheroids on $P_{DL}LA$ surface and hepatocytes in 2D monoculture. We also report for the first time the formation of 3D spheroids by co-culture of human hepatocytes and human HSCs on $P_{DL}LA$ surface. The utility of this system remains to be established and it may be that, due to limited availability and accessibility of primary human hepatocytes, hepatic cell line will remain an alternative option for hepatocyes *in vitro* studies. However, the potential of homologous human spheroids to contribute to liver tissue engineering and to provide an ideal substrate for drug metabolism studies is an exciting area for further work.

In the absence of a primary cell culture model, a novel immortalized human cell line, Fa2N-4, was tested in this thesis. The characterization of CYP1A2, CYP2C9, CYP3A4 and CYP2B6 induction in Fa2N-4 cells by a range of prototypical compounds at both activity level and mRNA level is reported. Fa2N-4 expresses a wider range of CYP functions than other available liver

cell lines and may be an effective alternative to primary human hepatocytes for the study of CYP1A2 and CYP3A4 induction.

6.2 The mechanism of improved hepatocyte specific functions in co-culture of hepatocyte and hepatic stellate cells (HSCs)

The mechanism for the enhancement of hepatocyte specific functions in co-cultures has not been elucidated yet. It has been reported to be caused by secretion of soluble factors, ECM production, cell-ECM interaction, cell-cell interaction or 3D spheroids (3D structure). Studies that have focused on separating these effects in co-culture are in disagreement. Ijima *et al.* shows the function of hetero-spheroids formed by co-culture of hepatocytes and bone marrow cells (BMCs) is caused by soluble factors derived from BMCs rather than a synergistic effect of spheroids formation and these factors (Ijima *et al*., 2008). Also, an initial hetero-cell-cell contact between hepatocytes and stroma followed by sustained soluble factors from stroma is essential to maintain hepatocyte viability and liver-specific functions (Hui and Bhatia, 2007). In addition, a combination of hetero-cell-cell interaction between hepatocytes and NPCs and sandwich configuration has a strong positive influence on hepatocyte phenotype and metabolic capability (Schmelzer *et al*., 2006). The improved liver-specific function of hepatocyte-hepatic stellate cell co-culture in collagen-Matrigel sandwich found in this thesis is consistent with a combination of hetero-cell-cell interaction, 3D spheroids and cell-ECM interaction. Our work does not distinguish between these possibilities and does not exclude a contribution from soluble factors derived from HSCs. The exact

factor or combination of factors playing a crucial role in maintaining hepatocyte function in this co-culture will be investigated in future.

6.3 Potential improvements and applications of the hepatocyte-stellate cell co-culture model

Cell functional benefits of hepatocyte-hepatic stellate cell co-culture are identified only after the formation of spheroids in culture on day 3, which implies the speed and manner of formation of spheroids is crucial. Supplement with growth factors (Selmer *et al*., 2000), addition of soluble factors such as plasmin and plasminogen activator (Hasebe *et al*., 2003), modification of isolation methods (Okubo *et al*., 2002) or pre-culture of a specific passage number of HSCs might provide an alternative faster method of establishment of spheroids. Also, the sizes of spheroids appear to be variable between 100 and 300 µm in diameter from different isolations or even on different plates from the same isolation. Hepatocytes in the central portion of the spheroids become necrotic if spheroids are bigger than 200 µm in diameter (Takabatake *et al*., 1991). This is consistent with the observation that oxygen maintains its ability to pass through only 100 µm depth in liver tissue (Takabatake *et al*., 1991). Limiting spheroid size to less than 200 µm in diameter may therefore improve function. A method using fluorocarbon as a gel or fluorocarbon-based carrier embedded in an ECM gel can effectively increase the oxygen supply *in vitro* (Nahmias *et al*., 2006) and may be applicable to our spheroid system. Application of patterned co-culture techniques, such as microfabrication and microcontact printing (Fukuda *et al.*, 2006; Nakazawa *et al*., 2006) are also useful to control spheroids sizes. Moreover, hepatic stellate cells (HSCs),

Kupffer cells (KCs) and sinusoidal endothelial cells (SECs) are the three major non-parenchymal cell types line the walls of the hepatic sinusoid *in vivo*. Hepatocytes co-cultured with more than one type of NPCs will more accurately replicate an *in vivo*-like environment, and may further enhance hepatocyte specific functions.

The model of co-culture of hepatocyte-hepatic stellate cell in collagen-Matrigel sandwich in this thesis may be valuable in the development of a bio-artificial liver system, toxicology model, or healthy/diseased model. However, hepatocytes functionality should be improved in a longer period for bio-artificial liver model; the sensitivity of spheroids responding to test compounds need to be tested for toxicology model; and the accessibility and permeability of plasmid or virus to the spheroids need to be investigated.

6.4 Application of the co-culture model for the study of disease pathogenesis

The development of the co-culture in this thesis is intended mainly to provide a model for the study disease pathogenesis, particularly that of hepatitis C. An estimated 200 million people carry hepatitis C virus (HCV) worldwide, which is a major cause of chronic hepatitis, liver cirrhosis and hepatocellular carcinoma (HCC) (Seeff and Hoofnagle, 2003; Chisari, 2005). Currently, the only available treatment for chronic HCV infections is the combination of pegylated interferon and ribavirin. However, this standard therapy is effective in only approximately half of the patients with chronic HCV hepatitis (Feld and Hoofnagle, 2005). As there are in addition no effective vaccines against the

infection, it is urgent to clearly understand the molecular virology of HCV infection.

Recently, a number of small animal models for HCV infection and hepatitis C have been developed to evaluate the efficacy of antiviral drugs and neutralizing monoclonal antibodies, including immunotolerated fetal rat (Wu *et al*., 2005), immunodeficient mice (Eren *et al*., 2006) and uPA mice (Kneteman *et al*., 2006). However, these models still have some limitations, such as over-expressed proteins of interest compared with natural HCV infection, and a possible influence of the integration site of the transgene on the outcome of the study. Also, the chimpanzee model, which can be experimentally infected with HCV, is threatened by the ethical and financial issues. USA, one of the countries to employ chimpanzees for biomedical research, has decided not to continue to breed them for research (Cohen, 2007).

The lack of robust and easily reproducible *in vivo* models leads to the study of *in vitro* models, but only limited areas have been investigated using *in vitro* models. Primary human or *Tupaia* hepatocytes have been mainly used for the study of HCV infection and of the mechanism of viral entry. For example, serum-derived virion is applied to primary Tupais hepatocytes for the study of scavenger receptor class B type I (Barth *et al*., 2005), and HCV-like particle (HCV-LP) infected in primary human hepatocytes is for the study of envelop glycoprotein E2 (Barth *et al*., 2003). For the study of viral replication processes, the establishment of the replicon systems and the production of recombinant infectious virions for HCV is a milestone in HCV research, but occur in a

limited cellular environment in which host cell lines have been selected for the capacity to sustain replication of the virus and may not be representative of primary cells in vivo. Consequently, an efficient cell culture system is required to investigate all steps of the viral life cycle and bring new insights in to the biology and molecular virology of HCV. A particular advantage of the co-culture model in this chapter is the capacity to study the signalling between hepatocytes and HSC and this system would therefore be an ideal model for the study of HCV replication. Work to establish HCV infection in our system is currently in progress.

Appendix

Appendix 1 Cell culture solutions

1.1 Preparation of HanksHEPES buffer (10×)

NaCl (Sigma, UK)	1.37 M (80g/L)
KCl (Sigma, UK)	54 mM (4g/L)
KH_2PO_4 (BDH, Dorset, UK)	4.4 mM (0.6g/L)
$Na_2HPO_4.12H_2O$ (Sigma, UK)	3.6 mM (1.2g/L)
HEPES (Sigma, UK)	200 mM (47.6g/L)
NaOH (Sigma, UK)	100 mM (4g/L)
Sterile distilled water	1000 ml

- Filter sterilized and stored at 4˚C
- To make up 1 × buffer, diluted with sterile distilled water and stored at 4˚C

1.2 Preparation of bicarbonate/glucose solution

NaHCO3 (Sigma, UK)	0.74 M (3.1g/50ml)
Glucose (Sigma, UK)	0.28 M (2.5g/50ml)
Methionine (Sigma, UK)	0.1 M (0.75g/50ml)
Sterile distilled water	50 ml

- Filter sterilized and stored in aliquots (12 ml) at -20˚C
- To make up working HanksHEPES buffer, 2 ml bicarbonate/glucose solution added to per 100 ml 1× HanksHEPES buffer
- Stored at 4˚C overnight

1.3 Preparation of 25 mM EGTA solution

EGTA (Sigma, UK)	0.48 g
Sterile 1x HanksHEPES (no bicarbonate/glucose)	25 ml

NaOH 1M (Sigma, UK)	2.5 ml

- Made up to 50 ml with 1× HanksHEPES buffer, filter sterilized and stored at 4˚C

1.4 Preparation of 250 mM $CaCl_2$ solution

$CaCl_2$ (FISONS Scientific Equipment, UK)	1.84 g
Sterile distilled water	50 ml

- Filter sterilized and stored at 4˚C

1.5 Preparation of perfusate buffer (EGTA chelating buffer)

HanksHEPES buffer (10×)	40 ml
Bicarbonate/glucose solution	8 ml
25 mM EGTA solution	8 ml
Sterile distilled water	360 ml

- stored at 4˚C overnight

1.6 Preparation of collagenase perfusate buffer

HanksHEPES buffer (10×)	20 ml
Bicarbonate/glucose solution	4 ml
250 mM $CaCl_2$ solution	4 ml
Sterile distilled water	180 ml

- stored at 4˚C overnight

1.7 Preparation of percoll solution

Percoll (Amersham, UK)	90 ml
HBSS (10×) (Sigma, UK)	10 ml

- Stored at 4˚C

1.8 Preparation of culture medium

1.8.1 Primary rat hepatocyte complete medium

Ingredient	*Volume*	*Final concentration*
Williams medium E (GibcoBRL, UK)	500 ml	N/A
L-glutamine (200 mM) (GibcoBRL, UK)	5 ml	2 mM
Antibiotic/antimycotic (100× solution) (GibcoBRL, UK)	5 ml	100 U penicillin 100 µg streptomycin 250 ng amphotericin B
Foetal calf serum (Sigma, UK)	50 ml	10 %

1.8.2 Primary rat hepatocyte incomplete medium

Ingredient	*Volume*	*Final concentration*
Williams medium E (GibcoBRL, UK)	500 ml	N/A
L-glutamine (200 mM) (GibcoBRL, UK)	5 ml	2 mM
Antibiotic/antimycotic (100× solution) (GibcoBRL, UK)	5 ml	100 U penicillin 100 µg streptomycin 250 ng amphotericin B
Insulin solution (10 mg/ml) (Sigma, UK)	500 µl	10 µg/ml
Nicotinamide (500 mM solution) (Sigma, UK)	5 ml	5 mM

1.8.3 Primary rat hepatic stellate cell medium

Ingredient	*Volume*	*Final concentration*
Dulbecco's modified Eagles Medium (DMEM) (GibcoBRL, UK)	500 ml	N/A
L-glutamine (200 mM) (GibcoBRL, UK)	5 ml	2 mM
Antibiotic/antimycotic (100× solution) (GibcoBRL, UK)	5 ml	100 U penicillin 100 µg streptomycin 250 ng amphotericin B
Foetal calf serum GOLD (Sigma, UK)	50 ml	10 %

1.8.4 Primary human hepatocyte plating medium

Ingredient	*Volume*	*Final concentration*
Williams medium E (GibcoBRL, UK)	500 ml	N/A
Antibiotic (100× solution) (GibcoBRL, UK)	5 ml	100 U penicillin 100 µg streptomycin
Insulin solution (10 mg/ml) (Sigma, UK)	2 µl	0.1 µM
Dexamethasone (Sigma, UK)	50 µl	0.1 µM
L-glutamine (200 mM) (GibcoBRL, UK)	5 ml	2 mM

1.8.5 Primary human hepatocyte culture medium

Ingredient	*Volume*	*Final concentration*
Dulbecco's modified Eagles Medium (DMEM) (GibcoBRL, UK)	500 ml	N/A
Antibiotic (100× solution) (GibcoBRL, UK)	5 ml	100 U penicillin 100 µg streptomycin
Insulin solution (10 mg/ml) (Sigma, UK)	2 µl	0.1 µM
Dexamethasone (Sigma, UK)	500 µl	1 µM
Foetal calf serum (Sigma, UK)	25 ml	5 %

1.8.6 Primary human hepatocyte isolation medium

Ingredient	*Volume*	*Final concentration*
Dulbecco's modified Eagles Medium (DMEM) (GibcoBRL, UK)	500 ml	N/A
L-glutamine (200 mM) (GibcoBRL, UK)	5 ml	2 mM
Antibiotic/antimycotic (100× solution) (GibcoBRL, UK)	5 ml	100 U penicillin 100 μg streptomycin
Foetal calf serum (Sigma, UK)	50 ml	10 %

1.8.7 Primary human hepatic stellate cell medium

Ingredient	*Volume*	*Final concentration*
Dulbecco's modified Eagles Medium (DMEM) (GibcoBRL, UK)	500 ml	N/A
L-glutamine (200 mM) (GibcoBRL, UK)	5 ml	2 mM
Antibiotic/antimycotic (100× solution) (GibcoBRL, UK)	5 ml	100 U penicillin 100 μg streptomycin
Human serum (Sigma, UK)	75 ml	15 %

- Stored at 4˚C and expired in two weeks

Appendix 2 Assay buffers

2.1 Fluorescence assay for ethoxy resorufin-O-dealkylase (EROD) activity

2.1.1 Krebs buffer

NaCl (Sigma, UK)	120 mM (7.013 g)
KCl (Sigma, UK)	4.8 mM (0.358 g)
KH_2PO_4 (BDH, Dorset, UK)	1.2 mM (0.163 g)
$NaHCO_3$ (Sigma, UK)	24 mM (2.106 g)
$MgCl_2$ (Sigma, UK)	1.2 mM (0.244 g)
$CaCl_2$ (FISONS Scientific Equipment, UK)	1.8 mM (0.265 g)
HEPES (Sigma, UK)	10 mM (2.383 g)
Sterile distilled water	1000 ml

- Filter sterilized and stored at 4˚C

2.1.2 7-Ethoxyresorufin 1mM stock solution (200 ×)

7-Ethoxyresorufin (Sigma, UK)	2.63 mg
Dimethyl sulphoxide (DMSO) (Sigma, UK)	10 ml

- Stored at 4˚C in 200 µl aliquots and protected from light with foil
- Diluted to 5 µM with Krebs buffer

2.1.3 Dicoumarol 2 mM stock solution

Dicoumarol	1.0089 g
Dimethyl sulphoxide (DMSO) (Sigma, UK)	15 ml

- Diluted to 10 µM with Krebs buffer

2.1.4 Sodium acetate buffer (0.1 M) pH 4.5

$NaCH_3COO{\cdot}3H_2O$ (Fisher Scientific, UK)	4.101 g
Sterile distilled water	500 ml

- Ajusted to pH 4.5 and stored at 4˚C

2.1.5 β-glucuribudase enzyme stock solution (1600 units/ml)

β-glucuribudase enzyme (374000 units/g)	1.35 g
Krebs buffer	15.75 ml

- Stored at -20˚C in 500 µl aliquots
- Diluted to 32000 units/ml with sodium acetate buffer

2.1.6 7-hydroxyresorufin standards

Step	*Concentration*	*Stock*	*Krebs buffer (ml)*
1	0.1 mM	2.35 mg	10
2	0.1 µM	10 µl from step 1	1
3	100 pmol/ml	100 µl from step 2	10
4	50 pmol/ml	5 ml from step 3	5
5	25 pmol/ml	5 ml from step 4	5
6	12.5 pmol/ml	5 ml from step 5	5
7	6.25 pmol/ml	5 ml from step 6	5
8	3.125 pmol/ml	5 ml from step 7	5

2.2 Rat albumin enzyme-linked immunosorbent (ELISA) assay

2.2.1 ELISA coating buffer

Carbonate-bicarbonate capsule (Sigma, UK)	1 capsule
Sterile distilled water	100 ml

- stored at 4˚C

2.2.2 ELISA washing solution

Tris buffered saline pH 8 (TBS) (Sigma, UK)	1 sachet
Polyoxyethylene sorbitan monolaurate (Tween 20) (Sigma, UK)	0.5 ml (0.05% v/v)
Sterile distilled water	1000 ml

2.2.3 ELISA blocking solution

Tris buffered saline pH 8 (TBS) (Sigma, UK)	1 sachet
Bovine serum albumin (BSA) (Sigma, UK)	10 g (1% w/v)
Sterile distilled water	1000 ml

2.2.4 ELISA dilution solution

Tris buffered saline pH 8 (TBS) (Sigma, UK)	1 sachet
Bovine serum albumin (BSA) (Sigma, UK)	10 g (1% w/v)
Tween 20 (Sigma, UK)	0.5 ml (0.05% v/v)
Sterile distilled water	1000 ml

2.2.5 ELISA stop solution 2M H_2SO_4

- Made up to sterile distilled water and stored at room temperature

2.2.6 Dilutions of calibrator albumin

Step	*Concentration (ng/ml)*	*Volume of stock*	*Sample diluents (ml)*
1	500	5 µl	30
2	250	1 ml from step 1	1
3	125	1 ml from step 2	1
4	62.5	1 ml from step 3	1
5	31.25	1 ml from step 4	1
6	15.625	1 ml from step 5	1
7	7.8	1 ml from step 6	1
8	3.9	1 ml from step 7	1
9	1.95	1 ml from step 8	1
10	0.975	1 ml from step 9	1
11	0.49	1 ml from step 10	1

2.2.7 Dilutions of HRP conjugated anti-albumin

Step	*Concentration (ng/ml)*	*Volume of stock*	*Sample diluents (ml)*
1	1:1000	5 µl	5
2	1:10000	1 ml from step 1	9
3	1:20000	1 ml from step 2	1
4	1:40000	1 ml from step 3	1
5	1:80000	1 ml from step 4	1

2.3 High performance liquid chromatography (HPLC)

2.3.1 Mobile phase solution A

HPLC grade acetonitrile Far UV	50 ml
Formic acid	250 µl

Sterile distilled water	450 ml

2.3.2 Mobile phase solution B

HPLC grade acetonitrile Far UV	450 ml
Formic acid	75 µl
Sterile distilled water	50 ml

2.3.3 Testosterone working buffer

Testosterone (Sigma, UK)	11.6 mg
100 % methanol	1 ml

- 5µl of solution mixed with 2 ml EBSS (Fisher, UK) and stored at 4˚C

2.4 Estimation of DNA content using HOECHST 33258

2.4.1 Hoechst 33258 dilution buffer

Trizma base(Sigma, UK)	0.01 M
Ethylenediamine tetra-acetic acid (EDTA) (Sigma, UK)	0.01 M
Sodium chloride (Sigma, UK)	0.1 M
Sterile distilled water	Made up to 1 L

- Adjusted to pH 7 with 1 M HCl and stored at 4˚C

2.4.2 Hoechst 33258 stock solution

Bisbenzinide (Sigma, UK)	20 mg
Saline sodium citrate buffer (SSC)	20 ml

- Stored at -20˚C in 200 µl aliquots

2.4.3 Hoechst 33258 working solution (2 µg/ml)

Hoechst 33258 stock solution	200 µl
Hoechst 33258 dilution buffer	49.8 ml

2.4.4 DNA stock solution

DNA (sodium salt from salmon tests) (Sigma, UK)	20 mg
Saline sodium citrate buffer (SSC)	20 ml

- Stored at -20˚C in 200 µl aliquots

2.4.5 DNA working solution (100 µg/ml)

DNA stock solution	200 µl
Papain solution	1.8 ml

2.4.6 Papain buffer

Dibasic sodium phosphate (Sigma, UK)	0.1 M
L-Cysteine hydrochloride (Sigma, UK)	0.005 M
EDTA (Sigma, UK)	0.005 M
Sterile distilled water	Made up to 100 ml

- Adjusted to pH 6.5 with 1 M HCl and stored at 4˚C

2.4.7 Papain solution

Papain (Sigma, UK)	0.0264 g
Papain buffer	25 ml

- Made fresh on the day required

2.5 Oil red O stain for hepatic stellate cells

2.5.1 Oil read O stock solution

Oil red O (Sigma, UK)	0.5 g
Isopropanol (Fisher, UK)	100 ml

- stored at 4˚C

2.5.2 Oil red O staining solution

Oil red O stock solution (Sigma, UK)	60 ml
Sterile distilled water (Fisher, UK)	40 ml

- Allowed to stand for 10 minutes and filtered before use

Appendix 3 Optimization of technique of primary rat hepatocytes isolation

Rat hepatocytes functionalities were firstly assessed by albumin secretion, urea secretion and testosterone metabolism assay on 12-well plates (Chapter 3, Figure 3.2 and 3.3). However, hepatocytes spheroids were not successfully formed on 12-well $P_{DL}LA$ coated plates as expected (Chapter 3, Figure 3.1). After the studies of the effects of different passage number HSCs and seeding density on spheroids formation (Chapter 3), 6-well plates were used for cultured hepatocytes instead. Also, because of inaccuracy and insensitivity of testosterone metabolism assay, and absence of DNA normalization of data by 12-well plates, LC-MS/MS and DNA content assay by QIAamp® DNA Mini Kit were introduced to hepatocytes cultured on 6-well plates. As a result, the spheroids were successfully developed in all culture systems except monoculture in collagen-Matrigel sandwich. In addition, the data of albumin secretion, urea secretion and CYP activities by LC-MS/MS were normalized to DNA level. However, after the first successful experiment on 6-well plates (Chapter 3, Figure 3.5 and 3.6), the viability of rat hepatocytes dropped dramatically and the CYP activities of spheroids disappeared after only a few days. The viability decreased from approximately 80% to 30% before percoll. The CYP activities of spheroids maintained for only three days instead of over a week. More surprisingly, cells in monoculture showed better functionalities than those in culture configuration, but cells co-cultured with HSCs in collagen-Matrigel sandwich showed the best functionalities from previous experiment. Therefore, the influence of chemicals (HEPES, EGTA, $CaCl_2$ and collagenase), water, medium, perfusion time and deceleration speed on the

quality of hepatocytes were assessed in order to get better viable and functional rat hepatocytes. Indices of quality were: the viability of hepatocytes following isolation, as assessed by dye exclusion; the morphology of hepatocytes in monoculture and co-culture; subsequently, the results of CYP function assays. The following experiments were conducted:

	Solutions	Collagenase	Total cell number (million)	Viability before percoll	Spheroids formation	Functional analysis	Other
Exp 1	HanksHEPES prepared in Boots building	C5138 LOT 037K7691 715 units/ mg (Sigma)	100 heps + good yield of HSCs	80%	Yes, except monoculture in collagen-Matrigel sandwich	Chapter 3 Figure 3.6	
Exp 2	HanksHEPES prepared in CBS building (no de-ionized water)	C5138 LOT 037K7691 715 units/ mg (Sigma)	5 heps + no yield of HSCs	10%	NA	NA	Hard liver lobes during perfusion
Exp 3	HanksHEPES prepared in CBS building (no de-ionized water)	C5138 LOT 037K7691 715 units/ mg (Sigma)	No heps + no yield of HSCs	NA	NA	NA	Hard liver lobes during perfusion
Exp 4	New HanksHEPES prepared by new chemicals	C5138 LOT 037K7691 715 units/ mg (Sigma)	No heps + no yield of HSCs	NA	NA	NA	Hard liver lobes during perfusion
Exp 5	New HanksHEPES prepared by new chemicals in de-ionized water	C5138 LOT 037K7691 715 units/ mg (Sigma)	10 heps + no yield of HSCs	20%	NA	NA	Less harder liver lobes during perfusion
Exp 6	New HanksHEPES prepared by new chemicals in de-ionized water	C5138 LOT 037K7691 715 units/ mg (Sigma)	8 heps + no yield of HSCs	23%	NA	NA	Less harder liver lobes during perfusion
Exp 7	New HanksHEPES, same as Exp 6 but with new HEPES Catalogue No. H4043, Sigma	C5138 LOT 037K7691 715 units/ mg (Sigma)	20 heps + no yield of HSCs	35%	NA	NA	Soft liver lobes during perfusion

Exp 8	Same as Exp 7	C5138 LOT 116K7681 715 units/ mg (Sigma)	20 heps + no yield of HSCs	35%	NA	NA	Soft liver lobes during perfusion
Exp 9	New HanksHEPES prepared as Exp 7 but with different Cat No. E3889 EGTA and Cat No. C8106 $CaCl_2$	C5138 LOT 116K7681 715 units/ mg (Sigma)	98 heps + good yield of HSCs	50%	NA	NA	Soft liver lobes during perfusion + big liver lobes (rat in 450 g)
Exp 10	Same as Exp 9	C5138 LOT 116K7681 715 units/ mg (Sigma)	30 heps + good yield of HSCs	50%	NA	NA	Small liver lobes (rat in 200 g)
Exp 11	Same as Exp 9	C5138 LOT 116K7681 715 units/ mg (Sigma)	50 heps + good yield of HSCs	45%	NA	NA	Normal liver lobes (rat in 300 g)
Exp 12	Same as Exp 9	C5138 LOT 116K7681 715 units/ mg (Sigma)	8.2 heps + no yield of HSCs	35%	NA	NA	Normal liver lobes (rat in 300 g)
Exp 13	Same as Exp 9, but 10% serum in collagenase buffer	C5138 LOT 116K7681 715 units/ mg (Sigma)	28 heps + no yield of HSCs	45%	NA	NA	Normal liver lobes (rat in 300 g)
Exp 14	Same as Exp 9	C1889 LOT 077K8613 (Sigma)	20 heps + very low yield of HSCs	40%	NA	NA	Normal liver lobes (rat in 300 g)
Exp 15	Same as Exp 9	C5138 with lower collagenase activity 455 units/mg (Sigma)	40 heps + very low yield of HSCs	45%, 90% after percoll	Yes, except monoculture in collagen-Matrigel sandwich and coculture on collagen gel	Appendix 3 Figure 3.1	Normal liver lobes (rat in 300 g)
Exp 16	Same as Exp 9, but 160 mg collagenase in 200 ml buffer	Cat No. 11 088793 001 (Roche)	72 heps + no yield of HSCs	60%	Yes, except monoculture in collagen-Matrigel sandwich	Appendix 3 Figure 3.2	15 mins collagenase buffer perfusion time
Exp 17	Same as Exp 9, but 80 mg collagenase in 200 ml buffer	Cat No. 11 088793 001 (Roche)	28 heps + no yield of HSCs	40%	NA	NA	15 mins collagenase buffer perfusion time
Exp 18	Same as Exp 9, but 100mg collagenase in 200 ml buffer	Cat No. 11 088793 001 (Roche)	70 heps + good yield of HSCs	60.5%	NA	NA	20 mins collagenase buffer perfusion time
Exp 19	Same as Exp 18	Cat No. 11 088793 001 (Roche)	40 heps + good yield of HSCs	65.3%	NA	NA	20 mins collagenase buffer perfusion time
Exp 20	Same as Exp 18	Cat No. 11 088793 001 (Roche)	82 heps + good yield of HSCs	63.3%	NA	NA	20 mins collagenase buffer perfusion time

Exp 21	Same as Exp 18	Cat No. 11 088793 001 (Roche)	15 heps + no yield of HSCs	20%	NA	NA	20 mins collagenase buffer perfusion time
Exp 22	Prepared in Astrazeneca	Cat No. 11 088793 001 (Roche)	40 heps	80%	Yes, except monoculture in collagen-Matrigel sandwich	Appendix 3 Figure 3.3	Viability dropped to 60% due to transport but back to 84% after percoll
Exp 23	Same as Exp 9	C5138 LOT 116K7681 715 units/ mg (Sigma)	60 heps + good yield of HSCs	60%	NA	NA	Fresh william E medium
Exp 24	Same as Exp 9	C5138 LOT 116K7681 715 units/ mg (Sigma)	80 heps + good yield of HSCs	72%	NA	NA	Fresh william E medium
Exp 25	Same as Exp 9	C5138 LOT 116K7681 715 units/ mg (Sigma)	50 heps + good yield of HSCs	65%	NA	NA	Fresh william E medium
Exp 26	Same as Exp 9	C5138 LOT 116K7681 715 units/ mg (Sigma)	60 heps + good yield of HSCs	63%	Yes, except monoculture in collagen-Matrigel sandwich	Appendix 3 Figure 3.4 (no 20 mins activities in raw data)	Fresh william E medium
Exp 27	Same as Exp 18	Cat No. 11 088793 001 (Roche)	50 heps + good yield of HSCs	70%	NA	NA	Fresh william E medium
Exp 28	Same as Exp 18	Cat No. 11 088793 001 (Roche)	40 heps + good yield of HSCs	65%	Yes, except monoculture in collagen-Matrigel sandwich	Appendix 3 Figure 3.5	Fresh william E medium
Exp 29	Same as Exp 9	Cat No.17465 (AMS Biotechnology Ltd.)	40 heps + good yield of HSCs	64%	NA	NA	Low deceleration speed
Exp 30	Same as Exp 9	Cat No.17465 (AMS Biotechnology Ltd.)	43 heps + good yield of HSCs	63%	NA	NA	Low deceleration speed
Exp 31	Same as Exp 9	Cat No.17465 (AMS Biotechnology Ltd.)	38 heps + good yield of HSCs	61%	Yes, except monoculture in collagen-Matrigel sandwich	Appendix Figure 3.6	Low deceleration speed

Although cell viability was back to approximately 70% before percoll after changing chemicals, medium, etc, it failed to reach 80% as previous isolations. In addition, Figure 3.1, 3.2, 3.3, 3.4, 3.5 and 3.6 show the CYP activities of rat hepatocytes in different culture configurations. From all the data, cells monocultured in collagen-Matrigel sandwiches show better activities than cells in any other culture systems, which are conflict from previous experiments. In conclusion, despite this very extensive set of experiments assessing the contribution of key variables, we were unable to replicating the high hepatocyte viability and consistent results of earlier isolations.

A)

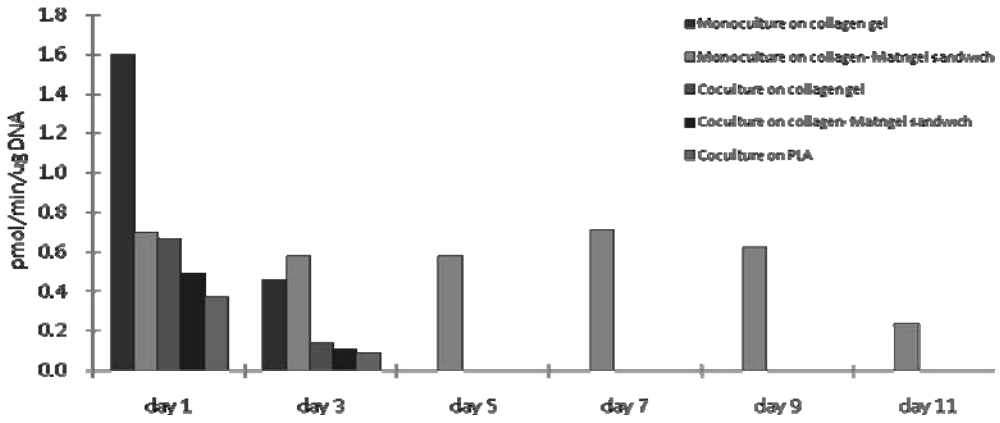

B)

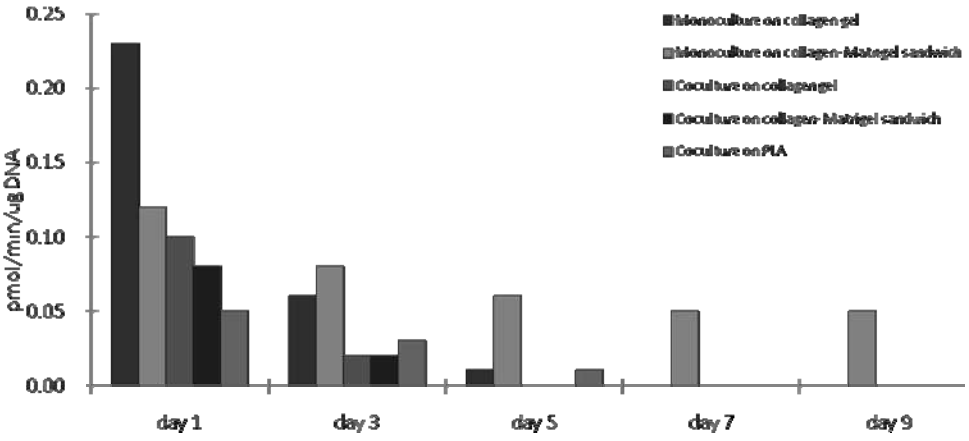

C)

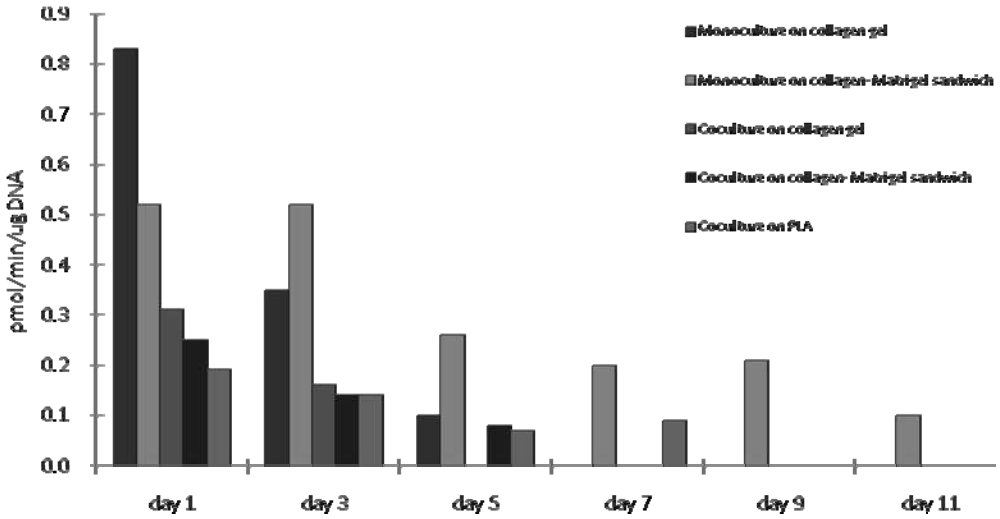

Figure 3.1 Paracetamol production (CYP1A2 activity) (A), 1'-hydroxymidazolam production (CYP3A1 activity) (B), and 1'-hydroxybuproprion (CYP2B6 activity) production (C) by rat hepatocytes on 6 well plates after 24 hours. (n=1)

A)

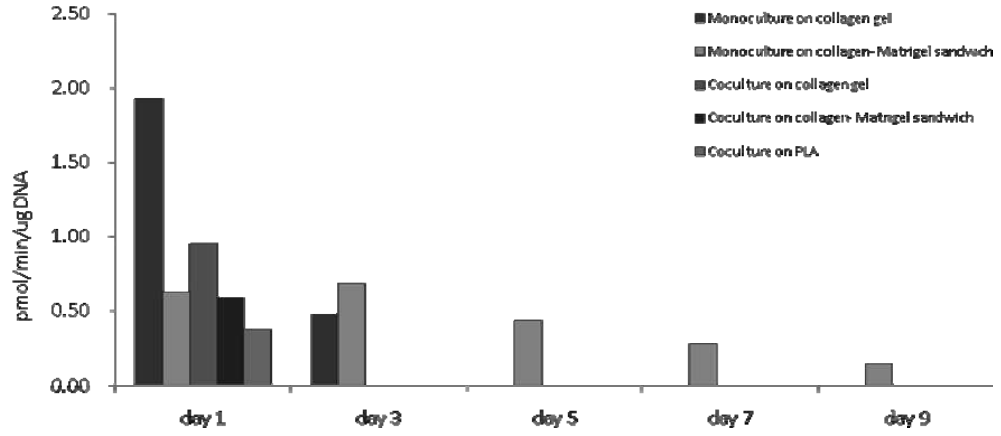

B)

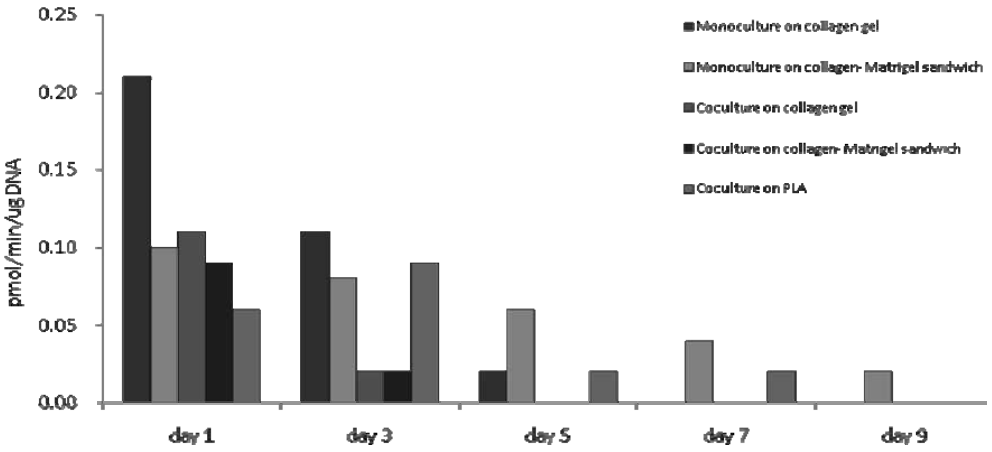

C)

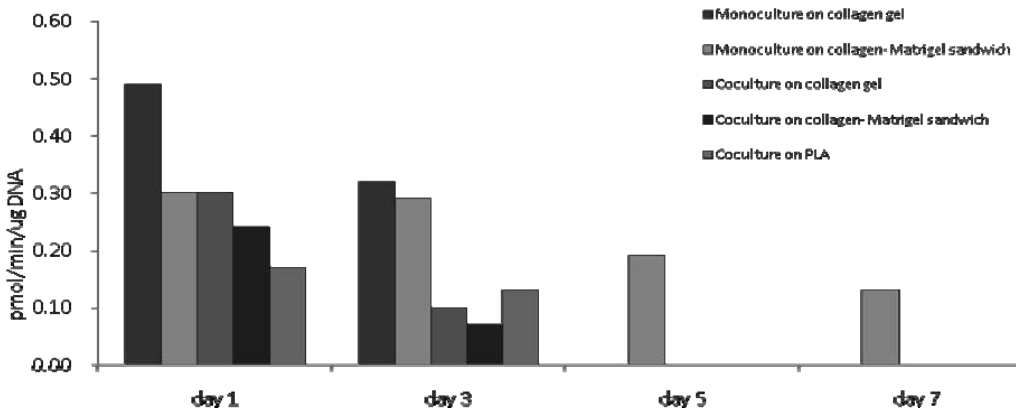

Figure 3.2 Paracetamol production (CYP1A2 activity) (A), 1'-hydroxymidazolam production (CYP3A1 activity) (B), and 1'-hydroxybuproprion (CYP2B6 activity) production (C) by rat hepatocytes on 6 well plates after 24 hours. (n=1)

A)

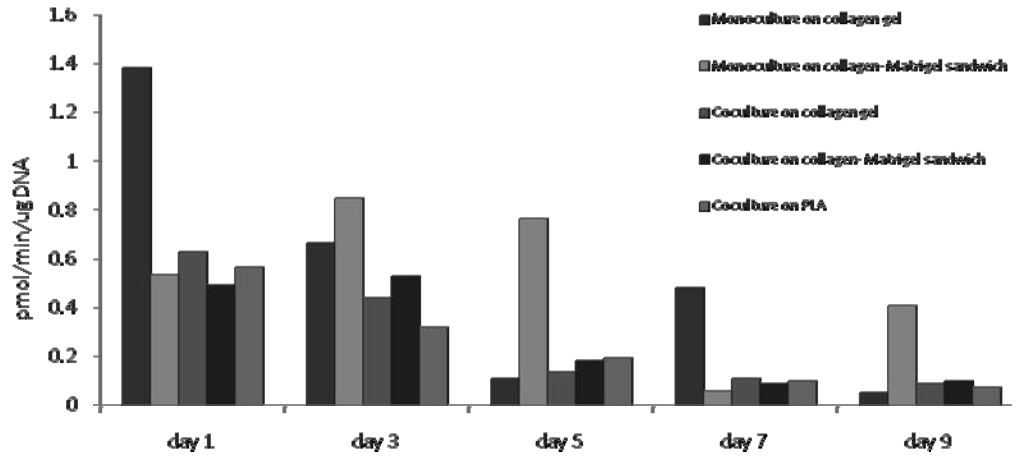

B)

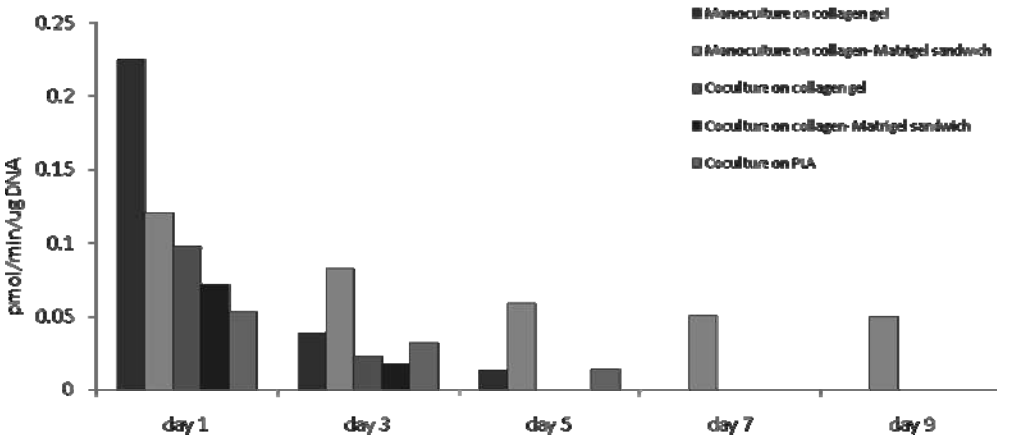

C)

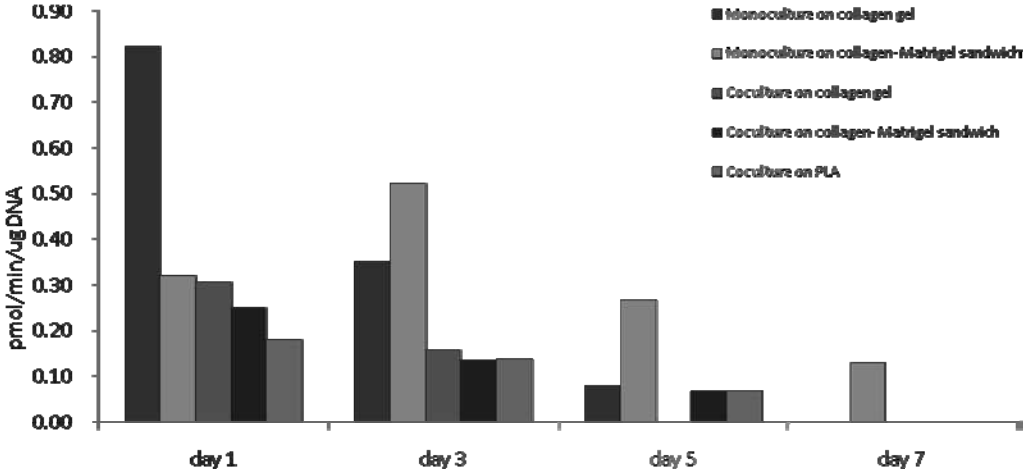

Figure 3.3 Paracetamol production (CYP1A2 activity) (A), 1'-hydroxymidazolam production (CYP3A1 activity) (B), and 1'-hydroxybuproprion (CYP2B6 activity) production (C) by rat hepatocytes on 6 well plates after 24 hours. (n=1)

A)

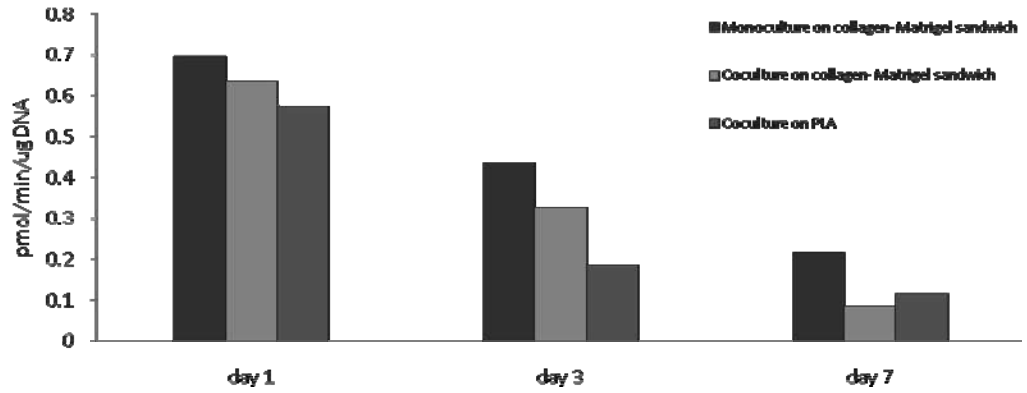

B)

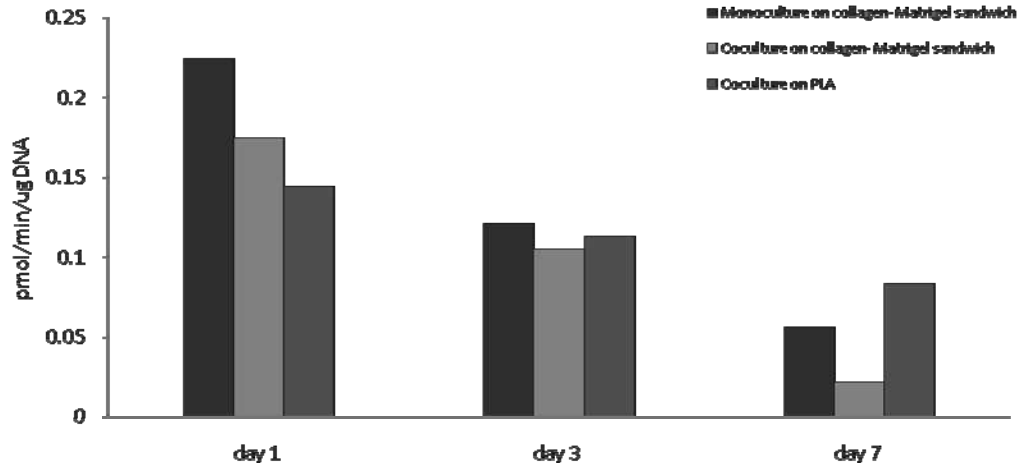

C)

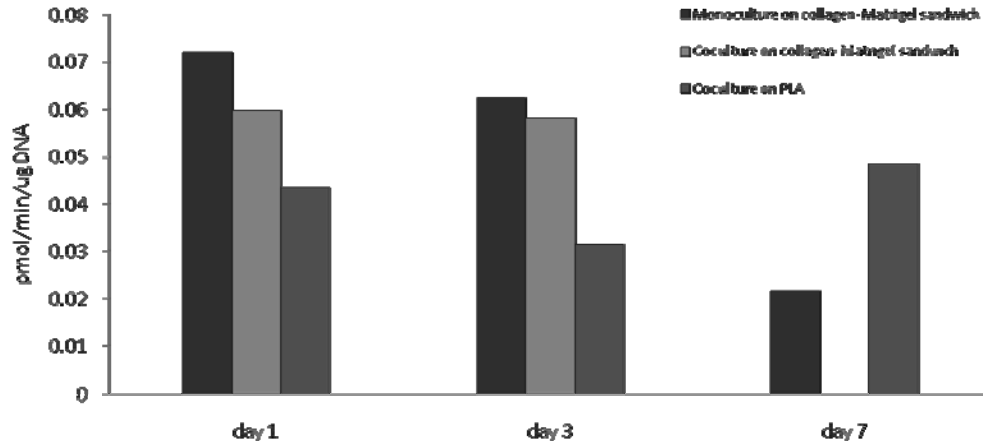

Figure 3.4 Paracetamol production (CYP1A2 activity) (A), 1'-hydroxymidazolam production (CYP3A1 activity) (B), and 1'-hydroxybuproprion (CYP2B6 activity) production (C) by rat hepatocytes on 6 well plates after 24 hours. (n=1)

A)

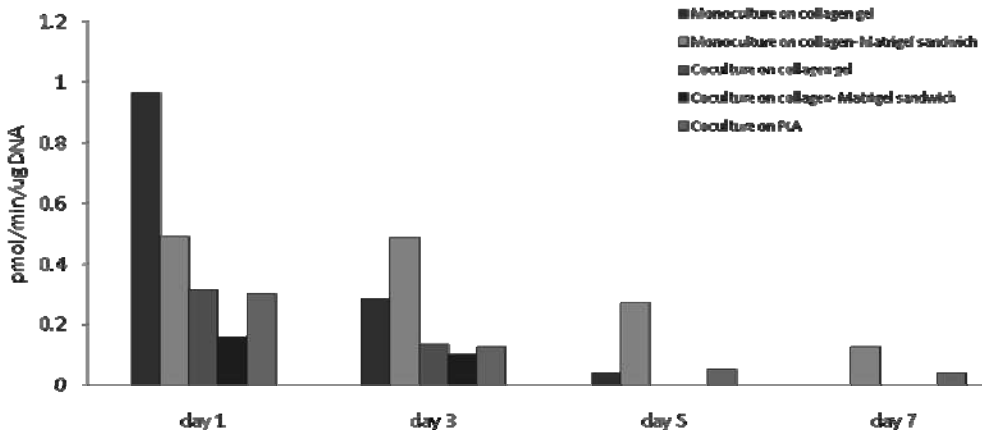

B)

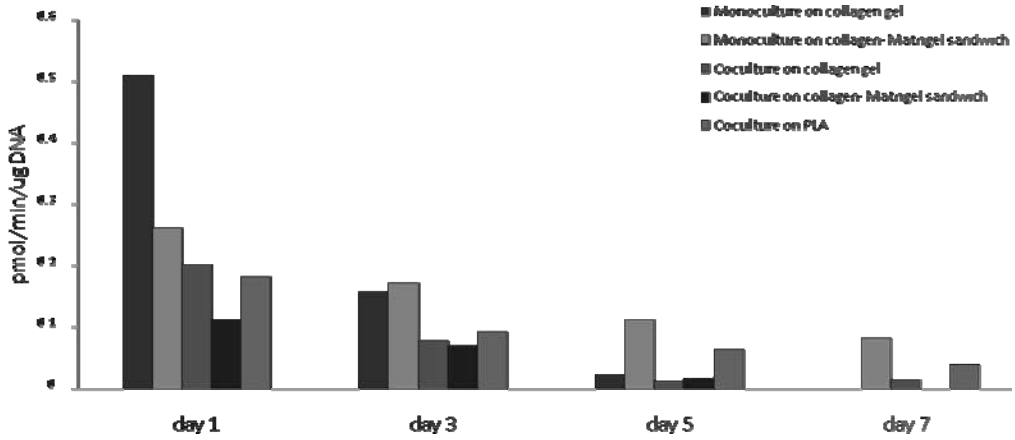

C)

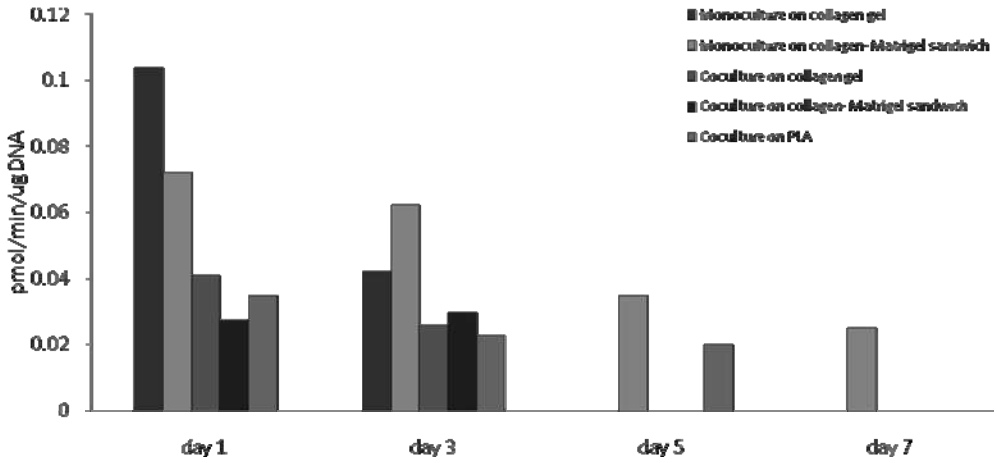

Figure 3.5 Paracetamol production (CYP1A2 activity) (A), 1'-hydroxymidazolam production (CYP3A1 activity) (B), and 1'-hydroxybuproprion (CYP2B6 activity) production (C) by rat hepatocytes on 6 well plates after 24 hours. (n=1)

A)

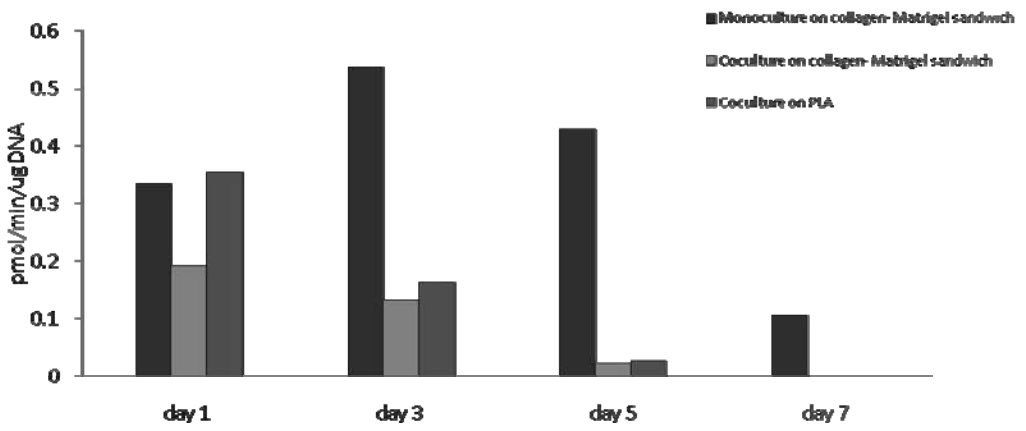

B)

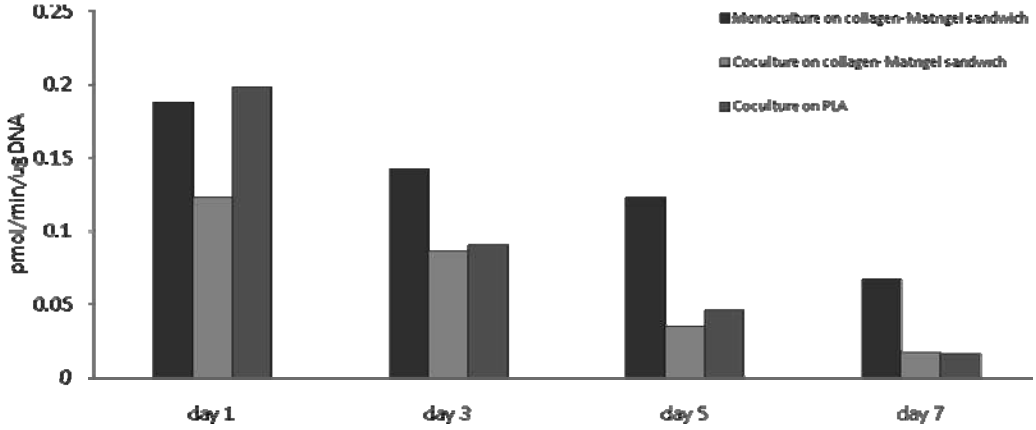

C)

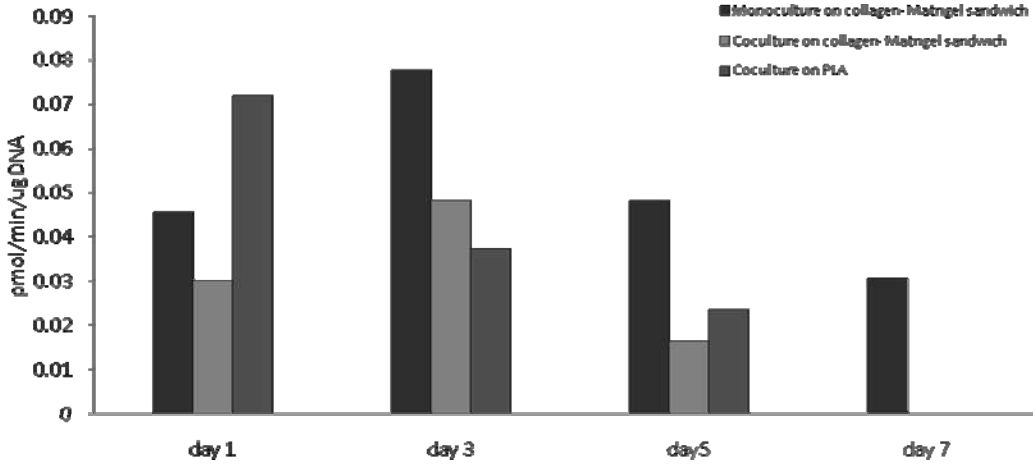

Figure 3.6 Paracetamol production (CYP1A2 activity) (A), 1'-hydroxymidazolam production (CYP3A1 activity) (B), and 1'-hydroxybuproprion (CYP2B6 activity) production (C) by rat hepatocytes on 6 well plates after 24 hours. (n=1)

References

Abdel-Razzak, Z., Loyer, P., Fautrel, A., Gautier, J.C., Corcos, L., Turlin, B., Beaune, P. and Guillouzo, A. (1993). Cytokines down-regulate expression of major cytochrome P-450 enzymes in adult human hepatocytes in primary culture. *Mol Pharmacol*, **44**, 707-715.

Abu-Absi, S.F., Friend, J.R., Hansen, L.K., Hu, W.S. (2002). Structural polarity ancl functional bile canaliculi in rat hepatocyte spheroids. *Exp Cell Res*, **274**(r), 56-67.

Abu-Absi, S.F., Hu, W.S. and Hansen, L.K. (2005). Dexamethasone effects on rat hepatocyte pheroid formation and function. *Tissue Eng*, **11**(3-4), 415-426.

Acosta, D., Sorensen, E.M., Anuforo, D.C., Mitchell, D.B., Ramos, K., Santone, K.S. and Smith, M.A. (1985). An in vitro approach to the study of target organ toxicity of drugs and chemicals. *In Vitro Cell Dev Biol*, **21**, 495-504.

Agius, L. and Peak, M. (1993). Intracellular binding of glucokinase in hepatocytes and translocation by glucose, fructose and insulin. *Biochem J*, **296**, 785-796.

Akon, H., Marie, K., Kenichi, K., Su, C.C., Toshihiro, A. and Mariko, H. (2005). Albumin and urea production by hepatocytes cultured on extracellular matrix protein-conjuaged poly (vinyl alcohol) membrances. *Journal of Biomaterials Science*, **16**, 847-860.

Aladag, M., Gurakar, A., Jalil, S. *et al*. (2004). A liver transplant center experience with liver dialysis in the management of patients with fulminant hepatic failure: a preliminary report. *Transplant Proc*, **36**, 203-205.

Alexander, E., Cahn, M., Abadie-Viollon, C., *et al*. (2002). Influence of pre-, inta-, and post-operative parameters of donor liver on the outcome of isolated human hepatocytes. *Cell Tissue Bank*, **3**, 223-233.

Alhelda, S.M., and Buck, C.A. (1990). Integrins and other cell adhesion molecules. *FASEB J,* **4**, 2868-2880.

Alison, M.R., Golding, M., Sarraf, C.E., *et al*. (1996). Liver damage in the rat induces hepatocyte stem cells from biliary epithelial cells. *Gastroenterology*, **110**, 1182-1190.

Allen, J.W., Hassanein, T. and Bhatia, S.N. (2001). Advances in bioartificial liver devices. *Hepatology*, **34**(3), 447-455.

Althaus, F.R., Lawrence, S.D., Sattler, G.L. and Pitot, H.C. (1982). ADP-ribosyltransferase activity in cultured hepatocytes. *J Biol Chem*, **257,** 5528-5535.

Andus, T., Geiger, T., Hirano, T., Kishimoto, T., and Heinrich, P.C. (1988). Action of recombinant human interleukin 6, interleukin 1 beta and tumor necrosis factor alpha on the mRNA induction of acute-phase proteins. *Eur J Immunol*, **18**, 739-746.

Appleton, I., Tomlinson, A., Chander, C.L., and Willoughby, D.A. (1992). Effect of endothelin-1 on croton oil-induced granulation tissue in the rat. A pharmacologic and immunohistochemical study. *Lab Investig*, **67**, 703–710.

Arnaud, A., Fontana, L., Angulo, A.J., Gil, A., Pez-Pedrosa, J.M.L. (2003). Proliferation, functionality, and extracellular matrix production of hepatocytes and a liver stellate cell line. *Digestive Diseases and Sciences*, **48**, 1406-1413.

Arthur, M.J. (2000). Fibrogenesis II. Metalloproteinases and their inhibitors in liver fibrosis. *Am J Physiol*, **279**, G245-G249.

Auth, M. K.H., Woitaschek, D., Beste, M., Schreiter, T., Kim, H.S., Oppermann, E., *et al*. (2005). Blaheta6 preservation of the synthetic and metabolic capacity of isolated human hepatocytes by coculture with human biliary epithelial cells. *Liver Transpl*, **11**, 410-419.

Backlund, M., and Ingelman-Sundberg, M. (2005). Regulation of aryl hydrocarbon receptor signal transduction by protein tyrosine kinases. *Cell Signal*, **17**(1), 39-48.

Ballardini, G., Groff, P., Badiali de Giorgi, L.B., Schuppan, D. and Bianchi, F.B. (1994). Ito cell heterogeneity: desmin-negative Ito cels in normal rat liver. *Hepatology*, **19**, 440-446.

Barbetta, A., Massimi, M., Di Rosario, B., Nardecchia, S., De Colli, M., Devirgiliis, L.C. and Dentini, M. (2008). Emulsion template scaffolds that include gelatine and glycosaminoglycans. *Biomacromolecules*, **9**(10), 2844-2856.

Barth, H., Cerino, R., Arcuri, M., *et al*. (2005). Scavenfer receptor class B type I and hepatitis C virus infection of primary tupaia hepatocytes. *J Virol*, **79**, 5774-5785.

Barth, H., Schafer, C., Adah, M.I., *et al*. (2003). Cellular binding of hepatitis C virus envelop glycoprotein E2 requires cell surface heparin sulphate. *J Biol Chem*, **278**, 41003-41012.

Bastien, M.C., Leblond, F., Pichette, V. and Villeneuve, J.P. (2000). Differential alteration of cytochrome P450 isoenzymes in two experimental models of cirrhosis. *Can J Physiol Pharmacol*, **78**(11), 912-919.

Bataller, R., Nicolás, J.M., Cinès, P., Gőrbig, M.N., Garcia-Ramallo, E., Lario, S., *et al*. (1998). Contraction of human hepatic stellate cells activated in culture: a role for voltage-operated calcium channels. *Journal of Hepatology*, **29**(3), 398-408.

Bedossa, P. and Paradis, V. (2003). Liver extracellular matrix in health and disease. *J Pathol,* **200**, 504-515.

Berthiaume, F., Moghe, P. V., Toner, M. and Yarmush, M. L. (1996). Effect of extracellular matrix topology on cell structure, function, and physiological responsiveness: hepatocytes cultured in a sandwich configuration. *FASEB Journal*, **10**, 1471-1484.

Bethanis, S.K. and Theocharis, S.E. (2006). Leptin in the field of hepatic fibrosis: a pivotal or an incidental player? *Dig Dis Sci*, **51**, 1685-1696.

Bissell, D.M., Arenson, D.M., Maher, J.J. and Roll, F.J. (1987). Support of cultured hepatocytes by a laminin-rich gel. Evidence for a functionally significant subendothelial matrix in normal rat liver. *J Clin Invest*, **79**(3), 801-812.

Block, G.D., Locker, J., Bowen, W.C. *et al*. (1996). Population expansion, clonal growth, and specific differentiation patterns in primary cultures of hepatocytes induced by HGF/SF, EGF, and TGFa in a chemically defined (HGM) medium. *J Cell Biol*, **132,** 1133-1149.

Boers, W., Aarrass, S., Linthorst, C., Pinzani, M., Oude Elferink, R. and Bosma, P. (2006). Transcriptional profiling reveals novel markers of liver fibrogenesis: gremlin and insulin-like growth factor binding proteins. *J Biol Chem*, **281**(24), 16289-16295.

Borkham-Kamphorst, E., Stoll, D., Gressner, A.M. and Weiskirchen, R. (2004). Antisense strategy against PDGF B-chain proves effective in preventing experimental liver fibrogenesis. *Biochem Biophys Res Commun*, **321**, 413-423.

Braet, F., Wisse, E., Bomans, P., Frederik, P., Geerts, W., Koster, A., Soon, L. and Ringer, S. (2007). Contribution of high-resolution correlative imaging techniques in the study of the liver sieve in threedimensions. *Microsc Res Tech*, **70**, 230-242.

Brandenburg, B., Stock, L., Gutzeit, C., *et al*. (2005). A novel system for efficient gene transfer into primary human hepatocytes via cell-permeable hepatitis B virus-like particle. *Hepatology*, **42**, 1300-1309.

Brenner, D. A., Koch, K. S., and Leffert, H. L. (1989). Transforming growth factor-alpha stimulates proto-oncogene c-jun expression and a mitogenic program in primary cultures of adult rat hepatocytes. *DNA*, **8**, 279-285.

Brieva, T.A. and Moghe, P.V. (2004). Engineering the hepatocyte differentiation–proliferation balance by acellular cadherin micropresentation. *Tissue Engineering*, **10**(3-4), 553-564.

Brown, P. J. and Juliano, R. L. (1985). Selective-inhibition of fibronectin mediated cell-adhesion by monoclonal-antibodies to a cell-surface glycoprotein. *Science*, **228**, 1448-1451.

Brown, S.E.S., Guzelian, C.P., Schuetz, E., Quattrochi, L.C.,Kleinman, H.K. and Guzelian, P.S. (1995). Critical role of extracellular matrix on induction by phenobarbital of cytochrome P450 2B1/2 in primary cultures of adult rat hepatocytes. *Lab Invest*, **73**, 818-27.

Bucher, N.L.R., Mcgowan, J.A. and Patel, U. (1978). Hormonal regulation of liver growth, ICN-UCLA Symp. *Mol Cell Biol*, **12,** 661-670.

Burke, L.J. and Baniahmad, A. (2000). Co-repressors. *FASEB J*, **14**(13), 1876-1888.

Burke, M. D. and Mayer, R. T. (1974). Ethoxyresorufin: direct fluorimetric assay of a microsomal O-dealkylation which is preferentially inducible by 3-methylcholanthrene. *Drug Metabolism and Disposition*, **2**, 583-589.

Butterworth, B.E., Smith-Oliver, T., Earle, L., Loury, D.J., White, R.D., Doolittle, D.J., Working, P.K., Cattley, R.C., Jirtle, R., Michalopoulos, G., *et al.* (1989). Use of primary cultures of human hepatocytes in toxicology studies. *Cancer Res*, **49**, 1075-1084.

Cable, E.E. and Isom, H.C. (1997). Exposure of primary rat hepatocytes in long-term DMSO culture to selected transition metals induces hepatocyte proliferation and formation of duct-like structures. *Hepatology*, **26**(6), 1444-1457.

Caron, J.M. (1990). Induction of albumin gene transcription in hepatocytes by extracellular matrix proteins. *Mol Cell Biol*, **10**, 1239-1243.

Carr, B. I., Hayashi, I., Branum, E. L., and Moses, H. L. (1986). Inhibition of DNA synthesis in rat hepatocytes by platelet-derived type transforming growth factor. *Cancer Res*, **46**, 2330-2334.

Castell, J.V., Jover, R., Martinez-Jimenez, C.P. and Gomez-Lechon, M.J. (2006). Hepatocyte cell lines: their use, scope and limitations in drug metabolism studies. *Expert Opinion on Drug Metabolism and Toxicology*, **2**, 183-212.

Cavallari, A., Cillo, U., Nardo, B., Filipponi, F., Gringeri, E., Montalti, R., *et al*. (2003). A multicenter pilot prospective study comparing Celsior and University of Wisconsin preserving solutions for use in liver transplantation. *Liver Transpl*, **9**(8), 814-821.

Chapman, D.E., Christensen, T.A., Michener, S.R. and Powis, G. (1993). In *Human drug metabolism form molecular biology to man*. (Eds, Jeffrey, E.H.), CRC Press, London, pp. 53-63.

Chia, S.M, Lin, P.C. and Yu, H. (2005). TGF-β1 regulation in hepatocyte-NIH3T3 co-culture is important for the enhanced hepatocyte function in 3D environment. *Biotechnol Bioeng*, **89**(5), 565-573.

Chisari, F.V. (2005). Unscrambling hepatitis C virus-host interactions. *Nature*, **436**, 930-932.

Cho, C.H., Berthiaume, F., Tilles, A.W. and Yarmush, M.L. (2008). A new technique for primary hepatocyte expansion in vitro. *Biotechnol Bioeng*, **101**, 345- 356.

Choksakulnimitr, S., Masuda, S., Tokuda, H., Takakura, Y. and Hashida, M. (1995). In-vitro cytotoxicity of macromolecules in different cell-culture systems. *J Control Release*, **34**, 233-241.

Clement, B., Guguen-Guillouzo, C., Campion, J.P., Glaise, D., Bourel, M. and Guillouzo, A. (1984). Long-term co-cultures of adult human hepatocytes with rat liver epithelial cells: modulation of albumin secretion and accumulation of extracellular material. *Hepatology*, **4**(3), 373-380.

Clement, B., Rissel, M. Peyrot, S. Mazurier, Y., Grimauct. J. A., and Guillouzo, A. (1985). A procedure for light and electron microscopic intracellularimmunolocalization of collagen and fibronectin in rat liver. *J Histodiem Cytochem,* **33**, 407-414.

Coecke, S., Vanhaecke, T., Foriers, A., Phillips, I.R., Vercruysse, A., Shephard, E.A. and Rogiers, V. (2000). Hormonal regulation of glutathione S-transferase expression in co-cultured adult rat hepatocytes. *Journal of Endocrinology,* **166**, 363-371.

Cohen, J. (2007). Animal studies: NIH to end chimp breeding for research. *Sciences*, **316**, 1265.

Corlu, A., Kneip, B., Lhadi, C., Leray, G., Glaise, D., Baffet, G., Bourel, D. and Guguen-Guillouzo, C. (1991). A plasma membrane protein is involved in cell contact-mediated regulation of tissue-specific genes in adult hepatocytes. *J Cell Biol*, **115**(2), 505-515.

Crosby, H.A., Hubscher, S., Fabris, L., Joplin, R., Sell, S., Kelly, D. and Strain, A.J. (1998). Immunolocalization of putative human liver progenitor cells in livers from patients with end-stage primary biliary cirrhosis and sclerosing cholangitis using the monoclonal antibody OV-6.culture of 3D hepatocyte monolayer. *Am J Pathol,* **152**, 771-779.

De Bartolo, L., Jarosch-Von Schweder, G., Haverich, A. and Bader, A. (2000). A novel full-scale flat membrane bioreactor utilizing porcine hepatocytes: Cell viability and tissue-specific functions. *Biotechnol Prog*, **16**,102-108.

De Zanger, R., Braet, F., Arnez, Camacho, M.R. and Wisse, E. (1997). Prolongation of hepatic endothelial cell cultures by phorbol myristate acetate. In *Cells of the Hepatic Sinusoid, Vol.6*. (Eds, Wisse, E., Knook, D.L., Balabaud, C.) Leiden: The Kupffer Cell Foundation, the Netherlands, pp. 97-101.

Decher, G. (1997). Fuzzy Nanoassemblies: Toward Layered Polymeric Multicomposites. *Science*, **277**, 1232-1237.

Decker, K. (1998).The response of liver macrophages to inflammatory stimulation. *Keio J Med*, **47**, 1-9.

Demetriou, A.A., Brown, R.S., Busuttil, R.W., *et al*. (2004). Prospective, randomized, multicenter, controlled trial of a bioartificial liver in treating acute liver failure. *Ann Surg*, **239**, 660-667.

Donato, M. T., Castell, J. V. & Gomezlechon, M. J. (1994). Cytochrome-P450 activities in pure and cocultured rat hepatocytes – effects of model inducers. *In Vitro Cellular & Developmental Biology-Animal* **30A**, 825-832.

Dong, J., Mandenius, C.F., Lu¨bberstedt, M., Urbaniak, T., Nu¨ ssler, A.K.N., Knobeloch, D., *et al*. (2008). Evaluation and optimization of hepatocyte culture media factors by design of experiments (DoE) methodology. *Cytotechnology*, **57**, 251-261.

Doré, E. and Legallais, C. (1999).A new concept of bioartificial liver based on a fluidized bed bioreactor. *Ther Apher*, **3**, 264-267.

Drocourt, L., Pascussi, J-M., Assenat, E., Fabre, J-M., Maurel, P. and Vilarem, M-J. (2001). Calcium channel modulators of the dihydropyridine family are human pregnane X receptor activators and inducers of CYP3A, CYP2B, and CYP2C in human hepatocytes. *Drug Metabolism and Disposition*, **29**, 1325-1331.

Du, Y., Han, R., Wen, F., Ng San San, S., Xia, L., Wohland ,T., *et al*. (2008). Synthetic sandwich culture of 3D hepatocyte monolayer. *Biomaterials*, **29**(3), 290-301.

Dunn, J.C., Tompkins, R.G., Yarmush, M.L. (1992). Hepatocytes in collagen sandwich: evidence for transcriptional and translational regulation. *J Cell Biol*, **116**(4), 1043-1053.

Dunn, J.C.Y., Yarmush, M.L., Koebe, H.G. and Tompkins, R.G. (1989). Hepatocyte function and extracellular marix geometry: long-term culture in a sandwich configuration. *FASEB J,* **3**, 174-177.

Eren, R., Landstein, D., Terkieltaub, D., Nussbaum, O., Zauberman, A., Ben-Porath, J., *et al*. (2005). Preclinical evaluation of two neutralizing human monoclonal antibodies against hepatitis C virus (HCV): a potential treatment to prevent HCV reinfection in liver transplant patients. *J Virol*, **80**, 2654-2664.

Evans, R.W. (1993). Organ procurement expenditures and the role of financial incentives. *JAMMA*, **269**, 3113-3156.

Faucette, S.R., Sueyoshi, T., Smith, C.M., Negishi, M., LeCluyse, E.L. and Wang, H. (2006). Differential regulation of hepatic CYP2B6 and CYP3A4 genes by constitutive androstane receptor but not pregnane X receptor. *Journal of Pharmacology and Experimental Therapeutics*, **317**, 1200-1209.

Faucette, S.R., Wang, H., Hamilton, G.A., Jolley, S.L., Gilbert, D., Lindley, C., *et al*. (2004). Regulation of CYP2B6 in primary human hepatocytes by prototypical inducers. *Drug Metabolism and Disposition*, **32**, 348-358.

Faucette, S.R., Zhang, T., Moore, R., Sueyoshi, T., Omiecinski, C.J., LeCluyse, E.L., Negishi, M. and Wang, H. (2007). Relative activation of human pregnane X receptor versus constitutive androstane receptor defines distinct classes of CYP2B6 and CYP3A4 inducers. *Journal of Pharmacology and Experimental Therapeutics*, **320**, 72-80.

Feld, J.J. and Hoofnagle, J.H. (2005). Mechanism of action of interferon and ribavirin in treatment of hepatitis C. *Nature*, **436**, 967-972.

Fiegel, H.C., Bruns, H., Höper, C., Lioznov, M.V. and Kluth, D. (2006). Cell growth and differentiation of different hepatic cells isolated from fetal rat liver in vitro. *Tissue Eng,* **12**, 123-130.

Fiegel, H.C., Kaufmann, P.M., Bruns, H., Kluth, D., Horch, R.E., Vacanti, J.P. and Kneser, U. (2008). Hepatic tissue engineering: from transplantation to customized cell-based liver directed therapies from the laboratory. *J Cell Mol Med*, **12**(1), 56-66.

Fiegel, H.C., Lioznov, M.V., Cortes-Dericks, L., Lange, C., Kluth, D., Fehse, B. and Zander, A.R. (2003). Liver-specifi c gene expression in cultured human hematopoietic stem cells. *Stem Cells*, **21**, 98-104.

Fiegel, H.C., Park, J.J., Lioznov, M.V., *et al*. (2003). Characterization of cell types during rat liver development. *Hepatology*, **37**, 148-154.

Fischer, R., Reinehr, R., Lu, T.P., Schonicke, A., Warskulat, U., Dienes, H.P. and Haussinger, D. (2005). Intercellular commnication via gap junctions in activated rat hepatic stellate cells. *Gastroenterology*, **128**, 433-448.

Folch, A. and Toner, M. (2000). Microengineering of cellular interactions. Ann *Rev Biomed Eng*, **2**, 227-256.

Folch, A., Jo, B.H., Hurtado, O., Beebe, D.J. and Toner M. (2000). Microfabricated elastomeric stencils for micropatterning cell cultures. *J Biomed Mater Res*, **52**, 346-353.

Foy, B.D., Rotem, A., Toner, M., Tompkins, R.G. and Yarmush, M.L. (1994). A device to measure the oxygen-uptake rate of attached cells—importance in bioartificial organ design. *Cell Transplant*, **3**(6), 515-527.

Friedman, S.J. (2006). Transcriptional regulation of stellate cell activation. *Journal of Gastroenterology and Hepatology*, **21**, S79–S83.

Friedman, S.L. (2000). Molecular regulation of hepatic fibrosis, an integrated cellular response to tissue injury. *J Biol Chem*, **275**, 2247-2250.

Friedman, S.L. (2004). Stellate cells: a moving target in hepatic fibrogenesis. *Hepatology*, **40**, 1041-1043.

Fujio, K., Evarts, R.P., Hu, Z., *et al*. (1994). Expression of stem cell factor and its receptor, c-kit, during liver regeneration from putative stem cells in adult rat. *Lab Invest*, **70**, 511-516.

Fujiwara, H., Kikkawa, Y., Sanzen, N. and Sekiguchi, K. (2001). Purification and characterization of human laminin-8. Laminin-8 stimulates cell adhesion and migration through a3b1 and a6b1 integrins. *J Biol Chem*, **276**, 17550-17558.

Fukuda, J., Khademhosseini, A., Yeo, Y., Yang, X., Yeh, J., Eng, G., *et al*. (2006). Micromolding of photocrosslinkable chitosan hydrogen for spheroid microarray and co-cultures. *Biomaterials*, **27**(30), 5259-5267.

Fukuda, J., Okamura, K., Nakazawa, K., Ijima, H., Yamashita, Y., Shimada, M., *et al*. (2003). Efficacy of a polyurethane foam/spheroid artificial liver by using human hepatoblastoma cell line (Hep G2). *Cell Transplant*, **12**(1), 51-58.

Fukuda, J., Sakai, Y. and Nakazawa, K. (2006). Novel hepatocyte culture system developed using microfabrication and collagen/polyethylene glycol microcontact printing. *Biomaterials*, **27**, 1061-1070.

Galli, A., Crabb, D., Price, D., Ceni, E., Salzano, R., Surrenti, C., *et al*. (2000). Peroxisome proliferator-activated receptor γ transcriptional regulation is involved in platelet-derived growth factor-induced proliferation in human hepatic stellate cells. *Hepatology*, **31**,101-108.

Gandol, A.J., Wijeweera, J. and Brendel, K. (1996). Use of precision-cut liver slices as an in vitro tool for evaluating liver function. *Toxicol Pathol*, **24**, 58-61.

Gant, T.W., Baus, P.R., Clothier, B., Riley, J., Davies, R., Judah, D.J., *et al*. (2003). Gene expression profiles associated with inflammation, fibrosis, and cholestasis in mouse liver after griseofulvin. *EHP Toxicogenomics*, **111**(1T), 37-43.

Gatmaitan, Z., Varticovski, L., Ling, L., Mikkelsen, R., Steffan, A.M. and Arias, I.M. (1996). Studies on fenestral contraction in rat liver endothelial cells in culture. *Am J Pathol*, **148**, 2027-2041.

Geerts, A. (2001). History, heterogeneity, developmental biology, and functions of quiescent hepatic stellate cells. *Semin Liver Dis*, **21**, 311-335.

Giancotti, F.G. and Ruoslahti, E. (1999). Integrin signaling. *Science*, **285**, 1028-1032.

Glicklis, R., Shapiro, L., Agbaria, R., Merchuk, J.C. and Cohen, S. (2000). Hepatocyte behavior within three-dimensional porous alginate scaffolds. *Biotechnol Bioeng*, **67**(3):344-353.

Gomez-Lechon, M.J., Castelli, J., Guillen, I., O'Connor, E., Nakamura, T., Fabra, R. and Trullenque, R. (1995). Effects of hepatocyte growth factor on the growth and metabolism of human hepatocytes in primary culture. *Hepatology*, **21**, 1248-1254.

Gomez-Lechon, M.J., Donato, M.T., Castell, J.V. and Jover, R. (2003). Human hepatocytes as a tool for studying toxicity and drug metabolism. *Curr Drug Metab*, **4**(4), 292-312.

Gomez-Lechon, M.J., Donato, M.T., Castell, J.V. and Jover, R. (2004). Human hepatocytes in primary culture: the choice to investigate drug metabolism in man. *Curr Drug Metab*, **5**(5), 443-462.

Gonzalez, F.J. (1990). Molecular genetics of the P450 superfamily. *Pharmacol Ther*, **45**(1), 1-38.

Gotoh, Y., Niimi, S., Hayakawa, T., Miyashita, T. (2004). Preparation of lactose–silk fibroin conjugates and their application as a scaffold for hepatocyte attachment. *Biomaterials*, **25**, 1131-1140.

Goulet, F., Normand, C. and Morin, O. (1988). Cellular interactions promote tissuespecific function, biomatrix deposition and junctional communication of primary cultured hepatocytes. *Hepatology*, **8**, 1010-1018.

Gressner, A. M., Lotfi, S., Gressner, G., Haltner and E., Kropf, J. (1993). Synergism between hepatocytes and Kupffer cells in the activation of fat storing cells (perisinusoidal lipocytes). *J Hepatol* , **19**, 117-32.

Gressner, A.M. (1983). Hepatic proteoglycans: a brief survey of their pathobiochemical implications. *Hepato-Gastroenterol*, **30**, 225-229.

Gressner, A.M. (1998). The cell biology of liver fibrogenesis, an imbalance of proliferation, growth arrest and apoptosis of myofibroblasts. *Cell Tissue Res*, **292**, 447–452.

Grisham, J.W. and Hartroft, W.S. (1961). Morphologic identification by electron microscopy of "oval" cells in experimental hepatic degeneration. *Lab Invest*, **10**,317-332.

Gross-Steinmeyer, K., Stapleton, P.L., Tracy, J.H., Bammler, T.K., Lehman, T., Strom, S.C. and Eaton, D.L. (2005). Influence of Matrigel-overlay on constitutive and inducible expression of nine genes encoding drug-metabolizing enzymes in primary human hepatocytes *Xenobiotica*, **35**(5), 419-438.

Gu, J., Sumida, Y., Sanzen, N. and Sekiguchi, K. (2001). Laminin-10/11 and fibronectin differentially regulate integrin-dependent Rho and Rac activation via p130Cas-CrkII-Dock180 pathway. *J Biol Chem*, **276**, 27090-27097.

Guengerich, F. (1993). Cytochrome P450 enzymes. *American Scientist*, **81**(5), 440-447.

Guengerich, F.P. (1999). Cytochrome P450 3A3: regulation and role in drug metabolism. *Ann Rev Pharmacol Toxicol*, 39, 1-7.

Guillouzo, A., Morel, F., Fardel, O. and Meunier, B. (1993). Use of human hepatocyte cultures for drug metabolism studies. *Toxicology*, **82**, 209-219.

Gupta, B., Plummer, C., Bisson, I., Frey, P. and Hilborn, J. (2002). Plasma induced graft polymerization of acrylic acid onto poly(ethylene terephthalate) films: characterization and human smooth muscle cell growth on grafted films. *Biomaterials*, **23**, 863-871.

Hamilton, G.A., Jolley, S.L., Gilbert, D., Coon, D.J. Barros, S. and LeCluyse, E.I. (2001). Regulation of cell morphology and cytochrome P450 expression in human hepatocyes by extracellular matrix and cell-cell interactions. *Cell Tissue Res*, **306**, 85-99.

Haouzi, D., Baghdiguian, S., Granier, G., Travo, P., Mangeat, P. and Hibner, U. (2005). Three-dimensional polarization sensitizes hepatocytes to Fas/CD95 apoptotic signalling. *J Cell Sci*, **118**(Pt12), 2763-2773.

Harada, K., Mitaka, T., Miyamoto, S., Sugimoto, S., Ikeda, S., Takeda, H., Mochizuki, Y. and Hirata, K. (2003). Rapid formation of hepatic organoid in collagen sponge by rat small hepatocytes and hepatic nonparenchymal cells. *J Hepatol*, **39**(5), 716-723.

Harimoto, M., Yamato, M., Hirose, M., Takahashi, C., Isoi, Y., Kikuchi, A. and Teruo, O. (2002). Novel approach for achieving double-layered cell sheets co-culture: overlaying endothelial cell sheets onto monolayer hepatocytes utilizing temperature-responsive culture dishes. *J Biomed Mater Res*, **62**, 464-470.

Hariparsad, N., Carr, B.A., Evers, R. and Chu, X. (2008). Comparison of immortalized Fa2N-4 cells and human hepatocytes as in vitro models for cytochrome P450 induction. *Drug Metabolism and Disposition*, **36**, 1046-1055.

Hariparsad, N., Nallani, S.C., Sane, R, S., Buckley, D.J., Buckley, A.R. and Desai, P.B. (2004). Induction of CYP3A4 by efavirenz in primary human hepatocytes: Comparison with rifampin and phenobarbital. *Journal of Clinical Pharmacology*, **44**:1273–1281.

Hartung, T., Sauer, A., Hermann, C., Brockhaus, F., and Wendel, A. (1997). Overactivation of the immune system by translocated bacteria and bacterial products. *Scand J Gastroenterol Suppl*, **222**, 98-99.

Hasebe, Y., Akao, M., Okumura, N., Izumi, T., Koth, T., Seki, T., *et al*. (2003). Plasminogen activator/plasmin system regulates formation of the hepatocyte spheriod. *Bioehem Biophy Res Commun*, **308**, 852-857.

Hashimoto, Y., Hirohata, S., Kashiwado, T., Itoh, K. and Ishii, H. (1992). Cytokine regulation of hemostatic property and IL-6 production of human endothelial cells. *Inflammatio,* **16**, 613-621.

Hasirci, V., Berthiaume, F., Bondre, S.P., Gresser, J.D., Trantolo, D.J., Toner, M. and Wise, D.L. (2001). Expression of liver-specific functions by rat hepatocytes seeded in treated poly (lactic-co-glycolic) acid biodegradable foams. *Tissue Eng*, **7** (4), 385-394.

Hay, E.D. (1981). Extracellular matix. *J Cell Biol*, **91**, 205-223.

He, Q., Kim, J., and Sharma, R. P. (2005). Fumonisin B1 hepatotoxicity in mice is attenuated by depletion of Kupffer cells by gadolinium chloride. *Toxicology,* **207**, 137-147.

Hewitt, H.J., Lechón, M.J.G., Houston, J.B., Hallifax, D., Brown, H.S., Maurel, P., *et al*. (2007). Primary hepatocytse: current understanding of the regulation of metabolic enzymes and transporter proteins, and pharmaceutical practice for the use of hepatocytes in metabolism, enzyme induction, transporter, clearance, and hepatotoxicity studies. *Drug Metab Rev*, **39**, 159-234.

Higgins, G.M. and Anderson, R.M. (1931). Experimental pathology of the liver. I: Restoration of the liver of the white rat following partial surgical removal. *Arch Pathol*, **12**, 186-202.

Higuchi, A., Kurihara, M., Kobayashi, K., Cho, C.S., Akaike, T. and Hara, M. (2005). Albumin and urea production by hepatocytes cultured on extracellular matrix proteins-conjugated poly (vinyl alcohol) membranes. *J Biomater Sci Polymer Edn*, **16**(7), 847–860.

Hillesheim, W., Jaeschke, H. and Neumann, H.G. (1995). Cytotoxicity of aromatic amines in rat liver and oxidative stress. *Chem Biol Interact*, **98**, 85-95.

Hirai, Y., Nakagawa, S. and Takeichi, M. (1993). Reexamination of the properties of epimorphin and its possible roles. *Cell*, **73**(3),426-427.

Hobbs, K.E., Hunt, A.C., Palmer, D.B., Badric, F.E., Morris, A.M., Mitra, S.K., Peacock, J.H., Immelman, E.J. and Riddell, A.G. (1968a). Hypothermic perfusion as a method of short-term porcine liver storage. *Br J Surg,* **55**, 862.

Hobbs, K.E., Hunt, A.C., Palmer, D.B., Badrick, F.E., Morris, A.M., Mitra, S.K., Peacock, J.H., Immelman, E.J. and Riddell, A.G. (1968b). Hypothermic low flow liver perfusion as a means of porcine hepatic storage for six hours. *Br J Surg,* **55**, 696-703.

Hoebe, K.H.N., Witkamp, R.F., Fink-Gremmels, J., Van Miert, A.S.J.P.A.M. and Monshouwer, M. (2001). Direct cell-to-cell contact between Kupffer cells and hepatocytes augments endotoxin-induced hepatic injury. *Am J Physiol Gastrointest Liver Physiol*, **280**, G720-G728.

Hohne, M.W., Zieroth, S., Veser, U., Kahl, G.F. and Schwarz, L.R. (1993). Carcinogen-induced diploid hepatocytes: sensitive target cells for transformation by mutated c-Ha-ras oncogene. *Mol Carcinog*, **7**(3), 180-189.

Hollenberg, P.F. (2002). Characteristics and common properties of inhibitors, inducers and activators of CYP enzymes. *Drug Metabolism Reviews*, **34**, 17-35.

Holt, A.P., Haughton, E.L., Lalor, P.F., Filer, A., Buckley, C.D. and Adams, D.H. (2009). Liver myofibroblasts regulate infiltration and positioning of lymphocytes in human liver. *Gastroenterology*, in press

Hong, S.H., Gang, E.J., Jeong, J.A., Ahn, C., Hwang, S.H., Yang, I.H., *et al*. (2005). In vitro differentiation of human umbilical cord blood-derived mesenchymal stem cells into hepatocyte-like cells. *Biochem Biophys Res Commun*, **330**,1153-1161.

Hong, S.R., Lee, Y.M. and Akaike, T. (2003). Evaluation of a galactose-carrying gelatin sponge for hepatocytes culture and transplantation. *J Biomed Mater Res A*, **67**, 733-741.

Hoshiba, T., Cho, C.S., Murakawa ,A., Okahata, Y. and Akaike, T. (2006). The effect of natural extracellular matrix deposited on synthetic polymers on cultured primary hepatocytes. *Biomaterials*, **27**, 4519-4528.

Houck, K.A. and Michalopoulos G.K. (1985). Proline is required for the stimulation of DNA synthesis in hepatocyte cultures by EGF. *In Vitro*, **21**, 121-124.

Hu, W., Sorrentino, C., Denison, M. S., Kolaja, K., and Fielden, M. R. (2007). Induction of CYP1A1 is a nonspecific biomarker of aryl hydrocarbon receptor activation: results of large scale screening of pharmaceuticals and toxicants in vivo and in vitro. *Mol Pharmacol*, **71**(6), 1475-1486.

Huggett, A. C., Krutzsch, H. C., and Thorgeirsson, S. S. (1987). Characterization of a hepatic proliferation inhibitor (HPI): effect of HPI on the growth of normal liver cells - comparison with transforming growth factor beta. J *Cell Biochem,* **35**, 305-314.

Hui, E.E. and Bhatia, S.N. (2007). Micromechanical control of cell–cell interactions. *Proc Natl Acad Sci USA*, **104**(14), 5722-5726.

Hynes, R.O. (2002). Integrins: Bidirectional, allosteric signaling machines. *Cell*, **110**, 673-687.

Ijima, H., Matsuo, T. and Kawakami, K. (2008). The mixed co-culture effect of primary rat hepatocytes and bone marrow cells is caused by soluble factors derived from bone marrow cells. *Journal of Bioscience and Bioengineering*, **105**, 226-231.

Ijima, H., Matsushita, T., Nakazawa, K., Fujii, Y. and Funatsu, K. (1998). Hepatocyte spheroids in polyurethane foam: functional analysis and application for a hybrid artificial liver. *Tissue Eng*, **4**, 213-226.

Ijima, H., Nakazawa, K., Mizumoto, H., Matsushita, T. and Funatsu, K. (1998). Formation of a spherical multicellular aggregate (spheroid) of animal cells in the pores of polyurethane foam as a cell culture substratum and its application to a hybrid artificial liver. *J Biomater Sci Polym Ed*, **9**, 765-778.

Ijima, H., Wang, Y. and Langer, R. (2004). Spheroid formation and expression of liver-specific functions of primary rat hepatocytes co-cultured with bone marrow cells. *Biochem Eng J*, **20**, 223-228.

Ilynes, R.O. (1987). Integrins: a family of dell surface receptors. *Cell,* **48**, 549-554.

Ingelman-sundberg, M. (2004). Pharmacogenetics of cytochrome P450 and its application in drug therapy: the past, present and future. *Trends Pharmacology Sciences,* **25**(4), 193-200.

Inoue, C., Yamamoto, H., Nakamura, T., Ichihara, A. and Okamoto, H. (1989). Nicotinamide prolongs survival of primary cultured hepatocytes without involving loss of hepatocyte-specific functions. *J Biol Chem*, **264,** 4747-4750.

Irving, M.G., Roll, F.J., Huang, S. and Bissell, D.M. (1984). Characterization and culture of sinusoidal endothelium from normal rat liver: lipoproteinuptake and collagen phenotype. *Gastroenterology*, **87**, 1233-1247.

Ito, A., Jitsunobu, H., Kawabe, Y. and Kamihira, M. (2007). Construction of heterotypic cell sheets by magnetic force-based 3-d co-culture of HepG2 and NIH3T3 cells. *Journal of Bioscience and Bioengineering*, **104**(5), 371-378.

Ito, A., Takizawa, Y., Honda, H., Hata, K.I., Kagami, H., Ueda, M., *et al*. (2004). Tissue engineering using magnetite nanoparticles and magnetic force: heterotypic layers of cocultured hepatocytes and endothelial cells. *Tissue Eng*, **10**, 833-840.

Ito, T. and Nemeto, J. (1952). Uber die Kupfferschen Sternzellen und die "Fettspeicherungszellen" (fat-storing cells) in der Blutkapillarenwand der menschlichen Leber. *Okajima's Folia Anat Jpn*, **24**, 243-258.

Ito, Y., Bethea, N. W., Abril, E. R., and McCuskey, R. S. (2003). Early hepatic microvascular injury in response to acetaminophen toxicity. *Microcirculation*, **10**, 391-400.

Jefferson, D.M., Reid, L.M., Giambrone, M.A., Shafritz, D.A. and Zem, M.A. (1985).Effects of dexamethasone on albumin and collagen gene expression in primary cultures of adult rat hepatocytes. *Hepatology*, **5**, 14-20.

Jeschke, M.G, Rensing, H., Klein, D., Schubert, T., Mautes, A.E., Bolder, U. and Croner, R.S. (2005). Insulin prevents liver damage and preserves liver function in lipopolysaccharide-induced endotoxemic rats. *J Hepatol,* **42**, 870-879.

Jeschke, M.G., Mlcak, R.P., Finnerty, C.C. and Herndon, D.N. (2007). Changes in liver function and size after a severe thermal injury. *Shock,* **28**,172-177.

Jiang, X., Ferrigno, R., Mrksich, M. and Whitesides, G.M. (2003). Electrochemical desorption of self-assembled monolayers noninvasively releases patterned cells from geometrical confinements. *J Am Chem Soc*, **125**, 2366-2367.

Jigorel, E., Le Vee, M.m Boursier-Neyet, C., Bertrand, M. and Fardel, O. (2005). Functional expression of sinusoidal drug transporters in primary human and rat hepatocytes. *Drug Metab Dispos*, **33**(10), 1418-1422.

Jung, D., Biggs, H., Erikson, J. and Ledyard, P.U. (1975). New colorimetric reaction for end-point, continuous-flow, and kinetic measurement of urea. *Clin Chem*, **21**, 1136-1140.

Kaihara, S., Kim, S., Kim, B.S., Mooney, D.J., Tanaka, K. and Vacanti, J.P. (2000). Survival and function of rat hepatocytes cocultured with nonparenchymal cells or sinusoidal endothelial cells on biodegradable polymers under flow conditions. *J Pediatr Surg*, **35**, 1287-1290.

Kakinuma, S., Tanaka, Y., Chinzei, R., Watanabe, M., Shimizu- Saito, K., Hara, Y., *et al*. (2003). Human umbilical cord blood as a source of transplantable hepatic progenitor cells. *Stem Cells*, **21**, 217-227.

Kamihira, M., Yamada, K., Hamamoto, R., and Iijima, S. (1997). Spheroid formation of hepatocytes using synthetic poly- mer. *Ann. N.Y. Acad. Sci*., **831**, 398-407.

Kan, P., Miyoshi, H. and Ohshima, N. (2004). Perfusion of medium with supplemented growth factors changes metabolic activities and cell morphology of hepatocytenonparenchymal cell coculture. *Tissue Eng*, **10**(9-l 0), 1297 -1307.

Kanebratt, K.P. and Andersson, T.B. (2008). HepaRG cells as an in vitro model for evaluation of cytochrome P450 induction in humans. *Drug Metabolism and Disposition*, **36**, 1137-1145.

Kang, I.K., Kim, G.J., Kwon, O.H. and Ito, Y. (2004). Co-culture of hepatocytes and fibroblasts by micropatterned immobilization of β-galactose derivatives. *Biomaterials*, **25**, 4225-4232.

Kang, X.Q., Zang, W.J., Song, T.S., Xu, X.L., Yu, X.J., Li, D.L., *et al*. (2005). Rat bone marrow mesenchymal stem cells differentiate into hepatocytes in vitro. *World J Gastroenterol,* **11**, 3479-3484.

Kemp, D.C. and Brouwer, K.L. (2004). Viability assessment in sandwich-cultured rat hepatocytes after xenobiotic exposure. *Toxicol In Vitro*, **18**(6), 869-877.

Kemp, D.C., Zamek-Gliszczynski, M.J., Brouwer, K.L. (2005). Xenobiotics inhibit hepatic uptake and biliary excretion of taurocholate in rat hepatocytes. *Toxicol Sci*, **83**(2), 207-214.

Kenny, J. R., Chen, L., McGinnity, D. F., Grime, K., Shakesheff, K. M., Thomson, B. and Riley, R. (2008). Efficient assessment of the utility of immortalized Fa2N-4 cells for cytochrome P450 (CYP) induction studies using multiplex quantitative reverse transcriptase-polymerase chain reaction (qRT-PCR) and substrate cassette methodologies. *Xenobiotica*, **38**, (12), 1500-1517.

Kidambi, S., Sheng, L., Yarmush, M. L., Toner, M., Lee, I. and Chan, C. (2007). Patterned co-culture of primary hepatocytes and fibroblasts using polyelectrolyte multilayer templates. *Macromol Biosci*, **7**, 344-353.

Kim, S.H., Goto, M. and Akaike, T. (2001). Specific binding of glucosederivatized polymers to the asialoglycoprotein receptor of mouse primary hepatocytes. *J Biol Chem*, **276**, 35312-35319.

Kim, S.H., Hoshiba, T. and Akaike, T. (2003). Effect of carbohydrates attached to polystyrene on hepatocyte morphology on sugar-derivatized polystyrene matrices. *J Biomed Mater Res A*, **67**, 1351-1359.

Kiss, A., Schnur, J., Szabo, Z. and Nagy, P. (2001). Immunohistochemical analysis of atypical ductular reaction in the human liver, with special emphasis on the presence of growth factors and their receptors. *Liver*, **21**, 237-246.

Kligerman, A.D., Strom, S.C. and Michalopoulos, G. (1980). S ister chromatid exchange studies in human fibroblast-rat hephtocyte co-cultures: a new in vitro system to study SCEs. *Environ Mtttagen*, **2**(2), l57-165.

Kneteman, N.M., Weiner, A.J., O'Connell, J., Collett, M., Gao, T., Aukerman, L., *et al*. (2006). Anti-HCV therapies in chinmeric scid-Alb/uPA mice parallel outcomes in human clinical application. *Hepatology*, **43**, 1346-1353.

Koide, N., Sakaguchi, K., Koide, Y., Asano, K., Kawaguchi, M., Matsushima, H., *et al*. (1990). Formation of multicellular spheroids composed of adult rat hepatocytes in dishes with positively charged surfaces and under other nonadherent environments. *Exp Cell Res*, **186**(2), 227-235.

Kojima, T., Mochizuki, C., Tobioka, H., Saitoh, M., Takahashi, S., Mitaka, T. and Mochizuki, Y. (1997). Formation of actin filament networks in cultured rat hepatocytes treated with DMSO and glucagon. *Cell Struct Funct*, **22,** 269-278.

Koneru, B. and Dikdan, G. (2002). Hepatic steatosis and liver transplantation current clinical and experimental perspectives. *Transplantation*, **73**(3), 325-330.

Korbling, M., Katz, R.L., Khanna, A., Ruifrok, A.C., Rondon, G., Albitar, M., *et al*. (2002).Hepatocytes and epithelial cells of donor origin in the recipients of peripheral blood stem cell transplantation. *N Engl J Med,* **346**, 738-746.

Kramer, L., Bauer, E., Schenk, P., Steininger, R., Vigl, M. and Mallek, R. (2003). Successful treatment of refractory cerebral oedema in ecstasy/cocaine-induced fulminant hepatic failure using a new high-efficacy liver detoxification device (FPSA-Prometheus). *Wien Klin Wochenschr*, **115**, 599-603.

Krausel, P., Markus, P.M., Schwartz, P., Unthan-Fechner, K., Peste, S., Fandrey, J. and Probst, I. (2000). Hepatocytmupported serum-free culture of rat liver sinusoidal endothelial cells. Journal *of Hepatology,* **32**, 718-726.

Kresse, M., Latta, M., Kunstle, G., Riehle, H. M., van Rooijen, N., Hentze, H., Tiegs, G., Biburger, M., Lucas, R., and Wendel, A. (2005). Kupffer cellexpressed membrane-bound TNF mediates melphalan hepatotoxicity via activation of both TNF receptors. *J Immunol*, **175**, 4076-4083.

Kumar, A. and Whitesides, G.M. (1993). Features of gold having micrometer to centimeter dimensions can be formed through a combination of stamping with an elastomeric stamp and an alkanethiol 'Ink' followed by chemical etching. *Appl Phys Lett*, **63**, 2002-2004.

Kwon, Y. (2001). Metabolism. In *Handbook of essential pharmacokinetics, pharmacodynamics and drug metabolism for industrial scientists*. Kluwer Academic Publishers, pp.121-165.

Lagasse, E., Connors, H., Al-Dhalimy, M., Reitsma, M., Dohse, M., Osborne, L., *et al*. (2000). Purified hematopoietic stem cells can differentiate into hepatocytes *in vivo*. *Nat Med*, **6**, 1229-1234.

Landry, J., Bernier, D., Ouellet, C., Goyette, R. and Marceau, N. (1985). Spheroidal aggreagate culture of rat liver cells: histotypic reorganization, biomatrix depostition, and maintenance of functional activities. *Journal of Cell Biology*, **101**, 914-923.

Lange, C., Bassler, P., Lioznov, M.V., Bruns, H., Kluth, D., Zander, A.R. and Fiegel, H.C. (2005). Hepatocytic gene expression in cultured rat mesenchymal stem cells. *Transplant Proc,* **37**, 276-279.

Lange, C., Bruns, H., Kluth, D., Zander, A.R. and Fiegel, H.C. (2006). Hepatocytic differentiation of mesenchymal stem cells in cocultures with fetal liver cells. *World J Gastroenterol,* **12**(15), 2394-2397.

LeCluyse, E. L., Alexandre, E., Hamilton, G. A., Viollon-Abadie, C., Coon, D. J., Jolley, S. and Richert, L. (2005). Isolation and culture of primary human hepatocytes. *Methods in Molecular Biology*, **290**, 207-229.

LeCluyse, E., Madan, A., Hamilton, G., Carroll, K., DeHaan, R. and Parkinson, A. (2000). Expression and regulation of cytochrome P450 enzymes in primary cultures of human hepatocytes. *Journal of Biochemical and Molecular Toxicology*, **14**, 177-188.

LeCluyse, E.L. (2001). Human hepatocyte culture systems for the in vitro evaluation of cytochrome P450 expression and regulation. *European Journal of Pharmaceutical Sciences*, **13**, 343-368.

LeCluyse, E.L., Audus, K.L. and Hochman, J.H. (1994). Formation of extensive canalicular networks by rat hepatocytes cultured in collagensandwich configuration. *Am J Physiol*, **266**(1), 1764-1774.

Lee, D.H., Yoon, H.H., Lee, J.H., Lee, K.W., Lee, S.K., Kim, S.K., *et al*. (2004). Enhanced liver-specific functions of endothelial cell-covered hepatocyte hetero-spheroids. *Biochemical Engineering Journal*, **20**, 181-187.

Lee, J., Morgan, J. R., Thmpkins, R. G. and Yarmush, M. L. (1993). Proline-mediated enhancement of hepatocyte function in collagen gel sandwich culture configuration. *FASEB J*, **7**, 586-591.

Lee, K., Yoon, K.R., Woo, S.I. and Choi, I.S. (2003). Surface modification of poly (glycolic acid) (PGA) for biomedical applications. *Journal of Pharmaceutical Sciences*, **92**(5), 933-937.

Lee, Y.K., Dell, H., Dowhan, D.H., Hadzopoulou-Cladaras, M. and Moore, D.D. (2000). The orphan nuclear receptor SHP inhibits hepatocyte nuclear factor 4 and retinoid X receptor transactivation: two mechanisms for repression. *Mol Cell Biol*, **20**(1), 187-195.

LeGuilly, Y., Lenoir, P. and Bourel, M. (1973). Production of plasma proteins by subcultures of adult human liver. *Biomedicine*, **19**, 361-364.

Lemaire, G., Delescluse, C., Pralavorio, M., Ledirac, N., Lesca, P., and Rahmani, R. (2004). The role of protein tyrosine kinases in CYP1A1 induction by omeprazole and thiabendazole in rat hepatocytes. *Life Sci*, **74**(18), 2265-2278.

Lemmer, E.R., Shepard, E.G., Blakolmer, K., *et al*. (1998). Isolation from human fetal liver of cells co-expressing CD34 haematopoietic stem cell and CAM 5.2 pancytokeratin markers. *J Hepatol*, **29**, 450-454.

Lerche, C., Fautrel, A., Shaw, P.W., Glaise, D., Ballet, F., Cuillouzo, C and Corcos, L. (1997). Regulation of the major detoxication functions by phenobarbital and 3-methylcholanthrene in co-cultures of rat hepatocytes and liver epithelial cells. *Eur J Biochem*, **244***,* 98-106.

Levy, M.T., Trojanowska, M. and Reuben, A. (2000). Oncostatin M: a cytokine upregulated in human cirrhosis, increases collagen production by human hepatic stellate cells*. Journal of Hepatology*, **32**, 218-226.

Li, A.P. (2007). Human hepatocytes: isolation, cryopreservation and applications in drug development. *Chem biol Interact*, **168,** 16-29.

Li, D. and Friedman, S.L. (1999). Liver fibrogenesis and the role of hepatic stellate cells: new insights and prospects for therapy. *J Gastroenterol Hepatol*, **14**, 618-633.

Li, J., Li, L., Yu, H., Cao, H., Gao, C. and Gong, Y. (2006). Growth and metabolism of human hepatocytes on biomodified collagen poly (lactic-co-glycolic acid) three dimensional scaffold. *ASAIO J*, **52**(3), 321-327.

Li., J, Liao, Z., Ping, J., Xu, D. and Wang, H. (2008). Molecular mechanism of hepatic stellate cell activation and antifibrotic therapeutic strategies. *J Gastroenterol*, **43**, 419-428.

Lieber, C.S. (2005). Metabolism of alcohol. *Clin Liver Dis* , **9**, 1-35.

Lin, J.H. and Lu, A.Y.H. (1998). Inhibition and induction of cytochrome P450 and the clinical implications. *Clin Pharmacokinet*, **35**, 361-390.

Lipinski, H.G. (1989). Model calculations of oxygen supply to tissue slice preparations. *Phys Med Biol*, **34**, 1103-1111.

Liu, J., Kuznetsova, L.A., Edwards, G.O., Xu, J., Ma, M., *et al*. (2007). Purcell WM Functional three-dimensional HepG2 aggregate cultures generated from an ultrasound trap: comparison with HepG2 spheroids. *J Cell Biochem*, **102**(5), 1180-1189.

Liu, X., Chism, J.P., LeCluyse, E.L., Brouwer, K.R. and Brouwer, K.L. (1999). Correlation of biliary excretion in sandwich-cultured rat hepatocytes and in vivo in rats. *Drug Metab Dispos*, **27**(6), 637-644.

Lloyd, T.D., Orr, S., Patel, R., *et al*. (2004). Effext of patient, operative and isolation factors on subsequent yield and viability of human hepatocytes for research use. *Cell Tisuue Bank*, **5**, 81-87.

Loreal, O., Levavasseur, F., Fromaget, C., Gros, D., Guillouzo, A. and Clement, B. (1993). Cooperation of Ito cells and hepatocytes in the deposition of an extracellular matrix in vitro. *American Journal of Pathology*, **143**, 538-544.

Lozzo, R.V. (1985). Proteoglycans: structure, fitnctton. and role in neoplasia. *Lab Invest,* **53,** 373-396.

Lu, H.F., Chua, K. N., Zhang, P.C., Lim, W.S., Ramakrishna, S., Leong, K.W. and Mao, H.Q. (2005). Three-dimensional co-culture of rat hepatocyte spheroids and NIH/3T3 fibroblasts enhances hepatocyte functional maintenance. *Acta Biomaterialia*, **1**, 399-410.

Lu, H.F., Lim, W.S., Wang, J., Tang, Z.Q., Zhang, P.C., Leong, K.W., *et al*. (2003). Galactosylated PVDF membrane promotes hepatocyte attachment and functional maintenance. *Biomaterials*, **24**, 4893-903.

Mabuchi, A, Mullaney, I, Sheard, P, Hessian, P, Zimmermann, A, Senoo, H, and Wheatley, A.M. (2004). Role of hepatic stellate cells in the early phase of liver regeneration in rat: formation of tight adhesion to parenchymal cells. *Comp Hepatol,* **3** (Suppl 1), S29.

Madan, A., Graham, R.A., Carroll, K.M., Mudra, D.R., Burton, L.A., Krueger, L.A., *et al*. (2003). Effects of prototypical microsomal enzyme inducers on cytochrome P450 expression in cultured human hepatocytes. D*rug Metabolism and Disposition*, **31**, 421-431.

Margarita, K., Catherine, H. and Helen Grant, M. (2005). Metabolic studies of hepatocytes cultured on collagen substrata modified to contain glycosaminoglycans. *Tissue Engineering*, **11**, 1263-1273.

Marra, F., Valente, A.J., Pinzani, M. and Abboud, H.E. (1993). Cultured human liver fat-storing cells produce monocyte chemotactic protein-1 regulation by proinflammatory cytokines. *J Clin Invest*, **92**, 1674-1680.

Martin, G. R. and Garbion, J. (1987). Laminin and other basement membrane components. *Annu. Rev Cell Biol*, **3**, 57-85.

Martin-Aragon, S., De Las Heras, B., Sanchez-Reus, M. I. and Benedi, J. (2001). Pharmacological modification of endogenous antioxidant enzymes by ursolic acid on tetrachloride-induced liver damage in rat and primary cultures of rat hepatocytes. *Exp Toxicol Pathol*, **53**, 199-206.

Martinez-Hernandez, A. (1984). The hepatic extracellular matrix. I. Electron immunohistochemical studies in normal rat liver. *Lab Invest,* **51**, 57-74.

Martinez-Hernandez, A. and Amenta, P. (1995). The extracellular matrix in hepatic regeneration. *FASEB J*, **9**, 1401-1410.

Masubuchi, Y. (2006). Metabolic and non-metabolic factors determining troglitazone hepatotoxicity: A review. *Drug Metabolism and Pharmacokinetics*, **21**, 347-356.

Matsumoto , K., Fujii, H., Michalopoulos, G., Fung, J.J. and Demetris, A.J. (1994). Human biliary epithelial cells secrete and respond to cytokines and hepatocyte growth factors in vitro: interleukin-6, hepatocyte growth factor and epidermal growth factor promote DNA synthesis in vitro. *Hepatology*, **20**, 376-382.

Mazariegos, G.V., Patzer, J.F.II, Lopez, R.C. *et al*. (2002). First clinical use of a novel bioartificial liver support system (BLSS). *Am J Transplant*, **2**, 260-266.

Mead, J. E., and Fausto, N. (1989). Transforming growth factor TGFα may be a physiological regulator of liver regeneration by means of an autocrine mechanism. *Proc NaiL Sc. USA*, **86**, 1558-1562.

Mendeloff, J., Ko, K., Roberts, M.S., Byrne, M. and Dew, M.A. (2004). Procuring organ donors as a health investment: how much should we be willing to spend? *Transplantation*, **78**, 1704-1710.

Meneses-Lorente, G., Pattison, C., Guyomard, C., Chesne′, C., Heavens, R., Watt, A.P. and Sohal, B. (2007). Utility of long-term cultured human hepatocytes as an in vitro model for cytochrome p450 induction. *Drug Metabolism and Disposition*, **35**, 215-220.

Millis, J.M., Cronin, D.C., Johnson, R., *et al*. (2002). Initial experience with the modified extracorporeal liver-assist device for patients with fulminant hepatic failure: system modifications and clinical impact. *Transplantation*, **74**, 1735-1746.

Mills, J.B., Rose, K.A., Sadagopan, N., Sahi, J. and M.F.de Morais, S. (2004). Induction of drug metabolism enzyems and MDR1 using a novel human hepatocyte cell line. *The Journal of Pharmacology and Experimental Therapeutics,* **309**, 303-309.

Miura, K., Yoshino, R., Hirai, Y., Goto, T., Ohshima, S., Mikami, K., *et al*. (2007). Epimorphin, a morphogenic protein, induces proteases in rodent hepatocytes through NF-$_K$B. *Journal of Hepatology*, **47**, 834-843.

Mizuguchi, T., Mitaka, T., Kojima, T., Hirata, K., Nakamura, T. and Mochizuki, Y. (1996). Recovery of mRNA expression of tryptophan 2,3-dioxygenase and serine dehydratase in long-term cultures of primary rat hepatocytes. *J Biochem* (Tokyo), **120,** 511-517.

Monga, S.P., Tang, Y., Candotti, F., *et al*. (2001). Expansion of hepatic and hematopoietic stem cells utilizing mouse embryonic liver explants. *Cell Transplant*, **10**, 81-89.

Monga, S.P.S., Micsenyi, A., Germinaro, M., Apte, U. and Bell, A. (2006). *β*-Catenin regulation during matrigel-induced rat hepatocyte differentiation. *Cell Tissue Res*, **323**, 71-79.

Mooney, D. J. and Langer, R. (1992). Induction of hepatocyte differentiation by the extracellular matrix and an RGD-containing synthetic peptide. *Mater Res Soc Symp Proc*, **252**, 199–204.

Mooney, D.J., Mazzoni, C.L., Breuer, C., McNamara, K., Hern, D., Vacanti, J.P. and Langer, R. (1996). Stabilized polyglycolic acid fibre-based tubes for tissue engineering. *Biomaterials*, **17**(2), 115-124.

Moreira, R.K. (2007). Hepatic Stellate Cells and Liver Fibrosis. *Arch Pathol Lab Med*, **131**, 1728–1734.

Morin, O. and Normand, C. (1986). Long-term maintenance of hepatocyte functional activity in co-culture: requirements for sinusoidal endothelial cells and dexamethasone. *J. Cell. Physiol*, **129**, 103-110.

Morita, M., Watanabe, Y. and Akaike, T. (1995). Protective effect of hepatocyte growth factor on interferon gamma–induced cytotoxicity in mouse hepatocytes. *Hepatology*, **21**, 1585-1593.

Morsiani, E., Pazzi, P., Puviani, A.C. *et al*. (2002). Early experiences with a porcine hepatocyte-based bioartificial liver in acute hepatic failure patients. *Int J Artif Organs*, **25**, 192-202.

Muhanna, N.M., Doron, S., Wald, O., Horani, A., Eid, A., Pappo, O., *et al*. (2008). Activation of hepatic stellate cells after phagocytosis of lymphocytes: a novel pathway of fibrogenesis. *Hepatology*, **48**, 963-977.

Mundt, A., Puhl, G., Muller, A. *et al*. (2002). A method to assess biochemical activity of liver cells during clinical application of extracorporeal hybrid liver support. *Int J Artif Organs*, **25**, 542-548.

Muntane-Relat, J., Ourlin, J.C., Domergue, J. and Maurel, P. (1995). Differential effects of cytokines on the inducible expression of CYP1A1, CYP1A2, and CYP3A4 in human hepatocytes in primary culture. *Hepatology*, **22**, 1143-1153.

Musat, A.I., Sattler, C., Sattler, G.L., Pitot, H.C. (1993). Reestablishment of cell polarity of hepatocytes in primary culture. *Hepatology*, **18**, 198-205.

Myung, S.J., Yoon, J.H., Gwak, G.Y., Kim, W., Yang, J.I., Lee, S.H., Jang, J.J. and Lee, H.S. (2007). Bile acid-mediated thrombospondin-1 induction in hepatocytes leads to transforming growth factor-b-dependent hepatic stellate cell activation. *Biochemical and Biophysical Research Communications*, **353**, 1091-1096.

Nagaki, M., Shidoji, Y., Yamada, Y., Sugiyama, A., Tanaka, M., Akaike, T., Ohnishi, H., Morwaki, H. and Muto, Y. (1995). Regulation of hepatic genes and liver transcription factors in rat hepatocytes by extracellular matrix. *Biochem Biophys Res Commun*, **210**, 38.

Nagasue, N., Yukaya, H. and Ogawa, Y. (1987). Human liver regeneration after liver resection. A study of normal livers and livers with chronic hepatitis and cirrhosis. *Ann Surg*, **206**, 30-39.

Nahmias, Y., Kramvis, Y., Barbe, L., Casali, M., Berthiaume, F. and Yarmush, M.L. (2006). A novel formulation of oxygen-carrying matrix enhances liver-specific function of cultured hepatocytes. *FASEB J,* **20**(14), 2531-2534.

Najimi, M. and Sokal, E. (2005). Liver cell transplantation. *Minerva Pediatr*, **57**, 243-257.

Nakamura, T., Arakaki, R., and Ichihara, A. (1988). Interleukin-1is a potent growth inhibitor of adult rat hepatocytes in primary culture. *Exp Cell Res,***179**, 488-497.

Nakamura, T., Teramoto, H., Tomita, Y. and Ichihara, A. (1984). L-proline is an essential amino acid for hepatocyte –growth in culture. *Biochem Biophys Res Commun*, **122**, 884-891.

Nakazawa, K., Lee, S.W., Fukuda, J., Yang, D.H. and Kunitake, T. (2006). Hepatocyte spheroid formation on titanium dioxide gel surface and hepatocyte long-term culture. *J Mater Sci: Mater Med*, **17**, 359-364.

Naughton, B.A., Sibanda, B., Weintraub, J.P., San Román, J. and Kamali, V.A. (1995). Stereotypic, transplantable liver tissue-culture system. *Appl Biochem Biotechnol*, **54**(1-3), 65-91.

Newman, S. and Guzelian, P.S. (1982). Stimulation of de novo synthesis of cytochrome P-450 by phenobarbital in primary nonproliferating cultures of adult rat hepatocytes. *Proc Natl Acad Sci USA*, **79,** 2922-2926.

Nierhoff, D., Ogawa, A., Oertel, M., *et al*. (2005). Purification and characterization of mouse fetal liver epithelial cells with high in vivo repopulation capacity. *Hepatology*, **42**,130-139.

Nieto, N. and Cederbaum, A.I. (2003). Increased Sp1-dependent transactivation of the LAMγ1 promoter in hepatic stellate Cells co-cultured with HepG2 cells overexpressing cytochrome P4502E1. *The Journal of Biological Chemistry*, **278**(17), 15360–15372.

Nieto, N., Friedman, S.L. and Cederbaum, A.I. (2002). Cytochrome P450 2E1-derived reactive oxygen species mediate paracrine stimulation of collagen I protein synthesis by hepatic stellate cells. *The Journal of Biological Chemistry*, **277**(12), 9853–9864.

Nishikawa, M., Kojimam, N., Komori, K., Yamamotoa, T., Fujii, T. and Sakai, Y. (2008). Enhanced maintenance and functions of rat hepatocytes induced by combination of on-site oxygenation and coculture with fibroblasts. *Journal of Biotechnology*, **133**, 253-260.

Nishimura, M., Koeda, A., Suganuma, Y., Suzuki, E., Shimizu, T., Nakayama, M., Satoh, T., Narimatsu, S. and Naito, S. (2007). Comparison of inducibility of CYP1A and CYP3A mRNAs by prototypical inducers in primary cultures of human, cynomolgus monkey, and rat hepatocytes. *Drug Metabolism and Pharmacokinetics*, **22**, 178-186.

Niu, L., Wang, X., Li, J., Huang, Y., Yang, Z., Chen, F., *et al*. (2007). Leptin stimulates alpha 1(I) collagen expression in human hepatic stellate cells via the phosphatidylinositol 3-kinase/Akt signalling pathway. *Liver Int* , **27**, 1265-1272.

Noji, S.T.K., Koyama, E., Nohno, T., Ohyama, K., Taniguchi, S. and Nakamura, T. (1998). Expression of Hepatocyte Growth Factor in Endothelial and Kuffer Cells of Damaged Rat Livers, as revealed by in situ Hybridisation. *Biochemical and Biophysical Research Communications*, **173**, 42-47.

Nussler, A.K., Wang, A., Neuhaus, P., Fischer, J., Yuan, J., Liu, L., *et al*. (2001). The suitability of hepatocyte culture models to study various aspects of drug metabolism. *Altex*, **18**(2), 91-101.

Obermayer, N., Busse, B., Grünwald, A., Mönch, E., Müller, C., Neuhaus, P. and Gerlach, J.C. (2001). Biochemical characterization of bioreactors for hybrid liver support: serum-free liver cell coculture of nonparenchymal and parenchymal cells. *Transplant Proc*, **33**, 1930–1931.

Oblender, M. and Carpentieri, U. (1991a). Control of the growth of leukemic cells (L1219) through manipulation of trace metals. *Anticancer Res*, **11,** 1561-1564.

Oblender, M. and Carpentieri, U. (1991b). Growth, ribonucleotide reductase and metals in murine leukemic lymphocytes. *J Cancer Res Clin Onc*, **117,** 444-448.

Oda, H., Yoshida,Y., Kawamura, Y. and Kakinuma, A. (2008). Cell shape, cell–cell contact, cell–extracellular matrix contact and cell polarity are all required for the maximum induction of CYP2B1 and CYP2B2 gene expression by phenobarbital in adult rat cultured hepatocytes. *Biochemical pharmacology*, **75**, 1209-1217.

Odorico, J.S., Kaufman, D.S. and Thomson, J.A. (2001). Multilineage differentiation from human embryonic stem cell lines. *Stem cells*, **19**, 193-204.

Oh, E., Peirschbacher, M. and Ruoslahti, E. (1981). Deposition of plasma fibronectin in tissues. *Proc Nati Acad Sci USA*, **78**, 3218-3221.

Oh, S.H., Hatch, H.M. and Petersen, B.E. (2002). Hepatic oval 'stem' cell in liver regeneration. Semin Cell Dev Biol, **13**, 405-409.

Okubo, H., Mastsushita, M., Kamachi, H., Kawai, T., Takahashi, M., Fujimoto, T., *et al*. (2002). A novel method of faster formation of rat liver cell spheroids. *Artificial Organs*, **26**(6), 497-505.

Okumoto, K., Saito, T., Hattori, E., Ito, J.I., Adachi, T., Takeda, T., *et al*. (2003). Differentiation of bone marrow cells into cells that express liver-specific genes *in vitro*: implication of the Notch signals in differentiation. *Biochem Biophys Res Commun,* **304**, 691-695.

Olaso, E. and Friedman, S.L. (1998). Molecular mechanisms of hepatic fibrogenesis. *J Hepatol*, **29**, 836-847.

Omiecinski, C. J., Remmel, R. P., Hosagrahara, V. P. (1999). Concise review of the cytochrome P450s and their roles in toxicology. *Toxicol Sci*, **48**, 151-156.

Ostuni E., Kane, R., Chen, C.S., Ingber, D. E. and Whitesides G. M. (2000). Patterning mammalian cells using elastomeric membranes. *Langmuir*, **16**, 7811-7819.

Otsuka, H., Hirano, A., Nagasaki, Y., Okano, T., Horiike, Y. and Kataoka, K. (2004). Two-dimensional multiarray formation of hepatocyte spheroids on a microfabricated PEG-brush surface. *Chem Bio Chem*, **5**, 850-855.

Paine, A. J., Villa, P. and Hockin, L. J. (1980). Evidence that ligand formation is a mechanism underlying the maintenance of cytochrome P450 in rat liver cell culture. Potent maintenance by metryrapone. *Biochemical Journal*, **188,** 937-939.

Paine, A.J., Hockin, L.J. and Legg, R.F. (1979). Relationship between the ability of nicotinamide to maintain nicotinamide adenine dinucleotide in rat liver cell culture and its effect on cytochrome P-450. *Biochem J*, **184,** 461-463.

Panin, L.E., Maksimov, V.F., khoshchenko. O.M. and Korostyshevskaia, I.M. (2002). Effect of combined glucocorticoids and low density lipoproteins on structural and functional changes in hepatocytes and Kupffer cells. *Tsitologiia*, **44**(12), 1149-1156.

Park, I.K., Yang, J., Jeong, H.J., Bom, H.S., Harada, I., Akaike, T., Kim, S.I. and Cho, C.S. (2003). Galactosylated chitosan as a synthetic extracellular matrix for hepatocytes attachment. *Biomaterials*, **24**, 2331-2337.

Park, J., Li, Y., Berthiaume, F., Toner, M., Yarmush, M.L. and Tilles, A.W. (2008). Radial Flow hepatocyte bioreactor using stacked microfabricated grooved substrates. *Biotechnol Bioeng*, **99**, 455-467.

Patzer, J.F., Mazariegos, G.V. and Lopez, R. (2002). Preclinical evaluation of the Excorp Medical, Inc, bioartificial liver support system. *J Am Coll Surg*, **195**, 299-310.

Petersen, B.E., Bowen, W.C., Patrene, K.D., Mars, W.M., Sullivan, A.K., Murase, N., *et al*. (1999). Bone marrow as a potential source of hepatic oval cells. *Science,* **284**, 1168-1170.

Pinzani, M., Gentilini, A., Caligiuri, A., De Franco, R., Pellegrini, G., Milani, S., Marra, F. and Gentilini, P. (1995). Transforming growth factor β-1 regulates platelet-derived growth-factor receptor-β subunit in human liver fat-storing cells. *Hepatology*, **21**, 232-239.

Pinzani, M., Gentilini, P. and Abboud, H.E. (1992). Phenotypical modulation of liver fat-storing cells by retinoids. Influence on unstimulated and growth factor-induced cell proliferation. *J Hepatol*, **14**, 211-220.

Powers, M.J., Rodriguez, R.E. and Griffith, L.G. (1997). Cell-substratum adhesion strength as a determinant of hepatocyte aggregate morphology.*Biotechnol Bioeng*, **53**(4), 415-426.

Powers, M.J., Domansky, K., Kaazempur-Mofrad, M.R., Kalezi, A., Capitano, A., Udapadhaya, A., Kurzawski, P., Wack, K.E., Stolz, D.B., Kamm, R. and Griffith, L.G. (2002). A microarray perfusion bioreactor for 3D liver culture. *Biotech. Bioeng*, **78**, 257-269.

Prins, H. A., Meijer, C., Boelens, P. G., Diks, J., Holtz, R., Masson, S., Daveau, M., Meijer, S., Scotte, M., and van Leeuwen, P. A. (2004). Kupffer cell-depleted rats have a diminished acute-phase response following major liver resection. *Shock,* **21**, 561-565.

Putnam, A.J. and Mooney, D.J. (1996). Tissue engineering using synthetic extracellular matrices. *Nat Med*, **2**, 824-826.

Quintana, A.B., Rodriguez, J.V., Scandizzi, A.L. and Guibert, E.E. (2003). The benefit of adding sodium nitroprusside (NPNa) or S-nitrosoglutathion (GSNO) to the University of Wisconsin solution (UW) to prevent morphological alterations during cold preservation/reperfusion of rat livers. *Ann Hepatol*, **2**(2), 84-91.

Rago, R., Mitchen, J. and Wilding, J. (1990). DNA fluorometric assay in 96-well tissue culture plates using Hoechst 33258 after cell lysis by freezing in distilled water. *Anal Biochem*, **191**(1), 31-34.

Ramachandran, V., Kostrubsky, V.E., Komoroski, B.J., Zhang, S., Dorko, K., Esplen, J.E., Strom, S.C. and Venkataramanan, R. (1999). Troglitazone increases cytochrome P-450 3A protein and activity in primary cultures of human hepatocytes. *Drug Metabolism and Disposition*, **27**, 1194-1199.

Rang, H.P., Dale, M.M., Ritter, J.M. and Flower, R.J (2007). General Principles. In *Rang and Dale's pharmacolohy* (sixth ed.). (Eds, Dimock, K., McGrath, S. and Cook, L.) Churchill Livingstore Elsevier Ltd., Philadelphia, pp.114-118.

Ranucci, C.S., Kumar, A., Batra, S.P. and Moghe, P.V. (2000). Control of hepatocyte function on collagen foams: sizing matrix pores toward selective induction of 2-D and 3-D cellular morphogenesis. *Biomaterials*, **21**, 783-793.

Raucy, J.L. (2003). Regulation of CYP3A4 expression in human hepatocytes by pharmaceuticals and natural products.*Drug Metabolism and Disposition*, **31**, 533-539.

Riccalton-Banks, L., Liew, C., Bhandari, R., Fry, J. and Shakesheff, K. (2003). Long-term culture of functional liver tissue: three-dimensional co-culture of primary hepatocytes and stellate cells. Tissue Eng, **9**, 401-409.

Richert, L., Alexandre, E., Lloyd, T., *et al*. (2004). Tissue collection, transport and isolation proedures required to optimize human hepatocyte isolation from waste liver surgical resection. A multilaboratory study. *Liver Int*, **24**, 371-378.

Richman, R. A., Claus, T. H., Pilkis, S. J. and Friedman, D. L. (1976). Hormonal stimulation of DNA synthesis in primary cultures of adult rat hepatocytes. *Proc. Natl. Acad. Sci. USA*, **73**, 3589-3593.

Ries, K., Krause, P., Solsbacher, M., Schwartz, P., Unthan-Fechner, K., Christ, B., Markus, P.M. and Probst, I. (2000). Elevated expression of hormone-regulated rat hepatocyte functions in a new serum-free hepatocyte-stromal cell coculture model. *In Vitro Cell Dev Biol Anim*, **36**(8), 502-512.

Ripp, S.L., Mills, J.B., Fahmi, O.A., Trevena, K.A., Liras, J.L., Maurer, T.S. and De Morais, S.M. (2006). Use of immortalized human hepatocytes to predict the magnitude of clinical drug–drug interactions caused by CYP3A4 induction. *Drug Metabolism and Disposition*, **34**, 1742-1748.

Robert, J. T., Rena, B., David, A.B., Andrew, J. B., Jeffrey, R. F., Desmond, P., Brian, J. T. and Kevin, M. S. (2005). The effects of three-dimensional co-culture of hepatocytes and hepatic stellate cells on key hepatocyte functions in vitro. *Cells Tissue Organs*, **181**, 67-79.

Rockey, D.C. and Weisiger, R.A. (1996). Endothelin induced contractility of stellate cells from normal and cirrhotic rat liver: implications for regulation of portal pressure and resistance. *Hepatology*, **24**, 233–240.

Rodés, J., Benhamon, J.P., Blei, A., Reichen, J. and Rizzetto, M. (2007). Architecture of the liver. In *Textbook of hepatology* (third ed.). Blackwell Publishing Ltd., Australia, pp.3-71.

Rodriguez-Antona, C., Bort, R., Jover, R., *et al*. (2003). Transcriptional regulation of human CYP3A4 basal expression by CCAAT enhancer-binding protein-α and hepatocyte nuclear factor-3γ. *Mol Pharmacol*, **63**(5), 1180-1189.

Rojkind, M. and Ponce-Noyola, P. (1982). The extracellular matrix of the liver. *Collagen Related Res*, **2**, 151-175.

Rojkind, M., Novikoff, P.M. and Greenwel, P. (1995). Characterization and func- tional studies on rat liver fat-storing cell line and freshly isolated hepatocyte coculture system. *Am J Pathol*, **146**, 1508-1520.

Roymans, D., Van Looveren, C., Leone, A., Parker, J.B., McMillian, M., Johnson, M.D., *et al*. (2004). Determination of cytochrome P450 1A2 and cytochrome P450 3A4 induction in cryopreserved human hepatocytes. *Biochemical Pharmacology*, **67**, 427-437.

Saito, M., Matsuura, T., Nagatsuma, K., Tanaka, K., Maehashi, H., Shimizu, K., *et al*. (2007). The functional interrelationship between gap junctions and fenestrae in endothelial cells of the liver organoid. *J Membrane Biol*, **217**, 115-121.

Sakamoto, T., Liu, Z., Murase, N., Ezure, T., Yokomuro, S., Poli, V., *et al*. (1999). Mitosis and apoptosis in the liver of interleukin-6- deficient mice after partial hepatectomy. *Hepatology*, **29**,403-411.

Sandhu, J.S., Petkov, K.M., Dabeva, M.D. and Shafritz, D.A. (2001). Stem cell properties and repopulation of the rat liver by fetal liver epithelial progenitor cells. *Am J Pathol*, **159**, 1323-1334.

Sato, F., Mitaka, T., Mizuguchi, T., Mochizucki, Y. and Hirata, K. (1999). Effects of nicotinamide-related agents on the growth of primary rat hepatocytes and formation of small hepatocyte colonies. *Liver*, **19**, 481-488.

Sato, M., Suzuki, S. and Senoo, H. (2003). Hepatic stellate cells: unique characteristics in cell biology and phenotype. *Cell structure and function*, **28**, 105-112.

Saucer, I.M., Zeilinger, K., Obermayer, N. *et al*. (2002). Primary human liver cells as source for modular extracorporeal liver support: a preliminary report. *Int J Artif. Organs*, **25**, 1001-1005.

Sauer, I.M., Kardassis, D., Zeillinger, K., Pascher, A., Gruenwald, A., Pless, G., *et al*. (2003). Clinical extracorporeal hybrid liver support – phase I study with primary porcine liver cells. *Xenotransplantation*, **10**, 460-469.

Schaefer, B., Rivas-Estilla, A.M., Meraz-Cruz, N., Reyes-Romero, M.A., Hernández-Nazara, Z.H., Domínguez-Rosales, J.A., Schuppan, D., Greenwel, P. and Rojkind, M. (2003). Reciprocal modulation of matrix metalloproteinase-13 and type I collagen genes in rat hepatic stellate cells. *Am J Pathol*, **162**(6), 1771-1780.

Schiff, L. and Schiff, E. (1993). *Diseases of the liver* (first ed.). PA: J.B. Lippincott., Philadelphia.
Schmelzer, E., Acikgoez, A., Frühauf, N. R., Crome, O., Klempnauer, J., Christians, U. and Bader, A. (2006). Biotransformation of cyclosporin in primary rat, porcine and human liver cell co-cultures. *Xenobiotica*, **36**, 693-708.

Schnabl, B., Choi, Y.H., Olsen, J.C., *et al*. (2002). Immortal activated human hepatic stellate cells generated by ectopic telomerase expression. *Lab Invest*, **82**,323-333.

Schrem, H., Kleine, M., Borlak, J. and Klempnauer, J. (2006). Physiological incompatibilities of porcine hepatocytes for clinical liver support. *Liver Transplantation*, **12**, 1832-1840.

Schrem, H., Klempnauer, J. and Borlak, J. (2002). Liver-enriched transcription factors in liver function and development. Part I: the hepatocyte nuclear factor network and liver-specific gne expression. *Pharmacol Rev*, **54**(1), 129-158.

Schrem, H., Klempnauer, J. and Borlak, J. (2004). Liver-enriched transcription factors in liver function and development. Part II: the C/EBPs and D site-binding protein in cell cycle control, carcinogenesis, circadian gene regulation, liver regeneration, apoptosis, and liver-specific gene regulation. *Pharmacol Rev*, **56**(2), 291-330.

Schuppan, D. (1990). Structure of the extracellular matrix in normal and fibrotic liver: collagens and glycoproteins. *Semin Liver Dis,* **10**, 1-10.

Schuppan, D., Bei'ker, J., Boehm, H., and Hahn, E.G. (1986). Immunofluorescent localization of type V collagen as a librillar component of the interstitial connective tissue of hunsan oral mucosa, artery and liver. *Cell Tissue Res,* **243,** 535-543.

Schuppan, D., Schmid, M., Somasundaram, R., Ackermann,R., Ruehl,M., Nakamura,T. and Riecken, E.O. (1998). Collagens in the liver extracellular matrix bind hepatocyte growth factor. *Gastroenterology*, **114**,139-152.

Schworer, C.M. and Mortimore, G.E. (1979). Glucagon-induced autophagy and proteolysis in rat liver: Mediation by selective deprivation of intracellular amino acids. *Proc Natl Acad Sci USA*, **76,** 3169-3173.

Seeff, L.B. and Hoofnagle, J.H. (2002). Appendix: the national institutes of health consensus development conference management of hepatitis C. *Clin Liver Dis*, **7**, 261-287.

Segawa, D., Miura, K., Goto, T., Ohshima, S., Mikami, K.I., Yoneyama, K., *et al*. (2005). Distribution and isoforms of epimorphin in carbon tetrachloride-induced acute liver injury in mice. *J Gastrol Hepatol*, **20**, 1769-1780.

Seglen, P. O. (1976). Preparation of isolated liver cells. *Methods Cell Biol*, **13**, 29-83

Seglen, P.O. and Solheim, A.E. (1978). Effects of aminooxyacetate, alanine and other amino acids on protein synthesis in isolated rat hepatocytes. *Biochim Biophys Acta*, **520,** 630-641.

Seglen, P.O., Gordon, P.B. and Schwarze, P.E. (1983). Autophagy and protein degradation in rat hepatocytes. In *Isolation, Characterization, and Use of Hepatocytes*. (Eds. Harris, R.A. and Cornell, N.W.) Elsevier, New York, pp. 153-163.

Sellaro, T.L., Ravindra, A.K., Stolz, D.B. and Badylak, S.F. (2007). Maintenance of hepatic sinusoidal endothelial cell phenotype in vitro using organ-specific extracellular matrix scaffolds. *Tissue Eng*, **13**(9), 2301-2310.

Semler, E.J. and Moghe, P.V. (2001). Engineering hepatocyte functional fate through growth factor dynamics: the role of cell morphologic priming. *Biotechnol Bioeng*, **75**(5), 510-520.

Semler, E.J., Ranucci, C.S. and Moghe, P.V. (2000). Mechanochemical manipulation of hepatocyte aggregation can selectively induce or repress liver-specific function. *Biotechnol Bioeng*, **69**, 359-369.

Seo, S.J., Kima, I.Y., Choia, Y.J., Akaikeb, T. and Cho, C. (2006). Enhanced liver functions of hepatocytes cocultured with NIH 3T3 in the alginate/galactosylated chitosan scaffold. *Biomaterials*, **27**, 1487-1495.

Seo, S.J., Park, I.K., Yoo, M.K., Shirakawa, M., Akaike, T., Cho, C.S. (2004). Xyloglucan as a synthetic extracellular matrix for hepatocyte attachment. *J Biomater Sci Polym Ed*, **15**, 1375-1387.

Sérandour, A.L., Loyer, P., Garnier, D., Courselaud, B., Théret, N., Glaise, D., Guguen-Guillouzo, C. and Corlu, A. (2005). TNFalpha-mediated extracellular matrix remodeling is required for multiple division cycles in rat hepatocytes. *Hepatology*, **41**(3), 478-486.

Serralta, A., Donato, M.T., Orbis, F., Castell, J.V., Mir, J. and Gomez-Lechon, M.J. (2003). Functionality of cultured human hepatocytes from elective samples, cadaveric grafts and hepatectomies. *Toxicol in vitro*, **17**, 769-774.

Sherlock, S. and Dooley, J. (2005). Anatomy and function. *In Diseases of the liver and biliary system* (eleven ed.). Blackwell Science Ltd., London, pp. 1-17.

Shi-Wen, X., Chen, Y., Denton, C.P., Eastwood, M., Renzoni, E.A., Bou-Gharios, G., *et al*. (2004). Endothelin-1 promotes myofi broblast induction through the ETA receptor via a rac/phosphoinositide 3-kinase/Akt-dependent pathway and is essential for the enhanced contractile phenotype of fibrotic fibroblasts. *Mol Biol Cell*, **15**, 2707-2719.

Sidhu, J.S., Liu, F. and Omiecinski, C.J. (2004). Phenobarbital responsiveness as a uniquely sensitive indicator of hepatocyte differentiation status: Requirement of dexamethasone and extracellular matrix in establishing the functional integrity of cultured primary rat hepatocytes. *Experimental Cell Research*, **292**, 252-264.

Siegmund, S.V., Seki, E., Osawa, Y., Uchinami, H., Cravatt, B.F. and Schwabe, R.F. (2006). Fatty acid amide hydrolase determines anandamide-induced cell death in the liver. *The Journal of Biological Chemistry*, **281**, 10431-10438.

Sirica, A.E. (1997). Immortalizing hepatocytes with truncated MET: a little bit of gene goes a long way. *Hepatology*, **26**(2), 510-512.

Sivaraman, A., Leach, J. K., Townsend, S., Iida, T., Hogan, B. J., Stolz, D. B., Fry, R., Samson, L. D., Tannenbaum, S. R. and Griffith, L. G. (2005). A microscale in vitro physiological model of the liver: predictive screens for drug metabolism and enzyme induction. *Current Drug Metabolism*, **6**, 569-591.

Smart, D.E., Vincent, K.J., Arthur, M.J., Eicjelberg, O., Castellazzi, M., Mann, J., *et al*. (2001). JunD regulates transcription of the tissue inhibitor of metalloproteinases-1 and interleukin-6 genes in activated hepatic stellate cells. *J Biol Chem*, **276**, 24414-24421.

Smets, F., Najimi, M. and Sokal, E.M. (2008). Cell transplantation in the treatment of liver diseases. *Pediatric Transplantation*, **12**, 6-13.

Smith, P.F., Krack, G., Mckee, R.L., Johnson, D.G., Gandolfi, A.J., Hruby, V.J, *et al*. (1986). Maintenance of adult rat liver slices in dynamic organ culture. *In Vitro Cell Dev Biol*, **22**, 706-712.

Sonderfan, A.J., Arlotto, M.P. and Parkinson, A. (1989). Identification of the cytochrome P-450 isozymes responsible for testosterone oxidation in rat lung, kidney, and testis: evidence that cytochrome P-450a P450IIA1) is the physiologically important testosterone 7 alpha-hydroxylase in rat testis. *Endocrinology*, **125**, 857-866.

Spinelli, S.V., Rodríguez, J.V., Quintana, A.B., Mediavilla, M.G. and Guibert, E.E. (2002). Engraftment and function of intrasplenically transplanted cold stored rat hepatocytes. *Cell Transplant*, **11**(2), 161-168.

Stacey, G., Doyle, A. and Ferro, M. (2001). Cell culture model for hepatotoxicology. In *Cell culture methods for in vitro toxicology* (kindle ed.). Kluwer Academic Publisher, Netherlands, pp.83-96.

Stadlbauer, V. and Jalan, R. (2007). Acute liver failure: liver support therapies. *Curr Opin Crit Care*, **13**, 215–221.

Stange, J., Hassanein, T.I., Mehta, R., Mitzner, S.R. and Bartlett, R.H. (2002). The molecular adsorbents recycling system as a liver support system based on albumin dialysis: a summary of preclinical investigations, prospective, randomized, controlled clinical trial, and clinical experience from 19 centers. *Artif Organs*, **26**, 103-110.

Steen, D. (2004). Immortalized human hepatocytes: A new advance in convenience and performance. *Current Separations*, **20**, 137-140.

Stephenne, X., Najimi, M., Sibille, C., Nassogne, M.C., Smets, F. and Sokal, E.M. (2006). Sustained engraftment and tissue enzyme activity after liver cell transplantation for argininosuccinate lyase deficiency. *Gastroenterology,* **130**, 1317-1323.

Stow, J. L., Kjellen, L., Unger, E., Hook, M. and Farquhar, M. G. (1985). Heparan sulfate proteoglycans are concentrated on the sinusoidal plasmalemmal domain and in intracellular organelles of hepatocytes. *J Cell Biol,* **100**, 975-980.

Straatsburg, I.H., Abrahamse, S.L., Song, S.W., Hartman, R.J. and Van Gulik, T.M. (2002). Evaluation of rat liver apoptotic and necrotic cell death after cold storage using UW, HTK, and Celsior. *Transplantation*, **74**(4), 458-464.

Sugimoto, R., Enjoji, M., Nakamuta, M., Ohta, S., Kohjima, M., Fukushima, M., *et al*. (2005). Effect of IL-4 and IL-13 on collagen production in cultured LI90 human hepatic stellate cells. *Liver Int*, **25**, 420-428.

Sunman, J.A., Hawke, R.L., LeCluyse, E.L. and Kashuba, A.D.M. (2004). Kupffer cell-mediated IL-2 suppression of CYP3A activity in human hepatocytes. *Drug Metabolism and Disposition*, **32**,359-363.

Surapaneni, S., Pryor, T., Klein, M.D. and Matthew, H.W. (1997). Rapid hepatocyte spheroid formation: optimization and long-term function in perfused microcapsules. *ASAIO J*, **43**(5), M848-853.

't Hart, N.A., van der Plaats, A., Leuvenink, H.G., Wiersema-Buist, J., Olinga, P., van Luyn, M.J., *et al*. (2004). Initial blood washout during organ procurement determines liver injury and function after preservation and reperfusion. *Am J Transplant,* **4**(11), 1836-1844.

Takabatake, H., Koide, N., Sasaki, S., Matsushima, M., Takenami, T., Ono, R., *et al*. (1991). Bio-artificial liver using encapsulated hepatocyte spheroids. Jpn J Artif Organs, **20**, 139-144.

Takashi, H., Katsumi, M. and Toshihiro, A. (2007). Hepatocytes maintain their function on basement membrane formed by epithelial cells. *Biochem Biophys Res Commun*, **359**(1), 151-156.

Takezawa, T., Yamazaki, M., Mori, Y., Yonaha, T. and Yoshizato, K. (1992). Morphological and immuno-cytochemical characterization of a hetero-spheroid composed of fibroblasts and hepatocytes. *J Cell Sci*, **101** (Pt3), 495-501.

Talamini, M.A., Mccluskey, M.P., Buchman, T.G. and De Maio, A. (1998). Expression of α2-macroglobulin by the interaction between hepatocytes and endothelial cells in coculture. *Am J Physiol Regulatory Integrative Comp Physiol,* **275**, 203-211.

Tamura, T., Sakai, Y. and Nakazawa, K. (2008). Two-dimensional microarray of HepG2 spheroids using collagen/polyethylene glycol mircropatterned chip. *J Mater Sci: Master Med*, **19**, 2071-2077.

Taniguchi, H., Suzuki, A., Zheng, Y., Kondo, R., Takada, Y., Fukunaga, K., *et al*. (2000). Usefulness of flowcytometric cell sorting for the enrichment of hepatic stem and progenitor cells in the liver. *Transplant Proc*, **32**, 249-251.

Tanikawa, K. (1995). Hepatic sinusoidal cells and sinusoidal circulation. *J Gastroenterol Hepatol*, **10** (Suppl), S8–S11.

Tateno, C. and Yoshizato, k. (1996). Long-term cultivation of adult rat hepatoctes that undergo multiple cell divisions and express normal parenchymal phenotypes. *Am J Pathol*, **148**, 383-392.

Terry, T.L. and Gallin, W.J. (1994). Effects of fetal calf serum and disruption of cadherin function on the formation of bile canaliculi between hepatocytes. *Exp Cell Res*, **214**, 642-653.

Thomas, R.J., Bennett, A., Thomson, B. and Shakesheff, K.M. (2006). Hepatic stellate cells on poly (DL-lactic acid) surfaces control the formation of 3D hepatocyte co-culture aggregates in vitro. *European Cells and Materials*, **11**, 16-26.

Thomas, R.J., Bhandari, R., Barrett, D.A., Bennett, A.J., Fry, J.R., Powe, D., Thomson, B.J. and Shakesheff, K.M. (2005). The effect of three-dimensional co-culture of hepatocytes and hepatic stellate cells on key hepatocye functions in vitro. *Cells Tissues Organs*, **181**, 67-79.

Tirona, R.G. and Kim, R.B. (2004). Nuclear receptors and drug disposition gene regulation. *Journal of Pharmaceutical Sciences*, **94**, 1169-1186.

Tiwari, A., Punshon, G., Kidane, A., Hamilton, G., Seifalian, A.M. (2003). Magnetic beads (dynabead (tm)) toxicity to endothelial cells at high bead concentration: implication for tissue engineering of vascular prosthesis. *Cell Biol Toxicol*, **19**, 265-272.

Tsai, S.Y. and Tsai, M.J. (1997). Chick ovalbumin upsteam promoter-transcription factors (COUP-TFs): coming of age. *Endocr Rev*, **18**(2), 229-240.

Tsiaoussis, J., Newsome, P.N., Nelson, L.J., Hayes, P.C. and Plevris, J.N. (2001). Which hepatocyte will it be? Hepatocyte choice for bioartificial liver support systems. *Liver Transplantation*, **7**(1), 2-10.

Tsuda, Y., Kikuchi, A., Yamato, M., Chen, G. and Okano, T. (2006). Heterotypic cell interactions on a dually patterned surface. *Biochemical and Biophysical Research Communications*, **348**, 937-944.

Tsuda, Y., Kikuchi, A., Yamato, M., Nakao, A., Sakurai, Y., Umezu, M., *et al*. (2005). The use of patterned dual thermoresponsive surfaces for the collective recovery as co-cultured cell sheets. *Biomaterials*, **26**, 1885-1893.

Tulachan, S.S., Doi, R., Hirai, Y., Kawaguchi, Y., Koizumi, M., Hembree, M., *et al*. (2006). Mesenchymal epimorphin and its possible roles. *Cell*, **73**, 426-427.

Turncliff, R.Z., Tian, X. and Brouwer, K.L. (2006). Effect of culture conditions on the expression and function of Bsep, Mrp2, and Mdr1a/b in sandwichcultured rat hepatocytes. *Biochem Pharmacol*, **71**(10), 1520-1529.

Tuschl, G. and Mueller, S.O. (2006). Effects of cell culture conditions on primary rat hepatocytes-cell morphology and differential gene expression. *Toxicology*, **218**(2–3), 205-215.

Tzanakakis, E. S., Hansen, L. K. and Hu, W. S. (2001). The role of actin filaments and microtubules in hepatocyte spheroid self-assembly. *Cell Motility and the Cytoskeleton*, **48**, 175-189.

Ueda, K. and Hayaishi, O. (1985). ADP-ribosylation. Ann Rev Biochem, **54**, 73-100.
Uyama, N., Shimahara, Y., Kawada, N., Seki, S., Okuyama, H., Iimuro, Y. and Yamaoka, Y. (2002). Regulation of cultured rat hepatocyte proliferation by stellate cells. *Journal of Hepatology*, **36**, 590-599.

Van de Kerkhove, M.P., Di Florio, E., Scuderi, V. *et al*. (2002). Phase I clinical trial with the AMC-bioartificial liver. *Int J Artif Organs*, **25**, 950-959.

Verfaillie, C.M., Pera, M.F. and Lansdorp, P.M. (2002). Stem cells: hype and reality. *Hematology Am Soc Hematol Educ Program*, 369-391.

Vermeir, M., Annaert, P., Mamidi, R.N., Roymans, D., Meuldermans, W. and Mannens, G. (2005). Cell-based models to study hepatic drug metabolism and enzyme induction in humans. *Expert Opinion on Drug Metabolism and Toxicology*, **1**, 75-90.

Vickers, A.E. (1994). Use of human organ slices to evaluate the biotransformation and drug-induced side-effects of pharmaceuticals . *CellBiol Toxicol*, **10**, 407-414.

Vondran, F.W., Katenz, E., Schwartlander, R., Morgul, M.H., Raschzok, N., Gong, X., *et al*. (2008). Isolation of primary human hepatocyes after partial hepatectomy: critieria for identification of the most promsing liver specimen. *Artif Organs*, **32**(3), 205-213.

Von Kupffer, C. (1876).Ueber Sternzellen der Leber. Briefliche Mitteilung an Prof. Waldyer. *Arch mikr Anat,* **12**:353-358.

Wang, H. and LeCluyse, E.L. (2003).Role of orphan nuclear receptors in the regulation of drug-metabolising enzymes. *Clin. Pharmacokinet*, **42**(15), 1331-1357.

Wang, S., Nagrath, D., Chen, P.C., Berthiaume, F. and Yarmush, M.L. (2008). Three-dimensional primary hepatocyte culture in synthetic self-assembling peptide hydrogel. *Tissue Eng*, **14**(2), 227-236.

Wang, X., Foster, M., Al-Dhalimy, M., *et al*. (2003). The origin and liver repopulating capacity of murine oval cells. *Proc Natl Acad Sci USA*, **100**(suppl 1), 11881-11888.

Wang, Y.F., Nan, X., Li, Y.H., Zhang, R., Yue, W., Yan, F. and Pei, X.Y. (2005). Sustaining effect of gene-transferring hepatic stellate cell strain CFSC/HGF on hepatocytes development. *Zhonghua Gan Zang Bing Za Zhi*, **13**(1), 45-48.

Washizu J, Berthiaume F, Mokuno y, Tompkins RG, Toner M, yarmush ML. (2001). Long-term maintenance of cytochrome P450 activities by rat hepatocyte/3T3 cell co-cultures in heparinized human plasma. *Tissue Eng*, **7**(6):691-703.

Watanabe, T., Shibata, N., Westerman, K.A., Okitsu, T., Allain, J.E., Sakaguchi, M., *et al*. (2003). Establishment of immortalized human hepatic stellate scavenger cells to develop bioartificial livers. *Transplantation,* **75**(11), 1873-1880.

Wege, H., Le, H.T., Chui, M.S., *et al*. (2003). Telomerase reconstitution immortalizes human fetal hepatocytes without disrupting their differentiation potential. *Gastroenterology*, **124**(2), 432-444.

Weltman, M.D., Farrell, G.C., Hall, P., Ingelman-Sundberg, M. and Liddle, C. (1998). Hepatic cytochrome P450 2E1 is increased in patients with nonalcoholic steatohepatitis. *Hepatology,* **27**(1), 128-133.

Wen, F., Chang, S., Toh, Y.C., Arooz, T., Zhuo, L., Teoh, S.H. and Yu, H. (2008). Development of dual-compartment perfusion bioreactor for serial coculture of hepatocytes and stellate cells in poly(lactic-co-glycolic acid)-collagen scaffolds. *J Biomed Mater Res Part B: Appl Biomater*, **87B**, 154-162.

William, G.M., Bermudez, E. and Scaranyzzino, D. (1977). Rat hepatocye primary cell cultures. III. Improved dissociation and attachment techniques and the enhancement of survival by cultures medium. *In Vitro*, **13**, 809-817.

Winwood, P.J., Schuppan, D., Iredale, J.P., Kawser, C.A., Docherty, A.J. and Arthur, M.J. (1995). Kupffer cell-derived 95 kd type IV collagenase/gelatinase B: characterization and expression in cultured cells. *Hepatology*, **22**, 304-315.

Wu, F.J., Friend, J.R., Hsiao, C.C., Zilliox, M.J., Ko, W.J., Cerra, F.B. and Hu, W.S. (1995). Efficient assembly of rat hepatocyte spheroids for tissue engineering application. *Biotechnol Bioeng*, **50**, 404-415.

Wu, G. Y., Konishi, M., Walton, C.M., Olive, D., Hayashi, K and Wu, C.H. (2005). A novel immunocompetent rat model of HCV infection and hepatitis. *Gastroenterology*, **128**, 1416-1423.

Wu, R., Cui, X., Dong, W., Zhou, M., Simms, H.H. and Wang, P. (2006). Suppression of hepatocyte CYP1A2 expression by Kupffer cells via AhR pathway: the central role of proinflammatory cytokines. *International Journal of Molecular Medicine*, **18**, 339-346.

Wynn, T.A. (2004). Fibrotic disease and the T(H)1/T(H)2 paradigm. *Nat Rev Immunol*, **4**, 583-594.

Xia, Y. and Whitesides, G.M. (1998). Soft LithographyAngew. *Chem Int Ed*, **37**, 550-575.

Xu, L., Albanis, E., Arthur, M.J., O'Byrne, S.M., Blaner, W.S., Mukherjee, P., Friedman, S.L., Eng, F.J. (2005). Human hepaticstellate cell lines, LX-1 and LX-2: new tools for analysis of hepatic fibrosis. *Gut,* **54**, 142-151.

Yamada, K., Kamihira, M. and Iijima, S. (2001). Self-organization of liver constitutive cells mediated by artificial matrix and improvement of liver functions in long-term culture. *Biochemical Engineering Journal*, **8**, 135-143.

Yamada, S., Otto, P.S., Kennedy, D.L. and Whayne, T.F.Jr. (1980). The effects of dexamethasone on metabolic activity of hepatocytes in primary monolayer culture. *In Vitro*, **16**(7), 559-570.

Yekaterina S. Zinchenko, Laura W. Schrum and Mark Clemens, Robin N. Coger. (2006). Hepatocyte and Kupffer cells c-culture on micropatterned surface to optimize hepatocyte function. *Tissue Engineering*, **12**(4), 751-761.

Yamane, A., Seetharam, L., Yamaguchi, S., Gotoh, N., Takahashi, T., Neufeld, G., *et al*. (1994). A new communication system between hepatocytes and sinusoidal endothelial cells in liver through vascular endothelial growth factor and Flt tyrosine kinase receptor family. *Oncogene*, **9**, 2683-2690.

Yamato, M., Konno, C., Utsumi, M., Kikuchi, A. and Okano, T. (2002). Thermally responsive polymer-grafted surfaces facilitate patterned cell seeding and co-culture. *Biomaterials*, **23**, 561-567.

Yang, J., Goto, M., Ise, H., Cho, CS. and Akaike, T. (2002). Galactosylated alginate as a scaffold for hepatocytes entrapment. *Biomaterials*, **23**, 471-479.

Yang, S.M., Lee, D.H. and Park, J.K. (2000). Effects of degree of cell-cell contact on liver specific functions of rat primary hepatocytes. *Biotechnology and Bioprecess Engineering*, **5**(2), 99-105.

Yeo, W.S., Yousaf, M.N. and Mrksich, M. (2003). Dynamic interfaces between cells and surfaces: electroactive substrates that sequentially release and attach cells. *J Am Chem Soc*, **125**, 14994-14995.

Yin, C., Ying, L., Zhang, P.C., Zhuo, R.X., Kang, E.T., Leong, K.W., *et al*. (2003). High density of immobilized galactose ligand enhances hepatocyte attachment and function. *J Biomed Mater Res*, **67A**, 1093-1104.

Yoon, J.H., Lee, N.V.S., Lee, J.S., Park, J.B. and Kim, C.Y. (1999). Development of a non-transformed human liver cell line with differentiated-hepatocyte and urea-synthetic functions: applicable for bioartificial liver. *Int J Artif Organs*, **22**, 769-777.

Youdim, K.A., Tyman, C.A., Jones, B.C. and Hyland, R. (2007). Induction of cytochrome P450: Assessment in an immortalized human hepatocyte cell line (Fa2N-4) using a novel higher throughput cocktail assay. *Drug Metabolism and Disposition*, **35**, 275-282.

Zaret, K.S. (2000). Liver specification and early morphogenesis. *Mech Dev*, **92**, 83-88.

Zhang, S., Xia, L., Kang, C.H., Xiao, G., Ong, S. Mi., Toh, Y.C., Leo, H.L., Noort, D., Kan, S.H., Tang, H.H. and Yu, H. (2008). Microfabricated silicon nitride membranes for hepatocyte sandwich culture. *Biomaterials*, **29**, 3993-4002.